

Bentonite-Polymer Composites for Containment Applications

By

Joseph Scalia IV

A dissertation submitted in partial fulfillment of
the requirements for the degree of

Doctor of Philosophy
(Geological Engineering)

at the
UNIVERSITY OF WISCONSIN-MADISON
2012

Date of final oral examination: 8/9/2012

The dissertation is approved by the following members of the Final Oral Committee:

Craig H. Benson, Professor, Geological Engineering

Tuncer B. Edil, Professor, Geological Engineering

Samuel Kung, Professor, Soil Science

Huifang Xu, Associate Professor, Geoscience

Charles D. Shackelford, Professor, Civil and Environmental Engineering,
Colorado State University

Michael S. Donovan, Innovation Leader, AMCOL International

© Copyright by Joseph Scalia IV 2012
All Rights Reserved

ABSTRACT


BENTONITE-POLYMER COMPOSITES FOR CONTAINMENT APPLICATIONS

Joseph Scalia IV

Under the Supervision of Professor Craig H. Benson and
Professor Tuncer B. Edil at the University of Wisconsin-Madison

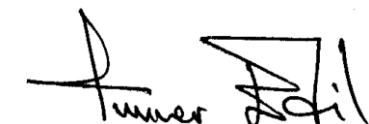
Bentonite was modified at the nanoscale so that low hydraulic conductivity (k) would be maintained under adverse conditions. Nanoscale modification consisted of polymerizing acrylic acid within bentonite slurry to form an interconnected super-swelling structure, and the resulting material is referred to as bentonite-polymer nanocomposite (BPN). Despite being super-swelling in dilute solutions, the swell of BPN decreased with increasing solution concentration and exhibited swells typical of low-swelling calcium-bentonite in aggressive solutions. Permeability tests were conducted on BPN, natural sodium bentonite (Na-B,) and superabsorbent polyacrylate (SAP). Thin layers of each material were assembled in flexible wall permeameters and permeated with a range of calcium chloride (CaCl_2) and extreme pH (0.3, 13.1) solutions that cause multiple order-of-magnitude increases in the k of Na-B. Tests were run to hydraulic and chemical equilibrium. Low k (less-than 8×10^{-11} m/s) was maintained by BPN for all solutions. In contrast, Na-B and SAP had k at-least three orders-of-magnitude higher in CaCl_2 solutions stronger-than 20 mM, and solutions with extreme pH. These results illustrate that BPN may be a superior waste-containment material for many containment applications. These results also demonstrate that the mechanism underlying the low k of BPN in aggressive solutions is decoupled from swell. Despite low swelling, BPN formed a homogeneous layer in all solutions tested. This structure was the result of the

cohesion of BPN granules by polyacrylate, and inter-granular consolidation during permeation. Additionally, of the 28.5% polymer (by mass) initially contained within BPN, up-to 75% was not superabsorbent, mobile, and had a weight average molecular weight of 280,000 g/mol. This polymer clogged permeameter tubing as well as the macroscale-porosity of Na-B in 50 mM CaCl_2 . Granular mixtures of BPN with Na-B resulted in k lower than pure BPN with mass-percentages as-low-as 1% when permeated with 50 mM CaCl_2 , but did not improve k to 500 mM CaCl_2 . Mixing of SAP and non-superabsorbent polyacrylate into Na-B and other mineral barrier layers was also investigated. Low mass percentages of polyacrylate with weight average molecular weights below 1,080,000 g/mol were effective at reducing the k of Na-B and kaolinite to 50 mM CaCl_2 .

 8/21/12

Signature Date

Craig H. Benson, Professor

 8/21/12

Signature Date

Tuncer B. Edil, Professor

ACKNOWLEDGEMENTS

Professors Craig Benson and Tuncer Edil, thank you for your guidance and mentorship throughout my years at the University of Wisconsin. This document would not exist without you. Many thanks are also due to my PhD committee: Professor Charles Shackelford of Colorado State University (CSU), Professor Samuel Kung, Professor Huifang Xu, and Dr. Mike Donovan of AMCOL International.

I would like to acknowledge Chris Bareither for his assistance, guidance, and friendship over the past five years. Gretchen Bohnhof, my co-project PhD student at Colorado State University, thank you for being my accomplice along this long journey.

Most importantly, I am grateful to my parents, Joseph and Lynne Scalia, and my fiancée, Nikki Woodward, for their love and unending support. My humble obeisance.

This is not a comprehensive list, for I have been blessed throughout my life with far more support than I can hope to acknowledge on a single page. So to everyone not mentioned...thank you, thank you, thank you.

Financial support for this study, which was a collaboration between the University of Wisconsin – Madison, Colorado State University, and Colloid Environmental Technologies Co. (CETCO), was provided by the U.S. National Science Foundation (NSF), under Grant No. CMMI-0757815. This support is gratefully acknowledged. The author thanks CETCO for providing the bentonites used in this study. The findings and recommendations that have been presented are solely those of the author, and do not necessarily represent the policies or opinions of the sponsors.

TABLE OF CONTENTS

ABSTRACT	i
ACKNOWLEDGEMENTS	iii
TABLE OF CONTENTS	iv
LIST OF FIGURES.....	x
LIST OF TABLES	xv
1. EXECUTIVE SUMMARY	1
1.1 INTRODUCTION	1
1.2 METHODS.....	3
1.3 MAJOR FINDINGS	4
1.4 REFERENCES	9
2. BACKGROUND: BENTONITES MODIFIED WITH ORGANIC MOLECULES FOR IMPROVED CHEMICAL COMPATIBILITY IN HYDRAULIC BARRIER APPLICATIONS	11
2.1 INTRODUCTION	11
2.2 MATERIALS IN THE LITERATURE	16
2.2.1 Multi-Swellable Bentonite (MSB).....	16
2.2.2 HYPER-Clay (HC).....	16
2.2.3 Dense-Prehydrated GCLs (DPH-GCLs)	16
2.2.4 Contaminant-Resistant Clay (CRC)	17
2.2.5 Bentonite-Polymer Alloy (BPA)	17
2.3 MECHANISMS FOR IMPROVED COMPATIBILITY.....	18
2.3.1 Intercalation and Activation of Osmotic Swell	18
2.3.2 Locking of Bound Cations	19
2.3.3 Independently Swelling Additives.....	21

	v
2.4 EXPERIMENTAL RESULTS	21
2.4.1 MSB	21
2.4.2 HC.....	24
2.4.3 DPH-GCLs	25
2.4.4 CRCs	27
2.4.5 BPA.....	27
2.5 MECHANISTIC ANALYSIS OF COMPILED RESULTS	28
2.6 DISCUSSION	31
2.7 REFERENCES	32
2.8 ABBREVIATIONS.....	39
2.9 FIGURES.....	40
3. LONG-TERM HYDRAULIC CONDUCTIVITY OF A BENTONITE- POLYACRYLATE NANOCOMPOSITE PERMEATED WITH AGGRESSIVE INORGANIC SOLUTIONS.....	45
3.1 ABSTRACT	45
3.2 INTRODUCTION	46
3.3 MATERIALS	49
3.3.1 Bentonite-Polyacrylate Nanocomposite (BPN).....	49
3.3.2 Na-Bentonite (Na-B)	50
3.3.3 Na-Polyacrylate (SAP)	51
3.3.4 Liquids	51
3.4 METHODS.....	55
3.4.1 Swell Index.....	55
3.4.2 Hydraulic Conductivity (k)	55
3.4.3 Termination Criteria	57

3.4.4 Inter-Laboratory Validation.....	58
3.4.5 Soluble Cations (SC), Bound Cations (BC), and Cation Exchange Capacity (CEC).....	58
3.4.6 Polymer Quantification.....	59
3.5 RESULTS.....	59
3.5.1 Swell Index.....	60
3.5.2 Temporal Hydraulic Behavior with DW.....	62
3.5.3 Temporal Behavior with 50 mM CaCl_2	64
3.5.4 Temporal Behavior with 500 mM CaCl_2	65
3.5.5 Temporal Behavior with Strong Acid and Base.....	66
3.5.6 Hydraulic Conductivity.....	67
3.5.7 Swelling and Specimen Water Content.....	68
3.5.8 Swelling and Hydraulic Conductivity.....	70
3.5.9 Polymer Retention.....	70
3.6 DISCUSSION.....	71
3.6.1 Polymer Content.....	71
3.6.2 SAP as a Hydraulic Barrier Material.....	72
3.6.3 Impact of Hydraulic Gradient on CaCl_2 Tests.....	72
3.6.4 Inter-Laboratory Duplication.....	74
3.7 IMPLICATIONS.....	75
3.8 CONCLUSIONS.....	76
3.9 REFERENCES.....	79
3.10 ABBREVIATIONS.....	87
3.11 TABLES.....	88
3.12 FIGURES.....	92

4. HYDRAULIC IMPACT OF MACROPORE SEALING IN A BENTONITE POLYMER-NANOCOMPOSITE EXPOSED TO AGGRESSIVE INORGANIC SOLUTIONS.....	105
4.1 ABSTRACT	105
4.2 INTRODUCTION	106
4.3 MATERIALS AND NON-STANDARDIZED METHODS	109
4.3.1 Bentonite-Polyacrylate Nanocomposite (BPN).....	109
4.3.2 Natural Na-bentonite (Na-B)	110
4.3.3 Permeants	111
4.3.4 Hydraulic Conductivity (k)	111
4.3.5 Polymer Content	112
4.4 BPN PROPERTIES AND BEHAVIOR	113
4.4.1 Intercalated Polymer	113
4.4.2 Cation Exchange.....	114
4.4.3 Carbonate Precipitation	115
4.4.4 BPN Monolith Formation	116
4.5 POLYMER CLOGGING NA-BENTONITE POROSITY	121
4.5.1 Clogging Experiments	122
4.5.2 Polymer Mobility.....	124
4.6 BPN AS A NA-BENTONITE ADDITIVE.....	128
4.6.1 Eluted Polyacrylate Clogged Bentonite	128
4.7 DISCUSSION	130
4.6.1 Unique Low Permeability Mechanisms	130
4.6.2 Future Work	132
4.8 CONCLUTIONS	134

4.9 REFERENCES	136
4.10 ABBREVIATIONS.....	141
4.11 FIGURES.....	142
5. NOVEL POLYMER ADDITIVES FOR ENHANCED HYDRAULIC PERFORMANCE OF MINERAL BARRIER LAYERS TO INCOMPATIBLE PERMEANTS	152
5.1 ABSTRACT	152
5.2 INTRODUCTION	153
5.3 MATERIALS	157
5.3.1 Na-Bentonite	157
5.3.2 Na-Polyacrylate.....	158
5.3.3 Other Soils	160
5.3.4 Permeant Liquids	160
5.4 METHODS.....	161
5.4.1 Na-B-SAP Mixture (BSM) Production	161
5.4.2 BB-SAP Composite (BSC) Production.....	162
5.4.3 Na-B-Polyacrylate (BPB) Production	164
5.4.4 Hydraulic Conductivity (k)	164
5.4.5 X-ray Diffraction (XRD)	166
5.5 RESULTS	166
5.5.1 SAP Mixtures Hydraulic Conductivity.....	166
5.5.2 SAP Mixtures Swell Index.....	168
5.5.3 SAP Mixtures – Hydraulic Conductivity and Swelling.....	169
5.5.4 Non-Superabsorbent-Na-B Composites	170
5.5.5 Non-Superabsorbent-Soil Composites.....	172

5.6 DISCUSSION	173
5.6.1 Problem with Bentonite-SAP Mixtures	173
5.6.2 Clogging of Hydraulically Governing Porosity	174
5.6.3 Other WSP Additive Applications.....	177
5.7 CONCLUSIONS	178
5.8 REFERENCES	182
5.9 ABBREVIATIONS.....	186
5.10 TABLES.....	188
5.11 FIGURES.....	193
 APPENDIX A.....	 203

LIST OF FIGURES

- Fig. 2.1 Hydraulic conductivity of GCLs permeated with solutions of varying ionic strength segregated by the type of cations in the synthetic permeant solutions used for testing. Data are from Shackelford et al. (2000), Jo et al. (2001), Kolstad et al. (2004), Jo et al. (2004), Jo et al. (2005), and Lee and Shackelford (2005)..... 40
- Fig. 2.2 Hydraulic conductivity of GCLs permeated in varying solutions versus the swell index of the bentonite component of the GCL in the permeant solutions. Data are from Shackelford et al. (2000), Jo et al. (2001), Kolstad et al. (2004), Jo et al. (2004), Jo et al. (2005), and Lee and Shackelford (2005)..... 41
- Fig. 2.3 Influence of ionic strength on the swell index of natural Na-bentonite and bentonites amended for hydraulic compatibility (multi-swellable bentonite, MSB; HYPER-clay, HC; dense-prehydrated GCLs, DPH-GCLs). Literature data for Na-bentonite are from Shackelford et al. (2000), Jo et al. (2001), Kolstad et al. (2004), Jo et al. (2004), Jo et al. (2005), and Lee and Shackelford (2005)..... 42
- Fig. 2.4 Influence of CaCl_2 concentration on the hydraulic conductivity of natural Na-bentonite and bentonites modified for hydraulic compatibility (multi-swellable bentonite, MSB; HYPER-clay, HC; dense-prehydrated GCLs, DPH-GCLs; contaminant-resistant clay, CRC). Literature data for Na-bentonite are from Shackelford et al. (2000), Jo et al. (2001), Kolstad et al. (2004), Jo et al. (2004), Jo et al. (2005), and Lee and Shackelford (2005)..... 43
- Fig. 2.5 Hydraulic conductivity versus swell index for natural Na-bentonite and bentonites amended for hydraulic compatibility (multi-swellable bentonite, MSB; HYPER-clay, HC; dense-prehydrated GCLs, DPH-GCLs). Literature data for Na-bentonite are from Shackelford et al. (2000), Jo et al. (2001), Kolstad et al. (2004), Jo et al. (2004), Jo et al. (2005), and Lee and Shackelford (2005). Model relating GCL hydraulic conductivity and swell index developed by Katsumi et al. (2008) is also included for comparison. 44
- Fig. 3.1 Swell index versus solution CaCl_2 concentration (a) and pH (b) for Na-bentonite (Na-B), superabsorbent Na-polyacrylate (SAP), and bentonite-polyacrylate nanocomposite (BPN). Swell indices in DW are shown at the method detection limit (MDL) of Ca^{2+} . Literature data from Jo et al. (2001), Lee and Shackelford (2005b), and Katsumi et al. (2008) are included for comparison. 92

- Fig. 3.2 Hydraulic conductivity profiles for bentonite-polyacrylate nanocomposite (BPN) (a) as well as superabsorbent Na-polyacrylate (SAP) and Na-bentonite (Na-B) (b) permeated with **deionized water** at varying hydraulic gradients (i). Average cumulative flow calculated as mean of cumulative inflow and cumulative outflow..... 93
- Fig. 3.3 Photograph of precipitated polymer being removed from clogged brass fitting. 94
- Fig. 3.4 Hydraulic conductivity versus average cumulative flow (ACF) (a) and time (b) for Na-bentonite (Na-B), superabsorbent Na-polyacrylate (SAP), and bentonite-polyacrylate nanocomposite (BPN), permeated with **50 mM CaCl₂** at varying hydraulic gradients (i). ACF calculated as mean of cumulative inflow and cumulative outflow..... 95
- Fig. 3.5 Hydraulic conductivity versus average cumulative flow (a) and time (b) for Na-bentonite (Na-B), superabsorbent Na-polyacrylate (SAP), and bentonite-polyacrylate nanocomposite (BPN), permeated with **500 mM CaCl₂** at varying hydraulic gradients (i). ACF calculated as mean of cumulative inflow and cumulative outflow..... 96
- Fig. 3.6 Hydraulic conductivity profiles for Na-bentonite (Na-B), superabsorbent Na-superabsorbent polyacrylate (SAP), and bentonite-polyacrylate nanocomposite (BPN) permeated with **1 M NaOH** (a) and **1 M HNO₃** (b). Average cumulative flow calculated as mean of cumulative inflow and cumulative outflow..... 97
- Fig. 3.7 Equilibrium hydraulic conductivities versus permeant solution CaCl₂ concentration (a) and pH (b) for Na-bentonite (Na-B), superabsorbent Na-polyacrylate (SAP) and bentonite-polyacrylate nanocomposite (BPN). The hydraulic conductivity of specimens permeated with deionized water is shown at method detection limit (MDL) of Ca²⁺. Bi-directional error bars represent maximum and minimum observed hydraulic conductivities..... 98
- Fig. 3.8 Gravimetric water content of specimens after permeation versus permeant solution CaCl₂ concentration (a) and corresponding swell index (b) in the same permeant solution for Na-bentonite (Na-B), superabsorbent polyacrylate (SAP), and bentonite-polyacrylate nanocomposite (BPN). The gravimetric water content of specimens permeated with deionized water is shown at method detection limit (MDL) of Ca²⁺. Bi-directional error bars represent maximum and minimum observed gravimetric water contents.. 99
- Fig. 3.9 Swell index in deionized water, DW, after permeation versus corresponding swell index on bulk (viz. new) material in permeant..... 100

Fig. 3.10 Equilibrium hydraulic conductivity versus swell index for Na-bentonite (Na-B), superabsorbent Na-polyacrylate (SAP), and bentonite-polymer nanocomposite (BPN). Literature data from Jo et al. (2005) included for comparison. Bi-directional error bars represent maximum and minimum hydraulic conductivities	101
Fig. 3.11 Polymer retained after long term hydraulic conductivity testing versus permeant solution CaCl_2 concentration (a) and cumulative inflow (b) for bentonite-polyacrylate nanocomposite. Bi-directional error bars represent maximum and minimum fractions of polymer remaining observed at a given CaCl_2 concentration.	102
Fig. 3.12 Equilibrium hydraulic conductivity versus polymer fraction remaining at the termination of bentonite-polyacrylate nanocomposite permeation. Bi-directional error bars represent maximum and minimum observed values.....	103
Fig. 3.13 Comparison of swell index (a) and hydraulic conductivity (b) results from paired replicate tests conducted at the University of Wisconsin – Madison (UW) and Colorado State University (CSU).....	104
Fig. 4.1 Mole fraction of bound monovalent cations at termination of long term testing versus the CaCl_2 concentration of the permeant solution. Data for DW are plotted at the method detection limit of Ca^{2+} within DW (0.05 mM Ca^{2+}).....	142
Fig. 4.2 Cross sections of bentonite-polymer nanocomposite, BPN (a, c, and e), and sodium bentonite, Na-B (b and d) specimens after permeation with DW (a and b) and 500 mM CaCl_2 (c, d, and e). Tests conducted by standard method (a, b, c, and d) and low change in effective stress method (e). Bottom scale in each image is in mm.....	143
Fig. 4.3 Granular hydration of bentonite-polyacrylate nanocomposite, BPN (a, c, and e), and sodium bentonite, Na-B (b, d, and f)	144
Fig. 4.4 Effective stress history of GCL specimens during permeation by standard method used for long term hydraulic conductivity tests, and low change (Δ) in effective stress (σ') low hydraulic gradient (i) method.	145
Fig. 4.5 Void ratio (e) at the termination of long term permeation versus final equilibrium hydraulic conductivity (k) from Chapter 3.....	146
Fig. 4.6 Schematics of permeameter assemblages for BPN clogging experiments where (a) BPN was placed up-gradient from granular Na-bentonite layer and (b) BPN was placed down-gradient from granular Na-bentonite layer.	147

Fig. 4.7	Conceptual models for observed hydraulic behavior. The swell of dry granules of Na-bentonite (a) depends on the ionic strength of the hydrating solution, with low swell occurring with 50 mM CaCl_2 and consequently a high hydraulic conductivity (k) (b). Na-bentonite granules hydrated with a dilute solution exhibit gel formation and low hydraulic conductivity (c). Clogging of hydraulically active porosity by low-molecular-weight polyacrylate in bentonite permeated with 50 mM CaCl_2 yields a low k (d).	148
Fig. 4.8	Fraction of polymer (P) retained in specimen determined by loss-on-ignition after long term hydraulic conductivity (k) testing and polymer-mobility basket testing in varying concentration CaCl_2 solutions. Data for DW are plotted at the method detection limit of Ca^{2+} within DW (0.05 mM Ca^{2+}).	149
Fig. 4.9	Hydraulic conductivity versus fraction of BPN in permeated specimen.	150
Fig. 4.10	Fraction of polymer remaining after permeation versus fraction of polymer initially contained.	151
Fig. 5.1	Comparison of results by expedited swell index (ESI) method and the standard ASTM D5890 swell index (SI) method.	193
Fig. 5.2	Schematic of cell assembly used for testing polyacrylate clogging in compacted (down-gradient) soils.	194
Fig. 5.3	Hydraulic conductivity versus the CaCl_2 concentration of the permeant solution.	195
Fig. 5.4	Surface of BSM 100:1 specimen after permeation with 50 mM CaCl_2 . Arrows denote some of the locations of visible SAP granules. Scale across top of picture is in mm.	196
Fig. 5.5	Expedited swell index of Na-bentonite (Na-B), superabsorbent polymer (SAP), a granular Na-B-SAP mixture, and base-bentonite-SAP composites (BSCs) in the range of CaCl_2 concentrations used as permeants.	197
Fig. 5.6	Hydraulic conductivity of Na-bentonite (Na-B), superabsorbent polymer (SAP), a granular Na-B-SAP mixture, and base-bentonite-SAP composites (BSCs) versus swell index of the materials in corresponding solutions.	198
Fig. 5.7	Hydraulic conductivity at varying permeant CaCl_2 concentrations versus the mass fraction of polyacrylate granularly blended into granular Na-bentonite.	199

Fig. 5.8	Final fractional mass of water-soluble polyacrylate (WSP) in bentonite-WSP specimens relative to initial fractional mass of polymer mixed into specimen. Data are segregated by WSP weight average molecular weight (Mw) and the strength (in mM) of CaCl_2 used as a permeant solution.....	200
Fig. 5.9	Hydraulic conductivity of varying mineral-barrier layers for unmodified and water-soluble-polyacrylate up-gradient (+Poly.) specimens.	201
Fig. 5.10	Conceptual models for hydraulic behavior of granular Na-bentonite (Na-B) and water-soluble polyacrylate (WSP) clogged granular bentonite. The swell of dry granules of Na-B (a) depends on the ionic strength of the hydrating solution, with low swell occurring with 50 mM CaCl_2 and consequently a high hydraulic conductivity (k) (b). Na-bentonite granules hydrated with a dilute solution exhibit low k (c). Clogging of hydraulically active porosity by soluble WSP in within granular Na-B permeated with 50 mM CaCl_2 still yields a low k (d).....	202
Fig. A1	Schematic of pseudo-GCL assembled in flexible wall permeameter.....	204

LIST OF TABLES

Table 3.1	Properties of Na-bentonite (Na-B) used in hydraulic conductivity tests, Na-bentonite used to produce BPN (BB), superabsorbent Na-polyacrylate (SAP), and bentonite-polyacrylate nanocomposite (BPN).....	88
Table 3.2	Soluble cations, bound cation, and cation exchange capacity (CEC) of Na-bentonite (Na-B) used in hydraulic conductivity tests, Na-B used to produce BPN (BB), and bentonite-polyacrylate nanocomposite (BPN).....	89
Table 3.3	Average measured parameters of permeant solutions.....	90
Table 3.4	Swell index and hydraulic conductivity of Na-bentonite (Na-B), superabsorbent Na-polyacrylate (SAP), and bentonite-polyacrylate nanocomposite (BPN) in varying calcium chloride (CaCl_2) solutions, 1 M NaOH, and 1 M HNO_3 . All data are the average of two or more duplicate tests, with the exception of hydraulic conductivities at Colorado State University (CSU) and hydraulic conductivities with 5 mM CaCl_2 at the University of Wisconsin – Madison.....	91
Table 5.1	Properties of Na-bentonite (Na-B), base bentonite (BB), Na-polyacrylate (SAP), BB-SAP mixture (BSM) at a BB-SAP ratio of 100:1, and Na-B-SAP composites (BSC) at Na-B-to-SAP ratios of 100:1 and 1280:1	188
Table 5.2	Cation exchange capacity (CEC) and hydraulic conductivity (k) of soils used in porosity clogging experiments with water-soluble polyacrylate (WSP).	189
Table 5.3	Measured indicator parameters of permeant solutions.	190
Table 5.4	Swell index (SI) or expedited swell index (ESI) and hydraulic conductivity (k) of sodium-bentonite (Na-B), superabsorbent-polymer (SAP), bentonite-SAP mixture (BPM) at a ratio of 100:1, and bentonite-SAP composites (BPC) at ratios of 100:1 and 1280:1.....	191
Table 5.5	Hydraulic conductivity (k) tests performed on polymer clay composites.....	192

CHAPTER ONE

EXECUTIVE SUMMARY

1.1. INTRODUCTION

Sodium bentonites (Na-B) are used in barriers for waste containment because they have low hydraulic conductivity (k) to water (typically $< 10^{-10}$ m/s). The low k of Na-B results from the osmotic adsorption of water molecules around platelets of montmorillonite (MMT) which is the dominant mineral constituent of bentonite. Once adsorbed, osmotically associated water does not participate in flow (McBride 1994). The manifestation of the osmotic adsorption of water is swelling of the immobile phase, and consequently reduced pathways for flow and transport within the mobile phase. However, two factors are requisite for osmotic swelling to occur: monovalent cations (e.g., Na^+) must dominate the MMT exchange complex, i.e., the collection of cations that satisfy the negative structural charge of MMT, and the ionic strength of the hydrating water must be below approximately 0.3 M (Norrish and Quirk 1954).

Unfortunately, many waste containment applications involve leachates with high ionic strengths (e.g., alumina refinery leachates, acid mine drainage) that may retard swell of Na-B and result in high k (Bouazza 2010). Na-B is also thermodynamically unstable in environments where multivalent cations (e.g., Ca^{2+}) are present (Sposito 1989); including most naturally occurring pore waters. When present, multivalent cations replace monovalent cations originally in the exchange complex thereby reducing or eliminating the ability of bentonite to swell osmotically (Kolstad et al. 2004). Because

of the ubiquitous nature of multivalent cations in geoenvironmental applications, in the long term, exchange of multivalent cations for Na^+ should be anticipated.

Recognition of the potential for increases in the k of Na-B has spurred the development of bentonites amended with organic molecules for improved performance in containment applications (e.g., Onikata and Kondo 1996, Trauger and Darlington 2000, Ashmawy et al. 2002, Emidio et al. 2010). Amending bentonites for improved hydraulic behavior has predominantly focused on activating and maintaining osmotic swell through intercalation of an organic molecule (e.g., propylene carbonate or sodium carboxymethyl cellulose) between MMT platelets. Organic molecules are intercalated to increase the range of solutions in which the amended bentonite will osmotically swell as well as, in some cases, impede cation exchange (Onikata and Kondo 2000, Kolstad et al. 2004).

In this study, Na-B was combined with a superabsorbent polymer to both activate and supplement osmotic swell. To this end, Na-B was amended at the nanoscale by in-situ polymerization of acrylic acid to form the superabsorbent polymer polyacrylate (SAP) within the Na-B slurry. Superabsorbent polyacrylate was chosen because SAP is relatively inexpensive, is not readily biodegradable, and is nontoxic (Buchholz and Graham 1998). The resultant material was termed a bentonite-polymer nanocomposite (BPN).

The first objective of this study was to evaluate the k of BPN at chemical equilibrium with a wide variety of permeant solutions emphasizing solutions that typically result in high k of Na-B. Additionally, to discover if the hydraulic behavior of

BPN was indeed superior (i.e., lower k) to BPN's constituent materials, k tests to chemical equilibrium were performed on Na-B and SAP.

The second objective of this study was to evaluate the mechanisms underlying the observed hydraulic behavior of BPN. Understanding the mechanism responsible for the observed behavior is critical to predict hydraulic behavior to leachates outside of those tested in this study and to distill the properties that should be included in future generations of bentonites amended for hydraulic compatibility.

The third objective of this study was to determine if mixing of commercial-grade SAP or non-superabsorbent polyacrylate into Na-B could produce a material with similar properties to BPN. A bentonite-polyacrylate mixture would be far easier to produce (and therefore cheaper) than in-situ polymerized BPN.

1.2 METHODS

BPN was created in the laboratory by dissolving acrylic acid in water followed by neutralization with sodium hydroxide (NaOH). Na-bentonite then was added to the neutralized solution to form bentonite-monomer slurry. Sodium persulfate ($\text{Na}_2\text{S}_2\text{O}_8$) was added as a thermal initiator. Polymerization was commenced by raising the temperature of the slurry above the decomposition temperature of the initiator. After polymerization, the solution was oven dried at 105 °C, and the resulting BPN was milled and screened to the desired gradations.

Hydraulic compatibility tests were conducted on thin layers (< 6 mm dry thickness) of granular BPN, Na-B, and SAP using flexible-wall permeameters. To investigate the impact of ionic strength and divalent cations on the hydraulic behavior of

BPN, 5, 20, 50, 200, and 500 mM CaCl_2 were used as permeant solutions; deionized water (DW) was also used to provide a baseline condition. To investigate the effect of extreme pH, 1 M nitric acid (HNO_3) and 1 M NaOH were used as permeant solutions. Specimens were not prehydrated with a dilute solution to investigate a worst-case condition.

Effluent samples from k tests were collected and analyzed for pH and electrical conductivity using bench-top meters. The water content (ASTM D2216), carbonate content (ASTM D4373), free swell (ASTM D5890), fluid loss (ASTM D5891), exchange complex (ASTM D7503), and polymer percentage of all samples before and after k testing were also determined.

Hydraulic compatibility tests were conducted on mixtures of Na-B with SAP and non-superabsorbent polyacrylate. Physical mixtures were prepared in two ways. The wet mixing method consisted of adding powdered Na-B to solutions containing varying concentrations of SAP in DW. The resultant slurry then was mixed in an end-over-end rotator and subsequently dried at 105 °C. Dry mixing was conducted with granular SAP or non-superabsorbent polyacrylate mixed into granular Na-B with the same gradation. Granular non-superabsorbent polyacrylate also was placed upstream from clean sand, non-plastic silt, low-plasticity silt, and kaolinite to investigate the resulting hydraulic impact.

1.3. MAJOR FINDINGS

This study is presented in four chapters. The first chapter (i.e., Chapter 2), titled “Background: Bentonites Modified with Organic Molecules for Improved Chemical

Compatibility in Hydraulic Barrier Applications,” presents the state-of-art in bentonites modified for hydraulic barrier applications. Amending Na-B for improved compatibility in containment applications has focused on activating and maintaining osmotic swell through intercalation of an organic molecule within the MMT interlayer, such as multi-swelling bentonite, or MSB (Onikata and Kamon 1996, Onikata et al. 2000, Katsumi et al. 2008, Mazzieri et al. 2010) as well as in some cases attempting to “lock” monovalent cations onto the exchange complex with a polymeric molecule, such as dense-prehydrated GCLs, or DPH-GCLs (Flynn et al. 1998, Schroeder et al. 2001, Kolstad et al. 2004, Katsumi et al. 2008). These materials show increased swelling relative to Na-B in dilute solutions, but are still sensitive to ionic strength and exhibit swell indices identical to Na-B in high-ionic-strength solutions. Similar to Na-B, the k of modified bentonites correlates to swell, with improved (lower) k relative to Na-B in a mid-range of ionic strengths (< 200 mM), and similar (high) k to solutions with high ionic strength (> 1000 mM). The exception is DPH-GCLs that maintain a low k irrespective of the ionic strength of the permeant (Kolstad et al. 2004, Katsumi et al. 2008). However, DPH-GCLs rely on both densification and pre-hydration in addition to organic compound additives to achieve a low k , which were shown by Kolstad et al. (2004) as the likely basis for the majority of hydraulic improvement.

The second chapter (i.e., Chapter 3), titled “Long Term Hydraulic Conductivity of a Bentonite-Polyacrylate Nanocomposite Permeated with Aggressive Inorganic Solutions,” presents the k at hydraulic and chemical equilibrium and the swell index of BPN, Na-B, and SAP in aqueous solutions having a range of Ca^{2+} concentrations of 5, 20, 50, 200, 500 mM and extreme pHs (i.e., 0.3 for 1 M HNO_3 and 13.1 M NaOH). For k

testing, thin layers (< 6 mm dry thickness) of granular BPN, Na-B, or SAP were permeated under low-stress conditions in flexible-wall permeameters.

BPN exhibited greater than three-orders-of-magnitude lower k relative to Na-B or SAP with aggressive inorganic solutions (50, 200, and 500 mM CaCl_2 , 1 M NaOH, and 1 M HNO_3), and swelled almost three times more than Na-B in DW. Similar to Na-B, and other modified bentonites, the swell of BPN decreased with increasing CaCl_2 concentration and exhibited a similar swell to Na-B in 500 mM CaCl_2 . Thus, in aggressive inorganic solutions, the k of BPN was decoupled from swelling. During long-term k testing, BPN eluted low-molecular-weight polyacrylate, with a decreasing quantity of polymer eluted with increasing permeant CaCl_2 concentration. Precipitated polymer clogged permeameter tubing during the initial phase of k testing, and required numerous cleaning cycles.

The third chapter (i.e., Chapter 4), titled “Hydraulic Impact of Macropore Sealing in a Bentonite-Polyacrylate Nanocomposite Exposed to Aggressive Inorganic Solutions,” presents an examination of the mechanisms underlying the observed k of BPN in solutions that dramatically reduced swell. The BPN maintained a low k ($< 9 \times 10^{-11}$ m/s) to all dilute solutions (DW, 5, and 20 mM CaCl_2) and all aggressive solutions (50, 200, and 500 mM CaCl_2 , 1 M HNO_3 , and 1 M NaOH) and exhibited superior swelling in dilute solutions due to the addition of SAP. However, similar to Na-B, the swell of BPN decreased with increasing solution concentration, and BPN exhibited swells typical of Ca-bentonite in aggressive solutions. Thus, the mechanism underlying the low k of BPN in aggressive inorganic solutions was decoupled from swell.

Despite low swell and low effective stress (~ 20 kPa), granular BPN was visually observed to form a homogeneous layer in all permeant solutions tested. This matrix was the result of the cohesion of BPN granules by polyacrylate resulting from the consolidation of hydrated granules during permeation that eliminated inter-granular macroporosity that typically conducts flow in high- k bentonite. In addition, BPN initially contained 28.5% polymer (by mass) with at least 75% of that polymer soluble and mobile low-molecular-weight polyacrylate (viz. not SAP). This polymer clogged permeameter tubing as well as the macroporosity of Na-B permeated with 50 mM CaCl_2 . Because of mobile polyacrylate, mixtures of granular BPN with granular Na-bentonite that were permeated with 50 mM CaCl_2 yielded up to 3,900-times reduction in k relative to pure Na-B. Granular BPN additions to granular Na-B as low as 1% (by mass) resulted in an equilibrium k less than pure BPN in 50 mM CaCl_2 . Granular mixing of BPN with Na-B did not consistently result in improvements to k when permeated with 500 mM CaCl_2 until at least 90% (by mass) BPN addition.

The fourth chapter (i.e., Chapter 5), titled “Novel Polymer Additives for Enhanced Performance of Mineral Barrier Layers to Incompatible Permeants,” presents an evaluation of enhancing the hydraulic compatibility of Na-B and other mineral-barrier layers by addition of SAP or non-superabsorbent polyacrylate. To supplement the swelling of Na-B and, thus, enhance the mechanism by which Na-B derives low k , SAP was investigated as an additive. Dry mixing of granular-SAP with Na-B did not result in an improved k relative to pure Na-B or SAP when permeated directly, i.e., without prehydration with a dilute solution, with 50 or 500 mM CaCl_2 ; these solutions result in high k in Na-B. Wet mixing of SAP with Na-B did not result in improved k relative to

pure Na-B or SAP when permeated directly with 500 mM CaCl_2 , but resulted in a modicum of k reduction (up to 2 orders-of-magnitude) when permeated with 50 mM CaCl_2 . In contrast to the traditional methodology of swell enhancement for improved performance, the use of water-soluble polyacrylate to improve performance was investigated by permeation of granular Na-B-PA mixtures with 50 and 500 mM CaCl_2 . The hydraulic impact of polyacrylate on other mineral barrier layers also was examined. When the weight-average molecular weight (M_w) of the polyacrylate additive was less than 1,080,000 g/mol, mass-percentage additions as low as 0.75% resulted in greater than three-orders-of-magnitude reduction in the k to 50 mM CaCl_2 . Conversely, granular mixing of PA did not improve k to 500 mM CaCl_2 . Polyacrylate with a M_w of 255,000 g/mol added upgradient to kaolinite also reduced the k of the composite system by three orders-of-magnitude when permeated with 500 mM CaCl_2 , but did not impact the k of clean sand, non-plastic silt, or low-plasticity silt.

1.4. REFERENCES

- Ashmawy, A. K., Darwish, E.H., Sotelo, N., and Muhammad, N. (2002). "Hydraulic performance of untreated and polymer-treated bentonite in inorganic landfill leachates." *Clays and Clay Minerals*, 50(5), 546-552.
- Bouazza, A. (2010). "Geosynthetics lining in mining applications." *Proceedings of Sixth International Conference on Environmental Geotechnics*, International Society for Soil Mechanics and Geotechnical Engineers, New Delhi, India, 221-259.
- Buchholz, F., Graham, A. 1998. *Modern Superabsorbent Polymer Technology*, John Wiley and Sons, New York.
- Di Emidio, G., Van Impe, W., Mazzieri, F. (2010). "A polymer enhanced clay for impermeable geosynthetic clay liners." *Proceedings of Sixth International Conference on Environmental Geotechnics*, International Society for Soil Mechanics and Geotechnical Engineers, New Delhi, India, 963-967.
- Flynn, B., Carter, G. (1998). "Waterproofing material and method of fabrication thereof." *US Patent Number: 6,537,676 B1*.
- Katsumi, T., Ishimori, H, Onikata, M., and Fukagawa, R. (2008). "Long-term barrier performance of modified bentonite materials against sodium and calcium permeant solutions." *Geotextiles and Geomembranes*, 26(1), 14-30.
- Kolstad, D., Benson, C., and Edil, T. (2004). "Hydraulic conductivity and swell of nonprehydrated GCLs permeated with multi-species inorganic solutions." *J. of Geotech. and Geoenviron. Engr.*, 130(12), 1236-1249.

- Mazzieri, F., Di Emidio, G., and Van Impe, P. (2010). "Diffusion of calcium chloride in a modified bentonite: Impact on osmotic efficiency and hydraulic conductivity." *Clays and Clay Minerals*, 58(3), 351-363.
- McBride M. (1994). *Environmental Chemistry of Soils*. Oxford University Press, New York.
- Norrish, K., and Quirk, J. (1954). Crystalline swelling of montmorillonite, use of electrolytes to control swelling, *Nature*, 173, 255-257.
- Onikata, M., Kondo, M., and Kamon, M. (1996). "Development and characterization of a multishrinkable bentonite." *Environmental Geotechnics*. Taylor and Francis, Rotterdam, 587-590.
- Onikata, M., Kondo, M., Hayashi, N., and Yamanaka, S. (2000). "Complex formation of cation-exchanged montmorillonites with propylene carbonate: osmotic swelling in aqueous electrolyte solutions." *Clays and Clay Minerals*, 47(5), 672-677.
- Schroeder, C., Monjoie, A., Illing, P., Dosquet, D., and Thorez, J. (2001). "Testing a factory-prehydrated GCL under several conditions." *Proceedings, Sardinia 2001, 8th International Waste Management and Landfill Symposium*, CISA Environmental Sanitary Engineering Centre, Cagliari, Italy, 187-196.
- Sposito, G. (1984). *The Surface Chemistry of Soils*, Oxford University Press, New York.
- Trauger R. and Darlington J. (2000). "Next-generation geosynthetic clay liners for improved durability and performance." *TR-220*. Colloid Environmental Technologies Company, Arlington Heights, 2-14.

CHAPTER TWO

BACKGROUND: BENTONITES MODIFIED WITH ORGANIC MOLECULES FOR IMPROVED CHEMICAL COMPATIBILITY IN HYDRAULIC BARRIER APPLICATIONS

2.1. INTRODUCTION

Sodium (Na) bentonite (Na-B) is used extensively to control flow and contaminant transport because Na-B has low hydraulic conductivity (k) to water. Within bentonite, montmorillonite (MMT), a member of the smectite group of clay minerals (Grim 1968), governs hydraulic behavior. The effectiveness of MMT as a barrier for waste containment depends on the osmotic adsorption of water molecules between MMT layers (McBride 1994) that is manifest as swelling of the immobile phase, reducing the size and increasing the tortuosity of the hydraulically active pores that conduct flow and transport. Osmotic swelling only occurs when monovalent cations, such as Na^+ , dominate the exchange complex (i.e., the collection of cations satisfying the negative structural charge of MMT) (McBride 1994). If multivalent cations dominate the exchange complex, osmotic swelling of MMT does not occur, resulting in much higher k (Shackelford et al. 2000, Jo et al. 2001, 2005, Kolstad et al. 2004, Katsumi et al. 2008). Unfortunately, waste liquids with high ionic strengths and multivalent cations are commonplace in modern environmental containment applications. Sodium satisfying the exchange complex of MMT is also thermodynamically unstable in environments where multivalent cations (e.g., calcium, Ca^{2+}) are present (Sposito 1989) including most naturally occurring pore waters and most leachates. When present, multivalent cations replace monovalent cations originally comprising the exchange complex,

thereby reducing or eliminating osmotic swell and the ability of the bentonite to function as a hydraulic barrier (Vasko et al. 2001, Kolstad et al. 2004, Lee and Shackelford 2005). Solutions with high ionic strength, even from monovalent solutions, also limit or eliminate osmotic swell (McBride 1994).

A common application of Na-B in environmental containment systems is within a geosynthetic clay liner (GCL). A GCL is comprised of a thin layer (≈ 0.7 mm) of Na-bentonite sandwiched between two carrier layers (typically thin geotextiles). Because GCLs contain a barrier layer of Na-B, GCLs exhibit hydraulic conductivities (k) $< 2\text{--}3 \times 10^{-10}$ m/s in dilute solutions at low effective stresses (< 30 kPa), and typically exhibit k on the order of 10^{-11} m/s in deionized water (DW). Unfortunately, because the hydraulic barrier component of GCLs is Na-B, and the osmotic swell of Na-B is sensitive to ionic strength and cation exchange, the range of leachate chemistries that can be contained by GCLs are limited.

Fig. 2.1 shows the relationship between GCL k and the ionic strength of the permeant liquid for tests conducted at effective stresses < 30 kPa, and with leachates of circumneutral pH. At ionic strengths below 60 mM, GCLs exhibit $k < 2\text{--}3 \times 10^{-10}$ m/s, i.e., the upper limit of k for GCLs permeated with dilute solutions. Between 60 mM and 400 mM, GCLs exhibit both low ($< 2\text{--}3 \times 10^{-10}$ m/s) and high k depending on: The fraction of MMT in the bentonite, the fraction of the MMT exchange complex satisfied by Na^+ , the bentonite granule size, and pre-permeation hydration in a dilute solution. Above 400 mM, GCLs exhibit $k > \sim 10^{-9}$ m/s, and up to 10^{-6} m/s. These data illustrate that the range of leachate chemistries that can be contained by GCLs are limited. The data presented

in Fig. 2.1 also show that di- and tri- valent homoionic permeants represent a worst-case condition relative to monovalent or blended-valence solutions.

For GCLs, swelling of the bentonite component is quantified by the free swell index (SI) test (ASTM D5890) which is used as an indicator parameter for both k and bentonite quality. Swell index tests consist of adding 2.00 g of bentonite ground to pass the No. 200-US-Standard Sieve (ASTM E11) into a 100-mL graduated cylinder of DW (or other solution) filled to 90 mL. Bentonite is dusted over the surface of the water column in increments of no more than 0.1 g over a period of 30 s. Each increment is allowed to hydrate for at least 10 min prior to addition of the next increment. At the conclusion of bentonite addition, the graduated cylinder is filled to 100 mL and the bentonite is allowed to continue hydrating for 16 h, at which time, the volume (swell) of the bentonite at the bottom of the graduated cylinder is recorded in mL of swell per 2.00 g of bentonite solids.

Fig. 2.2 shows the relationship between GCL k and SI with corresponding solutions. A SI > 20 mL/2 g generally correlates to a low k , < $2\text{-}3 \times 10^{-10}$ m/s, while SI below 20 mL/2 g corresponds to a 5 order-of-magnitude range of k . The variation in k at SI < 20 mL/2 g results from factors including: the MMT fraction in the bentonite, the fraction of the MMT exchange complex satisfied by Na^+ , the bentonite granule size, and pre-permeation hydration in a dilute solution.

In addition to reductions in swell associated with ionic strength effects, numerous laboratory studies on GCLs have shown that Ca^{2+} -for- Na^+ exchange results in reduced swelling capacity and ultimately to decreased hydraulic performance (Lin and Benson

2000, Jo et al. 2001, 2005, Eggloffstein 2001, Shackelford and Lee 2003, Kolstad et al. 2004, Lee and Shackelford 2005). Field studies have confirmed that GCLs placed in contact with soils will undergo Ca^{2+} -for- Na^{+} exchange (ATU 1992, James et al. 1997, Benson et al. 2004, 2007, Meer and Benson 2007, Scalia and Benson 2011). The Ca^{2+} is derived from surrounding soils, and migrates into the GCL in response to hydraulic (pressure or suction) and/or chemical gradients (Meer and Benson 2007, Bradshaw et al. 2012). Even GCLs installed in the field with an overlying geomembrane (GM) to protect from the downward percolation of pore water have been shown to undergo Ca^{2+} for Na^{+} exchange (Meer and Benson 2007, Scalia and Benson 2011), deriving Ca^{2+} from the underlying pore water and dissolution of constituent calcite (CaCO_3) (Guyonnet et al., 2005). Calcite is frequently reported as an accessory mineral in natural Na-B (Shackelford et al. 2000, Kolsad et al. 2004, Jo et al. 2004, Guyonnet et al. 2005). Irrespective of the specific source (leachate, soil porewater, or native calcite) exchange of Ca^{2+} (or other divalent ions) for Na^{+} should be anticipated in the long term.

Recognition of the sensitivity of Na-B to adverse chemical interactions in hydraulic-barrier applications has spurred the development of bentonites amended for compatibility (BACs) in hydraulic barrier applications (Kondo 1996, Onikata and Kondo 1996, Flynn et al. 1998, Onikata et al. 1999, Onikata et al. 2000, Trauger and Darlington 2000, Katsumi et al. 2001, Schroeder et al. 2001, Ashmawy et al. 2002, Kolstad et al. 2004, Katsumi et al. 2008, Di Emidio 2010, Di Emidio et al. 2010, Mazzieri et al. 2010a, Mazzieri et al. 2010b, Di Emidio et al. 2011, Mazzieri 2011, Scalia et al. 2011). BACs are engineered to minimize transport processes by maintaining low k , membrane

behavior, and sealing ability in solutions typically incompatible with Na-B, such as high ionic strength and multivalent cation laden solutions.

Amending bentonite for improved compatibility in barrier applications has focused on activating and maintaining osmotic swell through the intercalation of an organic molecule within the MMT interlayer, such as in multi-swellable bentonite, MSB, and HYPER-clay, HC, (Onikata and Kamon 1996, Onikata et al. 1999, Onikata et al. 2000, Katsumi et al. 2001, Katsumi et al. 2008, Mazzieri et al. 2010a, Mazzieri et al. 2010b, Di Emidio 2010, Di Emidio et al. 2010) as well as in some cases attempting to “lock” monovalent cations onto the exchange complex with a polymeric molecule, such as in dense-prehydrated GCLs, DPH-GCLs (Flynn et al. 1998, Schroeder et al. 2001, Kolstad et al. 2004, Katsumi et al. 2008). Additionally, Trauger and Darlington (2000) developed a BAC that was intended to incorporate the aforementioned improvements and also add additional swelling with a superabsorbent polymer. Trauger and Darlington (2000) termed this material bentonite-polymer alloy (BPA). There has also been laboratory investigation of “contaminant-resistant clays” (CRCs) of proprietary composition (Shan and Daniel 1991, Ruhl and Daniel 1997, Vasko et al. 2001).

This chapter examines the materials, mechanisms, and in-lab performance of BACs. This chapter provides an overview of the state-of-art in BAC research.

2.2. MATERIALS IN THE LITERATURE

2.2.1. Multi-Swellable Bentonite (MSB)

Dry Na-Bs amended by mixing with 15-45% propylene carbonate (PC) solution (by mass) are termed multi-swellable bentonites (MSBs) (Kondo 1996, Onikata et al. 1996). The resultant materials are then dried at 105°C and ground. To improve compatibility, MSB relies on PC to activate osmotic swell (Kondo 1996, Onikata and Kamon 1996, Onikata et al. 1999, 2000)

2.2.2. HYPER-Clay (HC)

Dry bentonite amended by mixing with a solution containing 2% Na-carboxymethylcellulose (Na-CMC) (by mass) is termed HYPER-clay (HC) (Di Emidio 2010, Di Emidio et al. 2010, 2011). The resultant HC was then oven dried at 105°C and ground with a Resch Mortar Grinder RM 200. HC relies on Na-CMC to activate osmotic swell (Di Emidio 2010, Di Emidio et al. 2010, 2011).

2.2.3. Dense-Prehydrated GCLs (DPH-GCLs)

GCLs uniformly prehydrated to a water content of ~43% using a dilute aqueous solution containing Na-CMC and methanol followed by subsequent densification by calendaring are termed dense-prehydrated GCLs (DPH-GCLs) (Kolstad et al. 2004). To maintain a low k to typically incompatible solutions, DPH-GCLs rely on osmotic swell activation by intercalated Na-CMC and two established mechanisms that improve the performance of un-amended Na-B: prehydration with a dilute solution (Shan and Daniel 1991, Ruhl and Daniel 1997, Vasko et al. 2001) and densification (Shackelford et al. 2000, Jo et al. 2001). Kolstad et al. (2004) also hypothesized that Na-CMC could bond

to Na^+ ions in the interlayer (i.e., lock the native- Na^+ ions satisfying the CEC), thereby minimizing or eliminating cation exchange.

2.2.4. Contaminant-Resistant Clay (CRC)

Several GCL manufacturers sell products dosed with proprietary additives purported to improve bentonite performance upon exposure to contaminants (Ruhl and Daniel 1997 Kajita 1997, Ashmawy et al. 2002). Names for these products include contaminant-resistant clay (CRC) or polymer-treated bentonite. As CRCs are proprietary, no further information on their manufacture is available. Ashmawy et al. (2002) postulated that treatment with a cationic polymer could result in the polyelectrolyte replacing the native Na^+ or Ca^{2+} ions, and because of the high free-energy required for polyelectrolyte desorption, render the polymer un-exchangeable (this concept is discussed in greater detail in the “Locking of Bound Cations” section. Alternatively, Ashmawy et al. (2002) postulated that a cationic polymer could rely on a dipole attraction with the native Na^+ ions satisfying the CEC and effectively coat the Na-MMT in polymer. This polymer coating would then prevent exchange of the native- Na^+ ions.

2.2.5. Bentonite-Polymer Alloy (BPA)

Bentonite amended by in-situ polymerization of an organic monomer within a Na-B slurry to form a bentonite-superabsorbent-polymer composite was termed bentonite-polymer alloy (BPA) by Trauger and Darlington (2000). Trauger and Darlington (2000) did not provide the formulation of BPA, nor the specific superabsorbent polymer used. The addition of superabsorbent polymer was hypothesized by Trauger and Darlington

(2000) to improve contaminant resistance by structural reinforcement of the interlayer by intercalated polymer, locking of native Na^+ ions satisfying the CEC by polyelectrolyte adsorption, and supplemented swell via the absorption of water by superabsorbent polymer.

2.3. MECHANISMS FOR IMPROVED COMPATIBILITY

2.3.1. Intercalation and Activation of Osmotic Swell

To activate osmotic swelling in solutions that typically preclude such behavior, Onikata and Kondo (1996) intercalated a high polarity aprotic solvent, PC, within MMT to form MSB. Low angle X-ray diffraction (XRD) on MSB showed increased d001 spacing, illustrating one-or-two layers of intercalated PC. When PC-bentonite composites were produced with bentonites with exchange dominated by weakly polarizing cations (such as Na^+), a d001 spacing of 1.4 nm was exhibited corresponding to a monolayer of intercalated PC. Onikata et al. (1999) and Onikata et al. (2000) used Fourier-transform-infrared (FTIR) spectroscopy and thermo-gravimetric analysis (TGA) to ascertain that PC coordinates to interlayer cations through the hydration shells of these cations.

Intercalated PC increased MMT swell by expanding the space between adjacent MMT platelets, and activating osmotic swell in NaCl solutions up to 750 mM, (Onikata et al. 1999) which is ~450 mM stronger than the maximum strength which osmotic swell will occur in Na-B (~300 mM) (Norrish and Quirk 1954). The electrostatics of the activation of osmotic swell by PC is described in Onikata et al. (1999). In NaCl solutions

with ionic strengths in excess of 0.75 M, osmotic swell is not activated and only crystalline swell is manifest (Onikata et al. 1999).

Di Emidio et al. (2010) amended Na-B with 2-4% Na-CMC and termed the resultant mixture HC. Similarly, Schroeder et al. (2001) describes Na-B within a GCL prehydrated with a dilute solution containing Na-CMC and then densified to form a DPH-GCL. In both HC and DPH-GCLs, Na-CMC was shown by XRD to be intercalated, and was hypothesized to act as an osmotic-swell activator similar to PC (Schroeder et al. 2001, Kolstad et al. 2004, Katsumi et al. 2008, Di Emidio et al. 2010).

Intercalation of high-molecular-weight polymers is difficult to accomplish through physical mixing (Theng 1970). Thus, to insure intercalation of a high-molecular-weight polymer, Trauger and Darlington (2000) polymerized an organic monomer in bentonite slurry. The material developed by Trauger and Darlington (2000) was termed BPA. XRD on dried BPA showed an increase in the inter-platelet opening from 0.35 nm to from 1.0 to 1.5 nm indicating that polymer was intercalated in the bentonite interlayer. In addition to physically increasing the space between platelets in the dry state, the anionic polymer was hypothesized to activate osmotic swell (Trauger and Darlington 2000).

2.3.2. Locking of Bound Cations

Polyelectrolyte additives such as Na-CMC and the superabsorbent polymer produced by Trauger and Darlington (2000) have many functional groups that can potentially be adsorbed. Generally, the extent of adsorption is directly related to the molecular weight of the polymer and the number and type of functional groups (Stumm

1992, Stumm and Morgan 1996). Because many segments of a single polymer molecule can be in contact with a surface simultaneously, a low bonding energy for each individual bond is still capable of rendering the total adsorption effectively irreversible because of the high energy required to simultaneously desorb the entire molecule (Lyklema 1985, Stumm 1992, Stumm and Morgan 1996). Thermodynamically, desorbing a polyelectrolyte molecule is possible, but the equilibrium lies far to the sorbed state (Lyklema 1985).

Deng et al. (2006) used FTIR spectroscopy to probe the bonds involved in adsorption of an anionic polyelectrolyte to MMT. Based on experimental results, Deng et al. (2006) postulated that the mechanism for polyelectrolyte adsorption to MMT basal surfaces was through exchangeable cation bridging (ECB). In ECB, the anionic polyelectrolyte associates with the cations satisfying the CEC of the MMT. Thus, MMT amended with an intercalated anionic-polyelectrolyte should be more thermodynamically stable to aggressive leachates because the simultaneous association of the polyelectrolyte with numerous bound cations should effectively “lock” the bound cations in place, thereby reducing or eliminating cation exchange.

Flynn et al. (1998) stated that the addition of 8-16% Na-polyacrylate (Na-PA) in addition to Na-CMC should inhibit ion exchange and render the CEC of a DPH-GCL “nil or very low,” but did not verify this assertion experimentally. Because Na-CMC is a polymeric material, Di Emidio et al. (2010) hypothesized that this mechanism may also improve the stability of DPH-GCLs to incompatible solutions irrespective of treatment with Na-PA. The CEC of bentonite removed from a DPH-GCL is not reported in the

literature. However, Schroeder et al. (2001) reported that after drying and re-wetting the additives in a DPH-GCL were “extracted”, illustrating that the Na-CMC may not be immobile within a DPH-GCL. Correspondingly, Mazzieri (2011) showed that cycles of permeation, drying, and re-wetting resulted in removal of the Na-CMC initially contained within a DPH-GCL. Polymeric locking of Na^+ cations originally contained within BPA was similarly hypothesized by Trauger and Darlington (2000), but not proven experimentally.

2.3.3. Independently Swelling Additives

Trauger and Darlington (2000) amended Na-B with a super absorbent polymer in part to supplement swell in a wide range of chemical environments. However, the water absorptive capacity of superabsorbent polymers is highly sensitive to ionic strength (Buchholz and Graham 1998). Thus, while a bentonite amended with a superabsorbent polymer may demonstrate a very high swelling capacity in dilute solutions, the polymer amendment may provide minimal supplementary swelling in solutions that are typically incompatible with bentonite.

2.4. EXPERIMENTAL RESULTS

2.4.1. MSB

Preliminary swelling tests on MSB in DW conducted by Onikata and Kamon (1996) showed similar behavior between MSB (20.0 mL/2 g) and Na-B (24.0 mL/2 g). But, when freely swollen in artificial sea water, MSB swelled more than three-times Na-B (32.0 versus 9.0 mL/2 g) (Onikata and Kamon 1996). Initial comparative-*k* testing

with artificial sea water by Onikata and Kamon (1996) showed approximately two-orders-of-magnitude lower k in MSB-sand mixtures than Na-B-sand mixtures with the same constituent proportions.

Katsumi et al. (2008) investigated the swell index and long-term k of MSB and Na-B. The MSB studied by Katsumi et al. (2008) was 25% PC (by mass). Data from swell index tests at varying CaCl_2 concentrations conducted by Katsumi et al. (2008) are shown in Fig. 2.3, with tests in DW plotted at 0.001 M CaCl_2 . In CaCl_2 solutions, both MSB and Na-B exhibited similar systematic decreases in swell with increased concentration. At CaCl_2 concentrations ≥ 500 mM both materials exhibited swell indices typical of Ca-bentonite. Similar behavior was shown by Lin et al. (2000), and is presented in Fig. 2.3. Overall, in CaCl_2 concentrations in excess of 300 mM the swelling behavior of MSB is indistinguishable from Na-B. These data illustrate that the osmotic-swell-activation mechanism proposed by Onikata et al. (1999) is mitigated at CaCl_2 concentrations > 300 mM. In homoionic monovalent solutions, MSB exhibits an elevated swell relative to Na-B (Fig. 2.3), but the swell is still sensitive to concentration.

Hydraulic conductivities of MSB with permeants containing varying CaCl_2 concentrations are shown in Fig. 2.4. Data for Na-B also are shown in Fig. 2.4 for comparison. Tests conducted with DW are plotted at 0.001 M CaCl_2 . Katsumi et al. (2008) conducted k tests on MSB for up to 7 yr to ensure the establishment of chemical equilibrium. Similarly, Lin et al. (2000) ran k tests on MSB to chemical equilibrium defined by electrical conductivity. Permeation with DW resulted in similar k irrespective of the material tested (MSB or Na-B) ($\approx 1.0 \times 10^{-11}$ m/s). Katsumi et al. (2008) found that

MSB permeated with CaCl_2 solutions with molar concentrations ≤ 1000 mM, maintained k within the same order-of-magnitude as to DW. For example, when permeated with 1000 mM CaCl_2 , the k of MSB was 6.5×10^{-11} m/s. However, the k of MSB permeated by Lin et al. (2000) increased with the permeant CaCl_2 concentration, such that a k of 6.5×10^{-9} m/s was reported with 500 mM CaCl_2 . The correlation of MSB k to CaCl_2 concentration reported by Lin et al. (2000) is similar to Na-B; however, MSB is less hydraulically sensitive to increased CaCl_2 concentration in the permeant solution (Fig. 2.4). Katsumi et al. (2008) did not observe a large increase in the k of MSB with increasing permeant CaCl_2 concentrations, but observed similar (high) k to that of Na-B ($2\text{-}3 \times 10^{-7}$ m/s) with a 2000 mM NaCl permeant. The findings of Lin et al. (2000) and Katsumi et al. (2008) illustrate that the k of MSB is less sensitive to divalent-cations and ionic strength effects than unamended Na-B, but is not immune to increases in k .

The k of MSB is presented versus SI in Fig. 2.5. For comparison, a model between k and SI developed by Katsumi et al. (2008) as well as data for Na-B from the literature are included in Fig. 5. Similar to Na-B, the k of MSB is inversely related to SI. But, the k of MSB is somewhat less sensitive to SI than Na-B. For example, MSB still exhibits a low k (6.5×10^{-11} m/s) with corresponding SI as low as 9.2 mL/2 g. Thus the SI cusp corollary to dramatic increases in k reported in the literature (typically $\approx 18\text{-}20$ mL/2 g for Na-B) (Jo et al. 2001, Kolstad et al. 2004) is perhaps lower for MSB.

Mazzieri et al. (2010) investigated the diffusion and chemico-osmotic behavior of MSB with a 5 mM CaCl_2 solution. A 4.5 kg/m^2 (dry mass per area) layer of MSB, composed of 20% PC, by mass, was spread in the testing apparatus and allowed to

freely swell to a height of ~10 mm. The MSB specimen was then consolidated to a thickness of 7.4 mm and permeated with DW to remove soluble salts (i.e., the sample was prehydrated and pre-consolidated prior to testing, similar to a DPH-GCL). In the flushing phase, MSB equilibrated to a k of 1.1×10^{-11} m/s, typical of Na-B. During subsequent membrane behavior testing, Mazzieri et al. (2010) observed a total loss of osmotic potential after approximately 22 days in concert with Ca^{2+} -for- Na^{+} exchange. The data presented by Mazzieri et al. (2010) suggest that prehydration of MSB does not prevent ion exchange, or the loss of osmotic swelling potential associated with divalent-for-monovalent cation exchange (Shackelford and Lee 2003). Moreover, these results are similar to unamended Na-B tested by Shackelford and Lee (2003). After the termination of membrane behavior testing, Mazzieri et al. (2010) showed that the SI of the tested MSB was reduced to 11 mL/2g, from 23 mL/2 g initially.

2.4.2. HC

The SI of HC containing 4% CMC (by mass) measured by Di Emidio et al. (2010) is shown versus CaCl_2 concentration in Fig. 2.3. Similar to MSB, HC swelling was sensitive to CaCl_2 concentration, with SI identical to the base Na-B exhibited at CaCl_2 concentrations ≥ 100 mM. Di Emidio et al. (2010) also determined the k of HC and Na-B in DW, seawater, and 5 mM CaCl_2 . In DW, both HC and Na-B had similar k (6×10^{-12} m/s), but in seawater, HC exhibited a k approximately-two-times lower than the base Na-B (1.5×10^{-11} m/s versus 2.7×10^{-11} m/s). Similarly, with 5 mM CaCl_2 the k of HC was two-times lower than the base Na-B (1.5×10^{-11} m/s versus 3.0×10^{-11} m/s). These tests were only run for approximately 80 days, and the state of chemical equilibrium at test termination was not reported. Di Emidio et al. (2010) also determined that the CEC of

the base Na-B and HC to be similar (~ 44 cmol+/kg), illustrating that CMC did not prevent the removal of the initially bound cations by ammonium acetate ($\text{C}_2\text{H}_3\text{O}_2\text{NH}_4$) during exchange complex testing.

2.4.3. DPH-GCLs

Kolstad et al. (2004) investigated the k and swell index of a DPH-GCL prepared by pre-hydrating a 6.0 kg/m^2 unamended Na-bentonite GCL (T-GCL) to a gravimetric water content of 43% with a dilute solution of Na-CMC and methanol. The DPH-GCL was then calendared to a uniform thickness of 5 mm. The performance of the DPH-GCL was compared to a T-GCL with a dry mass per unit area of 4.3 kg/m^2 . Fig. 2.3 includes the SI of bentonite removed from the DPH-GCL in DW and 1 M CaCl_2 . Similar SI in DW ($\approx 35 \text{ mL/2 g}$) was observed for both materials. The free swell of material removed from both the DPH-GCL and Na-B likewise decreased in solutions known to cause dramatic increases in the k of T-GCLs (1 M NaCl, 1 M CaCl_2 , and HCl with $\text{pH} = 1.2$).

Kolstad et al. (2004) measured the k of a DPH-GCL to be $1.0 \times 10^{-12} \text{ m/s}$ for DW, 1 M NaCl, 1 M CaCl_2 , and $1.6 \times 10^{-10} \text{ m/s}$ for HCl with a $\text{pH} = 1.2$. In contrast, the k of the T-GCL was $1 \times 10^{-7} \text{ m/s}$ for all permeants except DW ($k = 1.2 \times 10^{-11} \text{ m/s}$). These results indicate a decoupling between k and SI in DPH-GCLs. However, the SI test does not measure the prehydrated DPH-GCL as permeated; during k testing, the DPH-GCL is not dried or ground prior to swelling. Kolstad et al. (2004) concluded that SI tests appeared to eliminate the benefits of prehydration, and therefore are not a valid index

test for DPH-GCLs. Swell index tests are also not representative of the reduced porosity in DPH-GCLs achieved through densification.

Katsumi et al. (2008) comparatively investigated the long-term k of a DPH-GCL, Na-B, T-GCL, and MSB. Results obtained with DW (plotted at 0.001 M) and CaCl_2 solutions are shown in Fig. 2.4. When permeated with DW, Na-B and the T-GCL had similar k , approximately 1.0×10^{-11} m/s, and the DPH-GCL had a one-order-of-magnitude lower k , at approximately 1.0×10^{-12} m/s. When permeated with solutions of NaCl and CaCl_2 with concentrations ≤ 1000 mM the DPH-GCL maintained a k similar to DW. For example, when permeated with 1000 mM CaCl_2 the k of the DPH-GCL was $1.6\text{--}1.8 \times 10^{-12}$ m/s. Because of the low k of DPH-GCLs, Katsumi et al. (2008) did not reach chemical equilibrium prior to termination of these tests. Thus, while DPH-GCLs exhibit superior k to aggressive solutions, the longevity of this low k is unknown. To the author's knowledge, no data exists in the literature for a DPH-GCL permeated to chemical equilibrium.

Mazzieri (2011) investigated the impact of desiccation on the k of DPH-GCL specimens permeated with DW and 0.0125 M CaCl_2 solutions. DPH-GCL specimens were hydrated to swelling equilibrium in odometers followed by drying to gravimetric water contents of 5-10%. The specimens were then permeated with the original hydrating solution (DW or 0.0125 M CaCl_2). After three desiccation-permeation-cycles, the k of a DPH-GCL with 0.0125 M CaCl_2 increased 62,500 fold (8.8×10^{-12} m/s to 5.5×10^{-7} m/s), similar to results reported by Lin and Benson (2000) and Benson and Meer (2009) for unamended Na-B. After desiccation cycle testing, SI of bentonite

removed from DPH-GCL specimens tested with DW showed an increase from the original 16 mL/2 g to 28 mL/2 g. Moreover, the turbidity of solution above the settled bentonite layer was greatly reduced after desiccation-cycle testing and visually appeared similar to the hydrating solution in SI testing with unamended Na-B. DPH-GCL specimens tested with 0.0125 M CaCl_2 exhibited a SI of 9 mL/2 g, typical of Ca-bentonite, and illustrating that the bentonite within the DPH-GCL specimen had undergone extensive exchange of Ca^{2+} for native Na^+ . From these results, Mazzieri (2011) concluded that the additives to a DPH-GCL were removed as a result of desiccation-permeation cycling.

2.4.4. CRCs

Ashmawy et al. (2002) investigated the k of three CRCs via permeation with ash-landfill leachates containing varying concentrations of Ca^{2+} and Mg^{2+} . Testing by Ashmawy et al. (2002) did not include a chemical equilibrium termination criterion. The CRCs tested were of commercial origin and proprietary in composition. These clays are touted to minimize increases in bentonite k upon exposure to contaminants. CRCs only partially performed as advertised, exhibiting k two-to-three orders-of-magnitude higher to aggressive ash landfill leachate relative to DW (Fig. 2.4), but approximately one-order-of-magnitude lower than a T-GCL. CRCs had lower SI compared to a T-GCL from the same manufacturer.

2.4.5. BPA

Trauger and Darlington (2000) developed and tested BPA deposited into a needle-punched non-woven geotextile (GT). The resultant material was then dried, and

subsequently permeated with seawater. The k of the BPA-GT was 4,000-times lower than a T-GCL (5×10^{-12} m/s versus 2×10^{-8} m/s). Because of the incorporation of BPA onto the GT, measurement of SI on the resultant material were not feasible; however, Trauger and Darlington (2000) reported that a BPA-GT was capable of hydration to a water content 10-to-15 times greater than a T-GCL. The high water absorptive capacity of BPA was likely the result of the added superabsorbent polymer, which is capable of water absorption far in excess of Na-B (Buchholz and Graham 1996).

2.5. MECHANISTIC ANALYSIS OF COMPILED RESULTS

Scant experimental results exist that focus on the locking of cations by intercalated polyelectrolytes, such as Na-CMC or the superabsorbent polymer used by Trauger and Darlington (2000). Schroeder et al. (2001) showed that after drying, additives to a DPH-GCL were extracted upon re-wetting; illustrating that Na-CMC is not locked within the bentonite matrix. Additionally, by the ammonium acetate method Mazzieri (2011) determined the CEC of bentonite removed from a DPH-GCL to be within the range typical for GCL bentonite (viz. the polymer did not impede cation exchange by ammonium, NH_4^+ , ions). These results are collaborated by the ability to measure the CEC of bentonite amended with 2% or 4% Na-CMC by Di Emidio et al. (2010). To the author's knowledge, no data exists for a BAC in which the cations of a bentonite-composite are locked in place, and no CEC, or a greatly reduced CEC, is exhibited.

Data showing relationship between SI and CaCl_2 concentration of the hydrating solution are depicted in Fig. 2.3. Irrespective of the additive, the swell of BACs is inversely related to CaCl_2 concentration. Intercalation of organic additives in the clay interlayer has been shown via XRD to occur with PC, Na-CMC, and the superabsorbent polymer used by Trauger and Darlington (2000) (Onikata et al. 1999, Schroeder et al. 2001, Kolstad et al. 2004, Katsumi et al. 2008, Di Emidio 2010, Di Emidio et al. 2010). Thus, intercalation of organic molecules, while measurable at the nanoscale, does not prevent reduction in swell in aggressive inorganic solutions as measured by SI tests.

Data illustrating the impact of CaCl_2 concentration on k are summarized in Fig. 2.4. Both Na-B and MSB show increased k with increasing CaCl_2 concentration, although MSB is considerably less sensitive. In contrast, DPH-GCLs show a slightly inverse relationship between k and CaCl_2 concentration, with the lowest observed k concurrent to the strongest solution tested.

Based on the observed decoupling of k and SI in DPH-GCLs, Kolstad et al. (2004) attempted to quantify the relative contributions towards maintaining a low k from prehydration and densification of DPH-GCLs. To assess the reduction in k resultant from prehydration, a T-GCL was permeated with DW for 5.5 pore volumes of flow prior to permeation with 1 M CaCl_2 for 20 pore volumes of flow. Prehydration resulted in a final k with 1000 mM CaCl_2 of 1.0×10^{-10} m/s, which was 8,100-times lower than the k obtained without prehydration (8.1×10^{-7} m/s), but 27 times higher than the k of the DPH-GCL with the same solution (3.7×10^{-12} m/s). To evaluate the reduction in k from densification, a T-GCL was permeated with 1000 mM CaCl_2 at an elevated effective

stress (420 kPa) to achieve T-GCL porosity equal to the porosity of a DPH-GCL (1.84). Densification resulted in a k of 4.1×10^{-9} m/s, which was 8.9 times lower than the k of a T-GCL in the same solution (4.0×10^{-8} m/s). Assuming reductions in k are independent and multiplicative Kolstad et al. (2004) calculated a 79,400-fold reduction in the k from simultaneous densification and prehydration. Applying this reduction factor to the k of a T-GCL with 1000 mM CaCl_2 yielded a calculated k of 1.0×10^{-11} m/s, which is approximately three-times higher than the k obtained for the DPH-GCL in the same solution. The lower k of the DPH-GCL was hypothesized by Kolstad et al. (2004) to be a result of intercalated Na-CMC, differences in montmorillonite content, or synergistic effects of prehydration and densification. Overall, these findings illustrate that intercalated Na-CMC was not the dominant factor underlying the low k of DPH-GCLs.

The correlation between swell index and k is shown in Fig. 2.5. The k of both Na-B and MSB are corollary to SI. These data illustrate the mechanism underlying k of MSB is correlated to swell, and that a SI test is a possible indicator parameter for the k of MSB. Because of osmotic swell activation, the range of SI corollary to k in the 10^{-11} m/s order-of-magnitude extended lower for MSB than for natural Na-B. The k of DPH-GCLs did not exhibit a corollary relationship between SI and k , but, the insensitivity of DPH-GCLs has not been explicitly linked to intercalated Na-CMC or other additives. Kolstad et al. (2004) hypothesized that the inverse relationship between k and SI illustrated in Fig. 2.4 might have been due to precipitation of calcite; but this conclusion was not verified experimentally. Additionally, data for the k of a DPH-GCL at chemical equilibrium does not yet exist in the literature.

2.6. DISCUSSION

The data presented in this chapter illustrate that BAHCs show promise for enhanced environmental containment systems. Discounting DPH-GCLs, which are both prehydrated and pre-densified, the mechanism underlying the enhanced performance of BAHCs is coupled to increased swelling capacity through activation of osmotic swell by an intercalated polymeric molecule or supplementary swell from a superabsorbent polymer. These mechanisms for enhanced or supplemental swelling are still sensitive to ionic strength effects and cation exchange. Thus, with the exception of DPH-GCLs, no BAHC has been shown to contain high-strength leachates. Tests with DPH-GCLs in these solutions have not yet been run to chemical equilibrium due to the low initial k resulting from prehydration and pre-densification, and the ultimate performance of this material is unknown. Additionally, intercalated polymers may be mobile when permeated with DW or other dilute permeants, and therefore the longevity of BAHCs is unknown. In BACs, experimental results have also not fully substantiated the locking of bound cations by polymeric additives. Additional research in this area is warranted.

2.7. REFERENCES

- Ashmawy, A. K., Darwish, E.H., Sotelo, N., and Muhammad, N. (2002). "Hydraulic performance of untreated and polymer-treated bentonite in inorganic landfill leachates." *Clays and Clay Minerals*, 50(5), 546-552.
- ATU (1992). "ClayMax sodium bentonite liner found degraded at New Jersey site." *Aboveground Tank Update*, 3(2), 1, 17-18.
- Benson, C. H., Jo, H. Y., and Abichou, T. (2004). "Forensic analysis of excessive leakage from lagoons lined with a composite GCL." *Geosynthetics International*, 11(3), 242-252.
- Benson, C., Thorstad, P., Jo, H., and Edil, T. (2007). "Case history: hydraulic performance of geosynthetic clay liners in a landfill final cover." *J. of Geotech. and Geoenviron. Engr.*, 133(7), 814-827.
- Benson, C.H. and Meer, S.H. (2009), "Relative abundance of monovalent and divalent cations and the impact of desiccation on geosynthetic clay liners." *J. of Geotech. and Geoenviron. Eng.*, 133(5), 814-827.
- Bradshaw, S., Benson, C., and Scalia, J. (2012). "Cation exchange during subgrade hydration and effect on hydraulic conductivity of GCLs." Submitted to *J. of Geotech. and Geoenviron. Eng.*, (in press).
- Buchholz, F., Graham, A. (1998). *Modern Superabsorbent Polymer Technology*, John Wiley and Sons, New York.
- Deng, Y., Dixon, J.B., White, G.N. (2006). Bonding between polyacrylamide and smectite. *Colloids and Surfaces*, 281(1), 82-91.

- Di Emidio, G. (2010). "Hydraulic and chemico-osmotic performance of polymer treated clays." Ph.D. dissertation, Ghent Univ., Belgium.
- Di Emidio, G., Van Impe, W., Mazzieri, F. (2010). "A polymer enhanced clay for impermeable geosynthetic clay liners." *Proceedings of Sixth International Conference on Environmental Geotechnics*, International Society for Soil Mechanics and Geotechnical Engineers, New Delhi, India, 963-967.
- Di Emedio, G., Van Impe, W., Flores, V. (2011). "Advances in geosynthetic clay liners: polymer enhanced clays." *GeoFrontiers 2011. Advances in Geotechnical Engineering*, American Society of Civil Engineers, Reston, USA, 1931-1940.
- Egloffstein, T. (2001). "Natural bentonites-influence of the ion exchange and partial desiccation on permeability and self-healing capacity of bentonites used in GCLs." *Geotextiles and Geomembranes*, 19, 427-444.
- Flynn, B., Carter, G. (1998). "Waterproofing material and method of fabrication thereof." *US Patent Number: 6,537,676 B1*.
- Grim, R. (1968). *Clay Mineralogy*, 2nd Edition, McGraw-Hill, New York.
- Guyonnet, D., Gaucher, E., Gaboriau, H., Pons, C., Clinard, C., Norotte, W., and Didier, G. (2005). "Geosynthetic clay liner interactions with leachate: Correlation between permeability, microstructure, and surface chemistry." *J. of Geotech. and Geoenviron. Eng.*, 131(6), 740-749.
- James, A., Fullerton, D., and Drake, R. (1997). "Field performance of GCL under ion exchange conditions." *J. of Geotech. and Geoenviron. Eng.*, 123(10), 897-901

- Jo, H., Benson, C., Shackelford, C., Lee, J., and Edil, T. (2005). "Long-term hydraulic conductivity of a non-prehydrated geosynthetic clay liner permeated with inorganic salt solutions." *J. of Geotech. and Geoenviron. Eng.*, 131(4), 405-417.
- Jo, H., Katsumi, T., Benson, C., and Edil, T. (2001). "Hydraulic conductivity and swelling of non-prehydrated GCLs permeated with single species salt solutions." *J. of Geotech. and Geoenviron. Engr.*, 127(7), 557-567.
- Kajita, L. (1997). "An Improved Contaminant Resistant Clay for Environmental Clay Liner Applications." *Clays and Clay Minerals* 45(5), 609-617.
- Katsumi, T., Onikata, M., Hasegawa, S., Lin, L., Kondo, M., and Kamon, M. (2001). "Chemical compatibility of modified bentonite permeated with inorganic chemical solutions." *Geoenvironmental Impact Management*, Thomas Telford, London, 419-424.
- Katsumi, T., Ishimori, Ho, Onikata, M., and Fukagawa, R. (2008). "Long-term barrier performance of modified bentonite materials against sodium and calcium permeant solutions." *Geotextiles and Geomembranes*, 26(1), 14-30.
- Kolstad, D., Benson, C., and Edil, T. (2004). "Hydraulic conductivity and swell of nonprehydrated GCLs permeated with multi-species inorganic solutions." *J. of Geotech. and Geoenviron. Engr.*, 130(12), 1236-1249.
- Kondo, M., (1996). "Method of activation of clay and activated clay" *US Patent Number: 5,573,583*.

- Lee, J. and Shackelford, C. (2005). "Impact of bentonite quality on hydraulic conductivity of geosynthetic clay liners." *J. of Geotech. and Geoenviron. Engr.*, 131(1), 64-77.
- Lin, L. and Benson, C. (2000). "Effect of wet-dry cycling on swelling and hydraulic conductivity of geosynthetic clay liners." *J. of Geotech. and Geoenviron. Engr.*, 126(1), 40-49.
- Lin, L., Katsumi, T., Kamon, M., Benson, C., Onikata, M., and Kondo, M. (2000). "Evaluation of chemical-resistant bentonite for landfill barrier applications." *Annals of Disas. Prev. Res. Inst.*, Kyoto Univ., No. 43 B-2, 525-533.
- Lyklema, J. (1985). "How polymers adsorb and affect colloid stability, flocculation, sedimentation, and consolidation." In *Flocculation, Sedimentation and Consolidation: Proceedings of the Engineering Foundation Conference, Sea Island, Georgia*, Moudgil, B. and Somasundaran, P. Eds., United Engineering Trustees, Inc., 3-21.
- Mazzieri, F., Emidio, G., Van Impe, P. (2010a). "Diffusion of calcium chloride in a modified bentonite: Impact on osmotic efficiency and hydraulic conductivity." *Clays and Clay Minerals*, 58(3), 351-363.
- Mazzieri, F., Pasqualini, E., Emidio, G. (2010b). "Migration of heavy metals through conventional and factory-prehydrated GCL materials." *Proceedings of Sixth International Conference on Environmental Geotechnics*, International Society for Soil Mechanics and Geotechnical Engineers, New Delhi, India, 963-967.
- Mazzieri, F. (2011). "Impact of desiccation and cation exchange on the hydraulic conductivity of factory-prehydrated GCLs.." *GeoFrontiers 2011. Advances in*

Geotechnical Engineering, American Society of Civil Engineers, Reston, USA, 976-985.

McBride M. (1994). *Environmental Chemistry of Soils*. Oxford University Press, New York.

Meer, S. and Benson, C. (2007). "Hydraulic conductivity of geosynthetic clay liners exhumed from landfill final covers." *J. of Geotech. and Geoenviron. Engr.*, 133(5), 550-563.

Norrish, K., and Quirk, J. (1954). "Crystalline swelling of montmorillonite, use of electrolytes to control swelling." *Nature*, 173, 255-257.

Onikata, M., Kondo, M., and Kamon, M. (1996). "Development and characterization of a multishrinkable bentonite." *Environmental Geotechnics*. Taylor and Francis, Rotterdam, 587-590.

Onikata, M., Kondo, M., Hayashi, N., and Yamanaka, S. (1999). "Complex formation of cation-exchanged montmorillonites with propylene carbonate: Osmotic swelling in aqueous electrolyte solutions." *Clays and Clay Minerals*, 47(5), 672-677.

Ruhl, J., and Daniel, D. (1997). "Geosynthetic clay liners permeated with chemical solutions and leachates." *J. of Geotech. and Geoenviron. Engr.*, 123(4), 369-381.

Scalia, J., and Benson, C.H. (2011). "Hydraulic conductivity of geosynthetic clay liners exhumed from landfill final covers with composite barriers." *J. of Geotech. and Geoenviron. Engr.*, 137(1), 1-13.

- Scalia, J., Benson, C. H., Edil, T. B., Bohnhoff, G. L., and Shackelford, C. D. (2011). "GCLs containing bentonite polymer nanocomposite." *GeoFrontiers 2011. Advances in Geotechnical Engineering*, American Society of Civil Engineers, Reston, USA, 2001-2009.
- Schroeder, C., Monjoie, A., Illing, P., Dosquet, D., and Thorez, J. (2001). "Testing a factory-prehydrated GCL under several conditions." *Proceedings, Sardinia 2001, 8th International Waste Management and Landfill Symposium*, CISA Environmental Sanitary Engineering Centre, Cagliari, Italy, 187-196.
- Shackelford, C., Benson, C., Katsumi, T., Edil, T., and Lin, L. (2000). "Evaluating the hydraulic conductivity of GCLs permeated with non-standard liquids." *Geotextiles and Geomembranes*, 18(2-3), 133-161.
- Shackelford, C. and Lee, J. (2003). "The destructive role of diffusion on clay membrane behavior." *Clays and Clay Minerals*, 51(2), 187-197.
- Shan, H., and Daniel, D. (1991). "Results of laboratory tests on a geotextile/bentonite liner material." *Geosynthetics 2001*, Industrial Fabrics Assoc. International, St. Paul, MN, 517-535.
- Sposito, G. (1989). *The Surface Chemistry of Soils*, Oxford University Press, New York.
- Stumm, W. (1992). *Chemistry of the Solid-Water Interface*, John Wiley and Sons, New York.
- Stumm, W., and Morgan, J. (1996). *Aquatic Chemistry*, 3rd ed., Wiley, New York.

- Theng, B. (1970). "Interactions of clay minerals with organic polymers. Some practical applications." *Clays and Clay Minerals*, 18, 357-362.
- Trauger R. and Darlington J. (2000). "Next-generation geosynthetic clay liners for improved durability and performance." *TR-220*. Colloid Environmental Technologies Company , Arlington Heights, 2-14.
- Vasko, S., Jo, H., Benson, C., Edil, T., and Katsumi, T. (2001). "Hydraulic Conductivity of Partially Prehydrated Geosynthetic Clay Liners Permeated with Aqueous Calcium Chloride Solutions." *Geosynthetics 2001*, Industrial Fabrics Assoc. International, St. Paul, MN, 685-699.

2.8. ABBREVIATIONS

BAHC – Bentonite amended for hydraulic compatibility

BPA – Bentonite-polymer alloy

CEC – Cation-exchange capacity

CRC – Contaminant-resistant clay

DW – Deionized water

DPH-GCL – Dense-prehydrated geosynthetic-clay liner

ECB – Exchangeable cation bridging

FTIR – Fourier-transform-infrared spectroscopy

GCL – Geosynthetic-clay liner

T-GCL – Traditional Na-bentonite geosynthetic-clay liner

GT – Geotextile

HC – HYPER clay

k – Hydraulic conductivity

MMT – Montmorillonite

MSB – Multi-swellable bentonite

Na-B – Sodium-bentonite

Na-CMC – Sodium carboxymethylcellulose

Na-PA – Sodium polyacrylate

PC – Propylene carbonate

SI – Swell index

TGA – Thermogravimetric analysis

XRD – X-ray diffraction

2.9. FIGURES

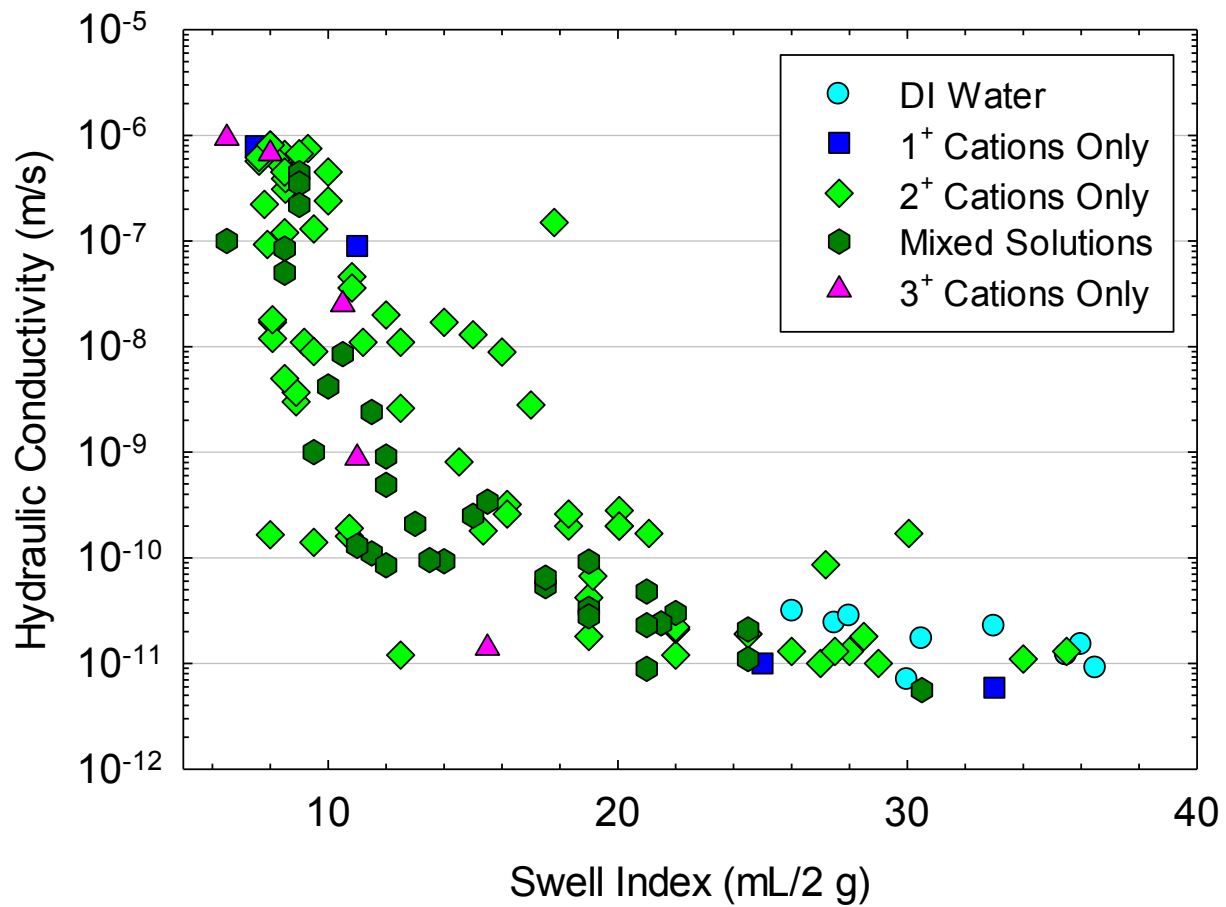


Fig. 2.1 Hydraulic conductivity of GCLs permeated with solutions of varying ionic strength segregated by the type of cations in the synthetic permeant solutions used for testing. Data are from Shackelford et al. (2000), Jo et al. (2001), Kolstad et al. (2004), Jo et al. (2004), Jo et al. (2005), and Lee and Shackelford (2005).

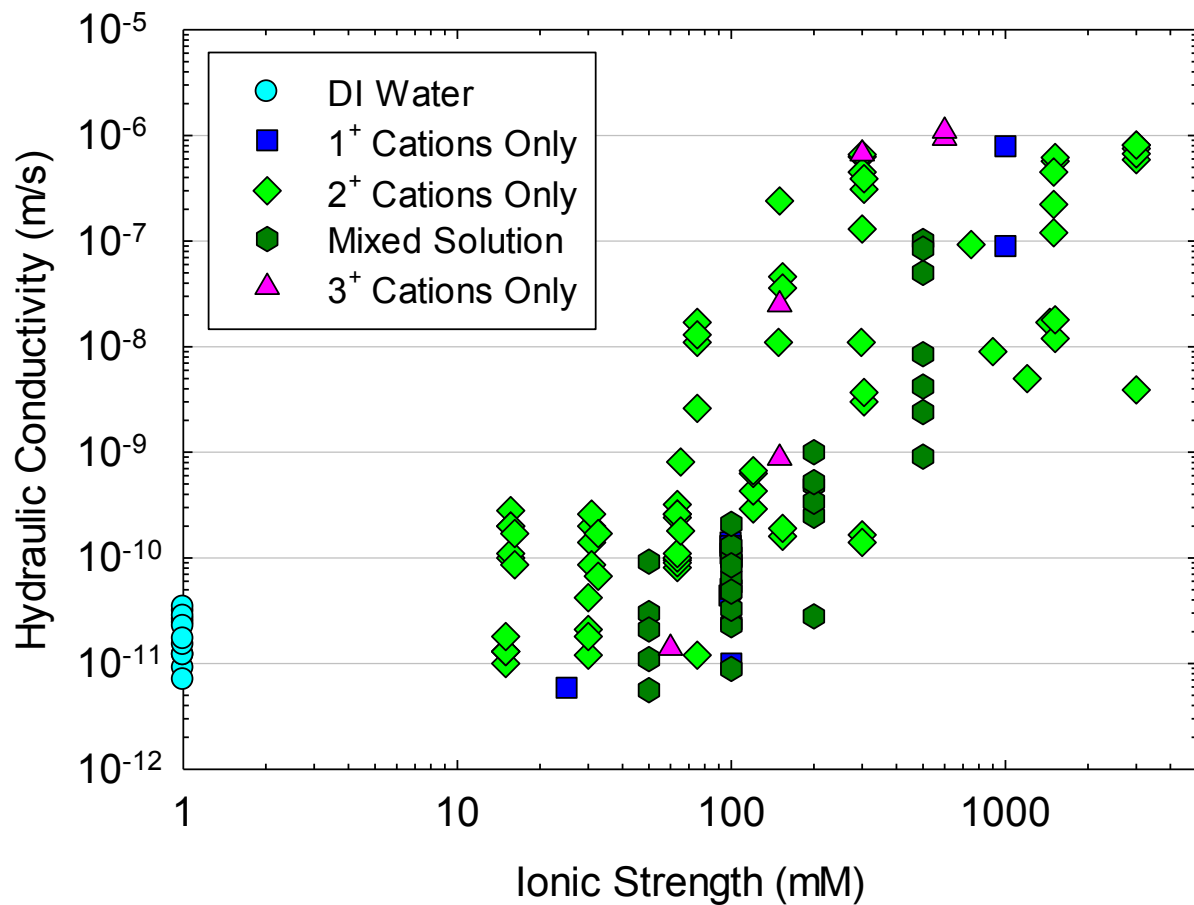


Fig. 2.2 Hydraulic conductivity of GCLs permeated in varying solutions versus the swell index of the bentonite component of the GCL in the permeant solutions. Data are from Shackelford et al. (2000), Jo et al. (2001), Kolstad et al. (2004), Jo et al. (2004), Jo et al. (2005), and Lee and Shackelford (2005).

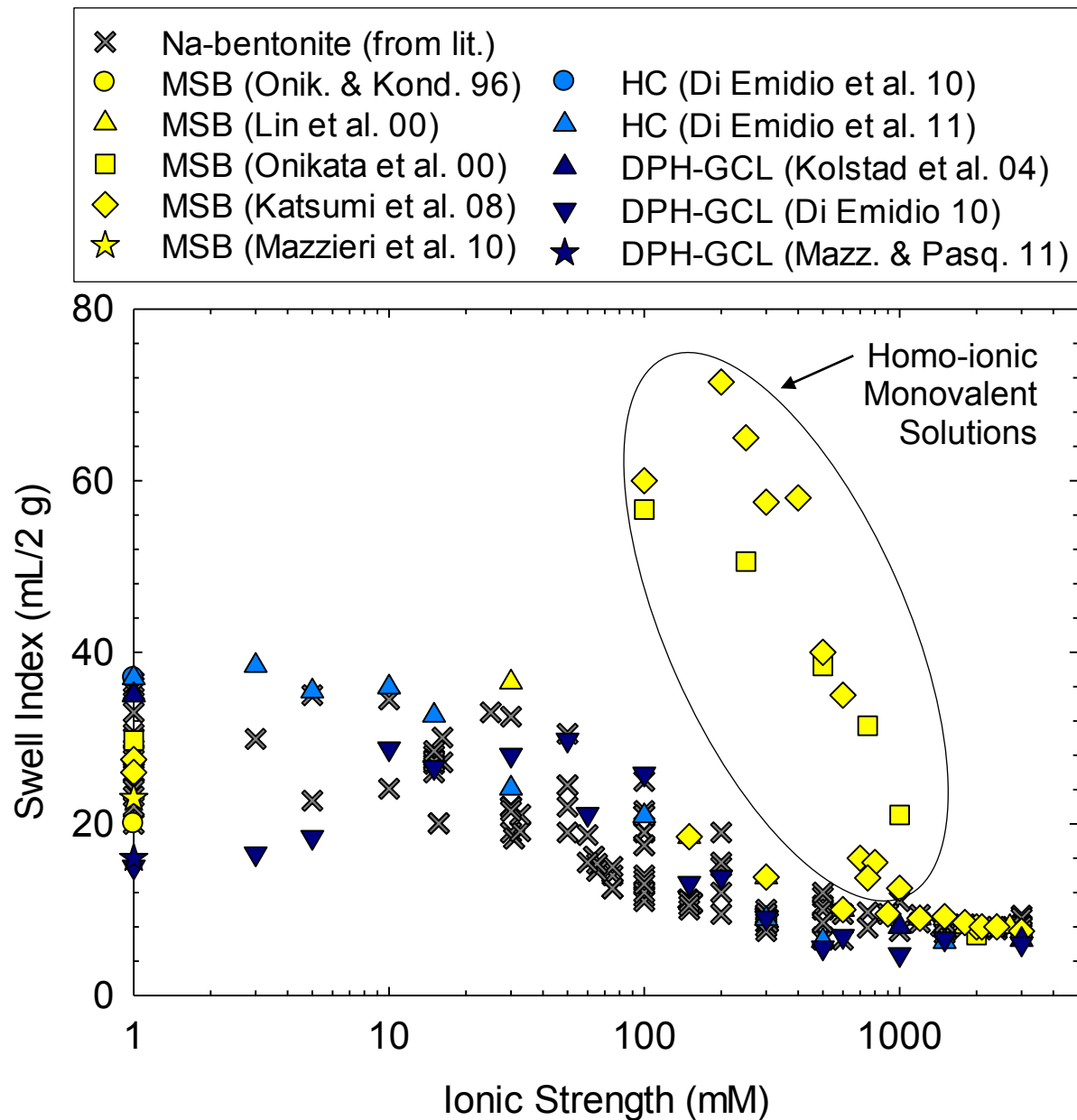


Fig. 2.3 Influence of ionic strength on the swell index of natural Na-bentonite and bentonites amended for hydraulic compatibility (multi-swellable bentonite, MSB; HYPER-clay, HC; dense-prehydrated GCLs, DPH-GCLs). Literature data for Na-bentonite are from Shackelford et al. (2000), Jo et al. (2001), Kolstad et al. (2004), Jo et al. (2004), Jo et al. (2005), and Lee and Shackelford (2005).

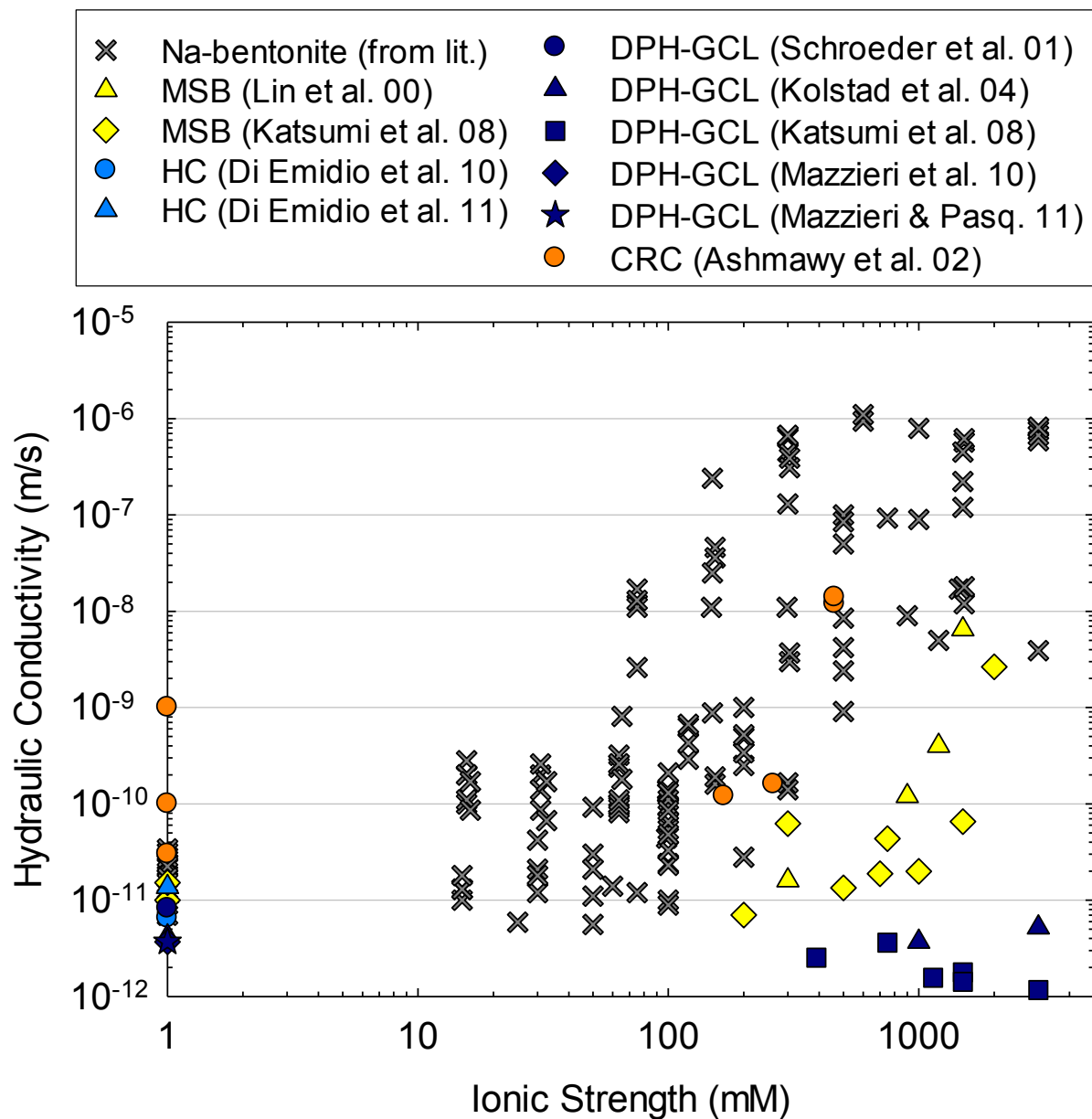


Fig. 2.4 Influence of CaCl_2 concentration on the hydraulic conductivity of natural Na-bentonite and bentonites modified for hydraulic compatibility (multi-swellable bentonite, MSB; HYPER-clay, HC; dense-prehydrated GCLs, DPH-GCLs; contaminant-resistant clay, CRC). Literature data for Na-bentonite are from Shackelford et al. (2000), Jo et al. (2001), Kolstad et al. (2004), Jo et al. (2004), Jo et al. (2005), and Lee and Shackelford (2005).

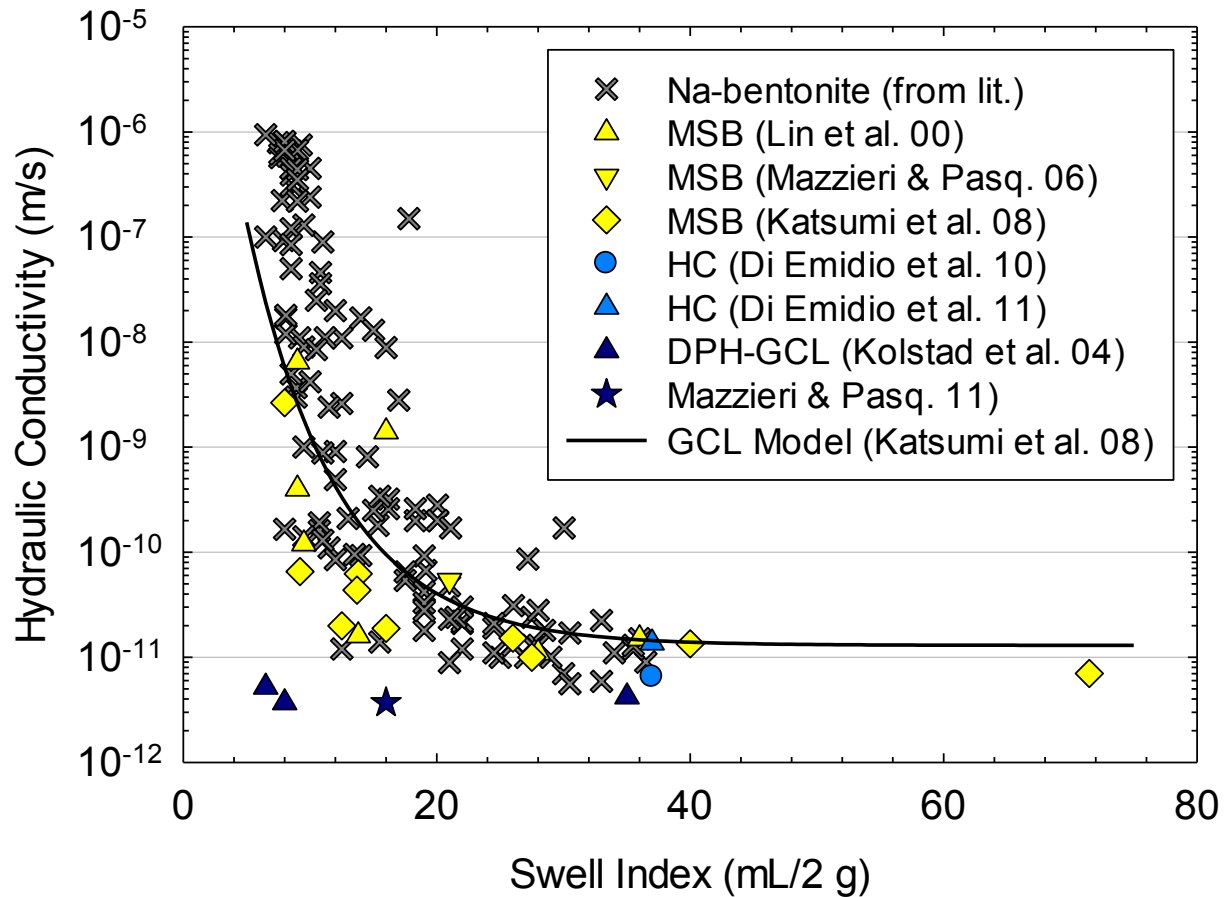


Fig. 2.5 Hydraulic conductivity versus swell index for natural Na-bentonite and bentonites amended for hydraulic compatibility (multi-swellable bentonite, MSB; HYPER-clay, HC; dense-prehydrated GCLs, DPH-GCLs). Literature data for Na-bentonite are from Shackelford et al. (2000), Jo et al. (2001), Kolstad et al. (2004), Jo et al. (2004), Jo et al. (2005), and Lee and Shackelford (2005). Model relating GCL hydraulic conductivity and swell index developed by Katsumi et al. (2008) is also included for comparison.

CHAPTER THREE

LONG-TERM HYDRAULIC CONDUCTIVITY OF A BENTONITE-POLYACRYLATE NANOCOMPOSITE PERMEATED WITH AGGRESSIVE INORGANIC SOLUTIONS

3.1. ABSTRACT

Bentonite was modified at the nanoscale so that low hydraulic conductivity (k) would be maintained under adverse conditions. Nanoscale modification consisted of polymerizing acrylic acid within bentonite slurry to form an interconnected super-swelling structure. This modified material is referred to as a bentonite-polymer nanocomposite (BPN). Index property tests indicated that BPN has different behavior than natural sodium bentonite (Na-bentonite). For example, in free swell tests, Na-bentonite (Na-B) swelled to approximately 30 mL in deionized water, whereas BPN swelled to 73 mL in the same solution. GCLs were assembled with BPN and permeated directly with a variety of calcium chloride (CaCl_2) solutions and solutions with extreme pH (0.3 and 13.1) known to cause large increases in the k of Na-bentonite. Low k ($< 8 \times 10^{-11}$ m/s) was maintained by BPN for all solutions for the duration of testing (> 2 years). In contrast, Na-bentonite and superabsorbent polyacrylate tested under the same conditions had k at least three orders-of-magnitude higher. These results illustrate that BPN may be a superior waste-containment material for extreme geoenvironmental applications and, therefore, warrants further exploration.

3.2. INTRODUCTION

Sodium (Na) bentonite (Na-B) is used to control flow and contaminant transport because Na-B has low hydraulic conductivity (k) to water. Within Na-B, montmorillonite (MMT), a member of the smectite group of clay minerals (Grim 1968), governs hydraulic behavior. The effectiveness of MMT as a barrier for waste containment is dependent on the osmotic adsorption of water molecules between MMT platelets (McBride 1994). Osmotic adsorption of water molecules is manifest as swelling of the immobile phase, reducing the size of the hydraulically active pores that conduct flow and transport and resulting in low k . The extent of osmotic swelling is a function of (1) the ionic strength of the hydrating solution (McBride 1994) and (2) the preponderance of when monovalent cations, such as Na^+ , dominating the exchange complex (i.e., the collection of cations adsorbed to the mineral surface) (McBride 1994). If multivalent cations dominate the exchange complex, or if the hydrating pore fluid has a high ionic strength, osmotic swelling does not occur, resulting in orders-of-magnitude higher k (Shackelford et al. 2000, Jo et al. 2001, 2005, Kolstad et al. 2004, Katsumi et al. 2008).

In addition to reduction or elimination of Na-B swell in high ionic strength solutions (Shackelford et al. 2000, Jo et al. 2001, 2005, Kolstad et al. 2004, Katsumi et al. 2008), Na^+ comprising the exchange complex is thermodynamically unstable in environments where multivalent cations (e.g., Ca^{2+}) are present (Sposito 1989), including most naturally occurring pore waters and most leachates. When present, multivalent cations replace monovalent cations originally comprising the exchange complex, thereby reducing or eliminating osmotic swell (Vasko et al. 2001, Kolstad et al. 2004, Lee and Shackelford 2005a).

Numerous laboratory studies on thin (~10 mm) Na-B barrier layers, viz geosynthetic clay liners (GCLs), have demonstrated that Ca^{2+} -for- Na^+ exchange results in reduced swelling capacity, as quantified by the swell index (SI) test (ASTM D5890), and ultimately decreased hydraulic performance (Lin and Benson 2000, Jo et al. 2001, 2005, Eggloffstein 2001, Shackelford and Lee 2003, Kolstad et al. 2004, Lee and Shackelford 2005a, b). Field studies have confirmed that GCLs placed in contact with soils will undergo Ca^{2+} -for- Na^+ exchange (ATU 1992, James et al. 1997, Benson et al. 2004, 2007, Meer and Benson 2007, Scalia and Benson 2011). Ca^{2+} is derived from surrounding soil pore water, and migrates into the GCL in response to hydraulic (pressure or suction) and/or chemical (diffusive) gradients (Meer and Benson 2007, Bradshaw et al. 2012). GCLs may also derive Ca^{2+} from the dissolution of calcite (CaCO_3) during hydration and permeation with dilute chemical solutions (Guyonnet et al. 2005). Calcite is extensively reported as an accessory mineral in bentonite removed from GCLs (Shackelford et al. 2000, Kolsad et al. 2004, Jo et al. 2004, Guyonnet et al. 2005). Cation exchange often occurs slowly, because the rate of exchange is controlled by the rate at which multivalent cations diffuse from the bulk pore water into the interlayer space (Jo et al. 2005, 2006). Irrespective of the source (leachate, soil porewater, or native calcite), exchange of Ca^{2+} for Na^+ should be anticipated in the long term.

Recognition of the potential for increases in k from Na-bentonite incompatibility has spurred the development of bentonites amended for compatibility (BACs) in hydraulic-barrier applications (Onikata and Kondo 1996, Flynn et al. 1998, Onikata et al. 1999, Onikata et al. 2000, Trauger and Darlington 2000, Katsumi et al. 2001, Schroeder

et al. 2001, Ashmawy et al. 2002, Kolstad et al. 2004, Katsumi et al. 2008, Di Emidio et al. 2010, Mazzieri et al. 2010a, Scalia et al. 2011, Di Emidio et al. 2011). In BACs, bentonite typically has been hydrated with an organic solution such as propylene carbonate (Onikata and Kondo 1996, Onikata et al. 1999, Katsumi et al. 2001, Kolstad et al. 2004, Katsumi et al. 2008), or carboxymethyl cellulose and methanol (Onikata and Kondo 1996, Flynn et al. 1998, Onikata et al. 1999, Onikata et al. 2000, Schroeder et al. 2001, Katsumi et al. 2008, Di Emidio et al. 2010, Mazzieri et al. 2010a, Di Emidio et al. 2011), to activate and maintain osmotic swelling in solutions with ionic strengths that would preclude osmotic swell in unmodified bentonite. The performance and underlying mechanisms of BACs in the literature were summarized in Chapter 2.

Trauger and Darlington (2000) developed a BAC in hydraulic barrier applications by polymerization of an organic monomer in Na-bentonite slurry. The material developed by Trauger and Darlington (2000) was termed bentonite-polymer alloy (BPA). To assess the impact of polymeric augmentation, BPA slurry was deposited into a needle-punched non-woven geotextile (GT) and permeated with seawater (ionic strength not provided). The k of the BPA-GT was 5×10^{-12} m/s compared to 2×10^{-8} m/s for a GCL containing natural Na-bentonite. X-ray diffraction (XRD) of dried BPA showed an increase in interlayer spacing from 0.35 nm (typical for dry MMT) to from 1.0 to 1.5 nm, indicating that the polymer was intercalated in the bentonite interlayer. The anionic polymer produced within BPA was hypothesized to bond with the Na^+ ions in the MMT interlayer.

A second generation of the BPA originally developed by Trauger and Darlington (2000) was investigated in this study. Na-bentonite was modified at the nanoscale by in-situ polymerization of acrylic acid to form sodium-polyacrylate. Polyacrylate was chosen because polyacrylate was expected to interact with Na-B via hydrogen bonding and has desirable characteristics such as being relatively inexpensive, similar to the super-absorbent and super-swelling polymers used in baby diapers, and is not readily biodegradable (Buchholz and Graham 1998). The resultant bentonite-polyacrylate nanocomposite (BPN) was comparatively tested against Na-bentonite and superabsorbent polypolyacrylate (SAP) for long-term hydraulic performance and SI in aqueous solutions having a range of Ca^{2+} concentrations (5, 20, 50, 200, 500 mM CaCl_2) and pHs (0.3, 13.1). For k testing, a thin layer (< 6 mm dry thickness) of BPN, Na-B, or SAP mimicking GCLs was permeated under low stress conditions (20 kPa effective stress). Corollary data also were included from replicate SI and k tests conducted at Colorado State University (CSU), and inter-laboratory reproducibility is discussed.

3.3. MATERIALS

3.3.1. Bentonite-Polyacrylate Nanocomposite (BPN)

BPN was created using a method comparable to that employed for conventional polymer nanocomposites (e.g., Muzny et al. 1996). Powdered Na-bentonite (base bentonite, BB) was mixed into a monomer solution prepared by dissolving acrylic acid in water, followed by slow neutralization with sodium hydroxide (NaOH) to allow

dissipation of the heat of neutralization. The properties of the BB used for BPN production are detailed in Tables 3.1 and 3.2. The mineralogical composition based on XRD was 73-77% MMT, 15-17% quartz, 4-5% plagioclase feldspar – andesine, and less than 3% illite/mica, heulandite, clinoptilolite, and calcite. BB was added to the neutralized solution in concentrations between 30-50% by weight to form bentonite-monomer slurry. During BB addition, the solution was vigorously agitated in an attempt to increase the surface area available for polyacrylate adsorption. Sodium persulfate ($\text{Na}_2\text{S}_2\text{O}_8$) was added as a thermal initiator.

Once the bentonite-monomer slurry was prepared, polymerization was initiated by raising the temperature of the slurry above the decomposition temperature of the initiator. This increase in temperature caused the initiator to decompose and form free radicals. During polymerization, free radicals ($\text{R}\bullet$) attack the double bond of the acrylic acid monomer to form new free radicals ($\text{RM}\bullet$), which then react with additional monomers to propagate the polymer chain ($\text{RMMM}\bullet$). After polymerization, the solution was oven dried at 105°C to remove water. The resulting BPN was milled and screened to match the gradation of Na-bentonite granules in a GCL as defined in Shackelford et al. (2000). The BPN used in this study was provided by the Colloid Environmental Technologies Company (CETCO, Hoffman Estates, IL).

3.3.2. Na-Bentonite (Na-B)

A natural Na-B from Wyoming, USA, was used for comparative testing to represent the current state of practice in GCLs. The Na-B was GCL grade and was provided by CETCO; Na-B is sold under the name Volclay CG-50 (Hoffman Estates, IL).

The range of granule sizes of the Na-B evaluated in this study was similar to that of the GCL bentonite studied by Shackelford et al. (2000), but with a smaller fraction of fine sand-size particles. The properties of Na-B are delineated in Tables 3.1 and 3.2. The mineralogical composition based on XRD was 85-91% MMT, 0-5% augite, 2-4% quartz, and less than 3% cristobalite, plagioclase feldspar – andesine, calcite, illite/mica, heulandite, gypsum, ferroan dolomite, and K-feldspar – microcline. As shown in Tables 3.1 and 3.2, Na-B and BB were not the same clay, but BB was not representative of bentonite currently used in GCLs (Jo et al. 2001, Guyonnet et al. 2005, Lee and Shackelford 2005) and was thus not chosen for comparative testing.

3.3.3. Na-Polyacrylate (SAP)

SAP ($[\text{C}_3\text{H}_3\text{NaO}_2]_n$) was tested to explore the swelling and hydraulic properties of the polymer component of BPN. In the SAP tested, the carboxyl group anionic (CH_3COO^-) charge is satisfied by a sodium ion (Na^+). This configuration is representative of SAP produced in Na-B slurry, in which the solution has a preponderance of Na^+ cations. SAP is also readily available commercially, and is commonly employed as the active component of baby diapers and other water absorbing products (Buckholz and Graham 1998). For k testing, granular SAP was used with granule sizes matching the grain size distribution of an average GCL as defined in Shackelford et al. (2000).

3.3.4. Liquids

To investigate the impact of divalent cations and ionic strength on the swelling and hydraulic behavior of BPN, deionized water (DW) as well as 5, 20, 50, 200 and 500

mM CaCl_2 were used as permeant solutions (Table 3.3). Jo et al. (2001) and Lee et al. (2005) showed that permeating GCLs originally containing Na-B with DW or dilute divalent solutions 5, or 20 mM CaCl_2 resulted in a low k ($\sim 2 \times 10^{-10}$ m/s) even after near complete exchange of Ca^{2+} for native Na^+ . In contrast, permeation of a GCLs originally containing Na-B with a strong divalent solutions such as 50, 200, or 500 mM CaCl_2 was shown by Lee et al. (2005a) to result in a k on the order of 10^{-8} to 10^{-7} m/s. Thus, DW and solutions containing 5 or 20 mM CaCl_2 were selected as permeant solutions to provide base-line conditions allowing for gradual cation exchange, whereas solutions containing 50, 200, or 500 mM CaCl_2 were chosen as permeant solutions to chemically stress BPN as a barrier layer. The DW used in solution preparation as well as testing was classified as Type-II water per ASTM D1193. The CaCl_2 solutions were prepared by dissolving reagent grade dihydrate-calcium-chloride salt ($\text{CaCl}_2 \cdot 2\text{H}_2\text{O}$) in DW. Concentrations of Ca^{2+} were verified by inductively coupled plasma-optical emission spectroscopy (ICP-OES) following USEPA Method 6010 B (USEPA 2007). The concentration of Ca^{2+} in DW was below the ICP-OES method detection limit (MDL) of 0.05 mM. Solutions were stored in collapsible carboys with no head space to limit interaction with atmospheric CO_2 .

A strong, acidic solution (1 M HNO_3) and a hyperalkaline solution (1 M NaOH) also were used as permeant solutions to investigate the effect of extreme pHs (Table 3.3). Extreme-pH solutions correlate to potential leachates generated in a wide variety of mining processes for which traditional GCLs have been investigated as a possible containment option (Bouazza 2010). Acidic leachates are of particular concern for GCLs because bentonite is thermodynamically unstable at $\text{pH} < 3\text{--}4$ (Gates et al. 2010)

resulting in dissolution of MMT (Jozefaciuk and Matyka-Sarzynska 2006). Shackelford et al. (2010) showed that both a GCL and a GCL “treated for contaminant resistance” had k to a synthetic acidic leachate (pH = 2.5) between 1,100 and 15,000 times higher than that permeated with a dilute groundwater. However, these increases in k were hypothesized to result from the high ionic strength, I , of the synthetic leachate ($I = 350$ mM) as dissolution was not visually observed.

Kashir and Yanful (2001), Lange et al. (2007), and Lange et al. (2009) permeated GCLs with acid mine drainage (AMD) containing high metal concentrations, high concentrations of SO_4 , and a low pH (2.5 to 3.3). Kashir and Yanful (2001) found that contact with AMD resulted in mineralogical alteration of the MMT, as evidenced by changes in XRD patterns. Kashir and Yanful (2001), Lange et al. (2007), and Lange et al. (2009) all found that the k of GCLs to AMD did not increase to more than 1×10^{-10} m/s; however, as a result of the documented dissolution of MMT, the longevity of these results is unknown. For this study, a 1 M HNO_3 with a pH = 0.3 was chosen to investigate the impact of a strong acidic solution on the BPN. The strong-acidic solution was prepared by diluting trace-metal grade 70% HNO_3 stock solution with DW.

Hyperalkaline NaOH solutions have been used as proxies for alumina refinery leachate (ARL) in GCL compatibility studies (Benson et al. 2010). Typically, ARL has a pH between 11.5-to-12.5 and contains high concentrations of Na salts and aluminum complexes (Benson et al. 2008). These solutions have the potential to dissolve the MMT component of GCLs as well as other accessory minerals (Gates and Bouazza 2010). Benson et al. (2010) investigated the impact of a 1 M NaOH solution (pH = 13.1)

on the k of GCLs composed of powdered Na-B and the Na-B amended with two dosages of a proprietary additive intended to reduce the adverse hydraulic impact due to chemical reactions. Permeation with the 1 M NaOH resulted in initial increases in k to < 50 times the k of the same product to DW permeation, followed by either a leveling out or a decreasing k with time. The observed decreasing trend was hypothesized by Benson et al. (2010) to result from pore filling by metal precipitates.

Data for bentonites contacted with realistic ARLs solutions containing high concentrations of cations in addition to a high pH also have shown clogging of pores by mineral precipitates (Claret 2002, Ramirez et al. 2002, Sanchez et al. 2006). To simulate a worst-case hyperalkaline solution, 1 M NaOH also was used to investigate the impact of high pH while simultaneously minimizing the potential k -lowering contribution of mineral precipitates. The 1 M NaOH was prepared by dissolving reagent grade NaOH in DW.

Electrical conductivity (EC) and pH of the permeant solutions were monitored on a monthly basis. EC was measured using an electrical conductivity probe (Con 5 series, Cole-Parmer Instrument Co., Vernon Hills, Illinois), and pH was measured using a pH probe (Accumet pH meter 50, Fisher Scientific Co., Waltham Massachusetts). The EC and pH of testing solutions are reported in Table 3.2.

3.4. METHODS

3.4.1. Swell Index

Swell index (SI) tests were performed on BPN and Na-B in general accordance with ASTM D5890. Materials were ground to 100% passing a standard No.-200 woven wire sieve (ASTM E11) with a mortar and pestle. In addition to baseline tests in DW (Table 3.1), 5, 20, 50, 200, and 500 mM CaCl_2 solutions, and 1 M HNO_3 and 1 M NaOH solutions were used as hydrating solutions. Swell indices are summarized in Table 3.4.

Although the SI tests (ASTM D5890) are only intended for analysis of the swelling capacity of bentonite, for comparative purposes a scaled-up SI method incorporating a 2-L graduated cylinder was used to determine the SI of SAP in DW, and in 5 and 20 mM CaCl_2 . This modified testing methodology was necessitated by the > 100-mL swelling capacity of 2 g of SAP. A 2-L graduated cylinder was filled to 1.8 L with DW, 5 mM CaCl_2 , or 20 mM CaCl_2 and 2 g of SAP were then added to the 2-L graduated cylinder following the methodology detailed in ASTM D5890. After all SAP was added, the graduated cylinder was filled to 2.0 L and allowed to equilibrate for 16 h prior to reading as per the methods described in ASTM D5890. The modified SI of SAP to DW, 5 mM CaCl_2 , and 20 mM CaCl_2 is included in Tables 3.1 and 3.4. The SI of SAP in 50, 200, and 500 mM CaCl_2 , 1 M NaOH , and 1 M HCl were determined following ASTM D5890, and are reported in Table 3.4.

3.4.2. Hydraulic Conductivity (k)

Hydraulic conductivity tests were conducted using flexible-wall permeameters in general accordance with ASTM D5084. The falling headwater-constant tailwater

method was employed. Glass tubing with 5.2-mm inside diameter was used as the falling headwater reservoir. The tubing was fixed at 5° from horizontal to minimize the change in hydraulic gradient during testing but still allow sufficient influent solution for convenient and accurate long term testing. Gravity heads were used to apply cell and influent pressure. Backpressure was not applied to allow for convenient collection of effluent for chemical analyses (i.e., pH, EC). Long-term testing was conducted under an average effective stress of 20 kPa and an average influent head of 1.5 m, corresponding to an average hydraulic gradient of 200 for a 7.5-mm thick average specimen. This hydraulic gradient is typical for GCL testing (Shackelford et al. 2000). These testing conditions were chosen to allow for comparison with existing data on long-term k of GCLs to inorganic salt solutions (Lee and Shackelford 2005; Lee et al. 2005a, 2005b; Jo et al. 2005).

Test specimens were constructed with granular BPN, Na-B, or SAP in flexible-wall permeameters equipped with 6.4-mm outside-diameter tubing. Nonwoven geotextiles (GTs) were used in lieu of porous stones and filter paper. A latex membrane was attached to a 154-mm-diameter base pedestal with at least three O-rings. A 0.75-kg/m² non-woven needle-punched GT was then placed on the base pedestal, and topped with a non-woven GT that had been calendared and heat bonded. A calendared GT was used against the specimen to allow for convenient specimen removal at the termination of permeation. BPN or Na-B was placed with a dry mass per unit area of 4.8 kg/m² and manually leveled. This mass per area is the average of the GCLs previously studied with inorganic salt solutions (Jo et al. 2005). To account for the

super-absorbent nature of SAP in dilute solutions, SAP was placed with a dry mass per unit area of 0.48 kg/m^2 and manually leveled. During preliminary testing, higher mass per areas were shown to result in specimen explosion from within the latex membrane into the cell water of the permeameter which resulted in an inflow-burette geyser. Two GTs and a top pedestal were placed atop the specimen layer mirroring the lower assemblage. The top pedestal was secured to the latex membrane with at least three O-rings.

In-cell hydration with the permeant solution of interest was conducted for 48 h prior to flow. After the permeameter was assembled and connected to the falling headwater apparatus, cell pressure was applied and all tubing was saturated with the permeant liquid. The inflow line of the permeameter was left open to allow the specimen to hydrate while the effluent line remained closed. After 48 h, the lines were flushed to remove any air bubbles and flow was initiated by opening the effluent line. During testing, effluent was collected in evacuated fluorinated ethylene propylene bags and sampled for effluent chemistry.

3.4.3. Termination Criteria

Hydraulic conductivity tests were continued until at least the following criteria were met: no systematic trend in k over time, (per ASTM D5084); at least four consecutive k readings within $\pm 25\%$ of the mean (per ASTM D5084); at least four consecutive outflow-to-inflow ratios within 1.0 ± 0.25 (per ASTM D 5084); and establishment of chemical equilibrium. Chemical equilibrium was defined as the EC of the effluent solution within 1.0 ± 0.1 of EC in the influent solution (per ASTM D 6766)

and the pH of the effluent solution within 1.0 ± 0.1 of the pH of the influent solution (per ASTM D 6766). All other tests, with the exception of EC termination criteria not being met for tests conducted with DW, 1 M NaOH, and 1 M HCl, met all termination criteria. The failure of tests with DW to reach EC termination criteria was deemed acceptable, as the k to DW was only intended as a baseline measurement. Jo et al. (2005) showed that Na^+ was still eluted from GCLs permeated with DW after 2.5 years under similar testing conditions. The mechanisms underlying the measured EC outflow-to-inflow ratios for tests with 1 M NaOH and 1 M HCl are discussed later in the text.

3.4.4. Inter-Laboratory Validation

Colorado State University conducted duplicate k and SI tests on BPN and Na-B with replicate testing conditions. At CSU, BPN and Na-B were permeated with DW, 5 mM CaCl_2 , and 500 mM CaCl_2 and tested for SI in DW, 5 mM CaCl_2 , 50 mM CaCl_2 , and 500 mM CaCl_2 . Data from testing at CSU are included in the average material properties presented in Table 3.1, permeant chemistry in Table 3.3, and SI / k results presented in Table 3.4. Comparative analysis of inter-laboratory results is included in the discussion section.

3.4.5. Soluble Cations (SC), Bound Cations (BC), and Cation Exchange Capacity (CEC)

Soluble cations, BC, and CEC were determined for Na-B, BB, and BPN following the procedures detailed in ASTM D7503. Chemical analysis of extracts from SC and BC tests were conducted using ICP-OES following USEPA Method 6010 B (USEPA 2007). Bound cation mole fractions of the major exchangeable cations for each material

(Na^+ , K^+ , Ca^{2+} , and Mg^{2+}) are presented in Table 3.2. Bound cation mole fractions were calculated as the ratio of total soluble cation charge per mass of bentonite associated with a particular cation to the CEC. Soluble cation, BC, and CEC testing was attempted on SAP following ASTM D7503, however, SAP absorbed all testing solution resulting in no effluent for analysis.

3.4.6. Polymer Quantification

The polymer content of BPN before and after permeation was determined by loss-on-ignition. Base bentonite, BPN, and sodium-polyacrylate were ground to pass a No. 20 woven wire sieve (ASTM E11) and oven dried at 105°C until mass ceased to change. Oven-dried material was placed in a pre-ignited crucible and the mass was recorded. The crucible was then placed in a 550°C furnace for 4 h to ignite volatile substances. After 4 h, the crucible was removed from the furnace and allowed to cool in a water-free atmosphere. The mass of the crucible and material was then determined.

Base bentonite used to produce BPN was ignited to ascertain the contribution of mass loss from water bound to the MMT surface after oven drying. Base bentonite lost a mean of 1.6% mass on ignition, with a standard deviation of 0.10% from 10 replicate tests. This mass loss correlates to the removal of strongly bound water from the MMT interlayer (Grim 1968). The BPN supplier also provided a bentonite-free polyacrylate mimicking the polymer component of BPN. This polyacrylate lost 74.7% mass on ignition (the decomposition temperature of polyacrylate is approximately 200°C), with a standard deviation of 0.00% from 10 replicate tests. BPN lost a mean of 22.4% on

ignition, with a standard deviation of 0.01% from 10 replicate tests. From the relative mass-loss percentages of BB and polyacrylate, BPN used in this study was calculated to initially contain 28.5% polymer by mass assuming all mass loss in BPN was the sum of independent BB and polyacrylate mass losses. Based on the relative mass-loss percentages of BB and polyacrylate, the polymer contents of BPN at the termination of permeation were also determined.

3.5. RESULTS

3.5.1. Swell Index

The SI of Na-B, SAP, and BPN in solutions with varying CaCl_2 concentration are shown in Fig. 3.1a, and presented in Table 3.4. Following the established trend (Jo et al. 2001, Lee and Shackelford 2005b, and Katsumi et al. 2008), the SI of Na-B decreased with increasing CaCl_2 concentration, with the majority of swell decrease occurring between 5 and 50 mM CaCl_2 (28.7- to 10.2-mL/2 g). At CaCl_2 concentrations ≥ 50 mM, the SI of Na-B was in the range typical of Ca-bentonite (8-to-10 mL/2 g). Based on the experimentally derived correlations between SI and k proposed by Jo et al. (2001) and Kolstad et al. (2004), Na-B was anticipated to have $k > 1 \times 10^{-10}$ m/s in 50, 200, or 500 mM CaCl_2 solutions.

The trend of decreasing swell with increasing CaCl_2 concentration was also exhibited by SAP. Superabsorbent polyacrylate swelled to 1790-mL/2 g in DW, 58-times greater than Na-B, but the magnitude of swell reduction was also extenuated in SAP. In 500 mM CaCl_2 , SAP exhibited a SI only slightly greater than Na-B (13.2-mL/2 g

versus 8.0-mL/2 g) and 135-times less than in DW. In contrast, for Na-B only a 3.8-times reduction in SI was observed between DW and 500 mM CaCl_2 ; these results illustrate the tremendous sensitivity of SAP swell to CaCl_2 concentration.

The SI of BPN in DW was > two times the SI of Na-B (73.0- vs. 30.5-mL/2 g). However, similar to both Na-B and BPN, SI decreased with increasing CaCl_2 concentration, reaching a SI typical of Ca-bentonite in 200 and 500 mM CaCl_2 (< 8.0-mL/2g). In 50 mM CaCl_2 , BPN swelled to 18.8-mL/2 g, a SI correlated by Jo et al. (2001) and Kolstad et al. (2004) to a $k < 1 \times 10^{-10}$ m/s. Based on the SI correlations of Jo et al. (2001) and Kolstad et al. (2004) Na-B was anticipated to have a $k > 1 \times 10^{-10}$ m/s in 200 and 500 mM CaCl_2 .

The SI of Na-B, SAP, and BPN are presented at varying pHs in Fig. 3.1b. Circumneutral data are for tests in DW. The swell of Na-B in both 1 M NaOH and 1 M HNO_3 was in the range typical of bentonite that had only undergone crystalline swell (e.g., Ca-bentonite). Comparable low swells also were exhibited by BPN in both extreme pH solutions. Similar results were shown by Jo et al. (2001) for pH 1 HCl, and a pH 13 NaOH (0.1 M NaOH). Jo et al. (2001) showed that aluminum (Al) had been dissolved from the alumina sheets by analyzing the effluents from permeability tests by ICP-OES and postulated that Al^{3+} for Na^+ exchange might partially underlie the observed SI. Similar dissolution of alumina was not observed with the NaOH solution, although Jo et al. (2001) noted that this might have been due to alumina-complex formation and precipitation mediating Al^{3+} in the effluent solution. Jo et al. (2001) also hypothesized that a partial reason for the low swells in 0.1 M NaOH was the high Na^+

concentration in solution reducing osmotic swell. Both 1 M NaOH and 1 M HNO₃ had ionic strengths in the range shown by Jo et al. (2001) to result in swell indices typical of Ca-bentonite when tested with circumneutral pH solutions with identical monovalent cation concentrations. Thus, while dissolution of alumina and resultant Al³⁺ for Na⁺ exchange may have occurred in these solutions, the observed low SI were likely the result of high ion concentrations in the hydrating solutions. Both 1 M NaOH and 1 M HNO₃ had electrical conductivities higher than any of the CaCl₂ solutions tested (Table 3.3).

The swell of SAP was reduced relative to DW by a factor of 22.8 in 1 M NaOH, and by a factor of 66.3 in 1 M HNO₃ (Fig. 3.1b, Table 3.4). These data are consistent with trends reported by Elyashevich et al. (2009) for sodium-polyacrylate hydrogels. At low pH, Na⁺ ions in the SAP were replaced by H⁺ ions reducing polyelectrolyte dissociation and consequently reducing swelling (Elyashevich et al. 2009). At high pH, ion screening from the high concentration of Na⁺ from NaOH resulted in a decreased concentration gradient and consequently less osmotic swell.

3.5.2. Temporal Hydraulic Behavior with DW

Hydraulic conductivity profiles for tests conducted with DW are shown versus average cumulative flow (ACF) in Fig. 3.2. Average cumulative flow is calculated as the mean of the cumulative inflow and the cumulative outflow. Average cumulative flow, is used to quantify flow because of the poor initial agreement between inflow and outflow in BPN tests during flushing cycles (discussed subsequently). Pore volumes of flow were not used because the pore volume changed temporally due to solids-mass elution

during testing (discussed subsequently). In tests with BPN, k initially crashed to $\approx 1 \times 10^{-12}$ m/s, at which time all permeameter lines were flushed to remove possible clogging. Tests were then re-initiated, and k of $\approx 8 \times 10^{-11}$ m/s was measured, followed again by crashing. Upon re-flushing, precipitated polyacrylate was observed at brass fittings (Fig. 3.3). All brass fittings were subsequently replaced with flexible acrylic tubing with pinch-clamps, and permeation was re-initiated. Removal of brass fittings did not eliminate clogging, but did limit complete immobilization of flow by precipitated polymer in fitting constrictions. Eluted polyacrylate was observed in both the inflow and outflow lines during flushing.

Elutable polyacrylate in BPN was the result of early termination of polyacrylate chains during manufacture. A partial implication of these remnants was the permeameter clogging exhibited in most BPN- k tests (with the exception of 1 M HNO_3). Polymer eluted from tests with DW was determined by gel permeation chromatography to have a weight average molecular weight (M_w) of 280,000 g/mol, and a polydispersity index (weight average molecular weight over number average molecular weight) of approximately 6.0, illustrating a wide range of polyacrylate molecular weights were present. In contrast, a $M_w > 1,000,000$ g/mol is typical for SAP (Buckholz and Graham 1998), and was the intended M_w of SAP in BPN.

To expedite the flushing of mobile polymer and the attainment of equilibrium, the hydraulic gradient of one BPN test permeated with DW was increased from 75 to 500 after 380 d. The duplicate BPN test was maintained at a hydraulic gradient of 75 for the duration of testing. Hydraulic equilibrium was rapidly achieved at a hydraulic gradient of

500 (Fig. 3.2a), and yielded a similar equilibrium k to the test maintained at a hydraulic gradient of 75. To explore the impact of a higher hydraulic gradient on initial test clogging, a BPN specimen was assembled and permeated with DW at a 500-gradient. Reduced clogging as well as attainment of hydraulic equilibrium in a shorter duration was observed, although the hydraulic equilibrium occurred at a similar ACF (Fig. 3.2a). The equilibrium k of BPN tested at a high gradient was slightly lower than tests initially permeated at a hydraulic gradient of 75; this behavior is discussed later when examining the impact of hydraulic gradient on BPN k .

Na-B permeated with DW maintained a stable k between $1\text{--}2 \times 10^{-11}$ m/s irrespective of hydraulic gradient (Fig. 3.2b). SAP specimens absorbed water for the first 50-60 days of testing (crashing exhibited at low ACF in Fig. 3.2b), and then hydraulically equilibrated to a stable k approximately one order-of-magnitude lower than Na-B or BPN. All duplicate tests yielded similar hydraulic behavior.

3.5.3. Temporal Behavior with 50 mM CaCl_2

Hydraulic conductivity profiles for tests conducted with 50 mM CaCl_2 are shown versus ACF in Fig. 3.4a, and versus time in Fig. 3.4b. BPN permeated with 50 mM CaCl_2 initially exhibited a crash/flush pattern similar to BPN tests with DW. However, after an ACF of 275 mL, the k of BPN with 50 mM CaCl_2 equilibrated to 8.1×10^{-11} m/s in both tests (Fig. 3.4a). Similar crashing followed by eventual increase to an equilibrium k was exhibited by BPN in 5 and 20 mM CaCl_2 . The hydraulic gradient of the duplicate BPN specimen permeated with 50 mM CaCl_2 was increased to a hydraulic gradient of 500 after an approximate ACF of 2000 mL to expedite additional polymer

flushing and investigate the correlated impact on long term hydraulic behavior (Fig. 3.4). No long-term deviation in behavior was observed at the elevated hydraulic gradient tested.

Na-B permeated with 50 mM CaCl_2 maintained a high k ($> 7 \times 10^{-8}$ m/s) for the duration of testing (Fig. 3.4). Similarly, SAP maintained a $k > 3.3 \times 10^{-7}$ m/s for the duration of testing (Fig. 3.4). To ensure that the lower equilibrium k observed in BPN was not an artifact of permeameter clogging, after each BPN test was terminated, all geosynthetics were stripped from the clay specimens and reassembled in the same permeameter. The system was then re-permeated. In all cases, the rate of flow through the system was in excess of 5-orders-of-magnitude greater than the highest k observed during BPN testing.

3.5.4. Temporal Behavior with 500 mM CaCl_2

Hydraulic conductivity profiles for tests conducted with 500 mM CaCl_2 are shown versus ACF in Fig. 3.5a and versus time in Fig. 3.5b. BPN permeated with 500 mM CaCl_2 exhibited the greatest response to polymer clogging. Even after increasing the hydraulic gradient of one BPN test to 500, the pattern of crashing until flushing continued for approximately 400 days (Fig. 3.5b). Eventually, both BPN tests equilibrated to a k less than 6.9×10^{-13} m/s. Eventual equilibrium to a lower k only occurred in BPN with 200 and 500 mM CaCl_2 . Both Na-B and SAP exhibited stable and high k ($> 3.5 \times 10^{-7}$ m/s) from the onset of testing (Fig. 3.5), and met chemical equilibrium termination criteria from the onset of outflow.

3.5.5. Temporal Behavior with Strong Acid and Strong Base

Hydraulic conductivity profiles for tests conducted with 1 M NaOH are shown versus ACF in Fig. 3.6a. Permeation with 1 M NaOH did not prevent permeameter clogging, but did affectedly lessen the number of required cleanings to eliminate clogging. After only two clogging cycles, the k of BPN steadily increased to a final equilibrium of 1.8×10^{-11} m/s. This increasing trend is disconsolate with the precipitation of ions in hydraulically active pores causing long term reductions in k that was hypothesized to underlie observed long-term behavior of GCLs permeated with NaOH by Benson et al. (2010). Throughout permeation the ratio of EC_{out}/EC_{in} was approximately 0.40 for both tests, illustrating probable precipitation of cations within the BPN matrix. The observed increase in k is hypothesized to be the result of mobile-polymer flushing from the BPN layer. Permeation of Na-B with 1 M NaOH resulted in a steady and high $k > 1 \times 10^{-8}$ m/s. The high k observed from the onset of testing is likely an indicator that the high ionic strength of the permeant solution suppressing osmotic swell, and not hydraulically impactful mineral dissolution. These findings corroborate those of Ruhl and Daniel (1997) who showed that when a non-prehydrated GCL was permeated directly with 0.1 M NaOH (pH = 13), the GCL had a k of approximately 1×10^{-8} m/s. SAP was also permeated with 1 M NaOH, but dissolved during testing and is therefore not included in Fig. 3.6a. Dissolution was likely the result of gradual hydrolysis catalyzed by OH^- ions in the strongly alkaline permeant.

Hydraulic conductivity is shown versus ACF for tests with 1 M HNO_3 in Fig. 3.6b. BPN permeated with 1 M HNO_3 did not exhibit the permeameter clogging characteristic of BPN with other permeants, but maintained a $k < 4 \times 10^{-11}$ m/s. In contrast, Na-B

permeated with 1 M HNO_3 exhibited a steady and high $k > 1 \times 10^{-7}$ m/s. A similar k (1.5×10^{-7} m/s) was observed by Jo et al. (2001) when directly permeating a granular-Na-B GCL with pH = 1 HCl solution. SAP permeated with 1 M HNO_3 also exhibited a steady $k > 1.9 \times 10^{-7}$ m/s for the duration of testing. This high k is likely the result of extensive replacement of Na^+ ions with H^+ ions and resultant weakening of the osmotic swelling potential of the polyelectrolyte (Elyashevich et al. 2009) in the high ionic strength permeant solution.

3.5.6. Hydraulic Conductivity

Hydraulic conductivity of BPN, Na-B, and SAP at chemical equilibrium are summarized in Table 3.4 and shown versus permeant CaCl_2 concentration in Fig. 3.7a. BPN exhibits a $k < 8.5 \times 10^{-11}$ m/s in all CaCl_2 solutions tested. In contrast, both Na-B and SAP exhibit k at least 2500-times greater ($> 1.7 \times 10^{-7}$ m/s) in solutions of 20 (SAP only), 50, 200, and 500 mM CaCl_2 . When permeated with 500 mM CaCl_2 , the k of BPN is $>$ five orders-of-magnitude lower than Na-B or SAP.

Hydraulic conductivities of BPN, Na-B, and SAP are shown versus pH in Fig. 3.7b. Data for neutral pH are from tests with DW used as the permeant solution. The k of BPN is independent of pH between 0.3 and 13.1. In contrast, Na-B exhibits elevated k in both strong acidic and hyperalkaline solutions. The high observed k of Na-B is likely the result of the high ionic strength of both 1 M HNO_3 and 1 M NaOH suppressing osmotic swell as exhibited in swell index tests (Fig. 3.1b). These data illustrate the potential of BPN in mining waste containment applications where extreme pH leachates are commonplace.

3.5.7. Swelling and Specimen Water Content

Gravimetric water contents of BPN, Na-B, and SAP specimens after long term permeation are shown versus permeant solution CaCl_2 concentration in Fig. 3.8a. The gravimetric water content of BPN specimens had an inverse correlation to CaCl_2 concentration; a similar inverse relationship existed in Na-B, but the difference in gravimetric water content between DW and 500 mM CaCl_2 was only 70% (135% with DW to 65% with 500 mM CaCl_2), compared to 509% for BPN (554% with DW to 45% with 500 mM CaCl_2). Both BPN and Na-B had similar, low, gravimetric water contents with 500 mM CaCl_2 (45% to 66%), however, BPN swelled to more than four times the gravimetric water content of Na-B in DW.

Despite containing only $1/10^{\text{th}}$ the material, SAP adsorbs a similar total volume of water in DW by reaching a gravimetric water content of 4,420%. In contrast, the gravimetric water content of SAP specimens in 50 and 500 mM CaCl_2 ranges from 126-145%. These data underscore the hypersensitivity of SAP swell to permeation with CaCl_2 . The extreme sensitivity of SAP to varying CaCl_2 concentrations makes quantitative comparisons between SAP and Na-B / BPN difficult because of the varying specimen masses in each test. Nonetheless, qualitative SAP behavior should be comparable to Na-B / BPN since additional SAP not hypothesized to not result in unique behavior.

The gravimetric water content of BPN, Na-B, and SAP specimens after long-term permeation is shown at corresponding swell indices measured in the permeant solution in Fig. 3.8b. A linear relationship was evident between the gravimetric water content of

the specimen and swell index. These data illustrate that swell index correlates to swelling of specimens in the permeameter for all three materials, and is thus a reliable indicator of specimen swelling.

Swell index of Na-B and BPN from tests on the bulk materials in the permeant solutions are presented against swell indices in DW after permeation with CaCl_2 solutions in Fig. 3.9. In concentrated CaCl_2 solutions ($> 20 \text{ mM CaCl}_2$ for Na-B, $> 50 \text{ mM CaCl}_2$ for BPN) swell after permeation remained within the typical minimum swell range that was characteristic of Ca-bentonite. With the exception of tests with 50 mM CaCl_2 , BPN swell was similar before and after permeation, illustrating that in the dilute regime ($< 50 \text{ mM CaCl}_2$) long term exposure with divalent solutions does not result in further reductions in swell. But, in 50 mM CaCl_2 , BPN swell decreases from 18.8- to 7-8-mL/2 g; the mechanisms underlying this behavior are unknown.

Na-B exhibited lower swell after permeation with all solutions, with swell indices near those typical of Ca-bentonite after permeation with 5 and 20 mM CaCl_2 . These data illustrate the impact of rate limited cation exchange during the permeation of originally Na-B GCLs with dilute CaCl_2 solutions (Jo et al. 2006). The decrease of SI after permeation with DW illustrates that cation exchange occurred, and thus that there was a source of multivalent cations for exchange within the GCL. The calcite (CaCO_3) content of Na-B was determined by the methods described in ASTM D4373. Upon observing similar behavior, Guyonnet et al. (2005) determined that calcite dissolution within the GCL was the likely source of multivalent cations for exchange. Na-B initially contained 1.23% CaCO_3 (by mass); at the termination of permeation with DW, Na-B

retained, on average, only 0.21% calcite (by mass). Thus calcite dissolution likely contributed to the observed decrease in swelling via cation exchange.

3.5.8. Swelling and Hydraulic Conductivity

Hydraulic conductivity is presented versus SI in Fig. 3.10. The k of BPN was independent of SI. This decoupling of swell and k was in contrast to Na-B and SAP. In both Na-B, and SAP, $SI > 16\text{-mL/2 g}$ in solutions with CaCl_2 concentrations $\leq 20\text{ mM}$ corresponded to $k < 3 \times 10^{-11}\text{ m/s}$, while $SI < 11\text{-mL/2 g}$ in solutions with CaCl_2 concentrations $\geq 50\text{ mM}$ corresponded to $k > 1.7 \times 10^{-7}\text{ cm/s}$. The k of BPN remained $< 8 \times 10^{-11}\text{ m/s}$ in all permeant solutions, with the lowest SI (7-mL/2 g) corresponding to the lowest measured k (in 500 mM CaCl_2). Thus the mechanism underlying the superior hydraulic performance of BPN in CaCl_2 concentrations $\geq 50\text{ mM CaCl}_2$ does not correspond to the attainment and maintenance of osmotic swell. A detailed analysis of the mechanisms underlying the hydraulic performance of BPN is outside the scope of this paper, but is the subject of Chapter 4.

3.5.9. Polymer Retention

The fraction of polymer remaining within BPN specimens after long term permeation is presented at varying CaCl_2 concentrations in Fig. 3.11a. BPN initially contained 28.5% polymer by mass. The elution of mobile polymer showed a linear relationship to the permeant CaCl_2 concentration, with the greatest polymer elution occurring in specimens permeated with DW. A coefficient of determination of 0.99 was calculated for a linear regression through the data, demonstrating that a linear model was a good fit for the data. At the termination of long term permeation, BPN

permeated with DW retained only 23-24% of the original polymer content. In contrast, BPN permeated with 500 mM CaCl_2 retained 91-94% of original polymer.

The fraction of polymer remaining within BPN was a function of the cumulative permeameter inflow (Fig. 3.11b), with the largest polymer elution occurring at the initial stages of permeation. These results are supported by the temporal reduction of permeameter clogging shown in Figs. 3.2, 3.4, and 3.5. The elution of polymer was slowed in tests permeated with stronger CaCl_2 solutions, with the most gradual elution occurring in 500 mM CaCl_2 . Continued elution was evident for BPN permeated with 50 mM CaCl_2 between 2840 mL and 10370 mL; however the apparent longevity of continued elution only illustrates that elution continued beyond 2840 mL of total inflow and not that elution continued to 10370 mL (or beyond). BPN permeated with DW appeared to mobilize all elutable polymers by 1745 mL of cumulative inflow.

3.6. DISCUSSION

3.6.1. Polymer Content

The fraction of polymer remaining within BPN at the termination of permeation is shown against corresponding equilibrium k in Fig. 3.12. Across the range of CaCl_2 solutions tested, the minimum observed k corresponded to the greatest polymer retention (with 500 mM CaCl_2). Increased polymer retention correlated to decreased k in 50, 200, and 500 mM CaCl_2 . The SI of BPN at the termination of permeation with 50, 200, and 500 mM CaCl_2 were in the range typical of Ca-bentonite. Thus, increased

polymer within BPN is hypothesized to correlate to the observed, atypical, swell- k disconnect.

A general inverse correlation between k and polymer retention with DW, 5, 20, and 50 mM CaCl_2 illustrates that the retention of polymer is unlikely to govern k in these solutions. Potentially in 50 mM CaCl_2 and likely more dilute solutions, k was governed by the bulk immobilization of water by osmotic swelling, comparable to natural Na-bentonite. With DW, 5, 20, or 50 mM CaCl_2 , the SI of BPN in the permeant solution is within or above the range ($> 16\text{-mL/2 g}$) typically associated with low k in Na-bentonite under similar testing conditions (Jo et al. 2005).

3.6.2. SAP as a Hydraulic Barrier Material

As part of this study, the performance of SAP in long term hydraulic barrier applications was investigated. In DW, SAP exhibits a k one order-of-magnitude lower than either Na-B or BPN (2.7×10^{-12} m/s vs. $2.1\text{-}2.5 \times 10^{-11}$ m/s), and a corresponding swell index 58-times greater than Na-B and 24-times greater than BPN. Thus, on an index property level, SAP far outperformed Na-B. SAP also exhibited hypersensitivity to increased divalent cation concentrations, and extreme pHs, exhibiting $k \geq 1.0 \times 10^{-7}$ with CaCl_2 concentrations > 5 mM or in 1 M HNO_3 . In 1 M NaOH, SAP completely dissolved during k testing. The SI of SAP decreases from 1790-mL/2 g in DW, to 445-mL/2 g in 5 mM CaCl_2 , and to only slightly more than Na-B in 500 mM CaCl_2 (13.2-mL/2 g versus 8.0-mL/2 g). This behavior is anticipated in SAP, as ionic crosslinking by Ca^{2+} ions stitch together carboxyl groups and cause “catastrophic collapse” of the polymer gel (Buckholz and Graham 1998). Thus, while SAP exhibits a SI of 222-mL/2 g in 20 mM

CaCl₂, long-term k testing still revealed an equilibrium k of 3.1×10^{-7} m/s, 7950- to 11070-times > the k of Na-B or BPN with the same solution.

3.6.3. Impact of Hydraulic Gradient on CaCl₂ Tests

An unintended consequence of the large variability in BPN swell and corresponding specimen thicknesses was a wide range of applied hydraulic gradients during k testing. Nevertheless, the range of applied gradients was within the range typical for GCL testing (Shackelford et al. 2000). Additionally, Petrov et al. (1997) and others have shown that GCLs are insensitive to hydraulic gradients less than 550, and Rad et al. (1994) showed that the k of a GCL was unaffected by hydraulic gradients as large as 2800.

Yet, because the mechanism for low- k in BPN is dissimilar to that of Na-B (i.e., not correlated to swell), the impact of hydraulic gradient on BPN was investigated. Average hydraulic gradients of BPN tests initially ranged from 75 (with DW) to 375 (with 500 mM CaCl₂). In one replicate test with DW, 50 mM CaCl₂, and 500 mM CaCl₂ the hydraulic gradients were increased to 500 mid-test to speed the out-washing of mobile polymer and the onset equilibrium. The temporal impact of increasing the hydraulic gradient from 275 to 500 (for the test with 50 mM CaCl₂) is shown in Fig. 3.4, and for increasing the hydraulic gradient from 375 to 500 (for the test with 500 mM CaCl₂) in Fig. 3.5. These increases in hydraulic gradient did not result in a variation of k relative to the replicate test. The impact of increasing the hydraulic gradient from 75 to 500 (for the test with DW) is shown in Fig. 3.2. However, due to the thickness of BPN specimens in DW (≈ 18 mm) an increase of the average effective stress to 55 kPa was

required to achieve a hydraulic gradient of 500 while maintaining the inflow-end pressure < the cell pressure. This increase in effective stress and coupled increase of hydraulic gradient did not impact k with respect to the replicate test (Fig. 3.2). An additional test of BPN with DW was assembled to investigate the impact of increased effective stress on the hydration and polymer-elution of BPN (Fig. 3.2). The higher gradient reduced the severity of permeameter clogging, but did not eliminate this behavior. Equilibrium k was 1.4×10^{-11} m/s, on the order of, but slightly lower than, tests that were first hydrated and permeated at a lower effective stress (20 kPa versus 55 kPa). These data illustrate the potential sensitivity of BPN to effective stress during hydration. Additional research into the impact on k of increased effective stress during and after hydration is warranted.

3.6.4. Inter-Laboratory Duplication

Replicate tests were conducted at CSU to ensure the validity of experimental results. In general, excellent agreement between datasets was observed. Swell indices of Na-B and BPN determined at UW are compared to corollary data from CSU in Fig. 3.13a. In DW, 5 mM CaCl_2 , and 50 mM CaCl_2 , the standard deviation between corresponding swell indices was within 4% of the mean. For tests in 500 mM CaCl_2 , the standard deviation was within 14% of the mean (for Na-B, SI = 6.7-mL/2 g at CSU, 8.0-mL/2 g at UW; for BPN, SI = 8.5-mL/2 g at CSU, 7.0-mL/2 g at UW). No bias was evident in the paired SI data.

Replicate k tests were also conducted at CSU to ensure validity of long-term hydraulic behavior. Similar to SI, excellent agreement was observed. Nearly all tests were within a factor of two, the typical reproducibility associated with GCL k testing

(Petrov et al. 1997, Shackelford et al. 2000); the exception was BPN with 500 mM CaCl_2 . Replicate long term k testing on GCLs reported by Jo et al. (2005) warns of two potential sources of k -test inter-laboratory variation: Effective stress variation, and clogging of permeameter tubing by salt precipitates. Standardization of effective stress was easily accomplished. To minimize the potential for clogging during long term testing, both UW and CSU used permeameters that incorporated 6.4-mm outside-diameter (OD) tubing. Jo et al. (2005) reported clogging by salt precipitates only in tests with 3.2-mm OD tubing. Based on typical permeameter tubing, 6.4-mm OD tubing yields a factor of 5.4 increases in cross-sectional area relative to 3.2-mm OD tubing. No clogging was reported by Jo et al. (2005) when 6.4-mm tubing was employed, nor was any clogging observed for long-term testing of Na-B during the course of this study. The choice to use 6.4-mm OD tubing was also fortuitous based on the polymer-clogging by BPN during k testing. Exploratory tests on BPN in permeameters with 3.2-mm OD tubing yielded irremovable clogging within the first month of testing.

3.7. IMPLICATIONS

The results of comparative long-term testing for k illustrate that BPN is a more resistant alternative to traditional Na-B or SAP in waste containment applications. The data show that BPN may also allow for containment of high ionic strength leachates, mid-range-strength divalent leachates, and leachates with extreme pH that are typically incompatible with Na-B. As always, tests with site-specific leachates are recommended before extrapolating data from idealized testing conditions to field applications. These tests should also include field specific stress conditions.

The enhanced swell of BPN in DW as well as 5, 20, and 50 mM CaCl_2 was likely a result of the swelling contribution of the superabsorbent polymer component of BPN. Additional research is warranted to investigate if a physical mixture, viz. not an in-situ polymerized nanocomposite, can yield similar swelling behavior and hydraulic performance. The maintenance and even slight increase of BPN SI after permeation with dilute solutions illustrates that eluted polymer was likely not contributing to swell during preliminary SI tests. The high swelling of BPN relative to Na-B also illustrate the potential for BPN to be more effective than Na-B at closing defects in dilute solutions. Conversely, the enhanced swelling of BPN may lead to elevated risk of hydraulically significant desiccation effects (Benson and Meer 2009). The hydraulic impact of desiccation on BPN warrants further study.

In all permeants tested, BPN eluted polymer during permeation (Fig. 3.11) but maintained a $k < 8 \times 10^{-11}$ m/s (Fig. 3.12). These data illustrate that only a fraction of the polymer initially contained within BPN was necessary to maintain the low k observed at chemical equilibrium. Future generations of BPN manufactured with lower polymer loading may therefore be sufficient to produce similar hydraulic behavior. Further study of BPN as an additive to bentonite is discussed in Chapter 5.

3.8. CONCLUSIONS

Bentonite was modified at the nanoscale by polymerizing acrylic acid within sodium-bentonite slurry. The resulting bentonite-polymer nanocomposite (BPN) was then dried and ground to simulate the granule-size distribution typical within

geosynthetic clay liners (GCLs) composed of granular bentonite. Reference tests were conducted on GCL-grade Na-bentonite (Na-B) with similar granule size and super-absorbent polymer (SAP) representative of the intended polymeric constituent within BPN. BPN, Na-B, and SAP were tested for long term hydraulic conductivity (k) in deionized water (DW) (as a reference) as well as 5, 20, 50, 200, 500 mM CaCl_2 , 1 M NaOH, and 1 M HNO_3 . Dilute divalent solutions (5 and 20 mM CaCl_2) were chosen to investigate the impact of gradual cation exchange on long term k , and concentrated divalent solutions (50, 200, and 500 mM CaCl_2) were chosen to investigate the impact of high ionic strength coupled with divalent-for-monovalent cation exchange. Sensitivity to extreme pH (0.3 and 13.1) was investigated with 1 M HNO_3 and 1 M NaOH. Index property tests were performed on all materials. Replicate k and index property tests were conducted at CSU to validate experimental results. Based on the results reported in this study, the following conclusions can be distilled:

- Swell index tests indicate that BPN has greater swelling potential than Na-B in dilute solutions. For example, free swell tests with 2 g of Na-B swelled to 30.5 mL in DW, whereas the same amount of BPN swelled to 73 mL in the same solution.
- Similar to Na-B, the swell of BPN is sensitive to high concentrations of CaCl_2 , and extreme pHs. In 200 mM CaCl_2 , 500 mM CaCl_2 , 1 M NaOH, and 1 M HNO_3 BPN exhibits swell indices similar to calcium bentonite. These swells are within the range typically correlated to high k ($> 10^{-10}$ m/s).

- Low k ($< 8 \times 10^{-11}$ m/s) was maintained by BPN for all solutions tested. In contrast, matching tests on specimens prepared with Na-B and SAP had k approximately three orders-of-magnitude (at minimum) higher ($> 7 \times 10^{-8}$ m/s) when permeated with 50 mM CaCl_2 , 200 mM CaCl_2 , 500 mM CaCl_2 , 1 M NaOH, or 1 M HNO_3 .
- In aggressive solutions (200 mM CaCl_2 , 500 mM CaCl_2 , 1 M NaOH, or 1 M HNO_3) the k of BPN is decoupled from swell. In these solutions, BPN exhibits swell indices typically corollary to high k yet maintains a $k < 8 \times 10^{-11}$ m/s.
- During k testing, BPN eluted polyacrylate with all permeants. The extent of polymer elution was correlated to CaCl_2 concentration, with the least elution occurring in the strongest solution. Eluted polymer caused clogging of permeameter tubing that required manual flushing.
- SAP exhibits a swell index more than 58-times that of Na-B (1790- vs. 30.5-mL/2 g); however, similar to both BPN and Na-B, SAP swell decreases with increasing CaCl_2 concentration. In 500 mM CaCl_2 , the SI of SAP is only 13.2-mL/2 g, similar to Na-B or BPN. Similar to Na-B, solutions that produce large reductions in SAP swell concurrently result in $k > 1 \times 10^{-7}$ m/s, these solutions include: 20 mM CaCl_2 , 50 mM CaCl_2 , 200 mM CaCl_2 , 500 mM CaCl_2 , and 1 M HNO_3 . SAP was observed to dissolve during permeation with 1 M NaOH.

3.9. REFERENCES

- Ashmawy, A., Darwish, E., Sotelo, N., and Muhammad, N. (2002). "Hydraulic performance of untreated and polymer-treated bentonite in inorganic landfill leachates." *Clays and Clay Minerals*, 50(5), 546-552.
- ATU (1992). "ClayMax sodium bentonite liner found degraded at New Jersey site." *Aboveground Tank Update*, 3(2), 1, 17-18.
- Benson, C., Jo, H., and Abichou, T. (2004). "Forensic analysis of excessive leakage from lagoons lined with a composite GCL." *Geosynthetics International*, 11(3), 242-252.
- Benson, C. and Meer, S. (2009), "Relative abundance of monovalent and divalent cations and the impact of desiccation on geosynthetic clay liners." *J. of Geotech. and Geoenviron. Eng.*, 133(5), 814-827.
- Benson, C., Thorstad, P., Jo, H., and Edil, T. (2007). "Case history: hydraulic performance of geosynthetic clay liners in a landfill final cover." *J. of Geotech. and Geoenviron. Engr.*, 133(7), 814-827.
- Benson, C., Oren, A., and Gates, W. (2010). "Hydraulic Conductivity of Two Geosynthetic Clay Liners Permeated with a Hyperalkaline Solution." *J. Geotextiles and Geomembranes*, 28(2), 206-218.
- Bradshaw, S., Benson, C., and Scalia, J. (2012). "Cation exchange during subgrade hydration and effect on hydraulic conductivity of GCLs." Submitted to *J. of Geotech. and Geoenviron. Eng.*, (in press).
- Bouazza, A. (2010). "Geosynthetics lining in mining applications." *Proceedings of Sixth International Conference on Environmental Geotechnics*, International

- Society for Soil Mechanics and Geotechnical Engineers, New Delhi, India, 221-259.
- Buchholz, F., and Graham, A. (1998). *Modern Superabsorbent Polymer Technology*. John Wiley and Sons, New York.
- Claret, F. (2002). "Experimental investigation of the interaction of clays with high-pH solutions: a case study from the Callovo-Oxfordian formation, Haute Marne underground laboratory (France)." *Clays and Clay Minerals*, 50, 633–646.
- Di Emidio, G., Van Impe, W., Mazzieri, F. (2010). "A polymer enhanced clay for impermeable geosynthetic clay liners." *Proceedings of Sixth International Conference on Environmental Geotechnics*, International Society for Soil Mechanics and Geotechnical Engineers, New Delhi, India, 963-967.
- Di Emedio, G., Van Impe, W., Flores, V. (2011). "Advances in geosynthetic clay liners: polymer enhanced clays." *GeoFrontiers 2011. Advances in Geotechnical Engineering*, American Society of Civil Engineers, Reston, 1931-1940.
- Egloffstein, T. (2001). "Natural bentonites-influence of the ion exchange and partial desiccation on permeability and self-healing capacity of bentonites used in GCLs." *Geotextiles and Geomembranes*, 19, 427-444.
- Elyashevich, G., Bel'nikovich, N., and Vesnebolotskaya, S. (2009). "Swelling-concentration of sodium polyacrylate hydrogels in media with various pH values." *Polymer Science Series A*, 51(5), 550-553.
- Flynn, B., Carter, G. (1998). "Waterproofing material and method of fabrication thereof." *US Patent Number: 6,537,676 B1*.

- Gates, W. and Bouazza, A. (2010). "Bentonite transformations in strongly alkaline solutions." *Geotextiles and Geomembranes*, 28(2), 219-225.
- Gates, W., Anderson, J., Raven, M., and Churchman, G. (2002). "Mineralogy of a bentonite from Miles, Queensland, Australia and characterization of its acid activation products." *Applied Clay Science*, 20, 189-197.
- Grim, R. (1968). *Clay Mineralogy*, 2nd Edition. McGraw-Hill, New York.
- Guyonnet, D., Gaucher, E., Gaboriau, H., Pons, C., Clinard, C., Norotte, W., and Didier, G. (2005). "Geosynthetic clay liner interactions with leachate: Correlation between permeability, microstructure, and surface chemistry." *J. of Geotech. and Geoenviron. Eng.*, 131(6), 740-749.
- James, A., Fullerton, D., and Drake, R. (1997). "Field performance of GCL under ion exchange conditions." *J. of Geotech. and Geoenviron. Eng.*, 123(10), 897-901.
- Jo, H., Benson, C., and Edil, T. (2006). "Rate-limited cation exchange in thin bentonitic barrier layers." *Canadian Geotech. J.*, 43, 370-391.
- Jo, H., Benson, C., Shackelford, C., Lee, J., and Edil, T. (2005). "Long-term hydraulic conductivity of a non-prehydrated geosynthetic clay liner permeated with inorganic salt solutions." *J. of Geotech. and Geoenviron. Eng.*, 131(4), 405-417.
- Jo, H., Katsumi, T., Benson, C., and Edil, T. (2001). "Hydraulic conductivity and swelling of non-prehydrated GCLs permeated with single species salt solutions." *J. of Geotech. and Geoenviron. Engr.*, 127(7), 557-567.

- Jozefaciuk, G., and Matyka-Sarzynska, D. (2006). "Effect of acid treatment and alkali treatment on nanopore properties of selected minerals." *Clays and Clay Minerals*, 54, 220–229.
- Kashir, M., and Yanful, E. (2001). "Hydraulic conductivity of bentonite permeated with acid mine drainage". *Canadian Geotechnical Journal*, 38, 1034–1048.
- Katsumi, T., Onikata, M., Hasegawa, S., Lin, L., Kondo, M., and Kamon, M. (2001). "Chemical compatibility of modified bentonite permeated with inorganic chemical solutions." *Geoenvironmental Impact Management*, Thomas Telford, London, 419-424.
- Katsumi, T., Ishimori, Ho, Onikata, M., and Fukagawa, R. (2008). "Long-term barrier performance of modified bentonite materials against sodium and calcium permeant solutions." *Geotextiles and Geomembranes*, 26(1), 14-30.
- Kolstad, D., Benson, C., and Edil, T. (2004). "Hydraulic conductivity and swell of nonprehydrated GCLs permeated with multi-species inorganic solutions." *J. of Geotech. and Geoenviron. Engr.*, 130(12), 1236-1249.
- Lange, K., Rowe, R.K., and Jamieson, H. (2007). "Metal retention in geosynthetic clay liners following permeation by different mining solutions." *Geosynthetics International*, 14(3), 178–187.
- Lange, K., Rowe, R.K., Jamieson, H. (2009). "Diffusion of metals in geosynthetic clay liners." *Geosynthetics International* 16(1), 11-27.
- Lee, J. and Shackelford, C. (2005). "Impact of bentonite quality on hydraulic conductivity of geosynthetic clay liners." *J. of Geotech. and Geoenviron. Engr.*, 131(1), 64-77.

- Lee, J., Shackelford, C., Benson, C., Jo, H. and Edil, T. (2005). "Correlating index properties and hydraulic conductivity of geosynthetic clay liners." *J. Geotech. and Geoenviron. Engr.*, 131(11), 1319-1329.
- Lin, L. and Benson, C. (2000). "Effect of wet-dry cycling on swelling and hydraulic conductivity of geosynthetic clay liners." *J. of Geotech. and Geoenviron. Engr.*, 126(1), 40-49.
- McBride M. (1994). *Environmental Chemistry of Soils*. Oxford University Press, New York.
- McKelvey, J. (1997). "Geosynthetic clay liners in alkaline environments, Testing and acceptance criteria for geosynthetic clay liners." STP 1308, ASTM International, West Conshohocken, USA, 139-149.
- Mazzieri, F., Emidio, G., Van Impe, P. (2010a). "Diffusion of calcium chloride in a modified bentonite: Impact on osmotic efficiency and hydraulic conductivity." *Clays and Clay Minerals*, 58(3), 351-363.
- Mazzieri, F., Pasqualini, E., Emidio, G. (2010b). "Migration of heavy metals through conventional and factory-prehydrated GCL materials." *Proceedings of Sixth International Conference on Environmental Geotechnics*, International Society for Soil Mechanics and Geotechnical Engineers, New Delhi, India, 963-967.
- Meer, S. and Benson, C. (2007). "Hydraulic conductivity of geosynthetic clay liners exhumed from landfill final covers." *J. of Geotech. and Geoenviron. Engr.*, 133(5), 550-563.

- Muzny, C., Butler, B., Hanley, H., Tsvetkov, F., and Pfeiffer, D. (1996). "Clay platelet dispersion in a polymer matrix." *Materials Letters*, 28, 379-384.
- Onikata, M., Kondo, M., and Kamon, M. (1996). "Development and characterization of a multiswellable bentonite." *Environmental Geotechnics*. Taylor and Francis, Rotterdam, 587-590.
- Onikata, M., Kondo, M., Hayashi, N., and Yamanaka, S. (1999). "Complex formation of cation-exchanged montmorillonites with propylene carbonate: Osmotic swelling in aqueous electrolyte solutions." *Clays and Clay Minerals*, 47(5), 672-677.
- Petrov, R., Rowe, R., and Quigley, R. (1997). "Selected Factors Influencing GCL Hydraulic Conductivity." *J. of Geotech. and Geoenviron. Engr.*, 123(8), 683-695.
- Ramirez, S., Cuevas, J., Vigil, R., and Leguey, S. (2002). "Hydrothermal alteration of "La Serrata" bentonite (Almería, Spain) by alkaline solutions." *Applied Clay Science*, 21, 257-269.
- Rad, N., Jacobson, B., Bachus, R. (2004). "Compatibility of geosynthetic clay liners with organic and inorganic permeants." *Proc. Fifth International Conference on Geotextiles, Geomembranes and Related Products*, International Geosynthetics Society, Singapore, 1165-1168.
- Ruhl, J., and Daniel, D. (1997). "Geosynthetic clay liners permeated with chemical solutions and leachates." *J. of Geotech. and Geoenviron. Engr.*, 123(4), 369-381.
- Sanchez, L., Cuevas, J., Ramirez, S., Riuiz De Leon, D., Fernandez, R., Vigi Dela Villa, R., and Leguey, S. (2006). "Reactions of FEBEX bentonite in hyperalkaline

conditions resembling the cement–bentonite interface.” *Applied Clay Science*, 33, 125–141.

Scalia, J., and Benson, C.H. (2011). “Hydraulic conductivity of geosynthetic clay liners exhumed from landfill final covers with composite barriers.” *J. of Geotech. and Geoenviron. Engr.*, 137(1), 1-13.

Scalia, J., Benson, C. H., Edil, T. B., Bohnhoff, G. L., and Shackelford, C. D. (2011). “GCLs containing bentonite polymer nanocomposite.” *GeoFrontiers 2011. Advances in Geotechnical Engineering*, American Society of Civil Engineers, Reston, USA, 2001-2009.

Schroeder, C., Monjoie, A., Illing, P., Dosquet, D., and Thorez, J. (2001). “Testing a factory-prehydrated GCL under several conditions.” *Proceedings, Sardinia 2001, 8th International Waste Management and Landfill Symposium*, CISA Environmental Sanitary Engineering Centre, Cagliari, Italy, 187-196.

Shackelford, C., Benson, C., Katsumi, T., Edil, T., and Lin, L. (2000). “Evaluating the hydraulic conductivity of GCLs permeated with non-standard liquids.” *Geotextiles and Geomembranes*, 18(2-3), 133-161.

Shackelford, C. and Lee, J. (2003). “The destructive role of diffusion on clay membrane behavior.” *Clays and Clay Minerals*, 51(2), 187-197.

Shackelford, C., Sevic, G., and Eykholt, G. (2010). “Hydraulic conductivity of geosynthetic clay liners to tailings impoundment solutions.” *Geotextiles and Geomembranes*, 28(2), 149-162.

- Sposito, G. (1984). *The Surface Chemistry of Soils*. Oxford University Press, New York.
- Stumm, W. (1992). *Chemistry of the Solid-Water Interface*. John Wiley and Sons, New York.
- Stumm, W., and Morgan, J. (1996). *Aquatic Chemistry*, 3rd ed. Wiley, New York.
- Trauger R. and Darlington J. (2000). "Next-generation geosynthetic clay liners for improved durability and performance." *TR-220*, Colloid Environmental Technologies Company, Arlington Heights, IL, 2-14.
- U.S. EPA. (2007). *Method 6010B: Inductively coupled plasma-atomic emission spectrometry, physical/chemical methods SW846*, 3rd Ed. US Environmental Protection Agency, Office of Solid Waste and Emergency Response, Washington, DC.
- Vasko, S., Jo, H., Benson, C., Edil, T., and Katsumi, T. (2001). "Hydraulic Conductivity of Partially Prehydrated Geosynthetic Clay Liners Permeated with Aqueous Calcium Chloride Solutions." *Geosynthetics 2001*, Industrial Fabrics Assoc. International, St. Paul, Minnesota, 685-699.

3.10. ABBREVIATIONS

ACF – Average cumulative flow

ARL – Alumina refinery leachate

BAC – Bentonite amended for compatibility

BB – Na-bentonite base clay

BPA – Bentonite-polymer alloy

BPN – Bentonite-polyacrylate nanocomposite

DW – Deionized water

EC – Electrical conductivity

GCL – Geosynthetic clay liner

GT – Geotextile

k – Hydraulic conductivity

SAP – Superabsorbent polymer

SI – Swell index

MMT - Montmorillonite

Na-B – Sodium bentonite

Na-PA – Sodium polyacrylate

XRD – X-ray diffraction

3.11. TABLES

Table 3.1 Properties of Na-bentonite (Na-B) used in hydraulic conductivity tests, Na-bentonite used to produce BPN (BB), superabsorbent Na-polyacrylate (SAP), and bentonite-polyacrylate nanocomposite (BPN).

Material	ASTM D5890	ASTM D2216	ASTM D4373	ASTM D2487
	Swell index (mL/2 g)	Water content as received (%)	Carbonate content (%)	Soil classification
Na-B	31.4*	13.2	1.3	SP
BB	19.0*	0.8	0.6	-
SAP	1790	4.8	0.0	SP
BPN	72.7*	2.7	0.0	SP

*Average between Colorado State University and the University of Wisconsin.

Table 3.2 Soluble cations, bound cation, and cation exchange capacity (CEC) of Na-bentonite (Na-B) used in hydraulic conductivity tests, Na-B used to produce BPN (BB), and bentonite-polyacrylate nanocomposite (BPN).

Material	Soluble cations (cmol+/kg)				Bound cations (mole fractions)				CEC
	Na ⁺	K ⁺	Ca ²⁺	Mg ²⁺	Na ⁺	K ⁺	Ca ²⁺	Mg ²⁺	cmol+/kg
Na-B	18.1	0.4	0.2	0.1	0.44	0.02	0.36	0.17	78.0
BB	23.3	0.4	0.2	0.1	0.42	0.04	0.42	0.12	85.5
BPN	118	0.4	9.5	1.6	0.90	0.02	0.06	0.02	142.6

Table 3.3 Average measured parameters of permeant solutions.

Testing Liquid	Electrical conductivity (mS/cm)		pH	
	UW	CSU	UW	CSU
<0.05 mM CaCl_2	0.005	0.001	6.7	7.4
5 mM CaCl_2	1.34	1.05	6.1	5.3
20 mM CaCl_2	4.20	-	6.2	-
50 mM CaCl_2	11.0	-	6.5	-
200 mM CaCl_2	41.2	-	6.4	-
500 mM CaCl_2	98.9	64.3	6.8	5.4
1 M NaOH	112	-	13.1	-
1 M HNO_3	431	-	0.3	-

Table 3.4 Swell index and hydraulic conductivity of Na-bentonite (Na-B), superabsorbent Na-polyacrylate (SAP), and bentonite-polyacrylate nanocomposite (BPN) in varying calcium chloride (CaCl_2) solutions, 1 M NaOH, and 1 M HNO_3 . All data are the average of two or more duplicate tests, with the exception of hydraulic conductivities at Colorado State University (CSU) and hydraulic conductivities with 5 mM CaCl_2 at the University of Wisconsin – Madison.

Test Liquid	Na-B				SAP		BPN			
	Swell index (mL/2 g)		Hydraulic conductivity (m/s)		Swell index (mL/2 g)	Hydraulic conductivity (m/s)	Swell index (mL/2 g)		Hydraulic conductivity (m/s)	
	UW	CSU	UW	CSU			UW	CSU	UW	CSU
<0.05 mM CaCl_2	30.5	32.2	2.1×10^{-11}	1.6×10^{-11}	1790	2.7×10^{-12}	73.0	72.3	2.5×10^{-11}	6.2×10^{-12}
5 mM CaCl_2	28.7	30.2	2.3×10^{-11}	3.3×10^{-11}	445	2.1×10^{-11}	46.7	49.3	1.8×10^{-11}	2.4×10^{-11}
20 mM CaCl_2	16.0	-	2.8×10^{-11}	-	222	3.1×10^{-7}	30.5	-	3.9×10^{-11}	-
50 mM CaCl_2	10.2	10.3	1.7×10^{-7}	-	80.4	2.5×10^{-7}	18.8	19.5	8.1×10^{-11}	-
200 mM CaCl_2	9.0	-	4.3×10^{-7}	-	22.0	2.3×10^{-7}	8.0	-	2.8×10^{-11}	-
500 mM CaCl_2	8.0	6.7	4.5×10^{-7}	4.0×10^{-7}	13.2	4.0×10^{-7}	7.0	8.5	6.5×10^{-13}	9.7×10^{-13}
1 M NaOH	8.0	-	5.1×10^{-7}	-	78.4	x	10.5	-	1.8×10^{-11}	-
1 M HNO_3	10.0	-	3.4×10^{-7}	-	27.0	1.7×10^{-7}	13.3	-	3.3×10^{-11}	-

3.12. FIGURES

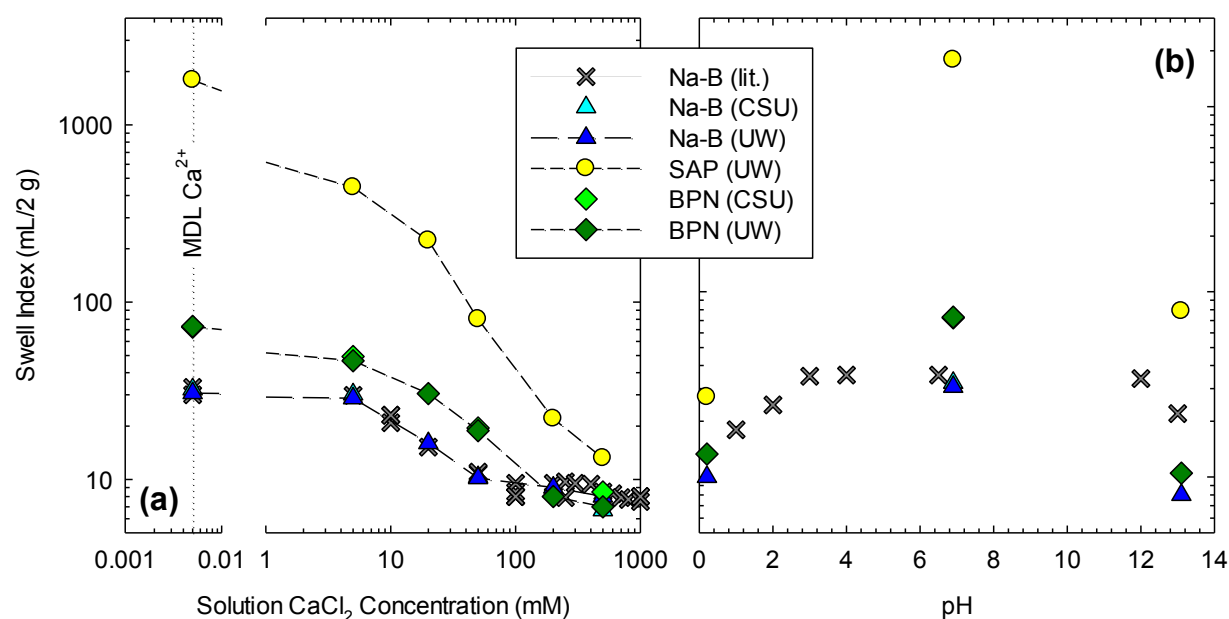


Fig. 3.1 Swell index versus solution CaCl_2 concentration (a) and pH (b) for Na-bentonite (Na-B), superabsorbent Na-polyacrylate (SAP), and bentonite-polyacrylate nanocomposite (BPN). Swell indices in DW are shown at the method detection limit (MDL) of Ca^{2+} . Literature data from Jo et al. (2001), Lee and Shackelford (2005b), and Katsumi et al. (2008) are included for comparison.

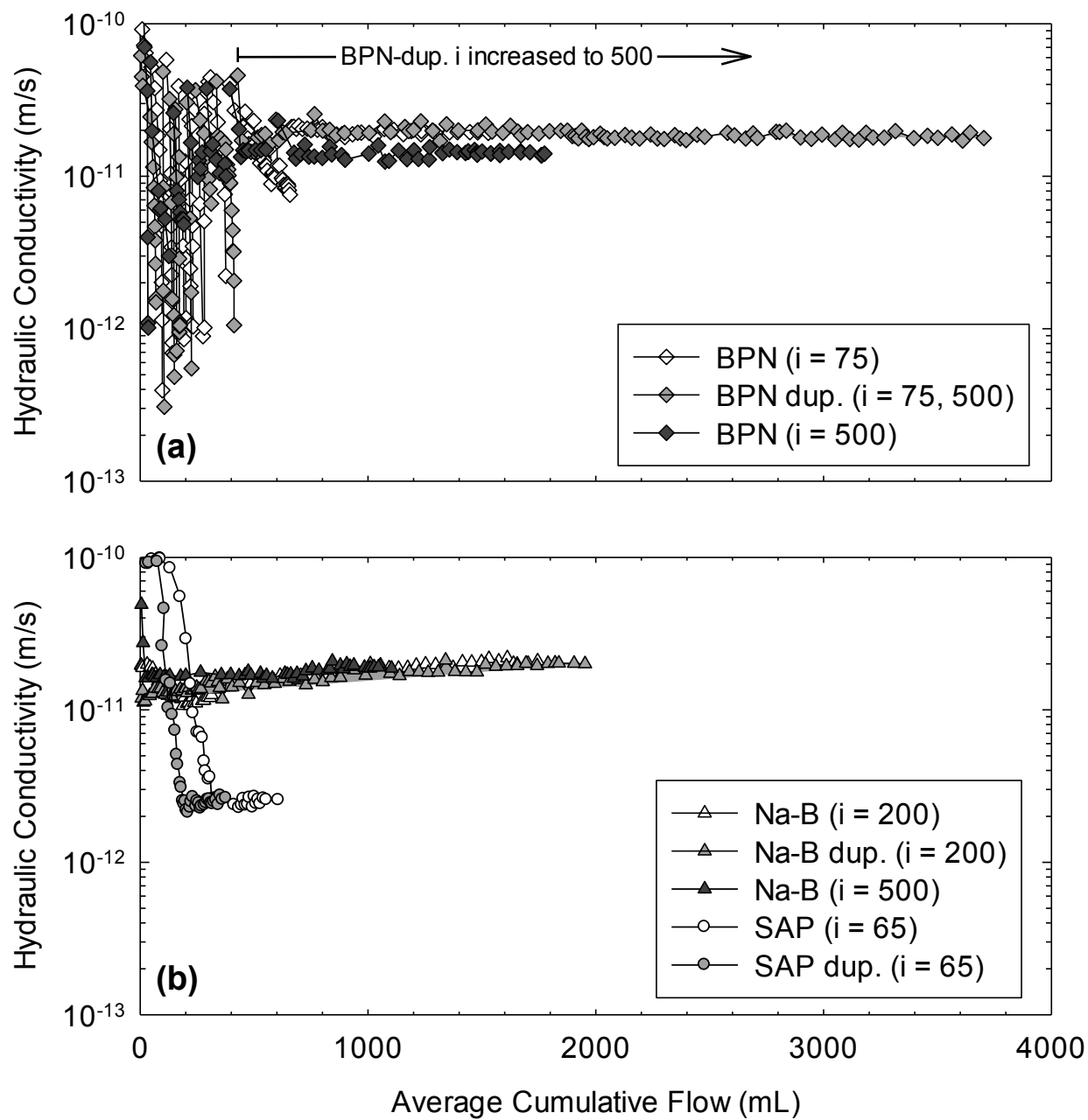


Fig. 3.2 Hydraulic conductivity profiles for bentonite-polyacrylate nanocomposite (BPN) (a) as well as superabsorbent Na-polyacrylate (SAP) and Na-bentonite (Na-B) (b) permeated with **deionized water** at varying hydraulic gradients (i). Average cumulative flow calculated as mean of cumulative inflow and cumulative outflow.

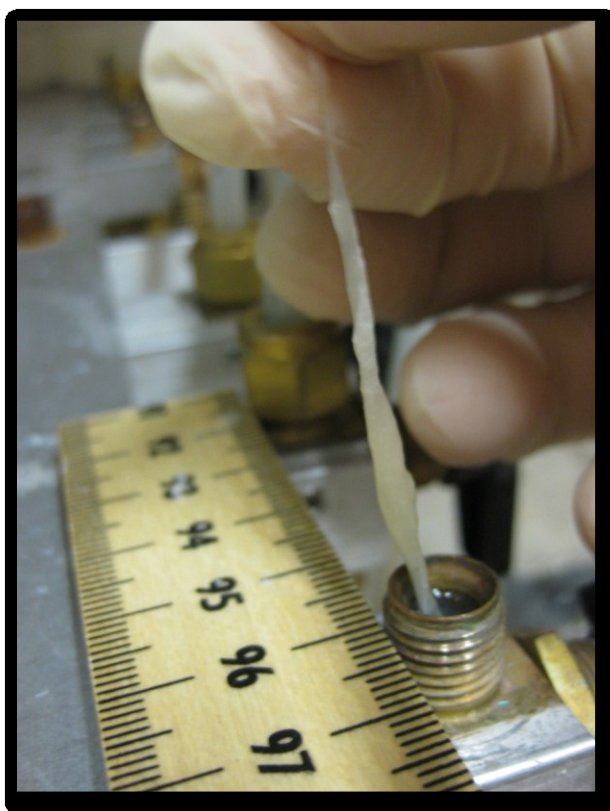


Fig. 3.3 Photograph of precipitated polymer being removed from clogged brass fitting.

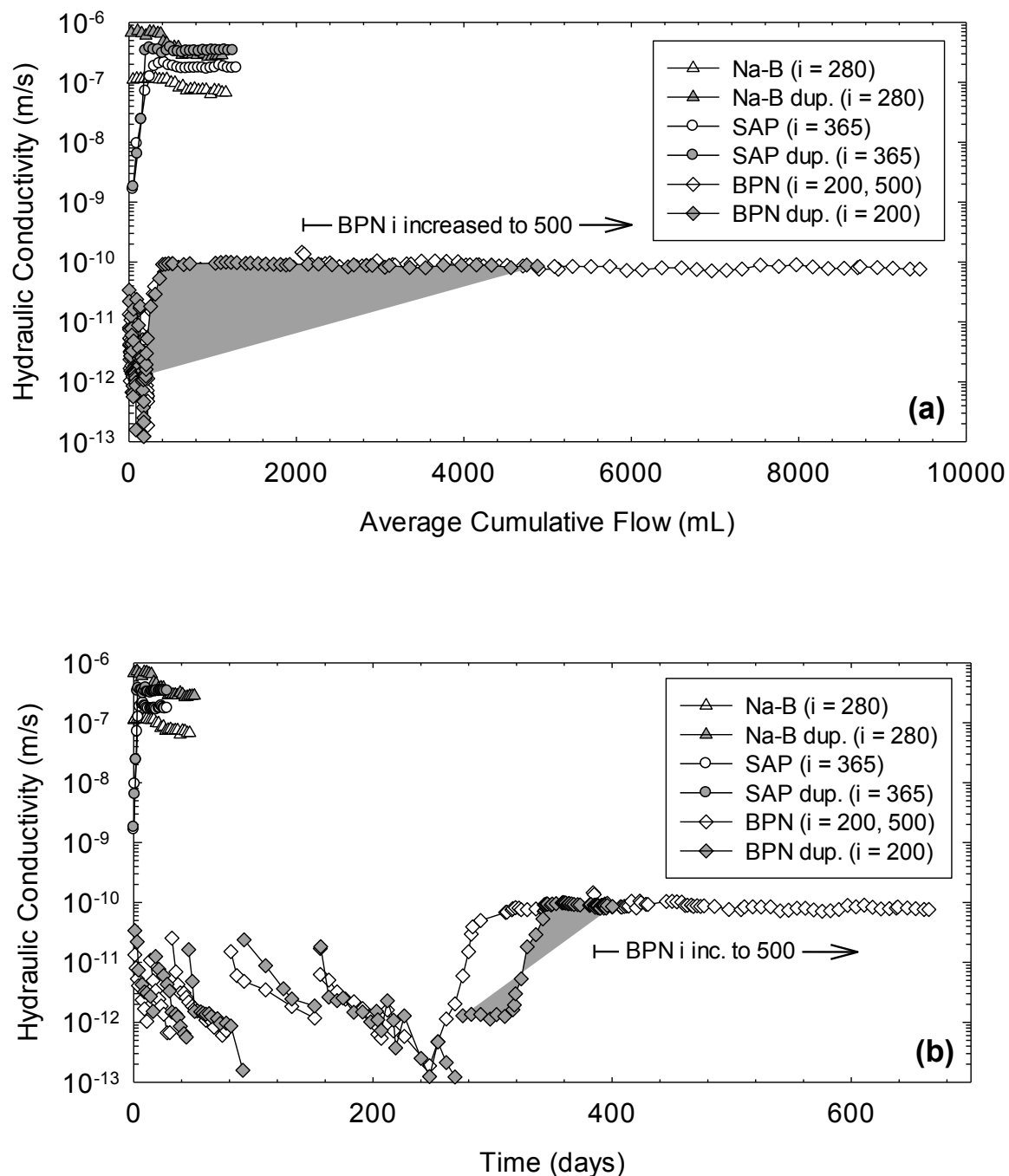


Fig. 3.4 Hydraulic conductivity versus average cumulative flow (ACF) (a) and time (b) for Na-bentonite (Na-B), superabsorbent Na-polyacrylate (SAP), and bentonite-polyacrylate nanocomposite (BPN), permeated with **50 mM CaCl_2** at varying hydraulic gradients (i). ACF calculated as mean of cumulative inflow and cumulative outflow.

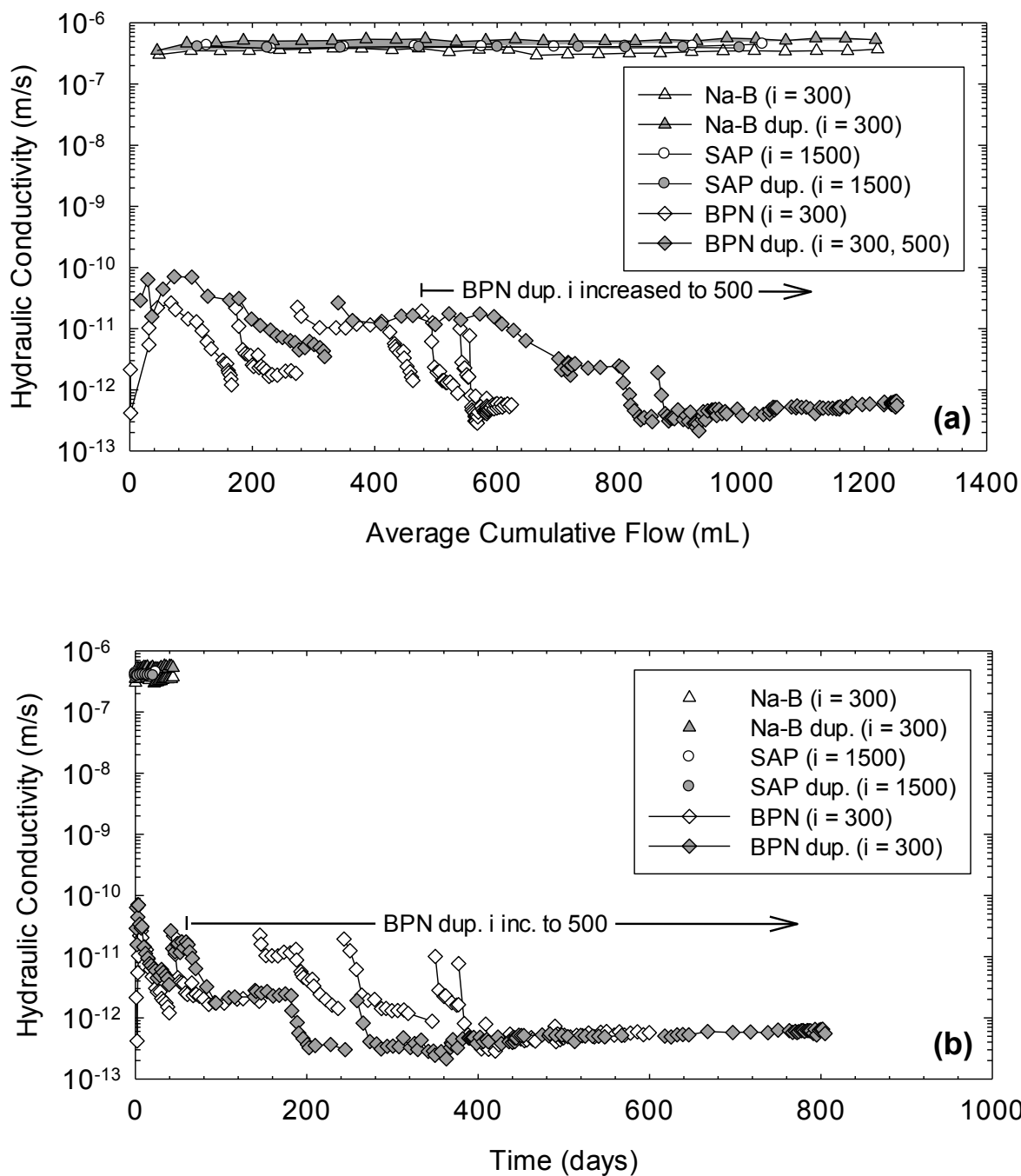


Fig. 3.5 Hydraulic conductivity versus average cumulative flow (a) and time (b) for Na-bentonite (Na-B), superabsorbent Na-polyacrylate (SAP), and bentonite-polyacrylate nanocomposite (BPN), permeated with **500 mM CaCl_2** at varying hydraulic gradients (i). ACF calculated as mean of cumulative inflow and cumulative outflow.

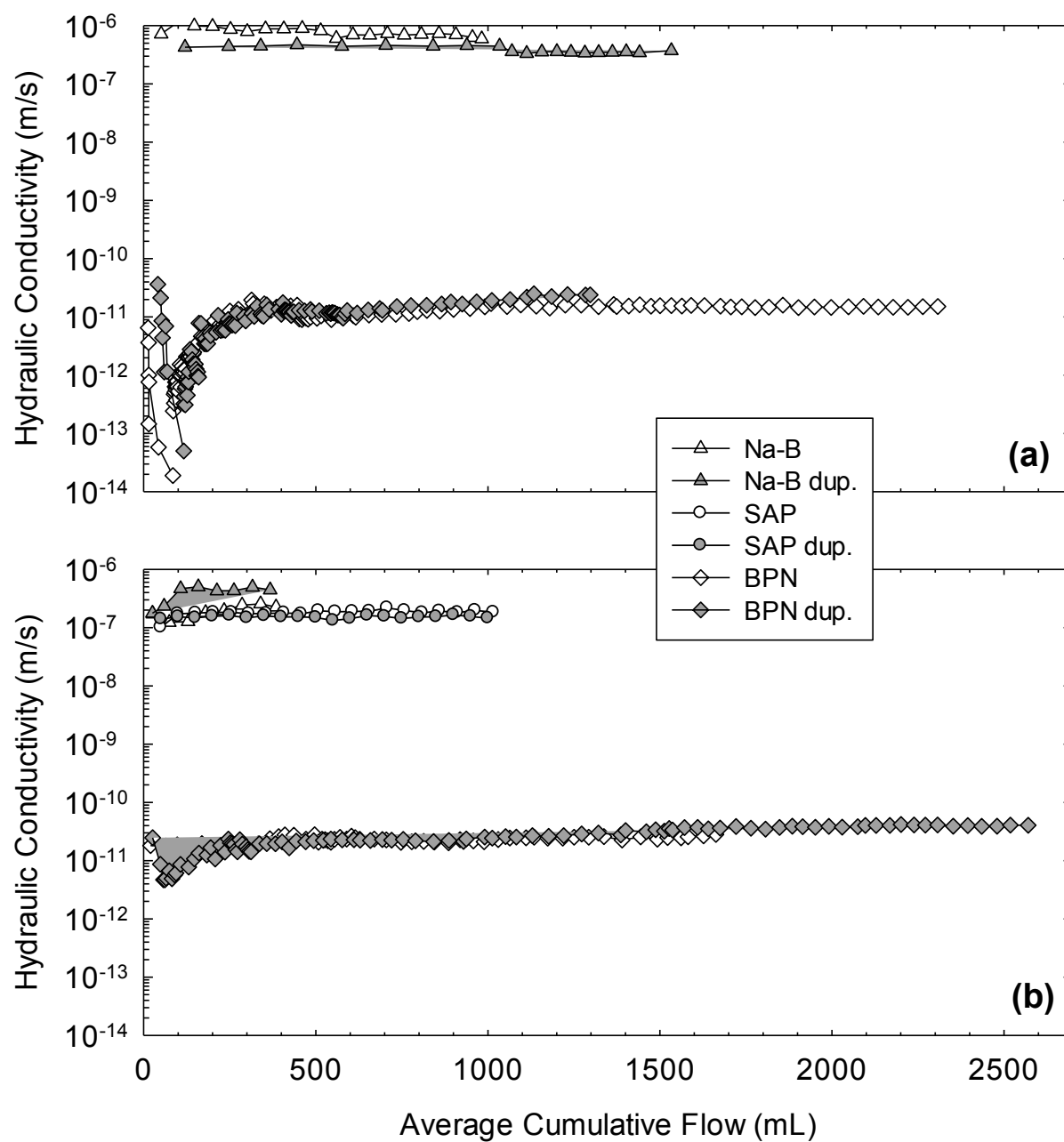


Fig. 3.6 Hydraulic conductivity profiles for Na-bentonite (Na-B), superabsorbent Na-superabsorbent polyacrylate (SAP), and bentonite-polyacrylate nanocomposite (BPN) permeated with **1 M NaOH** (a) and **1 M HNO₃** (b). Average cumulative flow calculated as mean of cumulative inflow and cumulative outflow.

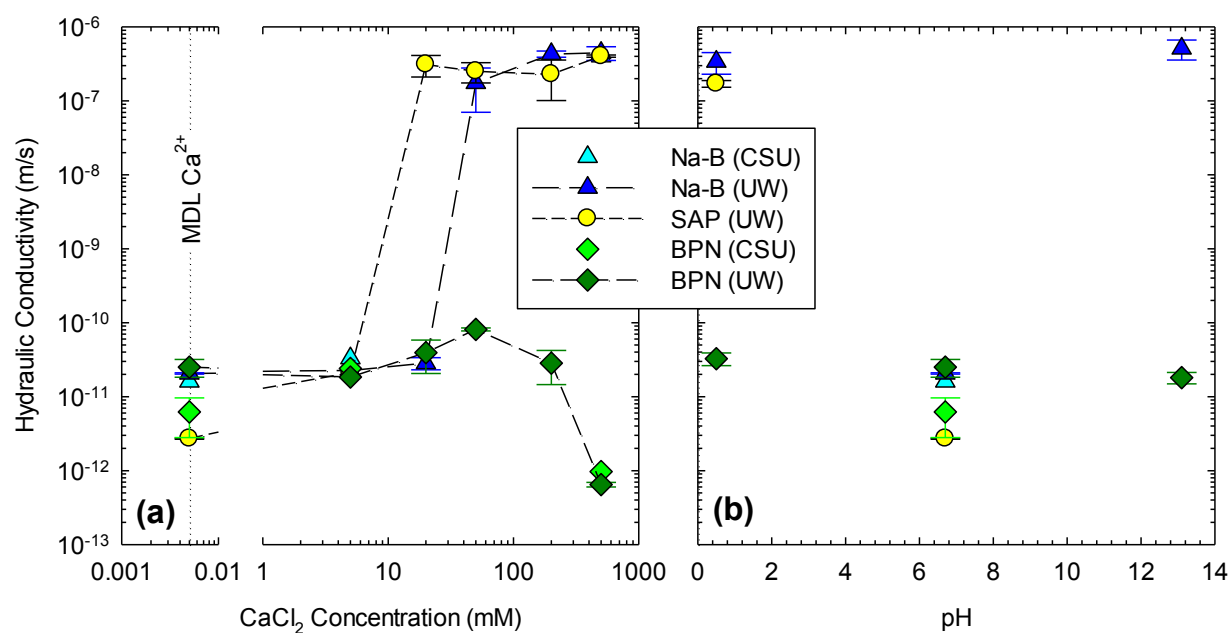


Fig. 3.7 Equilibrium hydraulic conductivities versus permeant solution CaCl_2 concentration (a) and pH (b) for Na-bentonite (Na-B), superabsorbent Na-polyacrylate (SAP) and bentonite-polyacrylate nanocomposite (BPN). The hydraulic conductivity of specimens permeated with deionized water is shown at method detection limit (MDL) of Ca^{2+} . Bi-directional error bars represent maximum and minimum observed hydraulic conductivities.

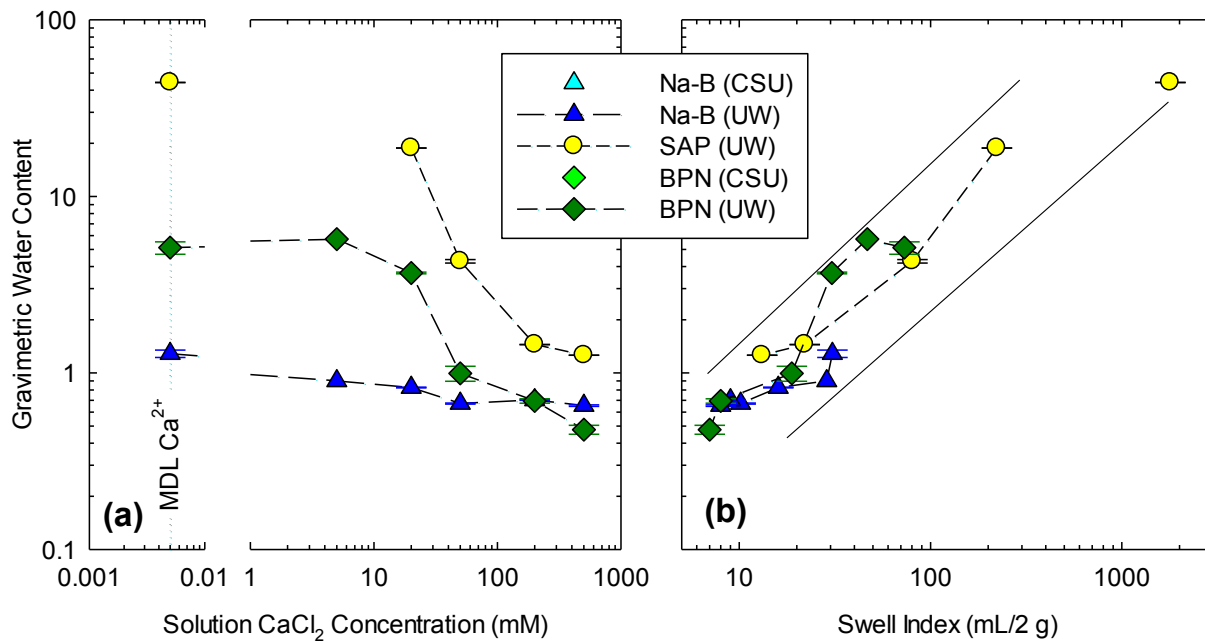


Fig. 3.8 Gravimetric water content of specimens after permeation versus permeant solution CaCl_2 concentration (a) and corresponding swell index (b) in the same permeant solution for Na-bentonite (Na-B), superabsorbent polyacrylate (SAP), and bentonite-polyacrylate nanocomposite (BPN). The gravimetric water content of specimens permeated with deionized water is shown at method detection limit (MDL) of Ca^{2+} . Bi-directional error bars represent maximum and minimum observed gravimetric water contents.

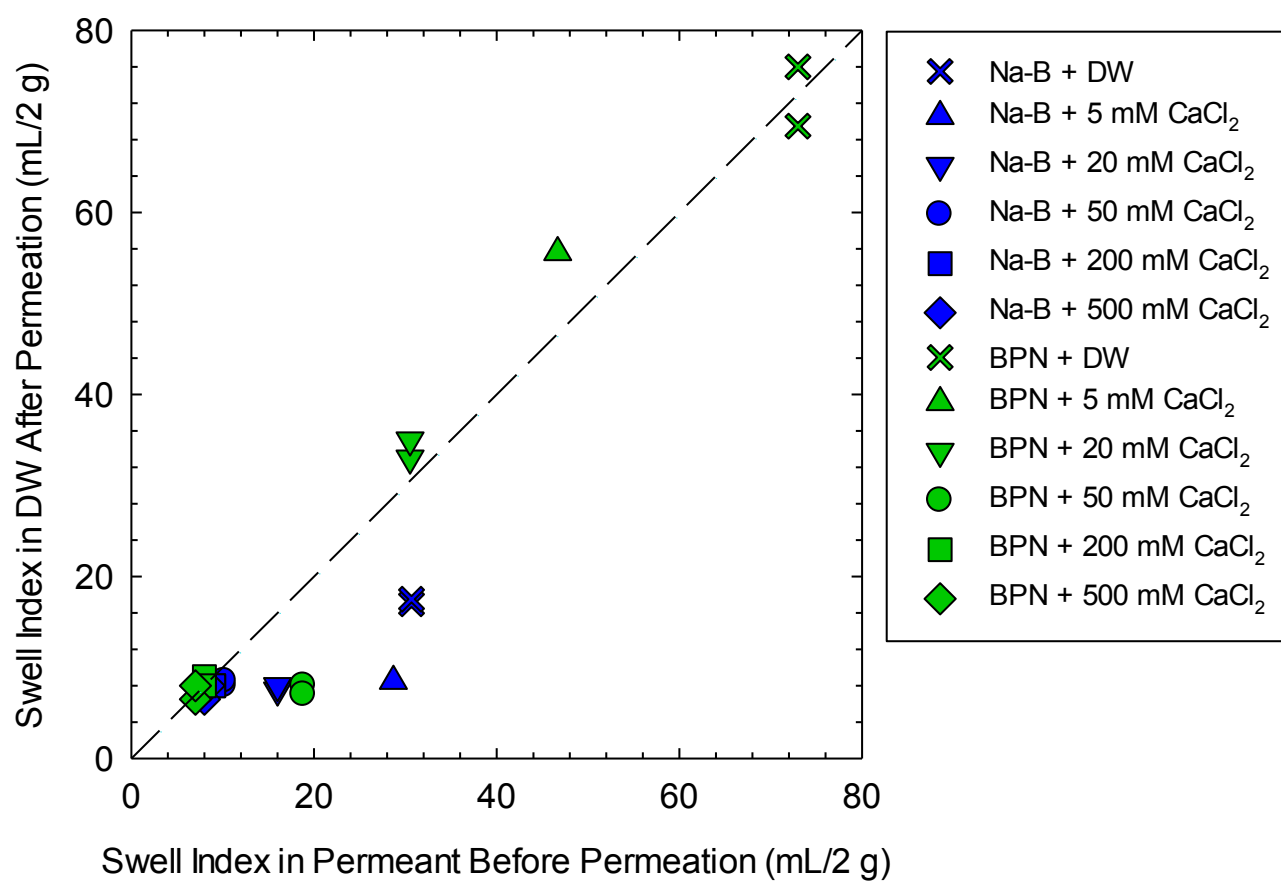


Fig. 3.9 Swell index in deionized water, DW, after permeation versus corresponding swell index on bulk (viz. new) material in permeant.

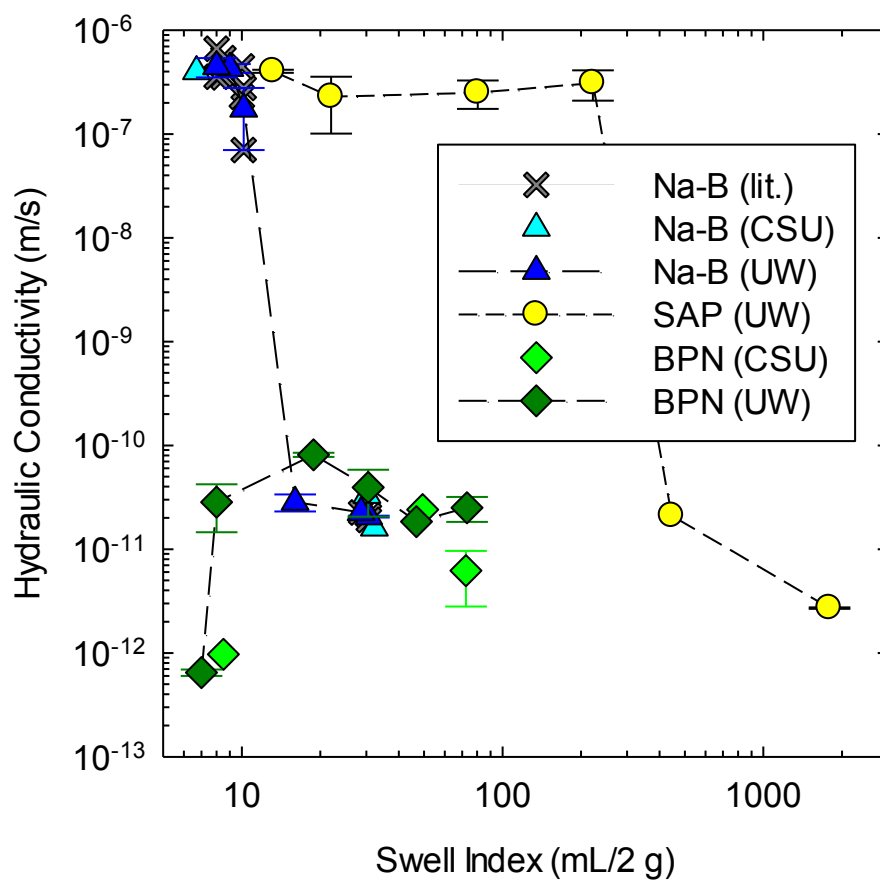


Fig. 3.10 Equilibrium hydraulic conductivity versus swell index for Na-bentonite (Na-B), superabsorbent Na-polyacrylate (SAP), and bentonite-polymer nanocomposite (BPN). Literature data from Jo et al. (2005) included for comparison. Bi-directional error bars represent maximum and minimum hydraulic conductivities.

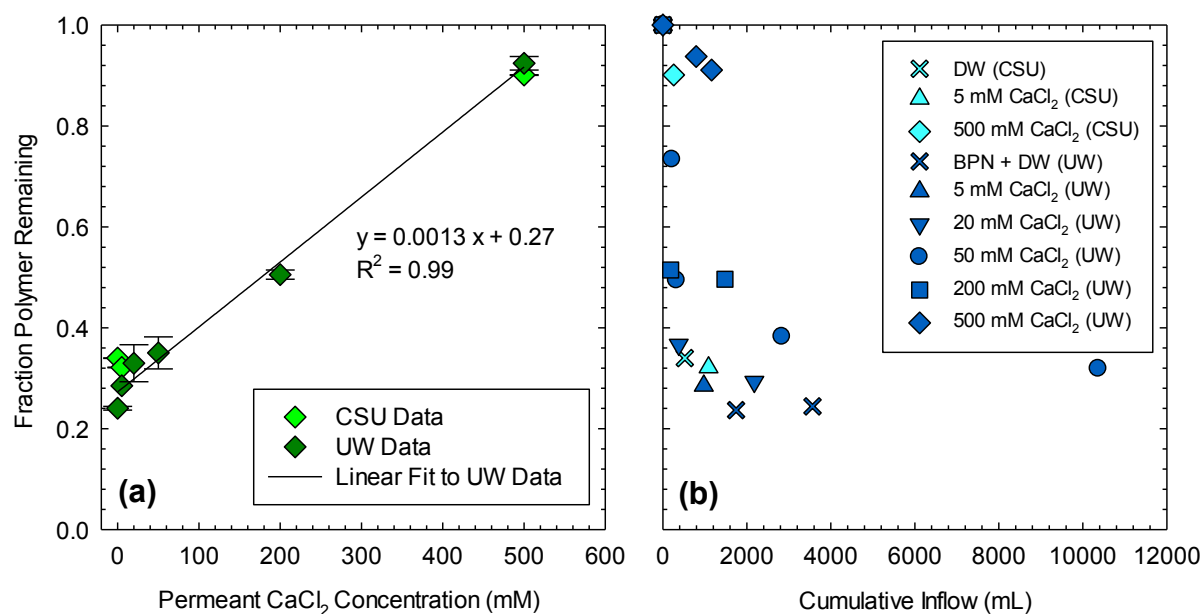


Fig. 3.11 Polymer retained after long term hydraulic conductivity testing versus permeant solution CaCl_2 concentration (a) and cumulative inflow (b) for bentonite-polyacrylate nanocomposite. Bi-directional error bars represent maximum and minimum fractions of polymer remaining observed at a given CaCl_2 concentration.

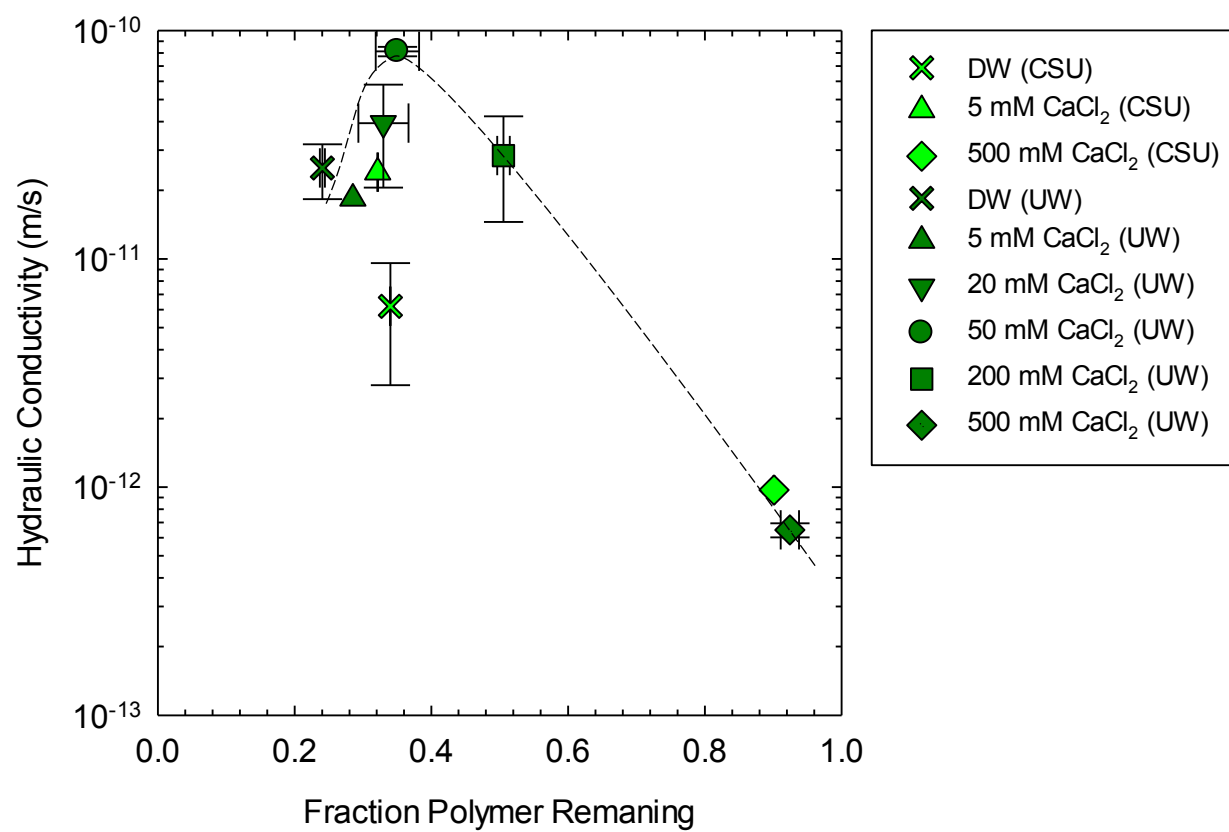


Fig. 3.12 Equilibrium hydraulic conductivity versus polymer fraction remaining at the termination of bentonite-polyacrylate nanocomposite permeation. Bi-directional error bars represent maximum and minimum observed values.

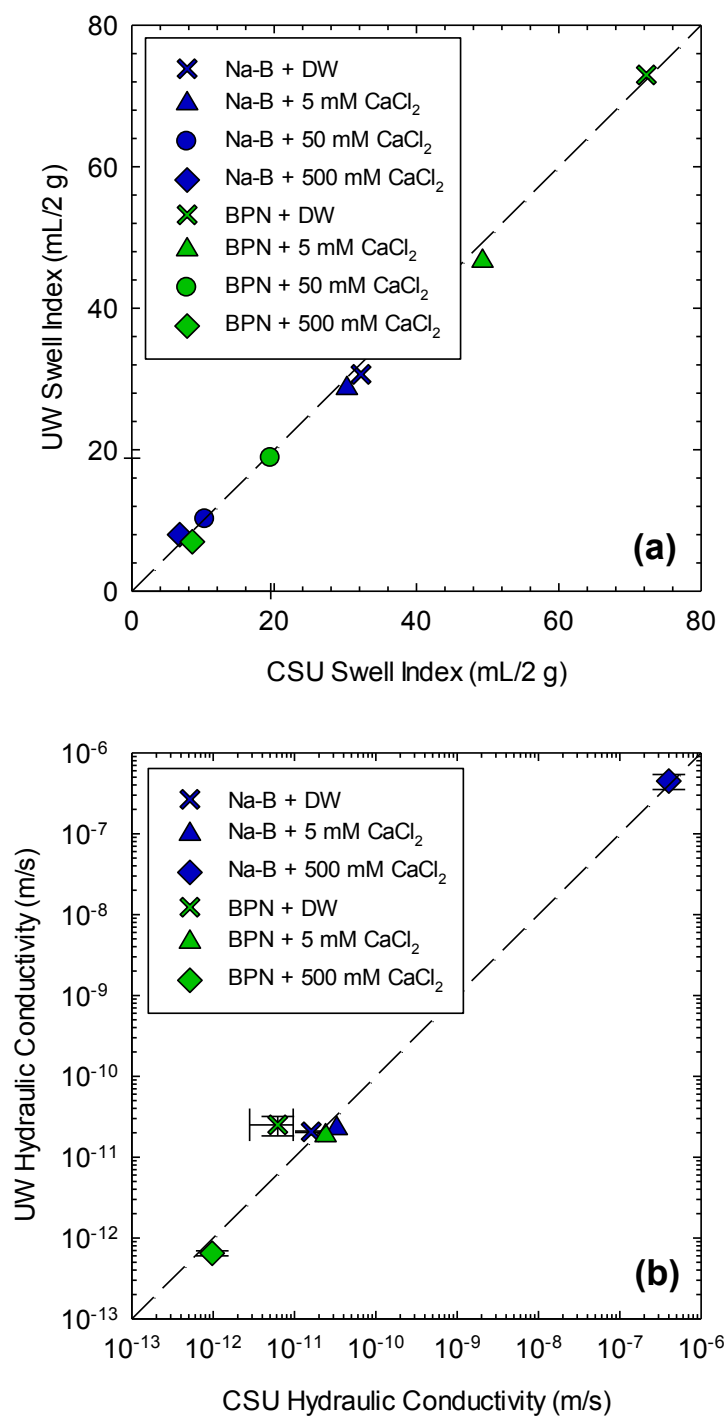


Fig. 3.13 Comparison of swell index (a) and hydraulic conductivity (b) results from paired replicate tests conducted at the University of Wisconsin – Madison (UW) and Colorado State University (CSU).

CHAPTER FOUR

HYDRAULIC IMPACT OF MACROPORE SEALING IN A BENTONITE POLYMER-NANOCOMPOSITE EXPOSED TO AGGRESSIVE INORGANIC SOLUTIONS

4.1. ABSTRACT

Bentonite-polymer nanocomposite (BPN) manufactured by in-situ polymerization maintained a low ($< 9 \times 10^{-11}$ m/s) hydraulic conductivity (k) to 50, 200, and 500 mM CaCl_2 , 1 M HNO_3 , and 1 M NaOH . BPN also exhibited superior swelling in dilute solutions (DW, 5, and 20 mM CaCl_2) due to the addition of the superabsorbent polymer sodium-polyacrylate. But, similar to sodium bentonite, the swell of BPN decreased with increased solution concentration, and exhibited swells typical of Ca-bentonite in aggressive solutions (50, 200, 500 mM CaCl_2 , 1 M HNO_3 , 1 M NaOH). Thus, the mechanism underlying the low k of BPN in aggressive solutions was decoupled from swell. Despite low swell and low effective stress (on average 20 kPa), granular BPN was visually observed to form a homogeneous matrix in all permeants tested. This matrix was the result of the stitching together of BPN inter-granules by polyacrylate, and granular consolidation during permeation. Additionally, of the 28.5% (by mass) polymer initially contained within BPN, up to 75% was soluble and mobile (viz. not superabsorbent) polyacrylate. This polymer was highly effective at clogging permeameter tubing, as well as the macroscale porosity of Na-bentonite in 50 mM CaCl_2 . Granular mixtures of BPN with Na-bentonite resulted in up to a 3,900-times

reduction in k relative to pure Na-bentonite. Granular BPN additions to granular Na-bentonite of mass percentages as low as 1% resulted in equilibrium $k <$ pure BPN.

4.2. INTRODUCTION

Natural sodium bentonites (Na-bentonites) used for hydraulic and contaminant containment are highly sensitive to chemical interactions that reduce swell and result in increases in hydraulic conductivity (k) (Petrov and Rowe 1997, Shackelford et al. 2000, Jo et al. 2001, etc.). Reductions in swell occur during hydration when the permeant solution has a high ionic strength (McBride 1994). To prevent reduced swelling and coupled increases in k , recent research has focused on chemical modification of bentonites to improve compatibility in environmental-containment applications (Onikata et al. 1996, Flynn et al. 1998, Onikata et al. 1999, Onikata et al. 2000, Trauger and Darlington 2000, Schroeder et al. 2001, Ashmawy et al. 2002, Kolstad et al. 2004, Katsumi et al. 2008, Emidio et al. 2010, Mazzieri et al. 2010a, Mazzieri et al. 2010b, Emidio et al. 2011, Scalia et al. 2011).

Published efforts to modify bentonite and produce more stable low- k barriers have mechanistically focused on intercalating organic molecules (e.g., propylene carbonate or Na-carboxymethyl cellulose) in the montmorillonite (MMT) interlayer to activate or maintain osmotic swell in typically incompatible solutions; for example: multi-swellable bentonite, MSB, (Onikata et al., 1996, Onikata et al. 1999), HYPER-Clay, HC, (Emidio et al. 2010, Emidio et al. 2011), and dense-prehydrated geosynthetic clay liners, DPH-GCLs (Flynn and Carter 1998, Kolstad et al. 2004). Norrish and Quirk

(1954) showed that CaCl_2 solutions with ionic strengths > 300 mM suppress the osmotic absorption of water that is manifest as high swelling. At concentrations more dilute than 300 mM, Norrish and Quirk (1954) found that the extent of osmotic swelling was linearly related to one over the square root of the hydrating solution concentration, with greater swell occurring in more dilute solutions. Bentonites modified to activate osmotic swell shift osmotic swelling behavior to a higher concentration regime. Data from tests on polymer modified bentonites has shown promise, but, while polymer intercalation and swell activation have been demonstrated (e.g., Onikata et al. 1996), bentonites modified for hydraulic barrier applications have not shown greatly improved swelling in divalent solutions and are still sensitive to high ionic strength solutions for polymer intercalation and gradual replacement of monovalent cations by divalent cations.

Chapter 3 examined the long term hydraulic performance of a bentonite modified at the nanoscale by in situ polymerization of acrylic acid. The resultant material was termed a bentonite-polyacrylate nanocomposite (BPN). BPN and a similar material tested by Trauger and Darlington (2000) differ from other polymer modified bentonites in that a superabsorbent polymer (viz. sodium polyacrylate), typically encountered in incontinence products (Buckholtz and Graham 1998), was incorporated to add swell. Hydraulic conductivity at chemical equilibrium was determined with aggressive inorganic solutions that yielded high k ($> 10^{-7}$ m/s) with Na-bentonite (50, 200, 500 mM CaCl_2 , 1 M HNO_3 , and 1 M NaOH) in flexible-wall permeameters at an average effective stress of 20 kPa. A base-line k was also determined with dilute solutions typically compatible with Na-bentonite (deionized water, DW, 5, and 20 mM CaCl_2). At chemical equilibrium,

BPN maintained a $k < 9.0 \times 10^{-11}$ m/s in all solutions tested. In contrast, Na-bentonite exhibited a k at least 2,500-times greater ($> 2.4 \times 10^{-7}$ m/s) in aggressive solutions. When permeated with 500 mM CaCl_2 solution, the k of BPN was $>$ five orders-of-magnitude lower than the k of Na-bentonite.

Swell indices (SI) of BPN were determined per ASTM D5890 in all permeant solutions. In DW, BPN swelled to 73-mL/2 g, greater than 3.5-times the base bentonite used to produce BPN (19.0 mL/2 g). Unlike k , the SI of BPN showed a strong inverse correlation to CaCl_2 concentration, such that in 500 mM CaCl_2 , BPN had a SI similar to Ca-bentonite (< 10 mL/2 g). The SI of BPN similarly was low in 1 M HNO_3 (13.3 mL/2 g) and 1 M NaOH (10.5 mL/2 g). At the termination of k testing, specimen gravimetric water contents correlated to SI in the same solution (viz. high swell index = high water content specimen).

The reduction of swell with increased concentration was consistent with Na-bentonite and other polymer-modified bentonites, but BPN did not exhibit the corollary relationship between swell and k typical of these materials (Jo et al. 2001, Kolstad et al. 2004a, etc.). Thus, the mechanism underlying the improved hydraulic performance of BPN was not directly correlated to swell. Similar decoupling of swell and k has been shown for DPH-GCLs, but this behavior has been largely attributed to the in-factory densification and prehydration of the bentonite layer (Kolstad et al. 2004b) and the complete lack of data at chemical equilibrium (Katsumi et al. 2008).

This paper presents the mechanisms underlying the decoupling of swell and k in BPN. Three of the mechanisms presented have been previously shown or hypothesized

to underlie low k of bentonites or polymer modified bentonites in typically incompatible solutions. These mechanisms are:

- Activation of osmotic swelling by intercalated polymer in the MMT interlayer;
- Clogging of hydraulically active porosity by precipitated carbonate minerals;
- Impediment or prevention of the exchange of native sodium cations by absorbed polymer.

Two additional mechanism presented are based on observations made during long term k testing of BPN. These mechanisms are:

- Removal of inter-granular porosity by the stitching together of granules by in situ polymerized polyacrylate chains;
- Clogging of hydraulically active porosity by mobile low molecular weight (viz. soluble, non-super swelling) polyacrylate.

Optimization of BPN for use in inorganic environmental containment applications is also discussed.

4.3. MATERIALS AND NON-STANDARDIZED METHODS

4.3.1. Bentonite-Polyacrylate Nanocomposite (BPN)

BPN was extensively characterized in Chapter 3. In abstract, BPN was created by the in-situ polymerization of acrylic acid within a Na-bentonite slurry. BPN initially contained 28.5% polymer by weight, as determined by thermo-gravimetric analysis. Much of this polymer, > 73%, had a low weight average molecular weight, M_w (\approx

280,000 g/mol), and was mobile during permeation with dilute solutions. The swell index, SI (ASTM D5890), of BPN in DW was 73-mL/2 g, but 7-mL/2 g in 500 mM CaCl_2 . The granule size distribution of BPN used in *k* experiments was detailed in Scalia et al. (2011); BPN granules were classified as a SP according to the Unified Soil Classification System (USCS) (ASTM D2487).

Soluble cations (SC), bound cations (BC), and cation exchange capacity (CEC) were determined following the procedures detailed in ASTM D7503. Chemical analyses of extracts from SC and BC tests were conducted by inductively coupled plasma-optimal emission spectroscopy (ICP-OES) following USEPA Method 6010 B (USEPA 2007). BPN had a CEC of 143 cmol+/kg, while the Na-bentonite used to create BPN had a CEC of 86 cmol+/kg. These data show that the polyacrylate contributed CEC to the total CEC of the system. The BC within BPN were initially composed of 90% sodium (Na^+) and 6% calcium (Ca^{2+}), with the balance predominately satisfied by magnesium (Mg^{2+}) and (K^+). In contrast, the BC of the base Na-bentonite used to produce BPN were initially comprised of 42% Na^+ and 42% Ca^{2+} , with the balance predominately satisfied by Mg^{2+} and K^+ . The additional bound Na^+ in BPN resulted from the neutralization of acrylic acid by NaOH during BPN manufacture.

4.3.2. Natural Na-Bentonite (Na-B)

Na-bentonite from Wyoming, USA, was tested in Chapter 3 and used in this study, and is abbreviated as Na-B henceforth. Na-B was GCL grade and was provided by CETCO, and is sold commercially as Volclay CG-50. The SI of Na-B in DW was 31-mL/2 g, but 8-mL/2 g in 500 mM CaCl_2 . The granule size distribution of Na-B is

detailed in Scalia et al. (2011); Na-B granules were classified as a SP by the USCS (ASTM D2487). Soluble cations, BC, and CEC were determined following identical procedures to those described for BPN. Na-B had a CEC of 78 cmol+/kg, and the bound cations were initially comprised of 44% Na⁺ and 36% Ca²⁺, with the balance predominantly satisfied by Mg²⁺ and K⁺.

4.3.3. Permeants

Dilute (DW, 5, and 20 mM CaCl₂) and aggressive (50, 200, 500 mM CaCl₂, 1 M HNO₃, and 1 M NaOH) permeant solutions used in Chapter 3 are discussed in this study. Additionally, 50 and 500 mM CaCl₂ were tested as part of this study. The properties, preparation, and storage of these permeants are detailed in Chapter 3.

4.3.4. Hydraulic Conductivity (*k*)

The methods used for long term *k* testing on BPN are detailed in Chapter 3; a similar testing method was used for complimentary *k* tests described in this study. Specimens were constructed with a total dry mass per unit area of 4.8 kg/m² and manually leveled. Tests were conducted in flexible-wall permeameters in general accordance with ASTM D5084. The falling headwater-constant tailwater method was employed. Gravity heads were used to apply cell and influent pressure (gravity was assumed less likely to fail than a compressor and pressure transducer). Backpressure was not applied to allow convenient collection of effluents for chemical analysis. Specimens were tested under an average effective stress of 20 kPa and an average influent head of 1.5 m, corresponding to an average hydraulic gradient of 200 for a 7.5-mm thick specimen. This hydraulic gradient is typical of *k* tests on thin bentonite

specimens (viz. GCLs), and polymer modified bentonite specimens, tested in the laboratory (e.g., Shackelford et al. 2000, Jo et al. 2001, 2004, 2005, Kolstad et al. 2004a, 2004b, Katsumi et al. 2008).

In-cell hydration was conducted for 48 h prior to flow. After the permeameter was assembled and connected to the falling headwater apparatus, cell pressure was applied and all tubing was saturated with the permeant liquid. The inflow line of the permeameter was opened to allow the specimen to hydrate while the effluent line remained closed to prevent flow. After 48 h, flow was initiated by opening the effluent line. During testing, effluent was collected in fluorinated ethylene propylene bags and sampled for pH and electrical conductivity (EC) using bench-top meters. All tests were run until the hydraulic and chemical equilibrium termination criteria prescribed in ASTM D6766 were satisfied.

4.3.5. Polymer Content

The polymer content of BPN was determined by loss-on-ignition. BPN, the base clay used to produce BPN, and sodium-polyacrylate were ground to pass a No. 20 woven wire sieve (ASTM E11) and oven dried at 105°C until a constant mass was obtained. Oven dried materials were then placed in a 550°C furnace for 4 h to ignite volatile substances. BPN was determined have initially contained 28.5% polymer by mass. The sodium-polyacrylate used to quantify the loss-on-ignition of the polymer component of BPN was produced under identical conditions to BPN, but without the base bentonite. After testing, the crucible was allowed to cool in a water free atmosphere. The mass loss-on-ignition of each material was then determined. Polymer

content was calculated by assuming the mass loss percentages of base bentonite, sodium-polyacrylate, and BPN were independent, additive, and that the polymer tested was identical to the polymer contained within BPN. The net impact of these assumptions was verified by comparing the mass of specimens after long-term permeation to mass loss calculated based on initial and final polymer contents and taking into account measured changes in soluble and bound cations; the ratio of final specimen mass after permeation to specimen mass calculated by loss in polymer content were within 5% for all specimens.

4.4. BPN PROPERTIES AND BEHAVIOR

4.4.1. Intercalated Polymer

Activation of osmotic swelling by polymer intercalated between MMT platelets has been shown to underlie improved swelling and hydraulic behavior of MSB (Onikata et al. 1996, Onikata et al. 1999) and HYPER-clay (Emidio et al. 2010). These studies experimentally verified intercalation of polymer by powder X-ray diffraction of dried clay specimens. Increases in the dried d001 spacing measurably greater than the spacing typical of dried MMT (1.4 nm) were deemed indicative of interlayer polymer molecules physically propping open the interlayer.

Specimens of BPN and the base bentonite used to produce BPN were oven dried at 105°C and the d001 spacing was determined by low-angle XRD. A Scintag PAD V X-ray diffractometer with CuK α radiation was used at a power of 45 kV and 40 mA. Both the base bentonite and BPN exhibited d001 peaks at 1.4 nm, illustrating that

polyacrylate was not physically located in the interlayer of MMT within BPN. Because of the large hydrodynamic radius of polyacrylate in solution intercalation without prior full exfoliation of MMT platelets will not occur (Tran 2005). Based on the lack of intercalated polymer, the base bentonite used to produce BPN is hypothesized to have not been fully exfoliated during BPN production.

4.4.2. Cation Exchange

Because many segments of a single polymer molecule can be in contact with a surface, a low bonding energy for each individual bond is still capable of rendering the total adsorption effectively irreversible (Stumm 1992, Stumm and Morgan 1996). Thus, the high energy required to simultaneously desorb the entire molecule renders adsorbed polymers difficult to desorb (Lyklema 1985). Anionic polyacrylate is likely to be adsorbed to MMT via exchangeable cation bridging (Deng et al. 2006), where the negative carboxyl moieties off of the polyacrylate backbone associate with the cations that satisfy the net-negative-structural charge of the MMT platelets (viz. the bound cations). The theoretical result is the effective locking of the bound cations hypothesized by Trauger and Darlington (2000) and Flynn et al. (2008). Flynn et al. (2008) conjectured that locking of bound cations from absorbed polyacrylate could neutralize the cation exchange capacity (CEC) of the resulting composite. To the authors' knowledge, polymeric locking of bound cations has not been realized in an environmental containment material.

BPN had a CEC of 143 cmol+/kg, while the base bentonite used to produce BPN had a CEC of 86 cmol+/kg. Assuming polyacrylate in BPN does not lock bound cations,

the bentonite component of BPN should provide a CEC of 61 cmol+/kg BPN, and thus polyacrylate must provide a CEC of 82 cmol+/kg BPN (or 287 cmol+/kg of polymer). Based on the structure of polyacrylate, theoretically, fully anionic polyacrylate satisfied by sodium cations can have a maximum CEC of 1063 cmol+/kg polymer. But, realization of only a fraction of the theoretically possible exchangeability is anticipated due to neutralization during manufacture. Thus, while BPN had a higher CEC than the bentonite used for BPN production, the existence of bound cation locking is indeterminate within the scope of this study. Irrespective, BPN had a 167% greater CEC than the base bentonite used for production, and the swelling of BPN was susceptible to increased concentrations of divalent solutions (Chapter 3).

The theoretical utility of bound cation locking is the elimination of polyvalent-for-monovalent cation exchange. To explore exchange in BPN, the mole fraction of monovalent bound cations after long term permeation of BPN with a range of CaCl_2 solutions (as described in Chapter 3) is shown in Fig. 4.1. Na-B comparatively tested with identical solutions is included in Fig. 4.1 for comparison. Exchange of monovalent bound cations occurs in both materials in all permeants. In 50, 200, and 500 mM CaCl_2 , there was almost complete exchange of polyvalent cations (mainly Ca^{2+}) for native monovalent cations. These data show that in-situ polymerized polyacrylate does not prevent cation exchange in BPN.

4.4.3. Carbonate Precipitation

Precipitation of minerals from strong solutions in the pores of bentonite has been theorized to reduce k (Benson et al. 2010, Gates and Bouazza 2010). To ascertain if

carbonate mineral precipitation occurred in BPN permeated with CaCl_2 , the carbonate mineral content of BPN was determined by the methods prescribed in ASTM D4373. Carbonate content of BPN and Na-B were determined before and after long-term k testing; carbonate content of the base clay used to produce BPN was also determined for comparison. Base clay initially contained 0.6% carbonate minerals (by mass); while no carbonate minerals were detected within BPN. The carbonate minerals initially present in the base clay are believed to have dissolved during the production of BPN. After permeation, no carbonate minerals were detected in BPN at any concentration level. Na-B initially contained 1.2% carbonate minerals by mass. After long-term permeation with DW, only $1/6^{\text{th}}$ the original carbonate content remained (0.2% by mass). Similar dissolution of carbonate minerals during DW tests was shown by Guyonnet et al. (2005). Reduction in carbonate from permeation was observed in all test with Na-B, with the least reduction (to 1.1% by mass) observed with 500 mM CaCl_2 .

4.4.4. BPN Monolith Formation

The cross-sections of BPN and Na-B specimens after long-term permeation with DW and 500 mM CaCl_2 are displayed in Fig. 4.2. These cross sections represent the polar extremes of permeants used for long term k testing. When permeated with DW, both BPN (Fig. 4.2a) and Na-B (Fig. 4.2b) exhibit the homogeneous swollen gel that is characteristic of osmotically swollen MMT and, in the case of BPN, additionally swollen polyacrylate. As a counterpoint, BPN and Na-B permeated with 500 mM CaCl_2 (Fig. 4.2c and 4.2d) do not undergo osmotic swell, but, BPN exhibits a homogeneous cross-section while Na-B does not. Of the cross sections pictured in Fig. 4.2a, 4.2b, 4.2c, and 4.2d, the swollen-granule structure of Na-B permeated with 500 mM CaCl_2 was the only

specimen that exhibited a high k (4.8×10^{-7} m/s). High k across this cross-section occurs through macroscale-intergranular porosity. Similar macroscale-intergranular porosity was exhibited by Na-B permeated with 50 mM CaCl_2 , 200 mM CaCl_2 , 1 M NaOH, and 1 M HNO_3 (viz. specimens with high k) but was not evident in any BPN specimens.

BPN and Na-B granules behave differently during hydration in 500 mM CaCl_2 (Fig. 4.3) and other aggressive solutions. To illustrate this deviant behavior, dry BPN granules (Fig. 4.3a), and Na-B granules (Fig. 4.3b), were freely hydrated with 500 mM CaCl_2 . After 48 h, both BPN and Na-B granules had swollen as the result of intra-granular (crystalline) hydration (Figs. 4.3c and 4.3d). But, BPN granules (Fig. 4.3c) did not exhibit the granular spalling evident in Na-B (Fig. 4.3d). Na-B granule spalling is the result of coupled electrostatic repulsion and the loss of inter-particle matric potential. The lack of similar spalling of BPN granules during free hydration is theorized to result from the tying the MMT constituent of BPN by polyacrylate chains. These chains exist throughout the mineral matrix as a result of in situ polymerization during BPN manufacture. In addition to holding together the BPN granules and preventing spalling during free hydration, polyacrylate renders BPN granules cohesive via intermolecular forces. Thus, when two BPN granules are applied together the granules bond. Fig. 4.3e shows the hydrated BPN granules depicted in Fig. 4.3c stuck together by skewering one granule with a pin and gently pressing the granules together. Upon contact, the bonded granules could be freely moved. In contrast, disturbance of the hydrated Na-B granules depicted in Fig. 4.3d resulted in further disintegration of the granules (Fig. 4.3f)

The granular hydration behavior depicted in Fig. 4.3 coupled with the specimen effective stress history during permeation is hypothesized to underlie the formation of the homogenous BPN cross-section observed after permeation with 500 mM CaCl_2 (Fig. 4.2c) and other aggressive solutions. The effective stress history of specimens permeated by the methods described in Chapter 3 is shown in Fig. 4.4. Specimens were hydrated with the outflow-line closed for 48 h prior to permeation. During this phase, the effective stress across the specimen was effectively identical, and was similar to the stress that would ultimately be felt at the inflow-end of the specimen during permeation. As water hydrated the specimen, the effective stress increased slightly (up to 1 kPa) as the inflow head was reduced by water entering the specimen. After 48 h, but before permeation was initiated, the falling-headwater apparatus was filled, resulting in a slight (up to 2 kPa) decrease in effective stress across the specimen. To initiate permeation, the outflow line was opened, and the effective stress at the outflow end of the specimen increased as the pore water pressure transitioned from the inflow head. Ultimately during testing, the average effective stress applied to the middle of the specimen was 20 kPa, but because of the average 1.5-m inflow head, the effective stress at the inflow-end and outflow-end of the specimen varied by an average of 15 kPa. Stress changes during permeation due to changes in the inflow head were minimized to no more than 2 kPa by employing a sloping falling-headwater apparatus. Despite this precaution, the transition from prehydration to permeation resulted in an increase in effective stress by 15 kPa at the outflow end of the specimen, and 7.5 kPa at the middle of the specimen. This increase in effective stress is believed to have consolidated the hydrated BPN granules, resulting in the cohesion of granules as water

flowed from intergranular porosity and ultimately resulting in the formation of a homogeneous matrix, the k of which was governed by microscale-intragranular flow.

To test this hypothesis, a specimen of BPN was prepared by the methods described in Chapter 3 but hydrated and permeated under near-constant effective stress (Fig. 4.4). Hydration and permeation were conducted with a vertical burette with a cross sectional area of 28 cm^2 and an inflow head of 5 cm, equating to a hydraulic gradient of 10 for a 5-mm thick specimen (the average thickness reported in Chapter 3 for BPN permeated with 500 mM CaCl_2). A large cross-sectional-area burette was used to minimize changes in stress during hydration and permeation. An average effective stress of 20 kPa was applied to the specimen. After 48 h, permeation was initiated by opening the outflow line. A k of $9.1 \times 10^{-6} \text{ m/s}$ was measured, more than 6 orders-of-magnitude higher than the k of BPN to the same solution reported in Chapter 3 and > 2-times higher than the k of Na-B to the same solution reported in Chapter 3. The cross-section of BPN permeated under a low hydraulic gradient with 500 mM CaCl_2 is shown in Fig. 4.2e. BPN granules had not visibly coalesced, and macroscale flow-paths were visible between granules. Permeation of a replicate specimen with rhodamine-WT dye (Vasudevan et al. 2001) at the conclusion of testing confirmed inter-granular porosity as the dominant location of flow. While the low hydraulic gradient used for these stress-focused tests yielded informative data, a similar method would be impracticable for k testing of low conductivity materials to hydraulic and chemical equilibrium.

The homogeneous structure of BPN helps inform a plot of final void ratios and corresponding k at the end of long term permeation with DW, 5, 20, 50, 200, and 500

mM CaCl_2 (Fig. 4.5). For both BPN and Na-B, void ratio generally decreases with increasing CaCl_2 concentration, and higher k correlates to lower void ratio. Similar behavior is well documented in the literature (e.g., Petrov and Rowe 1997) and summarized in Shackelford et al. (2000). Comparably for BPN, k increases with increased concentration between 5 and 50 mM CaCl_2 correlate to decreased void ratio. In this range, decreased void ratios result from decreased swell in response to coupled ionic strength and cation exchange effects. When permeated with 50 mM CaCl_2 , BPN has a SI (19 mL/2) in the range typical for osmotic-gel driven low k in Na-bentonite.

In solutions stronger than 50 mM CaCl_2 (viz. 200 and 500 mM CaCl_2) the k of BPN decreases as void ratio decreases. Decrease in void ratio is in agreement with swell trends reported in Chapter 3. The direct correlation between k and void ratio is similar to the impact of increasing effective stress on a given bentonite-permeant system reported by Mesri and Olson (1971), and Petrov and Rowe (1997), but occurs at a (near) constant, and low, effective stress. BPN exhibits different behavior than Na-B because inter-granular porosity is not kept open by low-density arrangements of granule spalling at granule interfaces. BPN granules remain coalesced, and when consolidated, form a tight homogeneous matrix. Thus, in BPN, decreases in void ratio associated with decreased swell correlate to a denser matrix and consequently narrower intragranular flow paths.

4.5. POLYMER CLOGGING NA-BENTONITE POROSITY

During long-term k testing, BPN eluted low molecular weight polyacrylate (LMwP) (Chapter 3). LMwP in BPN was the result of chain termination during polymerization in the bentonite slurry, which is typically minimized in industrially produced superabsorbents (Buckholz and Graham 1998). LMwP eluted from 152.4-mm diameter samples with an initial dry mass per area of 4.8 kg/m^2 was clogged the 4.32-mm inside-diameter effluent lines of the permeameter. Manual cleaning of effluent lines was required to measure the k of BPN specimens and not clogged tubing. At the termination of long-term testing, BPN specimens permeated with DW retained only 13% polymer by mass (i.e., 21.5 g of polymer eluted from an 87.6 g specimen that initially contained 33.3 g polymer). Chapter 3 showed that the quantity of polymer retained, and correspondingly the amount of polymer eluted, was directly related to the CaCl_2 concentration of the permeant solution.

Preliminary elucidation of the potential impact of eluted LMwP was found during exploratory hydration tests in which a dry BPN GCL was placed atop clay compacted at 1% wet of optimum-water-content, sealed, and allowed to hydrate for 50 d. Hydration tests were conducted in accordance to the methods described in Bradshaw et al. (2012). When decommissioned, hydrated BPN was observed to stick to the surface of the subgrade via a low viscosity gel. This gel was visually evident in the top 3-4 mm of subgrade clay. The top 30 mm of the hydrating soil was removed and permeated in a flexible-wall permeameters following the falling-head constant-tail method detailed in ASTM D5084. The specimen was inverted for k testing, and permeated with tap water

from the bottom up to represent top-down flow. Hydraulic conductivity of the hydrating subgrade was also determined from a replicate test that incorporated a Na-bentonite GCL. Subgrade atop of which BPN had been hydrated exhibited a k two orders-of-magnitude lower than subgrade on which a Na-bentonite GCL had been hydrated (3×10^{-11} m/s versus 5×10^{-9} m/s). These results illustrate that a secondary mechanism for low k in BPN may be mobile and related to eluted polymer.

4.5.1. Clogging Experiments

A schematic of the experimental setup used to assess the potential impact of eluted LMwP on Na-B k is shown in Fig. 4.6. Non-contiguous layers of BPN granules were placed between two slit-film geotextiles (GTs) either up-gradient (Fig. 4.6a) or downstream (Fig. 4.6b) from granular Na-B layers. In the up-gradient testing configuration (Fig. 4.2a), eluted LM_wP was anticipated to advectively transport down-gradient into the Na-B layer. The down-gradient testing configuration (Fig. 4.2b) was used as a control to ensure that the permeability of the BPN layer was not governing the measured behavior. The sum amount of material in both layers was equal to the quantity used in long-term k tests (4.8 kg/m^2) with the Na-B layer comprising 98% of the total mass (4.7 kg/m^2) and BPN comprising 2% (0.1 kg/m^2). A low BPN loading was used to prevent the BPN layer from independently forming a hydraulic barrier. Both configurations were tested in flexible wall permeameters following the procedures previously for k testing. Specimens were permeated with 50 mM CaCl_2 , which yielded an average k of 8.1×10^{-11} m/s when permeated through pure BPN; Chapter 3 showed that 50 mM CaCl_2 yielded the highest k of the solutions tested (viz. stronger and weaker solutions yielded lower k). Tests were run until at least the hydraulic and chemical

equilibrium termination criteria specified in ASTM D6766 were satisfied. Both configurations were run in duplicate.

Elution of LMwP from BPN into Na-B (up-gradient configuration) resulted in a three order-of-magnitude reduction in k relative to the down-gradient configuration (9.0×10^{-11} versus 9.8×10^{-8} m/s). BPN placed down-gradient from the Na-B layer yielded a similar k (1.7×10^{-7} m/s on average) to pure Na-B tests with the same solution as reported in Chapter 3. These data illustrate that when permeated with 50 mM CaCl_2 , LMwP eluted from BPN has the potential to greatly reduce the k of Na-B. To assess the longevity of the observed reduction in k , BPN-up-gradient tests were run for 1 yr, and a total of 50 pore volumes of flow (PVF), during which time no significant changes in k were observed. At the termination of permeation, all Na-B specimens were disassembled and tested for SI in DW. Similar SI (8-10 mL/2 g) were observed for Na-B from both up-gradient and down-gradient testing configurations. This SI is in the range typical for bentonite fully exchanged with Ca^{2+} . Specimen thickness, water content, and void ratio were similar for specimens tested with both the up-gradient and down-gradient configurations.

The reduction in k by LMwP eluted from BPN is theorized to result from the clogging of k -governing porosity within the Na-B layer. The Na-B layer was initially comprised of Na-B granules (Fig. 4.7a) with swelling potential dependent on the ionic strength of the hydrating solution (Norrish and Quirk 1954). When hydrated in an aggressive solution (e.g., 50 mM CaCl_2), the Na-B granules only underwent crystalline swell and did not form the gel structure characteristic of low k bentonite. High k resulted

as flow passed through k -governing intergranular macroporosity (Fig. 4.7b). Alternatively, when Na-B granules were hydrated in a dilute solution, a high swell (crystalline + osmotic swell) was realized and intergranular macroporosity was sealed off. Flow through osmotically swollen bentonite occurred through narrow and tortuous intragranular microporosity resulting in low k (Fig. 4.7c). In the up-gradient configuration clogging experiments, the Na-B layer only swelled in the crystalline regime and a gel structure was not obtained. Low k is theorized to then have resulted from the clogging of k -governing intergranular macroporosity by LMwP (Fig. 4.7d).

4.5.2. Polymer Mobility

The extent of polymer elution from BPN during long-term k tests was shown in Chapter 3 to be linearly correlated to the permeant CaCl_2 concentration. In DW, 25% (on average) of the original polymer content within BPN was retained. In 50 mM CaCl_2 , the CaCl_2 concentration used for clogging experiments, 35% polymer (on average) was retained. At the extreme endpoint of testing, permeation with 500 mM CaCl_2 resulted in 92% polymer retention (on average). These data are from after permeation for in excess of two years. However, for mobile polymer to impact the k of Na-B during a permeability test, sufficient polymer must be mobilized during the 48 h hydration period to clog high- k governing porosity.

To assess the mobility of polyacrylate during the 48 h in-permeameter hydration phase, polymer elution tests were conducted on BPN in DW, 5, 20, 50, 200, and 500 mM CaCl_2 . Granular BPN was placed into baskets made from stainless steel wire woven at a No. 60-mesh standard sieve (ASTM E11). Baskets had square bottoms

measuring 5 cm in length/width and 3-cm height sides. Granular BPN was placed at a mass per area of 0.25 kg/m^2 and evenly distributed across the bottom of each basket. Baskets were then lowered into a dish containing 625 mL of solution (liquid-to-solid ratio of 1000:1), and were affixed in a suspended configuration with the bottom of the basket 2-cm below the solution surface. Polymer was allowed to solubilize and diffuse for 48 h, at which time, the baskets were removed and water was allowed to freely drain from the basket (inducing advective removal of solubilized polymer). Polymer content of material retained in the baskets was determined by loss-on-ignition.

The fraction of polymer retained in each basket after 48 h is shown for varying CaCl_2 concentrations in Fig. 4.8. The fraction of polymer retained in BPN after long-term k testing (Chapter 3) is also included in Fig. 4.8 for comparison. Elution test data follow the trend exhibited by BPN in long term k experiments. In more dilute solutions ($\leq 50 \text{ mM CaCl}_2$), BPN retained less polymer during 48-h elution than during > 2 years of permeation. This behavior is believed to result from the decreased specimen thickness of BPN during elution experiments, and the lower void ratio of BPN freely hydrated relative to BPN tested under a $\sim 13\text{-kPa}$ effective stress. In 500 mM CaCl_2 , similar (near complete) retention of polymer was observed. These data demonstrate that in more dilute solutions ($\leq 50 \text{ mM CaCl}_2$) up-to between 75% (with DW) and 82% (with 50 mM CaCl_2) of the polymer initially contained within BPN may mobilize, but polymer mobility may be minimal in CaCl_2 solutions with concentrations in excess of 200 mM . Consequently, clogging of hydraulically active porosity by mobile polyacrylate is

hypothesized to be minimal in solutions with CaCl_2 concentration stronger than 200 mM. This hypothesis is explored later in this chapter.

Quantification of the adsorptive capacity of Na-B for mobilized polymer from BPN was achieved through batch adsorption tests. Adsorption tests were conducted by adding Na-B ground to pass a No. 200 woven-wire sieve (ASTM E11) to DW, 5, 10, 20, 50, 200, and 500 mM CaCl_2 . Bentonite and a CaCl_2 , or DW, solution were mixed in an end-over-end rotator at 30 rpm for 1 h, at which time; LMwP eluted from BPN permeated with DW and dissolved at 25% (by mass) in DW was added. Prior to testing with all solutions, rotation time and liquid-to-solid ratio were systematically varied on specimens in DW and 50 mM CaCl_2 to determine the impact of these experimental parameters on adsorption. Exploratory testing was conducted with rotation times of 10 min, 16 h, 2 d, and 7 d as well as liquid-to-solid ratios of 10-to-1, 20-to-1, and 40-to-1; 40-to-1 was found to be the maximum ratio that would still generate filtrate. The polymer-to-bentonite ratio was kept constant at 3:1, because this ratio was expected to exceed the maximum adsorbed fraction based on the results of elution tests. Specimens were vacuum filtered through 2.5 μm glass microfiber filter paper after the requisite rotation time. Sequentially after all visible liquid had filtered, but prior to visible drying of the specimen, 5 50 mL aliquots of the eluent solution were added to ensure washing of free liquid. The filter paper was subsequently scraped, and the retained polymer quantity was determined by loss-on-ignition. No impact on polymer adsorption was detected, within the range of liquid-to-solid ratios and rotation times tested. Thus,

median parameters of 16 h rotation time and a liquid-to-solid ratio of 20-to-1 were chosen for further testing.

The fraction of polymer retained on the filter is presented in Fig. 4.8. With DW and 5 mM CaCl_2 , a low fraction of LMwP (16%) was retained, but, in solutions with CaCl_2 concentrations > 5 mM, near complete retention of LMwP was observed. Na-B polymer retention after permeation with DW and 5 mM CaCl_2 was similar to, but slightly higher than, polymer retention during elution experiments. Near complete retention in stronger solutions resulted from precipitated polymer globules. To determine if the formation of these globules was caused by interactions with Na-B, all tests were replicated without Na-B. The resultant retention data are also shown in Fig. 4.8. No polymer was retained in DW or 5 mM CaCl_2 , but similar to LMwP added to Na-B, near complete retention of polymer occurred in solutions with CaCl_2 concentrations > 5 mM. Polymer-only retention occurred by precipitated polymer globules. Stumm (1992) and Stumm and Morgan (1996) note that the ionic strength of a solution effect the configuration of anionic polyelectrolytes. At low ionic strength, polyelectrolytes have extended configurations (large hydrodynamic radii) because of intermolecular electrostatic repulsion. Conversely, at high ionic strength, the polyelectrolyte will have a coiled configuration. Multivalent cations (e.g., Ca^{2+}) can form crosslinks between negative carboxyl moieties off the polyacrylate backbone, and can then cause “catastrophic collapse by over-crosslinking” (Buckholz and Graham 1997). Buckholz and Graham (1997) showed that near-complete collapse of polyacrylate chains occurs, at the polymer concentration used in this study, at 27 mM CaCl_2 .

4.6. BPN AS A NA-BENTONITE ADDITIVE

4.6.1. Eluted Polyacrylate Clogged Bentonite

The results of polymer clogging experiments incorporating 2% BPN (by mass) illustrate that only a fraction of BPN may be a useful performance enhancing additive to Na-B. As such, granular mixtures of BPN and Na-B were permeated with solutions shown to result in high k when permeated through Na-B (viz. 50 and 500 mM CaCl_2). Malusis and Scalia (2007) showed that attempts to mix granular Na-B with a dissimilarly graded additive required stringent quality control to ensure uniform mixing throughout the specimen. For this reason, and because long term k tests on BPN were conducted in Chapter 3 on granular materials, BPN and Na-B granules with similar grain-size distributions (presented in Scalia et al. 2011) were used for mixture tests. Both materials had median granule diameters of approximately 0.9 mm. Mixing was accomplished following the methods described in Malusis and Scalia (2007). Permeability testing was conducted following the methods described in this study and Chapter 3. Specimens were permeated until all termination criteria detailed in ASTM D6766 were achieved.

The k of granular mixtures of BPN and Na-B to 50 and 500 mM CaCl_2 are shown by the mass fraction of BPN added in Fig. 4.9. BPN addition percentages of 0.1, 0.25, 0.5, 1, 2, 5, and 15% were tested with 50 mM CaCl_2 . At the quantitative bookends, Na-B permeated with 50 mM CaCl_2 resulted in an equilibrium k between 3×10^{-7} and 7×10^{-8} m/s while the k of BPN ranged from 9×10^{-11} to 8×10^{-11} m/s. A BPN addition of 0.1% resulted in a reduction in k between 350- and 1400-times relative to pure Na-B. Addition of 1% BPN reduced the k of the mixture to below the k of pure BPN. Lower k

was also observed with 2, 5, and 15% BPN additions. The lower k of BPN-Na-B mixtures relative to pure BPN is theorized to result from the lower granule void ratio of Na-B permeated with 50 mM CaCl_2 .

Although both BPN and Na-B exhibited similar total void ratios after long-term permeation (between 1.9 and 2.0) (Fig. 4.5), Na-B exhibited a higher k . Thus, the voids through which flow was dominated in Na-B must be larger than those in BPN. When LMwP eluted from BPN clogs these flow paths, the microscale, normally non-flow governing, porosity in Na-B becomes hydraulically dominant; this porosity is theorized to have less conductive flow paths than the evenly distributed monolithic matrix of pure BPN. Investigation of this behavior and detailed analysis of the flow behavior of high permeability (granular) bentonite warrants further research.

In contrast to mixtures permeated with 50 mM CaCl_2 , BPN-Na-B mixtures permeated with 500 mM CaCl_2 did not see marked improvement in k without substantial, > 50% by mass, addition of BPN. These data are congruous with the mobility of LMwP from BPN granules presented in Fig. 4.8. In 500 mM CaCl_2 , minimal polymer mobility (< 5%) was observed, thus polymer eluted from BPN is believed to be ineffectual at clogging flow-governing porosity in the Na-B matrix. At BPN concentrations between 50% and 80%, dramatic variability in measured k was observed. Thus four replicate tests each were conducted of mixtures with BPN percentages of 50, 60, 70, 80, and 90%. For tests that exhibited k in excess of 10^{-10} m/s, specimens were permeated with rhodamine-WT dye at the conclusion of testing to investigate the location of flow. In high- k mixtures, flow was observed to occur in inter-

granular conduits between Na-B granules (viz. not BPN granules). Therefore, the conductivity of these mixtures appears to be dependent on the presence of sufficient granular BPN content to remove cross-specimen Na-B intergranular flow paths. At BPN percentages in excess of 90%, sufficient BPN was present within the matrix that continuous inter-granular flow paths did not occur in the 4 specimens tested, and a low k was realized.

The retention of polymer in BPN mixtures is shown in Fig. 4.10 as fraction of polymer retained after permeation versus the initial fraction of polymer contained. Data for granular mixtures of BPN and Na-B permeated with 50 and 500 mM CaCl_2 are shown. Maximum initial polymer fractions represent pure BPN specimens, while zero polymer fractions correspond to pure Na-B. When permeated with 50 mM CaCl_2 , 100% polymer retention was exhibited in mixtures with up to 5% BPN (by mass), while at a BPN content of 15%, only 75% of polymer initially contained was retained. Near complete polymer retention occurred in granular mixtures permeated with 500 mM CaCl_2 . These data are congruous with polymer mobility data shown in Fig. 4.8, and illustrate that the tailoring of BPN additive percentages to specific permeants may be necessary to minimize excess polymer.

4.7. DISCUSSION

4.7.1. Unique Low Permeability Mechanisms

Three mechanisms underlie the improved hydraulic behavior of BPN to varying concentrations of CaCl_2 . At low concentrations in the hydrating and permeating

solution, $< 50 \text{ mM CaCl}_2$, BPN exhibited the gel structure characteristic of Na-bentonite that has undergone osmotic swelling. Both BPN and Na-B had low k ($< 10^{-10} \text{ m/s}$) in this range of solutions. The $>$ two-times swelling of BPN in DW did not result a reduced relative conductivity, but did result in a thicker specimen through which the time for diffusive transport processes that govern mass transport in low- k bentonite will be lengthened.

In stronger solutions ($\geq 50 \text{ mM CaCl}_2$), BPN exhibited homogeneous structures and k that was inversely related to swell. Polymer within BPN granules acted to provide tensile reinforcement and prevented the formation of low-density bentonite spalling along the interface of hydrated granules. After initial hydration, inter-granular water was consolidated from between granules resulting in the formation of a tight homogeneous matrix and relegating flow to low k intragranular pathways. Inter-granular consolidation occurred because of the increased effective stress induced after prehydration upon opening the outflow line to initiate permeation. Although this is an artifact of the testing method, numerous mechanisms exist by which increases in effective stress after hydration may occur in the field; for example, in a bottom liner application, the placement of additional waste in a containment facility. Nonetheless, future compatibility studies on in-situ polymerized bentonite should carefully control the application of stresses to mirror field conditions. All specimens in this study were tested under low average effective stress (on average 20 kPa). Additional research is warranted to investigate the impact on k of elevated effective stress before and during the hydration phase as well as during the permeation phase.

As produced, BPN contained a surplus of soluble, potentially mobile, LMwP. In 50 mM CaCl_2 , a solution shown hydraulically incompatible to Na-B, eluted LMwP eliminated hydraulically governing porosity in Na-B and resulted in > two orders-of-magnitude reductions in k . Clogging of hydraulically active porosity may also have occurred in BPN permeated with 50 mM CaCl_2 , although this system generated a higher porosity version of the homogeneous (viz. not granular) matrix shown in Fig. 4.2c. The use of BPN as a polymer reservoir for the clogging of hydraulically active porosity warrants further study. While elution was shown to be minimal in 500 mM CaCl_2 , weaker leachates that are still hydraulically incompatible with Na-B may be containable by tailored additions of BPN.

4.7.2. Future Work

This study identified the mechanisms underlying the observed hydraulic behavior of an in-situ polymerized bentonite-polyacrylate nanocomposite (viz. BPN). As a result of the atypical (non-swell derived) mechanisms underlying the superior hydraulic performance of BPN, correlations of hydraulic behavior to traditional Na-B hydraulic indicators are inappropriate. For this reason, additional research into the properties of BPN is needed to better understand this novel geo-material. These topics include:

- Impact of desiccation cycling on BPN. Because BPN exhibited superior water absorptivity relative to Na-B, BPN may be more able to maintain a gel structure under adverse environmental conditions. Conversely, the increased water absorptivity of BPN might increase the potential magnitude of desiccation cracks during extreme drying.

- The response of BPN to real leachates. The superior hydraulic resistance of BPN to the synthetic leachates detailed in Chapter 3 makes BPN an excellent candidate material for the hydraulic containment of extreme leachates, but, as always, field-representative compatibility studies must come first.
- Potential for preconditioning of a Na-B layer with mobile polymer, followed by permeation with stronger leachates (such as 500 mM CaCl_2). Although LMwP was not readily mobile in 500 mM CaCl_2 , once the polymer is in-place, the immobility of LMwP may become an asset.
- Impact of granule size and mixing method on k . Addition of well distributed powdered BPN may allow for better distribution of BPN and act to offset the reduced polymer mobility in stronger solutions.
- Potential of LMwP to clog hydraulically active porosity in other soils. The reduction in k of the underlying soil upon which BPN was hydrated may illustrate the potential for LMwP to improve the hydraulic behavior of other soil systems. This topic is currently under investigation.
- The LMwP tested in this study was a product of chain termination during the in-situ polymerization process. The necessity of in-situ polymerization to produce reinforced granules is unknown, as is the necessity of in-situ polymerization to produce LMwP capable of clogging the hydraulically active porosity of Na-B. These topics are currently under investigation.

4.8. CONCLUSIONS

The coupled low swell and low hydraulic conductivity (k) of a granular bentonite-polyacrylate nanocomposite (BPN) permeated with aggressive inorganic solutions results from a lack of flow-governing macroscale porosity. Typically, flow-governing macroscale-porosity is sealed during the osmotic swelling of Na-B and results in a homogeneous gel structure and consequently low k . Although super swelling in dilute solutions because of the inclusion of superabsorbent polymer, polymer was not intercalated in BPN as is the case in Multi-Swellable Bentonite (MSB) and HYPER-Clay (HC). BPN exhibited a higher cation exchange capacity than unamended bentonite (142 cmol+/kg), but still exhibited cation exchange in divalent solutions such that in CaCl_2 solutions near complete exchange of native sodium by calcium was observed.

Despite exhibiting low swelling in aggressive CaCl_2 solutions ($> 50 \text{ mM}$), the intergranular-macroscale porosity that normally governs high k of bentonite in swell retarding solutions were closed in BPN. This closure occurred because BPN granules did not disintegrate in aggressive solutions but were observed to hold together. After the hydration phase of k testing, specimens were consolidated by an increase in effective stress of as much as 15 kPa at the outflow end of the specimen, and 7.5 kPa at the middle of the specimen. Consolidation removed free inter-granular porosity and agglomerated cohesive BPN granules to form a homogeneous structure. Because of the low swell of BPN granules in aggressive solutions, the resultant homogeneous matrix had a very low void ratio (with 500 mM $\text{CaCl}_2 < 1/14^{\text{th}}$ BPN in DW; $\sim 1/2$ Na-B in the same solution), and consequently a very low k ($< 10^{-12} \text{ m/s}$)

A portion of polymer within BPN was in the form of soluble, low molecular weight polyacrylate. This polymer was highly mobile in dilute solutions, but exhibited decreased mobility with increased solution concentration. When permeated with 50 mM CaCl_2 , elution of mobile polymer from BPN into a granular Na-bentonite matrix resulted in up to a 3,900-times reduction in k relative to pure Na-bentonite. BPN additions of as low as 1% (by-mass) resulted in an equilibrium k less than pure BPN. In contrast, the low mobility of low molecular weight polymer eluted from BPN in 500 mM CaCl_2 translated to reductions in the k of a BPN-Na-bentonite granular mixture only when the BPN component formed a homogeneous matrix across the extent of the specimen. Mobile polymer is theorized to reduce the k of the granular Na-B matrix by clogging hydraulically active porosity that traditionally governs high k of Na-bentonite in hydraulically incompatible solutions.

The data presented in this study, and in Chapter 3, illustrate that BPN may allow for containment of a range of solutions typically uncontainable with Na-bentonite. Based on the observed conductivity governing mechanisms, pure BPN may be necessary to contain highly aggressive solutions (e.g., 500 mM CaCl_2). Tailored blends of BPN and Na-B may allow for containment of mid-range solutions (e.g., 50 mM CaCl_2) where pure BPN is not necessary or may yield slightly higher k . Due to the novelty of this mineral-based environmental containment material, additional research is warranted.

4.9. REFERENCES

- Ashmawy, A., Darwish, E., Sotelo, N., and Muhammad, N. (2002). "Hydraulic performance of untreated and polymer-treated bentonite in inorganic landfill leachates." *Clays and Clay Minerals*, 50(5), 546-552.
- Buchholz, F., Graham, A. (1998). *Modern Superabsorbent Polymer Technology*. John Wiley and Sons, New York.
- Benson, C., Oren, A., and Gates, W. (2010). "Hydraulic conductivity of two geosynthetic clay liners permeated with a hyperalkaline solution." *J. Geotextiles and Geomembranes*, 28(2), 206-218.
- Bradshaw, S., Benson, C., and Scalia, J. (2012). "Cation exchange during subgrade hydration and effect on hydraulic conductivity of GCLs." Submitted to *J. of Geotech. and Geoenviron. Eng.*, (in press).
- Deng, Y., Dixon, J., White, N., Loeppert, R., and Juo A. (2006). "Bonding between polyacrylamide and smectite." *Colloids and Surfaces A: Physiochem. Eng. Aspects*, 82-91.
- Di Emidio, G., Van Impe, W., Mazzieri, F. (2010). "A polymer enhanced clay for impermeable geosynthetic clay liners." *Proceedings of Sixth International Conference on Environmental Geotechnics*, International Society for Soil Mechanics and Geotechnical Engineers, New Delhi, India, 963-967.
- Di Emedio, G., Van Impe, W., Flores, V. (2011). "Advances in geosynthetic clay liners: polymer enhanced clays." *GeoFrontiers 2011. Advances in Geotechnical Engineering*, American Society of Civil Engineers, Reston, USA, 1931-1940.

- Flynn, B., Carter, G. (1998). "Waterproofing material and method of fabrication thereof." *US Patent Number: 6,537,676 B1*.
- Gates, W. and Bouazza, A. (2010). "Bentonite transformations in strongly alkaline solutions." *Geotextiles and Geomembranes*, 28(2), 219-225.
- Guyonnet, D., Gaucher, E., Gaboriau, H., Pons, C., Clinard, C., Norotte, W., and Didier, G. (2005). "Geosynthetic clay liner interactions with leachate: Correlation between permeability, microstructure, and surface chemistry." *J. of Geotech. and Geoenviron. Eng.*, 131(6), 740-749.
- Jo, H., Benson, C., and Edil, T. (2004). "Hydraulic conductivity and cation exchange in non-prehydrated and prehydrated bentonite permeated with weak inorganic salt solutions." *Clays and Clay Minerals*, 52(6), 661-679.
- Jo, H., Benson, C., Shackelford, C., Lee, J., and Edil, T. (2005). "Long-term hydraulic conductivity of a non-prehydrated geosynthetic clay liner permeated with inorganic salt solutions." *J. of Geotech. and Geoenviron. Eng.*, 131(4), 405-417.
- Jo, H., Katsumi, T., Benson, C., and Edil, T. (2001). "Hydraulic conductivity and swelling of non-prehydrated GCLs permeated with single species salt solutions." *J. of Geotech. and Geoenviron. Eng.*, 127(7), 557-567.
- Katsumi, T., Ishimori, Ho, Onikata, M., and Fukagawa, R. (2008). "Long-term barrier performance of modified bentonite materials against sodium and calcium permeant solutions." *Geotextiles and Geomembranes*, 26(1), 14-30.

- Kolstad, D., Benson, C., and Edil, T. (2004). "Hydraulic conductivity and swell of nonprehydrated GCLs permeated with multi-species inorganic solutions." *J. of Geotech. and Geoenviron. Eng.*, 130(12), 1236-1249.
- Kolstad, D., Benson, C., Edil, T., and Jo, H. (2004a). "Hydraulic conductivity of dense prehydrated GCL permeated with aggressive inorganic solutions." *Geosynthetics International*, 11(3).
- Lyklema, J. (1985). "How polymers adsorb and affect colloid stability, flocculation, sedimentation, and consolidation." *Flocculation, Sedimentation and Consolidation: Proceedings of the Engineering Foundation Conference, Sea Island, Georgia*, Moudgil, B. and Somasundaran, P. Eds., United Engineering Trustees, Inc., 3-21.
- Malusis, M. and Scalia, J. (2007). "Hydraulic conductivity of an activated carbon-amended geosynthetic clay liner." *GeoDenver 2007. New Peaks in Geotechnics*, American Society of Civil Engineers, Reston, VA, 1-13.
- Mazzieri, F., Emidio, G., Van Impe, P. (2010a). "Diffusion of calcium chloride in a modified bentonite: Impact on osmotic efficiency and hydraulic conductivity." *Clays and Clay Minerals*, 58(3), 351-363.
- Mazzieri, F., Pasqualini, E., Emidio, G. (2010b). "Migration of heavy metals through conventional and factory-prehydrated GCL materials." *Proceedings of Sixth International Conference on Environmental Geotechnics*, International Society for Soil Mechanics and Geotechnical Engineers, New Delhi, India, 963-967.

- McBride M. (1994). *Environmental Chemistry of Soils*. Oxford University Press, New York.
- Mesri, G. and Olson, R. (1971). "Mechanisms controlling the permeability of clays." *Clays Clay Minerals*, 19, 151-158.
- Norrish, K., and Quirk, J. (1954). "Crystalline swelling of montmorillonite, use of electrolytes to control swelling." *Nature*, 173, 255-257.
- Onikata, M., Kondo, M., and Kamon, M. (1996). "Development and characterization of a multiswellable bentonite." *Environmental Geotechnics*. Taylor and Francis, Rotterdam, 587-590.
- Onikata, M., Kondo, M., Hayashi, N., and Yamanaka, S. (1999). "Complex formation of cation-exchanged montmorillonites with propylene carbonate: Osmotic swelling in aqueous electrolyte solutions." *Clays and Clay Minerals*, 47(5), 672-677.
- Petrov, R. and Rowe, R. (1997). "Geosynthetic clay liner (GCL) – chemical compatibility by hydraulic conductivity testing and factors impacting its performance." *Canadian Geotechnical Journal*, 34, 863-885.
- Scalia, J., Benson, C. H., Edil, T. B., Bohnhoff, G. L., and Shackelford, C. D. (2011). "GCLs containing bentonite polymer nanocomposite." *GeoFrontiers 2011. Advances in Geotechnical Engineering*, American Society of Civil Engineers, Reston, USA, 2001-2009.
- Schroeder, C., Monjoie, A., Illing, P., Dosquet, D., and Thorez, J. (2001). "Testing a factory-prehydrated GCL under several conditions." *Proceedings, Sardinia 2001, 8th International Waste Management and Landfill Symposium*, CISA Environmental Sanitary Engineering Centre, Cagliari, Italy, 187-196.

- Shackelford, C., Benson, C., Katsumi, T., Edil, T., and Lin, L. (2000). "Evaluating the hydraulic conductivity of GCLs permeated with non-standard liquids." *Geotextiles and Geomembranes*, 18(2-3), 133-161.
- Stumm, W. (1992). *Chemistry of the Solid-Water Interface*, John Wiley and Sons, New York.
- Stumm, W., and Morgan, J. (1996). *Aquatic Chemistry*, 3rd ed. Wiley, New York.
- Trauger R. and Darlington J. (2000). "Next-generation geosynthetic clay liners for improved durability and performance." *TR-220*. Colloid Environmental Technologies Company, Arlington Heights, 2-14.
- Tran, N., Dennis, G., Milev, A., Kannangara, G., Wilson, M., and Lamb, R. (2005). "Interactions of sodium montmorillonite with poly(acrylic acid)." *Journal of Colloid and Interface Science*, 290(2), 392-396.
- USEPA (2007). Method 6010B: *Inductively Coupled Plasma-Atomic Emission Spectrometry, Physical/Chemical Methods SW846, Third Ed.* US Environmental Protection Agency, Office of Solid Waste and Emergency Response, Washington, DC.
- Vasudevan, D., Fimmen, R., and Francisco A. (2001). "Tracer-grade Rhodamine WT: structure of constituent isomers and their sorptive behavior." *Environmental Science and Technology*, 35(20), 4089-4096.

4.10. ABBREVIATIONS

BC – Bound cations

BPN – Bentonite-polyacrylate nanocomposite

CEC – Cation exchange capacity

DW – Deionized water

DPH-GCLs – Dense-prehydrated geosynthetic clay liner

EC – Electrical conductivity

HC – HYPER-clay

ICP-OES – Inductively coupled plasma-optical emission spectroscopy

k – Hydraulic conductivity

LMwP – Low molecular weight polyacrylate

MMT – montmorillonite

MSB – Multi-swellable bentonite

PVF – Pore volumes of flow

SC – Soluble cations

4.11. FIGURES

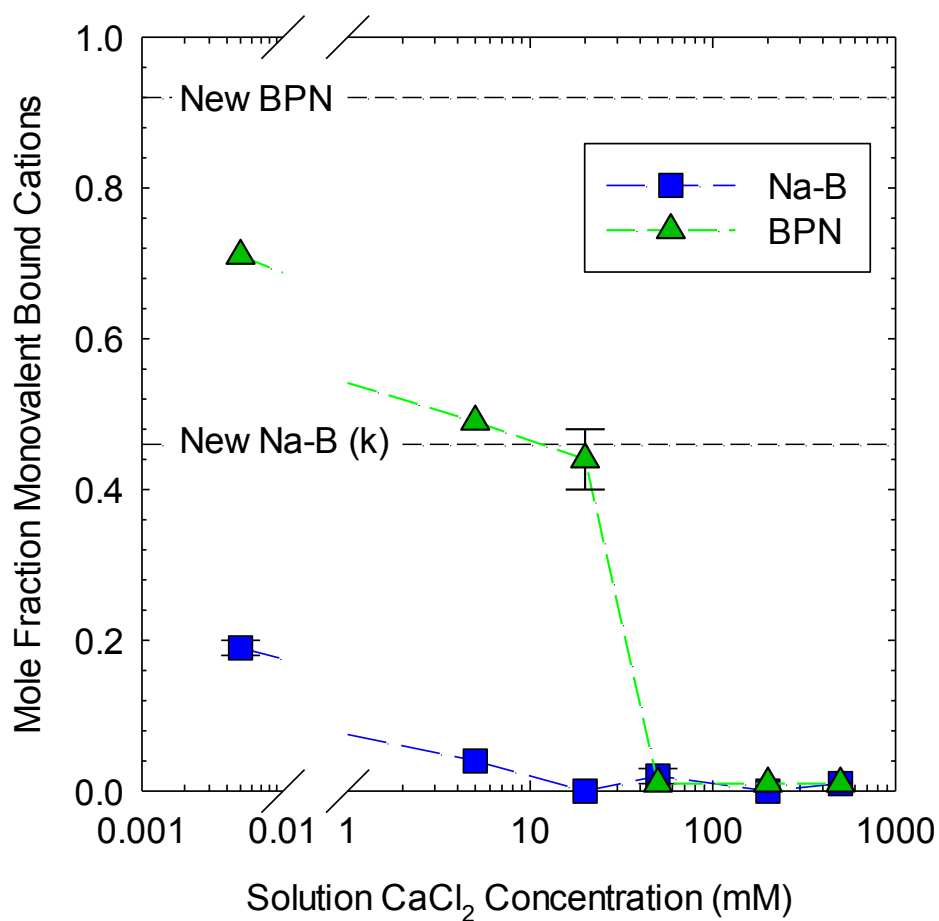


Fig. 4.1 Mole fraction of bound monovalent cations at termination of long term testing versus the CaCl_2 concentration of the permeant solution. Data for DW are plotted at the method detection limit of Ca^{2+} within DW (0.05 mM Ca^{2+}).

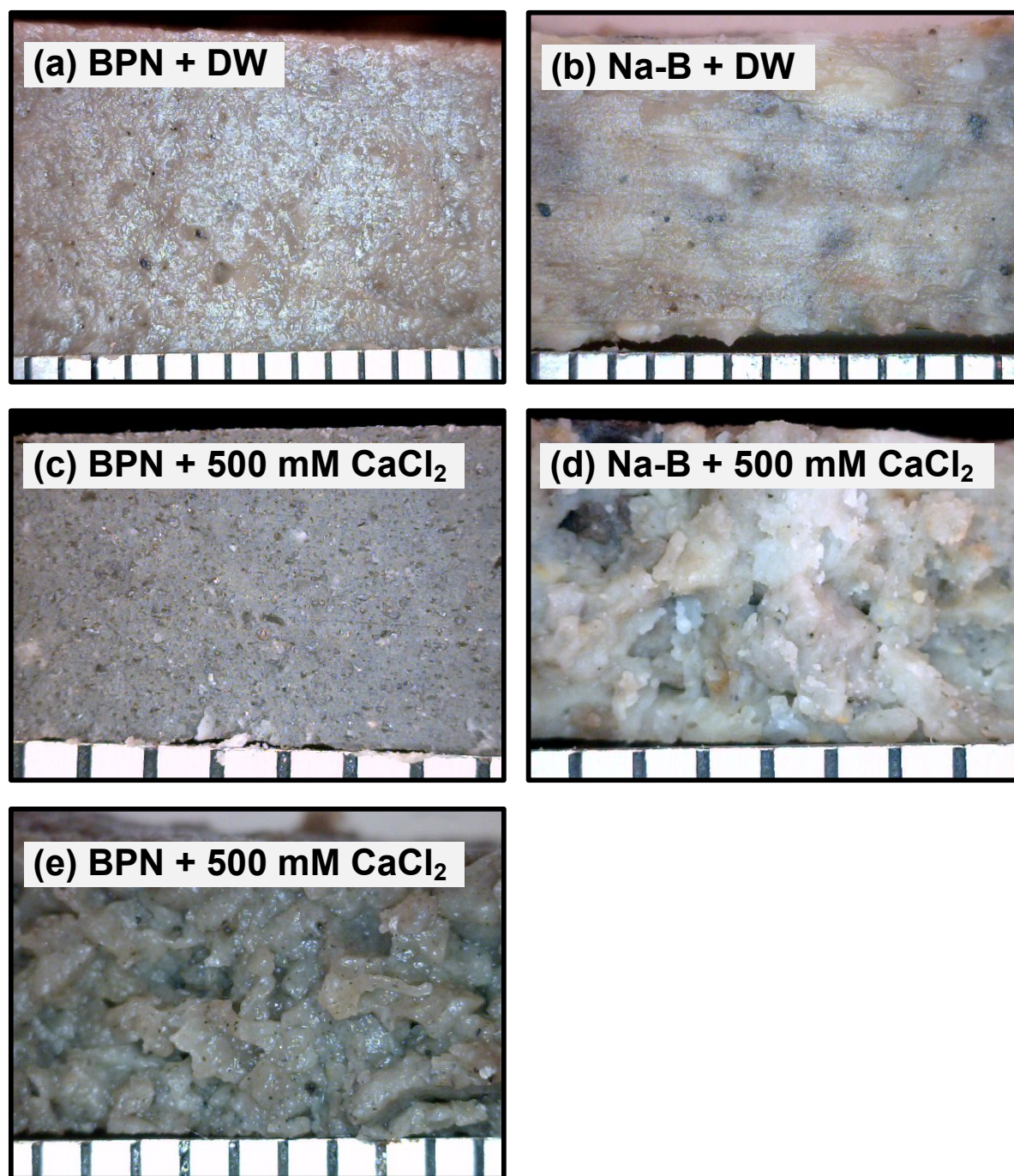


Fig. 4.2 Cross sections of bentonite-polymer nanocomposite, BPN (a, c, and e), and sodium bentonite, Na-B (b and d) specimens after permeation with DW (a and b) and 500 mM CaCl_2 (c, d, and e). Tests conducted by standard method (a, b, c, and d) and low change in effective stress method (e). Bottom scale in each image is in mm.

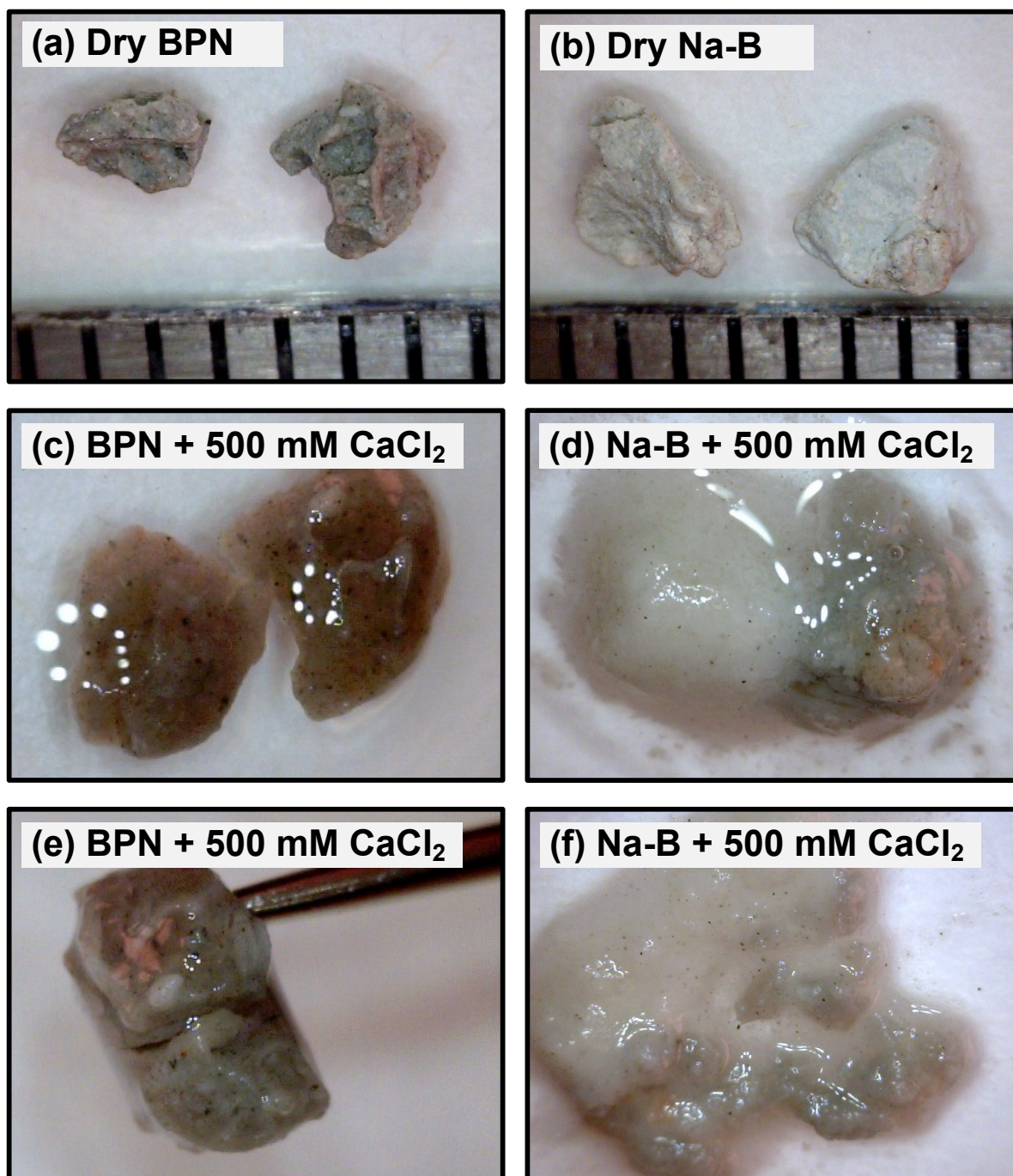


Fig. 4.3 Granular hydration of bentonite-polyacrylate nanocomposite, BPN (a, c, and e), and sodium bentonite, Na-B (b, d, and f).

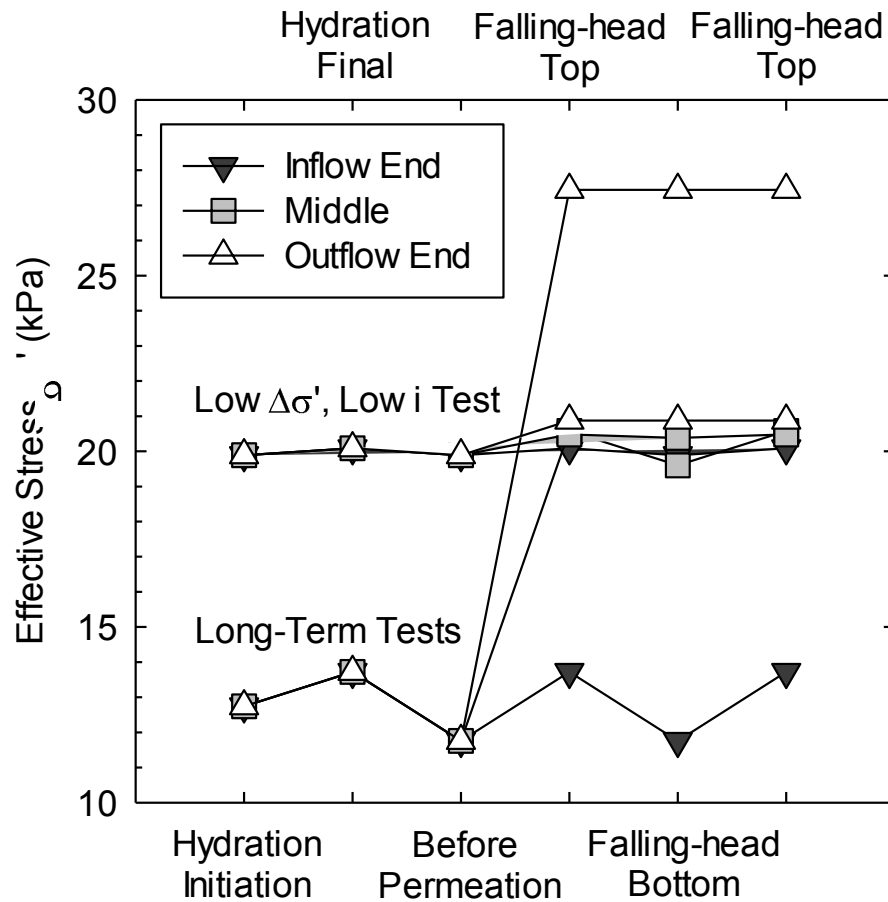


Fig. 4.4 Effective stress history of GCL specimens during permeation by standard method used for long term hydraulic conductivity tests, and low change (Δ) in effective stress (σ') low hydraulic gradient (i) method.

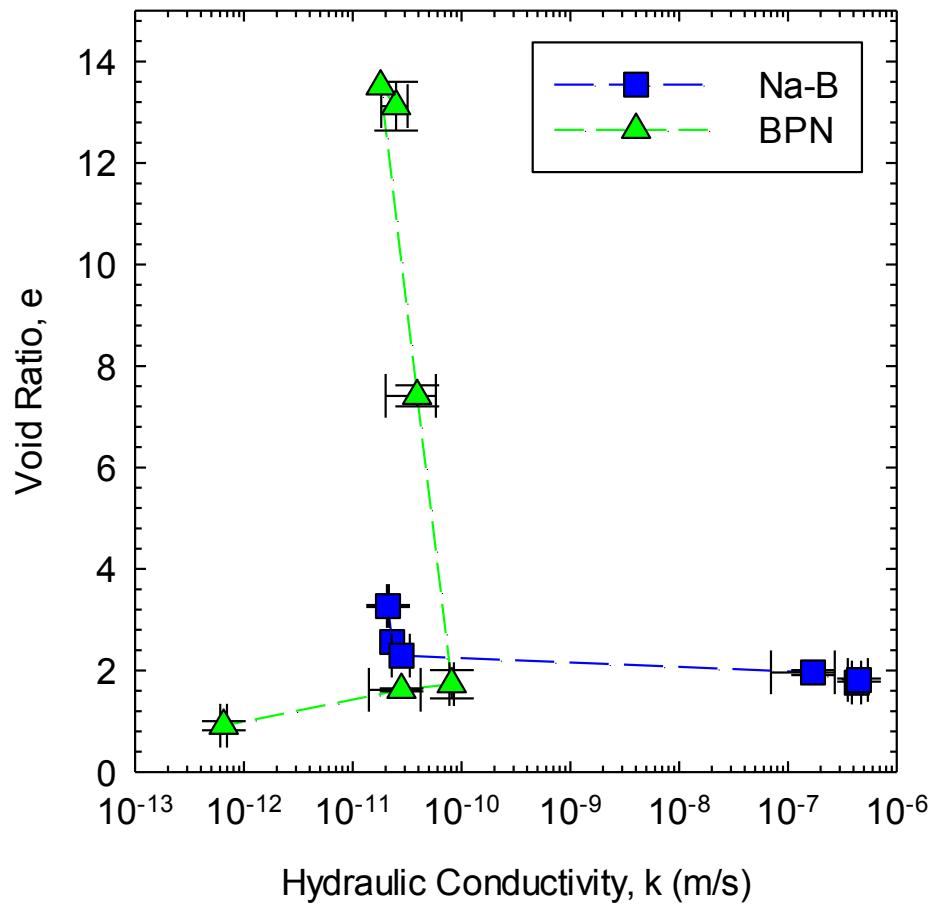


Fig. 4.5 Void ratio (e) at the termination of long term permeation versus final equilibrium hydraulic conductivity (k) from Chapter 3.

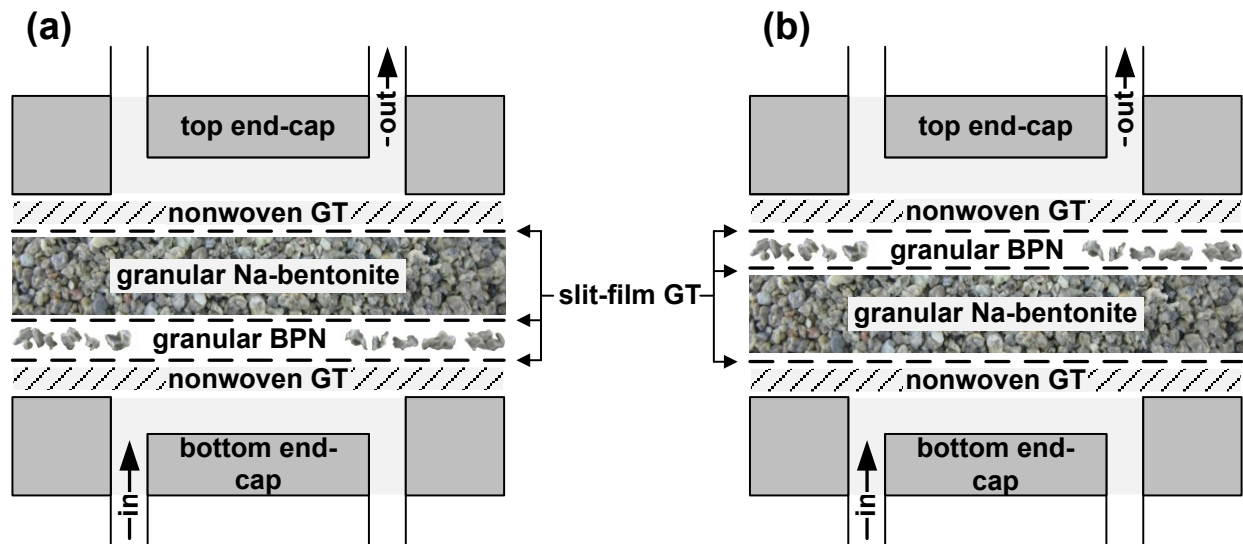


Fig. 4.6 Schematics of permeameter assemblages for BPN clogging experiments where (a) BPN was placed up-gradient from granular Na-bentonite layer and (b) BPN was placed down-gradient from granular Na-bentonite layer.

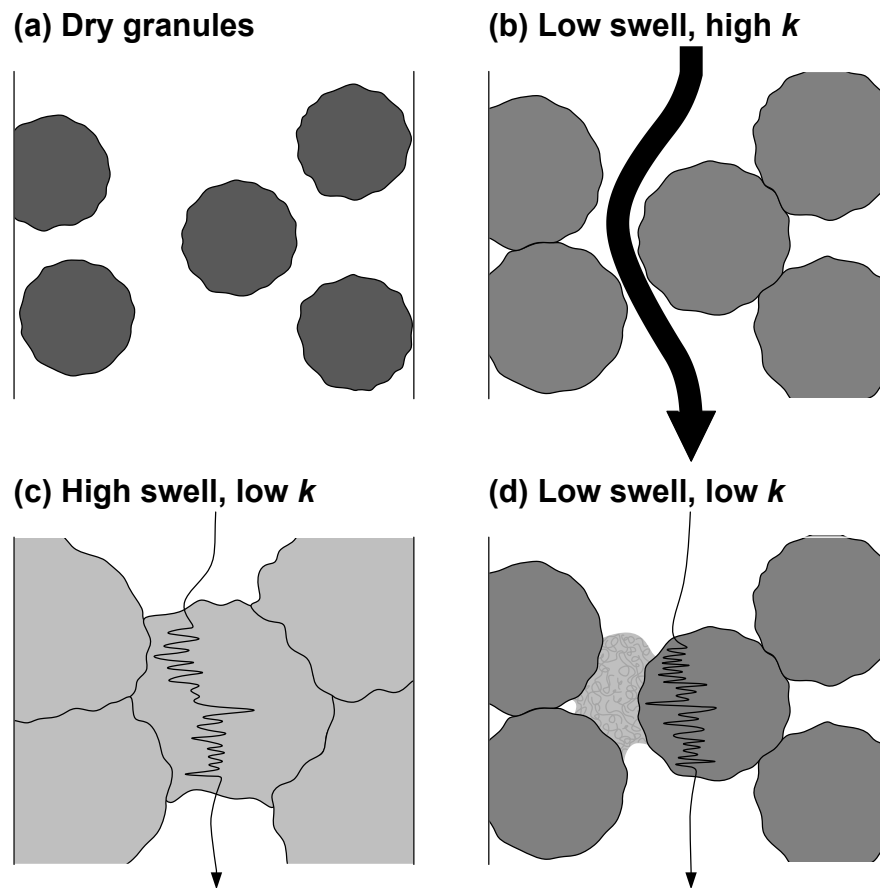


Fig. 4.7 Conceptual models for observed hydraulic behavior. The swell of dry granules of Na-bentonite (a) depends on the ionic strength of the hydrating solution, with low swell occurring with 50 mM CaCl_2 and consequently a high hydraulic conductivity (k) (b). Na-bentonite granules hydrated with a dilute solution exhibit gel formation and low hydraulic conductivity (c). Clogging of hydraulically active porosity by low-molecular-weight polyacrylate in bentonite permeated with 50 mM CaCl_2 yields a low k (d).

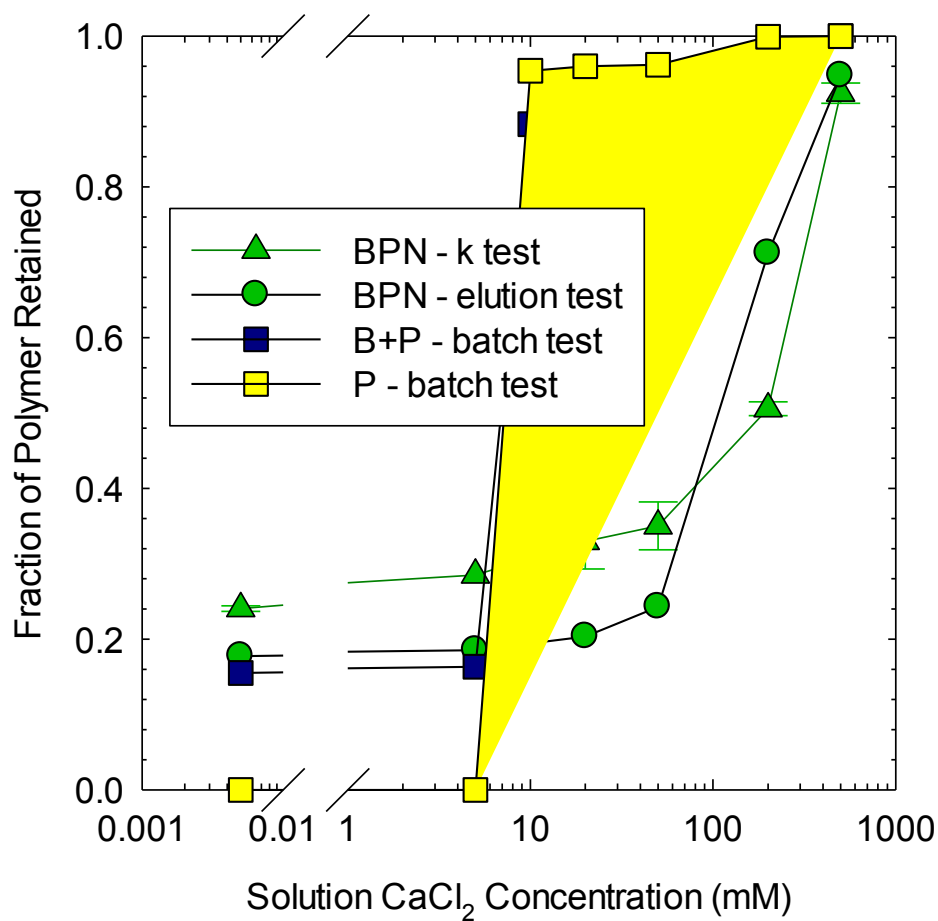


Fig. 4.8 Fraction of polymer (P) retained in specimen determined by loss-on-ignition after long term hydraulic conductivity (k) testing and polymer-mobility basket testing in varying concentration CaCl_2 solutions. Data for DW are plotted at the method detection limit of Ca^{2+} within DW (0.05 mM Ca^{2+}).

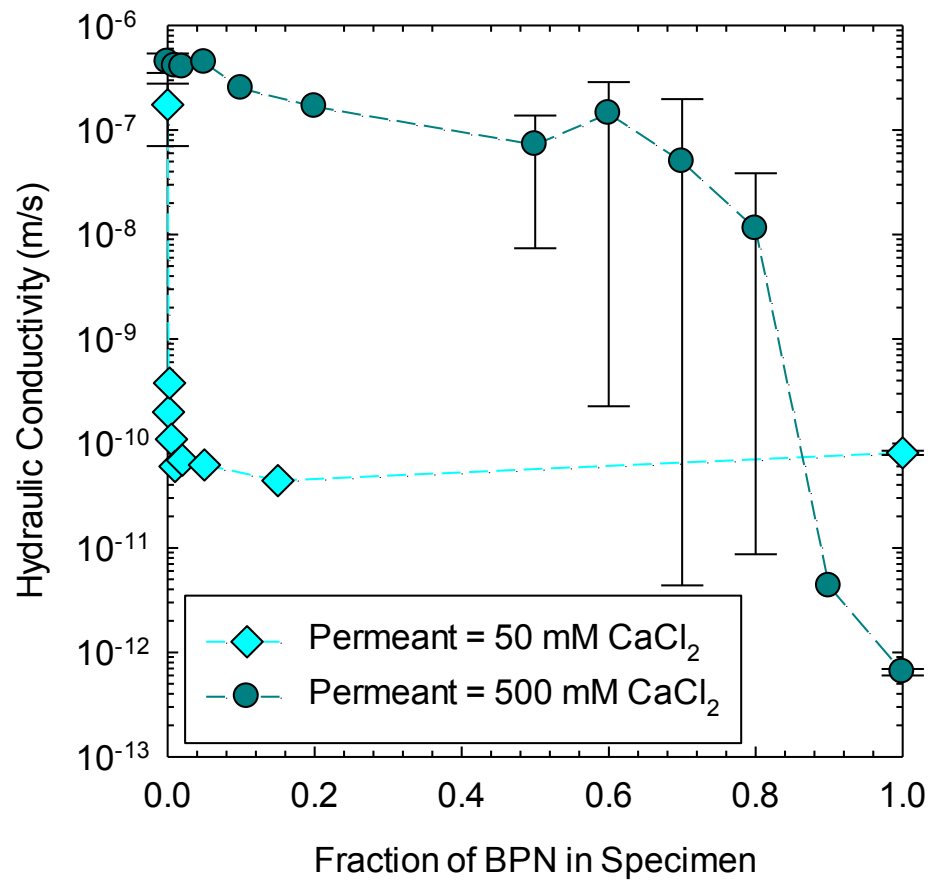


Fig. 4.9 Hydraulic conductivity versus fraction of BPN in permeated specimen.

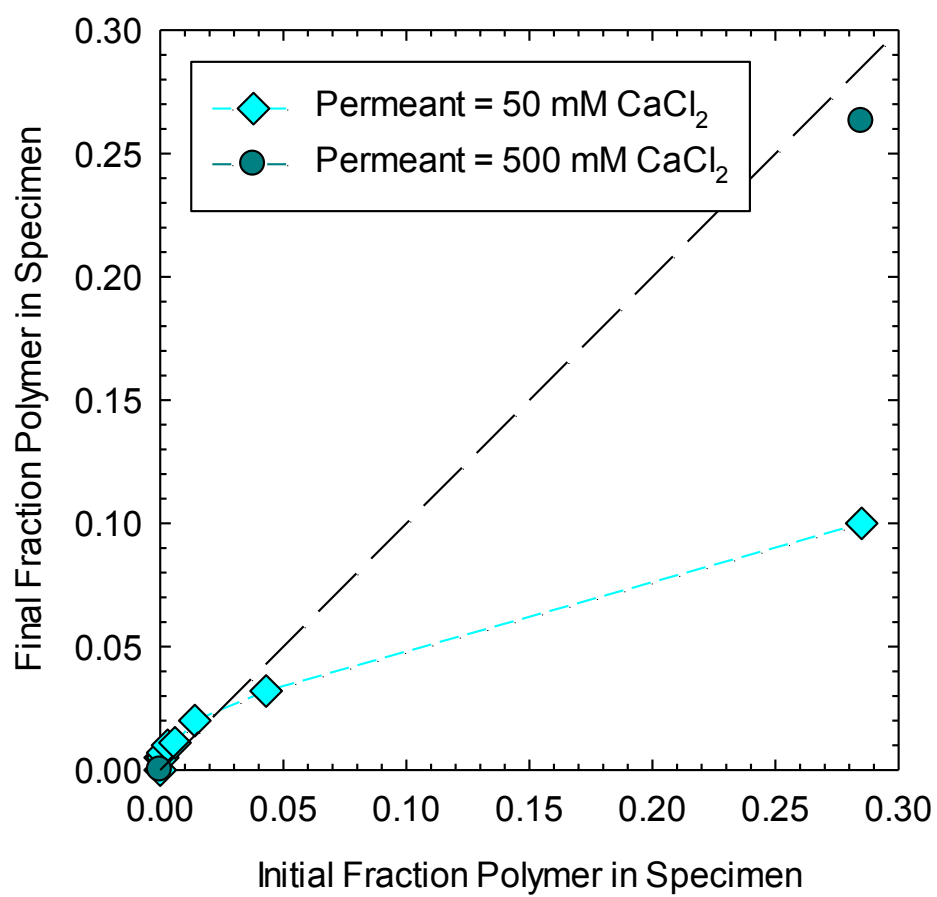


Fig. 4.10 Fraction of polymer remaining after permeation versus fraction of polymer initially contained.

CHAPTER FIVE

NOVEL POLYMER ADDITIVES FOR ENHANCED HYDRAULIC PERFORMANCE OF MINERAL BARRIER LAYERS TO INCOMPATIBLE PERMEANTS

5.1. ABSTRACT

Enhancement of the hydraulic conductivity (k) of Na-bentonite (Na-B) and other mineral barrier layers to incompatible permeant solutions by addition of polyacrylate was investigated. To boost the swelling of Na-B, and thus enhance the mechanism by which Na-B derives low k , superabsorbent Na-polyacrylate (SAP) was investigated as an additive. Dry mixing of granular SAP with Na-B did not result in an improved k relative to pure Na-B or SAP when directly permeated, i.e., without prehydration with a dilute solution, with 50 mM CaCl_2 or 500 mM CaCl_2 ; these solutions result in high k in Na-B). Wet mixing of SAP with Na-B does not result in improved k relative to pure Na-B or SAP when directly permeated with 500 mM CaCl_2 , but results in an up to two orders-of-magnitude reduction in k when permeated with 50 mM CaCl_2 . In a break from the traditional methodology of swell enhancement for improved performance, the use of water-soluble polyacrylate (WSP) to improve Na-bentonite hydraulic performance was investigated by permeation of granular Na-B-WSP mixtures with 50 mM CaCl_2 and 500 mM CaCl_2 . The hydraulic impact of WSP on other mineral barrier layers (clean sand, non-plastic silt, low-plasticity silt, and kaolinite) was also examined. When the weight-average-molecular weight (M_w) of the WSP additive was less than 1,080,000 g/mol, mass-percentage additions as low as 0.75% resulted in > three orders-of-magnitude reduction in k to 50 mM CaCl_2 . Conversely, granular mixing of WSP did not improve k

with 500 mM CaCl_2 . Water-soluble polyacrylate with an Mw of 255,000 g/mol added upstream to kaolinite also reduced the k of the composite system by three orders-of-magnitude.

5.2. INTRODUCTION

Sodium (Na) bentonite clay is used to control flow and contaminant migration in a variety of aqueous barrier applications such as barriers for waste containment (e.g., landfills, wastewater ponds, manure lagoons, radioactive-waste storage), groundwater cutoff walls, secondary containment in tank farms, and seals in monitoring and water supply wells. Na-bentonite excels in barrier applications because the characteristic swelling of Na-bentonite in dilute solutions results in narrow and tortuous flow paths that minimize the passage of dilute solutions. Unfortunately, Na-bentonite is chemically unstable in solutions containing polyvalent cations, high ionic strengths, or extreme pHs; conditions that are prevalent in waste containment applications. Chemical instability can lead to orders-of-magnitude increases in hydraulic conductivity (k) and contaminant transport.

Recognition of these limitations of Na-bentonite has spurred the development of bentonites modified with organic molecules, for example propylene carbonate or Na-carboxymethyl cellulose, to maintain low k in typically incompatible solutions (Onikata et al. 1996, Flynn et al. 1998, Onikata et al. 1999, Onikata et al. 2000, Trauger and Darlington 2000, Schroeder et al. 2001, Ashmawy et al. 2002, Kolstad et al. 2004, Katsumi et al. 2008, Emidio et al. 2010, Mazzieri et al. 2010a, Mazzieri et al. 2010b, Emidio et al. 2011). Efforts to date to produce more stable low- k bentonites have

mechanistically focused on activating or maintaining high bentonite swelling (osmotic swelling). In natural (unmodified) Na-bentonites, osmotic swelling occurs in dilute solutions in response to the high concentration gradient between the hydrated bound cations, viz. the cations satisfying the cation exchange capacity, and the free cations in the bulk pore water. Osmotic swelling only occurs when monovalent cations (e.g., Na^+) dominate the bound cations and when the hydrating solution has a low ion concentration. Polymeric additives that activate osmotic swell have been shown to shift this behavior to a higher concentration regime; examples of these materials include multi-swellable bentonite, MSB, (Onikata et al. 1996) and HYPER-Clay, HC (Emidio et al. 2010). In these systems, a large organic molecule is inserted into the interlayer of montmorillonite (the active ingredient within bentonite). The hydration of these intercalated molecules, in combination with hydration of the mineral surface and bound cations, increases swell and assists in overcoming the electrostatic attraction between platelets that can limit swell at high concentrations. Despite showing a partially improved hydraulic behavior with polymeric intercalation, swell activated bentonites do not show greatly improved swelling in divalent solutions and are still sensitive to high ionic strength solutions and gradual replacement of monovalent cations by divalent cations. Additionally, production of these materials requires intensive wet mixing of a dissolved organic molecule into Na-bentonite to successfully intercalate the polymeric additive.

As an alternative method to enhance the maintenance of low k in Na-bentonite to typically incompatible solutions, Trauger and Darlington (2000) modified Na-bentonite with superabsorbent polymer to both add swell and increase chemical stability. The

resultant material was termed bentonite-polymer alloy (BPA). To maximize interaction between the superabsorbent polymer and Na-bentonite, Trauger and Darlington (2000) produced BPA by polymerizing an on organic monomer within Na-bentonite slurry. A geotextile (GT) impregnated with BPA showed a 4,000-times reduction in k to seawater relative to a Na-bentonite impregnated GT. Based on these favorable results, Chapter 3 and 4 studied a second generation of BPA, termed bentonite-polymer nanocomposite (BPN), for long-term hydraulic performance to typically incompatible solutions.

Chapter 3 compared the k , at chemical equilibrium, of BPN, Na-bentonite, and superabsorbent Na-polyacrylate (SAP), to a range of solutions typically result in high k with Na-bentonites (50, 200, 500 mM CaCl_2 , 1 M HNO_3 , and 1 M NaOH). At chemical equilibrium, BPN maintained a $k < 9.0 \times 10^{-11}$ m/s in all solutions tested. In contrast, Na-bentonite exhibited a k at least 2,500-times greater ($> 2.4 \times 10^{-7}$ m/s) in typically incompatible solutions. When permeated with 500 mM CaCl_2 , the k of BPN was in excess of five orders-of-magnitude lower than Na-bentonite. Swell indices (SI) of BPN were determined per ASTM D5890 in the permeant solutions. In DW, BPN swelled to 73-mL/2 g, > 3.5 times the base bentonite used to produce BPN (19.0 mL/2 g). Unlike k , the SI of BPN showed a strong inverse correlation to CaCl_2 concentration, such that in 50 mM CaCl_2 , BPN had a SI of 18.8 mL/2 g (compared to 10.3 mL/2 g for the base bentonite), and in 500 mM CaCl_2 BPN had a SI similar to the base bentonite (< 10 mL/2 g). Reduction of swell with increased concentration was consistent with Na-bentonite and other polymer-modified bentonites, but BPN did not exhibit the corollary relationship between swell and k typical of Na-bentonite (Jo et al. 2001, Kolstad et al. 2004b, etc.).

Chapter 4 showed that three mechanisms underlie the improved hydraulic performance of BPN, all correlated to the sealing of flow-governing macroporosity. In mid-strength 50 mM CaCl_2 , the high swelling of BPN (relative to Na-bentonite) is in the range typically correlated to low- k bentonite. This increased swelling is believed to result from the SAP component of BPN. BPN also contained a large fraction of mobile (viz. non superabsorbent) polyacrylate. Polymer eluted from BPN was shown to reduce the k of granular Na-bentonite permeated with 50 mM CaCl_2 by up to 3,900 times via clogging the hydraulically active porosity that typically dominates high k of Na-bentonite in solutions that preclude osmotic swell. Finally, in 200 and 500 mM CaCl_2 , BPN swelling was in the range typical of Na-bentonite, and polymer mobility was shown to be low, but BPN exhibited lower k than in more dilute solutions. This behavior was the result of intergranular and intragranular cohesion resulting from the stitching of montmorillonite platelets together by polyacrylate chains and post-hydration consolidation during k testing. The intent of this study was to investigate the leveraging of most of these mechanisms without the intensive production process associated with BPN.

This study investigates the use of polyacrylate to improve the hydraulic compatibility of Na-bentonite without the rigor associated with production of an in-situ polymerized nanocomposite (viz. BPN). Addition by dry mixing of granular SAP with granular Na-B was studied, as well as combination by wet mixing. The resultant materials were dried (if wet mixed), and tested for swelling and k to 50 mM CaCl_2 and 500 mM CaCl_2 . The use of water-soluble polyacrylate to improve Na-bentonite

hydraulic performance was also investigated by permeation of granular mixtures of WSP and Na-bentonite with 50 and 500 mM CaCl_2 . The hydraulic impacts of WSP on other mineral barrier layers (clean sand, non-plastic silt, low-plasticity silt, and kaolinite) were also examined.

5.3. MATERIALS

5.3.1 Na-Bentonite

Two natural Na-bentonites from Wyoming, USA were used in this study. The properties of both bentonites are summarized in Table 5.1. Geosynthetic clay liner (GCL) grade Na-bentonite, henceforth abbreviated as Na-B, was used for mixture and water-soluble polyacrylate clogging experiments. Na-B is sold by CETCO (Hoffman Estates, IL) under the name VOLCLAY CG-50. The granule size distribution (GSD) of Na-B is detailed in Scalia et al. (2011) and was similar to the GSD for bentonite from a GCL studied by Shackelford et al. (2000), but had a smaller fraction of fine sand-size particles; Na-B granules were classified as a SP in accordance with the Unified Soil Classification System (USCS) (ASTM D2487). Soluble cations (SC), bound cations (BC), and cation exchange capacity (CEC) were determined following ASTM D7503. Chemical analyses of extracts from SC and BC tests were performed using inductively coupled-plasma optical emission spectroscopy (ICP-OES) following USEPA Method 6010 B (USEPA 2007). Na-B had a CEC of $78 \text{ cmol}^+/\text{kg}$, in the range typical for GCLs. The mineralogical composition of Na-B based on X-ray diffraction (XRD) was 85-91%

montmorillonite, 0-5% augite, 2-4% quartz, and less than 3% cristobalite, plagioclase feldspar – andesine, calcite, illite/mica, heulandite, gypsum, ferroan dolomite, and K-feldspar – microcline.

A second Na-bentonite from Wyoming, USA was also used for production of Na-bentonite-SAP wet-mixtures. This bentonite was the same material used to produce the BPN studied in Chapters 3 and Chapters 4, and is henceforth abbreviated as BB (base bentonite). Base bentonite was chosen for bentonite-SAP wet mixtures to investigate the swelling addition by SAP. The SC, BC, and CEC of BB were determined in accordance with ASTM D7503 and are presented in Table 5.1. The mineralogy of BB was determined by XRD; BB was composed of 73-77% montmorillonite, 15-17% quartz, 4-5% plagioclase feldspar – andesine, and less than 3% illite/mica, heulandite, clinoptilolite, and calcite. Base bentonite was used for BPN production instead of Na-B because the clay had lower concentrations of soluble trace elements that could prematurely initiate polymerization.

5.3.2 Na-Polyacrylate

Super-adsorbent polymers can be manufactured to be cationic, anionic, or charge neutral. This paper focuses on anionic polyacrylate (both superabsorbent, SAP, and water-soluble, WSP), in which the charge of some of the carboxyl groups is satisfied by a sodium cation was used that is produced from relatively inexpensive monomers (Buchholz and Graham 1998). The formula unit of polyacrylate when neutralized by sodium is $(-\text{CH}_2-\text{CH}(\text{COONa})-)_n$. The SAP used in this study was the same as that used in Chapter 3. For granular mixtures, granular SAP was screened to

match a GCL as defined in Shackelford et al. (2000). The CEC of SAP used in this study was determined following the methods described in ASTM D7503, but with different liquid-to-solid (L:S) ratios necessitated by the absorptive ability of SAP. Liquid-to-solid ratios of 200:1, 400:1, 500:1, 750:1, and 1000:1 were tested to assess the impact of varying polymer concentrations. All ratios resulted in similar calculated bound and soluble cations. SAP had an average CEC of 194 cmol+/kg, with a standard deviation of 3 cmol+/kg across the range of L:S ratios tested (Table 5.1). The CEC of SAP was satisfied by 95% Na^+ , with the balance comprised of Mg^{2+} . SAP eluted 173 cmol+/kg of Na^+ , with a standard deviation of 4 cmol+/kg across the range of L:S ratios tested, and no other soluble cations detected. These data illustrate that SAP has more than double the CEC of GCL-grade Na-bentonite (173 versus 78 cmol+/kg) by the same testing methodology. These data also illustrate that in addition to being super swelling, a SAP additive may increase the sorptive capacity of bentonite to inorganic contaminants of concern.

Water-soluble polyacrylate (WSP) eluted from BPN permeability tests with DW were determined by gel permeation chromatography to have a weight average molecular weight (M_w) of 280,000 g/mol, and a polydispersivity index (weight average molecular weight over number average molecular weight, PDI) of ~6.0, illustrating a wide range of molecule sizes. In contrast, a M_w in the millions of g/mol is typical for a SAP (Buckholz and Graham 1998). Three commercially available WSPs were used to study clogging of hydraulically active porosity: low- M_w WSP, M_w = 2,000 g/mol, with a PDI of 2.2, mid- M_w WSP, M_w = 255,000 g/mol, with a PDI of 6.1 intended to mimic polymer eluted from BPN, and a high-MW soluble WSP, M_w = 1,080,000 g/mol, with a

PDI of 8. Polyacrylates with a higher PDI were chosen because they are easier to produce and are less expensive (Buckholz and Graham 1998); viz. low-PDI WSP was deemed by the researchers to be too expensive for potential geoenvironmental-scale applications and was not included in this study.

5.3.3 Other Soils

Four soils, in addition to bentonite, were used to investigate the potential of WSP to enhance the k of other geomaterials: fine sand, non-plastic silt, low-plasticity silt, and kaolinite. The CEC of each soil was determined in accordance to the methods described in ASTM D7503 and are summarized in Table 5.2. Non-plastic silt, low-plasticity silt, and kaolinite were compacted with standard Proctor energy (ASTM D698) at their respective optimum water contents for k testing. Fine sand was poured into the flexible-wall permeameter using a removable rigid mold and then densified by vibrations until obtaining the dry density at standard Proctor energy in an air-dry condition.

5.3.4 Permeant Liquids

Calcium chloride solutions at concentrations of, 5, 50, and 500 mM were used to concurrently investigate the effect of ionic strength and cation exchange. Kolstad et al. (2004b) showed that homoionic-polyvalent permeants provide a worst-case condition relative to monovalent-polyvalent ion blends that are generally more representative of actual permeants. These solutions were also used in Chapters 3 and 4 and thus allowed for direct comparison with BPN. The pH and electrical conductivity of these solutions are summarized in Table 5.3. Lee et al. (2005) showed that thin bentonite layers (i.e., GCLs) permeated with dilute-divalent solutions, such as 5 mM CaCl_2 ,

exhibited a low k ($< 2 \times 10^{-10}$ m/s). In contrast, permeation of a thin Na-B layer with a mid-strength solution, such as 50 mM CaCl_2 , or a high-strength solution, such as 500 mM CaCl_2 , was shown to result in a k on-the-orders of 10^{-8} m/s to 10^{-7} m/s. Similar results were shown for Na-B and SAP in Chapter 3. Thus, 5 mM CaCl_2 was selected to provide a base-line condition, and 50 and 500 mM CaCl_2 were chosen as incompatible solutions. Dilute 5 mM CaCl_2 was not tested on mixture experiments with soluble WSP because Na-B alone was shown in Chapter 3 to provide a low k to this solution. All CaCl_2 solutions were prepared by dissolving dihydrate calcium chloride salt ($\text{CaCl}_2 \cdot 2\text{H}_2\text{O}$) in DW. The DW used in this study classified as Type II water per ASTM D1193. Solutions were stored in collapsible carboys with no headspace to minimize interactions with atmospheric carbon dioxide (CO_2).

5.4. METHODS

5.4.1 Na-B-SAP Mixture (BSM) Production

Granular SAP mixed into granular Na-B was tested for swelling behavior and k . The resulting material was termed a Na-B-SAP mixture (BSM). Prior to mixing, SAP was scalped to match the GSD of granular Na-B (see Scalia et al. 2011 for GSD). To allow for homogeneous mixing, Na-B and SAP were then combined and tumbled end-over-end at 30 rpm for 1 min. For swell index tests (ASTM D5890), the resultant material was then ground to pass a No. 40 woven wire sieve (ASTM E11) but retained on the No. 60 woven wire sieve with a mortar and pestle and an expedited testing method was used (discussed subsequently).

5.4.2 BB-SAP Composite (BSC) Production

Base-bentonite-SAP composites (BSC) were created by adding BB to solutions with varying concentrations of SAP to combine montmorillonite and SAP domains. Varying SAP concentrations were used to generate BSCs with BB-to-SAP mass ratios of 2000-to-1, 1000-to-1, 200-to-1, 100-to-1, 20-to-1, 10-to-1, and 5-to-1. The range of BB-to-SAP ratios tested was limited by formation of polyacrylate gel at BB-to-SAP ratios $> 5:1$, and by the sensitivity of the analytical balances used in the production process at BB-to-WSP ratios $< 2000:1$. To produce BSCs, SAP passing the No. 40 woven wire sieve (ASTM E11) but retained on the No. 60 woven wire sieve (ASTM E11) was added to a 2-L bottle filled with 1.75 L of DW. The SAP solution was then tumbled for 10 min at 30 rpm and transferred to a 2-L volumetric flask. The volumetric flask was filled to volume with DW, and the SAP solution was returned to the 2-L bottle. 20 g of BC passing the No. 40 woven wire sieve (ASTM E11) but retained on the No. 60 woven wire sieve (ASTM E11) was then added over 60 s by dusting across the solution surface, and the resulting mixture was tumbled for 1 h. After tumbling, the solution was air dried at 20 °C. The resultant BPC was ground with a mortar and pestle and scalped to an identical GSD to BPN shown in Scalia et al. (2011).

The swell index (SI) test (ASTM D5890) is used as an indicator of bentonite quality and as an indicator parameter for k . For the production of BSC the goal of swell tests was to mimic the swelling of BPN, therefore, to closer mimic the swelling of granular bentonite or BPN in a k test and save time, an expedited swell testing procedure was used. To expedite BSC, BPN, or BB, passing a No. 40 woven wire

sieve (ASTM E11) but be retained on No. 60 woven wire sieve (ASTM E11) was deposited in 0.5 g increments over 5 s with at least 2 min between additions. This modified method is abbreviated as expedited swell index (ESI).

The SI and ESI of BB and BPN are shown at varying CaCl_2 concentration in Fig. 5.1. The ESI of BC was within 8% of the corresponding SI for all solutions tested. Close agreement between the ESI and SI of BPN is also demonstrated in 50, and 500 mM CaCl_2 , but the ESI of BPN in 5 mM CaCl_2 and DW was up to 50% lower than the SI. Thus, the ESI of BPN in dilute solutions does not mirror SI. However, because the intent of swell testing in this study was relative comparison and not correlation to k , ESI was used for subsequent exploratory testing. A research paper on potential avenues to expedite the SI test (for natural bentonites), but produce results comparable to the standard method is in preparation for submittal to the Geotechnical Testing Journal.

Equivalent swelling between BPN (ESI = 38.8 mL/2 g) and BSC was found via linear interpolation at a BB-to-SAP ratio of 1280:1. This ratio is 12.3-times lower than the calculated ratio at which the ESI of a BSC would equal 38.8 mL/2 g assuming no interaction between materials (BB-to-SAP ratio of 100:1). For comparison, BPN in Chapter 3 was initially composed of BB-to-SAP at a ratio of 2.5:1 (although a large portion of the initial polymer was not superabsorbent). To investigate the compatibility of BSCs in divalent solutions, BSC with ESI equivalent to BPN (BB-to-SAP ratio of 1280:1) and at the calculated ratio for equivalent swell assuming no material interaction (BB-to-SAP ratio of 100:1) were chosen for k testing.

5.4.3 Na-B-Polyacrylate (BPB) Production

Blends of Na-B with low-, mid-, and high-Mw polyacrylate were created by granular mixing. These mixtures were termed bentonite-polymer blends (BPBs). To allow for homogenous mixing, polyacrylate was scalped to match the grain size distribution of granular Na-B (see Scalia et al. 2011 for GSD). To generate *k*-test specimens, the requisite masses of each material were then combined and tumbled end-over-end at 30 rpm for 1 min to ensure mixing.

5.4.4 Hydraulic Conductivity (*k*)

Hydraulic conductivity tests were conducted on BSM, BSC, and BPB specimens in flexible-wall permeameters following the procedures detailed in ASTM D5084 for a falling-head constant-tail test. Gravity heads were used to apply cell and influent pressure. Backpressure was not applied to allow convenient collection of effluent for chemical analysis (i.e., pH, electrical conductivity). Specimens were tested under an average effective stress of 20 kPa and an average influent head of 1.5 m, corresponding to an average hydraulic gradient of 200 for a (typical) 7.5-mm thick specimen.

Specimens were prepared within the flexible-wall permeameters. Geotextiles were used in lieu of porous stones and filter paper. A latex membrane was attached to a 154-mm diameter base pedestal with three O-rings. A 0.75-kg/m² non-woven needle-punched GT was then placed atop the base pedestal, and topped with a heat-bonded non-woven GT. Granular BSM or BSC was then placed with a dry mass per unit area of

4.8 kg/m² and manually leveled. Two GTs and a top pedestal were then placed atop the specimen mirroring the lower assemblage. The top pedestal was secured to the latex membrane with three O-rings.

In-cell hydration was conducted for 48 h prior to flow. After the permeameter was assembled and connected to the falling headwater apparatus, cell pressure was applied and all tubing was saturated with the permeant liquid. The inflow line of the permeameter was then opened to allow the specimen to hydrate while the effluent line remained closed. After 48 h, the influent line was flushed to remove any air bubbles and flow was initiated by opening the effluent line. During testing, effluent was collected in fluorinated ethylene propylene sample bags. All tests were run until the hydraulic and chemical criteria described in ASTM D6766 were satisfied.

Tests investigating the potential of mid-Mw WSP to lower the k of fine sand, non-plastic silt, low-plasticity silt, and kaolinite, were assembled using an experimental setup similar to the eluted-WSP (from BPN) clogging experiments detailed in Chapter 4. The permeameter assembly used for testing is shown in Fig. 5.2. Identical to BSM, BSC, and BPB k testing, a 0.75-kg/m² non-woven needle-punched GT was placed atop the base pedestal and topped with a heat-bonded non-woven GT. Atop the non-woven GT, a non-continuous layer of WSP granules passing a No. 40 woven wire sieve (ASTM E11), but be retained on a No. 60 woven wire sieve (ASTM E11), were placed between non-woven needle-punched GTs. A 3-cm thick layer of compacted soil was then placed over (viz. down-gradient from) the WSP layer and topped with GTs mirroring the up-

gradient textiles. Tests were run until at least the hydraulic and chemical equilibrium termination criteria detailed in ASTM D6766 were satisfied.

5.4.5 X-ray Diffraction (XRD)

Onikata et al. (1996), Onikata et al. (1999), and Emidio et al. (2010) experimentally verified intercalation of polymer within bentonite by low-angle X-ray diffraction (XRD) on dried samples. Increases in the dried d001 spacing measurably > the spacing typical of dried MMT (1.4 nm) were deemed to be indicate polymer molecules physically propping open the interlayer. Low-angle XRD was used to determine the d001 spacing of Na-B, BB, BSCs, and BSMs. A Scintag PAD V X-ray diffractometer with CuK α radiation was used at a power of 45 kV and 40 mA. Na-B and BB exhibited a d001 peak at 1.4 nm. Because of the large hydrodynamic radius of SAP in solution, intercalation without prior full exfoliation of MMT platelets was unlikely to occur (Theng 1970).

5.5. RESULTS

5.5.1 SAP Mixtures Hydraulic Conductivity

The k of BSM specimens permeated with 5, 50, and 500 mM CaCl $_2$ are shown in Fig. 5.3 and summarized in Table 5.4. BSM specimens were composed of a granular mixture of Na-B with SAP at a mass ratio of 100:1, the theoretical ratio for equivalent swelling assuming no material interactions. Data for the component materials Na-B and SAP permeated with DW, 5, 20, 50, 200, and 500 mM CaCl $_2$ are included in Fig. 5.3 for

comparison; the hydraulic behavior of these materials are presented in greater detail in Chapter 3. In dilute 5 mM CaCl_2 , BPM 100:1 exhibits a low k (1.9×10^{-11} m/s), effectively identical to both parent materials. But, in both 50 and 500 mM CaCl_2 , BPM 100:1, Na-B, and SAP all exhibit similar and high k ($> 6 \times 10^{-8}$ m/s). These data illustrate that granular mixing of Na-B with SAP at a low SAP content does not produce a unique hydraulic behavior. Disassembly of BSM k experiments revealed visible segregation of granular material domains as shown in Fig. 5.4. XRD on air-dried BSM post k testing showed that SAP intercalation did not occur during saturation and permeation.

To investigate if lower Na-B-to-SAP ratios result in composite hydraulic behavior (viz. lower system k), additional tests were conducted with 50 mM CaCl_2 . This solution was chosen because SAP retains an 8-times higher SI in 50 mM CaCl_2 relative to Na-B (80 vs. 10 mL/2 g). Hydraulic conductivity tests were conducted at Na-B-to-SAP ratios of 10:1 and 1:1. A Na-B-to-SAP ratio of 10:1 yielded an equilibrium k of 6.8×10^{-8} m/s, similar to pure Na-B, SAP, and BSM at a 100:1 Na-B-to-SAP ratio. At a Na-B-to-SAP ratio of 1:1, the specimen exploded from the flexible membrane during the hydration phase of testing. A Na-B-to-SAP ratio of 5:1 was then tested and resulted in an equilibrium k of 1.3×10^{-7} m/s. Thus, granular addition of SAP impacted system swelling, as illustrated by the outcome of testing a 1:1 specimen, but is not a hydraulically impactful additive due to the hydrated-granule nature of both Na-B and SAP in 50 mM CaCl_2 .

The k of BSC produced at BB-to-SAP ratios of 1280:1 and 100:1 are presented for varying CaCl_2 concentrations of the permeant liquid in Fig. 5.3 and summarized in

Table 5.4. In dilute 5 mM CaCl_2 , both BSCs exhibited low k effectively identical to both parent materials. Similarly, when permeated with 500 mM CaCl_2 , both BSCs exhibited high k (6×10^{-8} m/s to 3×10^{-7} m/s) comparable to both parent materials and illustrating that the incorporation of SAP with Na-B did not improve the system hydraulic behavior to a high strength solution (viz. 500 mM CaCl_2). To 50 mM CaCl_2 , BSCs exhibited superior hydraulic performance relative to the parent materials. The k of BSC produced at a Na-B-to-WSP ratio of 1280:1 is two orders-of-magnitude lower than the k of the parent materials, while the k of BSC 100:1 is nearly three orders-of-magnitude lower than the k of the parent materials and only two-times higher than the k of BPN to the same solution (8.1×10^{-11} m/s) (Chapter 3). Thus, even a small addition of wet-mixed SAP can reduce the k of Na-B in 50 mM CaCl_2 . Both BPCs were analyzed by XRD to assess if intercalation of SAP had occurred within the montmorillonite; intercalation was not found.

5.5.2 SAP Mixtures Swell Index

The swelling behavior of BSM 100:1 in varying concentrations of CaCl_2 solutions is shown in Fig. 5.5 and summarized in Table 5.4. In both DW and 5 mM CaCl_2 , BSM 100:1 exhibited lower ESI than Na-B (23.5 mL/2 g vs. 30.7 mL/2 g and 22.0 mL/2 g vs. 28.7 mL/2 g). This behavior is hypothesized to result from the agglomeration and flocculation of Na-B around hydrated SAP granules during ESI testing (Theng 1970). At higher CaCl_2 concentrations (viz. 50 and 500 mM CaCl_2), the swelling of BSM 100:1 is effectively identical to Na-B (i.e., in the low-swelling range typical of calcium bentonite).

The swelling behavior of BSC produced at Na-B-to-SAP ratios of 1280:1 and 100:1 at varying CaCl_2 concentrations are presented in Fig. 5.5 and summarized in Table 5.4. In DW and 5 mM CaCl_2 , both BSCs exhibit higher ESI than the additive combination of the ESIs of the parent materials (BSC was created using BB which had a swell index of 22 mL/2 g in DW and 20 mL/2 g in 5 mM CaCl_2). Constructive material interactions are hypothesized to result from a stair-step/card-house fabric created from large montmorillonite-SAP flocks (O'Brien 1971). Unlike BSM, in BSC production, SAP is allowed to obtain an extended configuration before insertion of bentonite. When BB is then introduced to the dissolved SAP, BB peripheral complexes interact along multiple segments of the polymer chain creating a structure that has been likened to a "string of beads" (Theng 1970). The resulting large flocks then create a more open stair-step/card-house configuration than did additive-free BB tactoids and resulted in a higher porosity gel (viz. higher ESI).

5.5.3 SAP Mixtures – Hydraulic Conductivity and Swelling

The relationship between k and ESI is shown for BSM 100:1, BSC 100:1, and BSC 1280:1 in Fig. 5.6. Data for Na-B and SAP are included in Fig. 5.6 for comparison, but are discussed greater detail in Chapter 3. All three Na-B-SAP mixtures exhibited essentially the same relationship between k and ESI as Na-B. SAP exhibited a similar relationship, but in an extended swelling regime. These data show that low-dosage SAP addition to a Na-B matrix by the methods used in this study did not decouple the normative k -swell relationship. Additionally, granularly adding SAP to add

swell to Na-B to achieve improved hydraulic compatibility to typically incompatible solutions is of minimal (if any) benefit.

5.5.4 Non-Superabsorbent-Na-B Composites

The k of specimens composted of varying percentages of soluble (viz. low molecular weight) WSP permeated with to 50 and 500 mM CaCl_2 are presented in Fig. 5.7 and summarized in Table 5.5. When permeated with 50 mM CaCl_2 , both low- and mid-Mw WSPs produce a > three order-of-magnitude reduction in k relative to unamended Na-B. Both low- and mid- Mw WSPs yielded k within a factor of 5.5 at 2%, 5%, and 10% additive levels. These k are within the range typical for a Na-B that has undergone long-term permeation with a dilute solution containing divalent cations (e.g., Ca^{2+}) (Jo et al. 2005). High-Mw WSP was not as effective as low- and mid-Mw WSP at reducing k at a 5% additive level, and demonstrated no beneficial effect at a 10% additive level.

Converse to the hydraulic impact of low- and mid- Mw WSP when permeating with 50 mM CaCl_2 , all specimens permeated with 500 mM CaCl_2 demonstrate high k ($> 5 \times 10^{-8}$ m/s) when permeated through specimens with 2% to 20% high-Mw WSP (Fig. 5.5). These k were similar in magnitude to the k of unmodified Na-B (4.5×10^{-7} m/s). For the combinations tested, high-Mw WSP showed an inverse correlation to k , with low-Mw polymer exhibiting an order-of-magnitude lower k than high-Mw WSP at a 5% additive level.

For k tests with low-, mid-, and high-Mw WSP additives, the gravimetric water content of each specimen after permeation was similar to unmodified Na-B specimens; water contents ranged from 67-68% for Na-B permeated with 50 mM CaCl_2 , and 65-66% for Na-B permeated with 500 mM CaCl_2 . The lack of increase in water content with polymeric addition is indicative of a non-swell derived mechanism underlying the observed increases in hydraulic performance with low- and mid-Mw WSP.

The final mass fraction of polymer retained in each permeated specimen is compared to the initial mass fraction of polymer included in each specimen in Fig. 5.8. The method used to determine the polymer content is based on loss-on-ignition testing at 550°C and is discussed in detail in Chapter 4. No specimen retains more than 5% polymer at the conclusion of permeation. Only high-Mw polymer permeated with 500 mM CaCl_2 retained the entirety of initially included polymer. Polymer retention was higher with 500 mM CaCl_2 than 50 mM CaCl_2 for a given polymer loading. This was likely due to decreased polymer mobility at increased ionic strength due to increased polymer coiling and interaction with montmorillonite via cation bridging at higher CaCl_2 concentrations (Stumm 1992, Stumm and Morgan 1996). Low- and mid-Mw polymer addition caused reductions in k to 50 mM CaCl_2 . For these additives, increases in polymer content did not result in increased retained polymer. These data illustrate that Na-B-WSP interactions that underlie the observed reductions in k only utilize a mass percent of 0.75% with low-Mw polymer and approximately 3% with mid-Mw polymer. Polymer retention also increased with increased polymer Mw across the range tested.

Increased polymer Mw equates to larger hydrodynamic radii polymer molecules, which are likely less mobile within the effective porosity of the Na-B matrix.

5.5.5 Non-Superabsorbent-Soil Composites

The relative contributions to reduction in k , with 50 mM CaCl_2 , of physical-only clogging of hydraulically dominant porosity and polymer-clay bonding between the polymer and clay matrix cannot be differentiated based on the data presented in Fig. 5.7. To differentiate these phenomenon, k tests were conducted in which polymer was placed up-gradient from compacted layers of clean sand, non-plastic silt, low-plasticity silt, and kaolinite. These soils exhibit both higher and lower k than Na-B permeated with 50 mM CaCl_2 (1.8×10^{-7} m/s). Assuming that soil layers with lower k than Na-B permeated with 50 mM CaCl_2 have less flow governing porosity and vice versa, if clogging is purely a physical phenomenon, soils with $k < 1.8 \times 10^{-7}$ m/s should see similar impacts of up-gradient polymer when permeated with 50 mM CaCl_2 . Soil layers were permeated with and without preceding layers (Fig. 5.1) of mid-Mw polymer additive. Mid-Mw polymer up-gradient was chosen because this additive demonstrated the greatest reductions in k to 50 mM CaCl_2 (Fig. 5.5). Granular mid-Mw SAP was placed up-gradient at a mass per area of 96 g/m^2 , equal to a 2%-by-mass inclusion within a Na-B specimen at the mass per area used in this study (4.8 kg/m^2).

The k of soil layers with and without mid-Mw up-gradient are shown in Fig. 5.9 and summarized in Table 5.2. Mid-Mw WSP did not impact the k of clean sand or non-plastic silt, and resulted in a 1.6-times reduction in the k of low-plasticity silt. In contrast, kaolinite exhibited an approximately four orders-of-magnitude in k reduction with mid-

Mw polymer upstream. This reduction was almost an order-of-magnitude greater than Na-B, which exhibited an approximately three orders-of-magnitude reduction in k . The lack of reduction in k from mid-Mw polymer in non-plastic silt, which had a k to 50 mM CaCl_2 14-times lower k than Na-B, indicates that polymeric reductions in k are mechanistically coupled to both polymer bonding and as well as pore clogging. These mechanisms are discussed in greater detail in the subsequent section.

5.6. DISCUSSION

5.6.1 Problem with Bentonite-SAP Mixtures

Analysis of BSM and BSCs by XRD did not show intercalation of SAP within the montmorillonite interlayer. These results corroborate the assertion by Trauger and Darlington (2000) and that simple mixing of a SAP with bentonite is not sufficient to intercalate SAP or produce a material with unique material properties. The inability of polyanions (e.g., Na-polyacrylate) to penetrate the interlayer was documented by Theng (1970). Thus, the observed increases in swell of BSM and BSC are not the result of swelling activation as is characteristic in MSB (Onikata et al. 1996) and HC (Emidio et al. 2010), but instead the added swelling and fabric impacts of SAP during swell tests. Unfortunately, the swelling of SAP is highly susceptible to ionic strength and multivalent cations; in high ionic strengths polyelectrolytes assume a coiled configuration (Stumm 1992, Stumm and Morgan 1996), and multivalent cations (e.g., Ca^{2+}) form crosslinks between negative carboxyl moieties off the polyacrylate backbone. Because of this

sensitivity, granular SAP and BSM, while capable of greater swelling in dilute solutions, do not exhibit superior hydraulic compatibility relative to Na-B in 50 and 500 mM CaCl_2 .

Wet-mixed BSC exhibited improved hydraulic performance in 50 mM CaCl_2 , but no improvement to 500 mM CaCl_2 . BSC is postulated to exhibit improved hydraulic behavior, despite swell similar to Na-B (10.0 mL/2 g vs. 10.2 mL/2 g), because of granular cohesion from inter-tactoid SAP bridging. Similar behavior was exhibited by BPN, and is discussed in Chapter 4. The difference is that BPN granules contain intermixed low-molecular-weight polyacrylate that results in inter-granular cohesion. These data illustrate that a cohesive WSP component is necessary to realize the intragranular cohesion exhibited by BPN in 500 mM CaCl_2 (Chapter 4).

5.6.2 Clogging of Hydraulically Governing Porosity

Granular Na-B mixed with low- or mid-Mw WSP produced a composite material that maintained a low k to 50 mM CaCl_2 , but did not reduce k to 500 mM CaCl_2 . Chapter 3 showed similar behaviors by WSP (with Mw of 280,000 g/mol) eluted from BPN and added to Na-B. The reduction in k from low- or mid-Mw WSP resulted from the elimination of hydraulically governing pores within the Na-B matrix. When initially dry Na-B granules, shown schematically in Fig. 5.10a, are hydrated and permeated with a strong divalent solution (e.g., 50 mM or 500 mM CaCl_2) the granules undergo only limited swelling and do not form the structure characteristic of low k bentonite. High k then results as flow occurs through conductivity-governing intergranular macroporosity (Fig. 5.10b) composed of low-density spillings from hydrated bentonite granules. If the same dry Na-B granules are hydrated in a dilute solution, a high swell is realized and

the resultant gel structure seals off macroscale porosity reappportioning governing flow to narrow and tortuous intragranular microporosity (Fig. 5.10c). Thus, the k of directly permeated Na-B (i.e. not prehydrated) is inversely related to total specimen void ratio (at low effective stresses). Soluble low- and mid-Mw WSP eliminated intergranular porosity and thereby removed macroscale (high k) flow (Fig. 5.10d).

Both clay minerals tested with mid-Mw WSP exhibited dramatic reductions in k when permeated with 50 mM CaCl_2 . In comparison, both non- and low-plastic(ity) silts did not exhibit large reductions in k despite having lower unmodified k (and less hydraulically governing pore volume). These results indicate that the elimination of high- k porosity by mid-Mw WSP is coupled to WSP interactions with the clay minerals. The adsorption of anionic polyelectrolytes to kaolinite and montmorillonite is well documented in the literature (e.g., Siffert and Espinasse 1980, Lee et al. 2001, Heller and Keren 2003), and is a function of the solution pH and ion concentration. The solution pH impacts the surface potential at the 'broken' mineral Si-O-Si or Al-O-Al mineral edges (Wieland 1988, Guven 1992, Wieland and Stumm 1992, McBride 1994). In solutions more acidic than the point-of-zero-net-proton charge (PZNPC) both montmorillonite and kaolinite platelet edges carry a positive charge, while at more basic pH, disassociation of silanol and aluminol groups yields negative charges (Tournassant et al. 2003a, 2003b). The PZNPC of montmorillonite edges occurs at a pH of approximately 8 (Kriaa et al. 2007) (although published PZNPC in the literature range from 2.6 to 8 (Avena et al. 1998, Zhuang and Gui-Rui 2002), and are nearly impossible to accurately measure due to the net negative structural charge of montmorillonite

(McBride 1994). The PZNPC of the edge surfaces of kaolinite is approximately 7.5 (Wieland 1988, Wieland and Stumm 1992). Initially, a pH of approximately 10 was exhibited by both Na-B and kaolinite incorporating WSP and permeated with 50 and 500 mM CaCl_2 . At a pH of 10, the edge surfaces of both kaolinite and montmorillonite should be above their PZNPC, and be slightly anionic. In this condition, polyelectrolyte adsorption occurs via cation bridging (Deng et al. 2006), where the negative carboxyl moieties off of the polyacrylate backbone associate with the cations that satisfy the net negative structural and anionic edge charges (viz. the CEC). Because many segments of a single polymer molecule can be in contact with a surface, a low bonding energy for each individual bond is still capable of rendering the total adsorption effectively irreversible (Stumm, 1992; Stumm and Morgan, 1996). The high energy required to simultaneously desorb the entire molecule renders adsorbed polymers difficult to desorb (Lyklema, 1985). Thus, polymer clogging may be an irreversible process.

Ion concentration effects the free and adsorbed configuration of the polyelectrolyte in solution. Stumm (1992) and Stumm and Morgan (1996) note that at low ionic strength, polyelectrolytes have extended shapes (large hydrodynamic radius) because of intramolecular electrostatic repulsion. When adsorbed at the interface of a surface and a solution of low ionic strength, the polyelectrolyte will have a flat configuration (small hydrodynamic thickness). Conversely, at high ionic strength, the polyelectrolyte will have a coiled configuration in solution (small hydrodynamic radius) and when adsorbed, will extend further from the surface (large hydrodynamic thickness). At high electrolyte concentrations, electrolyte screening can also cause

polyelectrolytes to behave similar to uncharged macromolecules (Stumm 1992, Stumm and Morgan 1996).

Water-soluble polyacrylate is ineffectual as a granular additive to Na-B when permeated with 500 mM CaCl_2 . Concurrent with reductions in the hydrodynamic radius of WSP at high electrolyte solutions, multivalent cations (e.g., Ca^{2+}) stitch together the WSP backbone. With 500 mM CaCl_2 , the resulting collapsed molecules are then insufficient to eliminate macroscale porosity despite higher polymer retention as shown in Fig. 5.8. These data illustrate that in 500 mM CaCl_2 WSP is less mobile within the Na-B matrix and WSP that is mobile does not sufficiently interact with macroscale porosity. In 500 mM CaCl_2 , low-Mw WSP is hypothesized to be less retained than higher-Mw WSP due to smaller collapsed molecule size. These data demonstrate that permeant specific k tests are necessary prior to application of Na-B-WSP composites with real leachates. Additionally, because much of the work on polyelectrolyte adsorption mechanisms has occurred via batch testing (viz. very high liquid-to-solid ratios) additional investigation into the adsorption and clogging mechanisms associated with low- and mid-Mw WSP and clay minerals is warranted.

5.6.3 Other WSP Additive Applications

Unlike other polymeric additives (e.g., propylene carbonate in MSB or carboxymethyl cellulose in HC), low- and mid-Mw WSP affects the k of Na-B without nanoscale mixing of a hydrated polymer-clay amalgam to ensure polymer intercalation. The simplicity of granular mixing may allow for reduced production costs relative to other polymer-modified GCLs. Unfortunately, the impact of dry-mixed WSP appears

limited to mid-range leachates (e.g. 50 mM CaCl_2), and did not yield $k < 10^{-12}$ m/s as was exhibited by BPN permeated with 500 mM CaCl_2 . Research is currently underway to determine if wet-mixing of mid-Mw WSP with BB will produce a composite material with similar hydraulic properties to BPN in 500 mM CaCl_2 . This may allow for the production of a range of low- and mid-Mw WSP amended bentonites that can be tailored depending on anticipated leachate chemistry. When mid strength leachates (e.g., 50 mM CaCl_2) are expected, dry mixing of low- or mid- Mw WSP has been shown to generate low k , while for high strength leachates (e.g., 500 mM CaCl_2) BPN (or potentially wet-mixed Na-B- WSP composites) will yield a low k .

Addition of WSP has a broader range of hydraulic barrier applications than existing bentonite amendment techniques that are solely applicable to bentonite. Although Na-B is generally favored in waste-containment applications when local materials are unsuitable, mid-Mw WSP was shown to lower the k of kaolinite, thus allowing for other WSP-enhanced mineral based lining systems. Such low- k barrier layers may have advantages over modified bentonite both in terms of material availability and desiccation potential. Chapter 4 also showed that WSP eluted from BPN hydrated atop a compacted clay layer reduced k by two orders-of-magnitude. Thus, WSP clogging will have applications outside of pure clay minerals.

5.7. CONCLUSIONS

The use of polyacrylate to improve the hydraulic compatibility of Na-bentonite and other mineral barrier layers was investigated. Addition by dry mixing of granular

superabsorbent (viz. cross-linked and high molecular weight) polyacrylate with Na-bentonite was investigated, as well as addition by wet blending of the constituents. The resultant materials were tested for swell index by an expedited method, and hydraulic conductivity (k) to 50 and 500 mM CaCl_2 . The use of water-soluble polyacrylate (viz. not cross-lined and low molecular weight, WSP) as a granular additive was also investigated. Granular polyacrylate with weight average molecular weights (M_w) of 2,000, 255,000, and 1,080,000 g/mol were mixed into granular Na-bentonite at mass percentages ranging from 0.75% to 20%. These blends were tested for k to 50 and 500 mM CaCl_2 . The hydraulic impacts of 96 g/m² of WSP with a weight average molecular weight of 255,000 g/mol on compacted layers of fine sand, non-plastic silt, low-plasticity silt, and kaolinite were also investigated.

The following conclusions can be distilled from research presented in this paper:

- Dry mixing of granular SAP with granular Na-bentonite did not result in improved hydraulic behavior to mid-strength (i.e., 50 mM CaCl_2) or high-strength (i.e., 500 mM CaCl_2) permeants relative to the parent materials.
- Wet mixing of SAP with Na-B resulted in minor improvements in k to 50 mM CaCl_2 (a mid-strength permeant), but not improve k to 500 mM CaCl_2 (a high-strength permeant).
- Granular mixing of WSP with $M_w < 1,080,000$ g/mol dramatically improved the k of the resulting composite to 50 mM CaCl_2 (a mid-strength permeant).

- Granular mixing of WSP with $M_w < 1,080,000$ g/mol did not greatly improve the k of the composite system to 50 mM CaCl_2 (a mid-strength permeant).
- Granular mixing of soluble WSP did not improve the composite system hydraulic behavior to 500 mM CaCl_2 (a high-strength permeant).
- WSP did not increase water absorption in tests with improved hydraulic behavior, but is believed to clog hydraulically governing (intergranular) porosity.
- Granular WSP with M_w of 255,000 g/mol added up-gradient improved the hydraulic performance of compacted kaolinite but did not impact clean sand, non-plastic silt, or low-plasticity silt.

5.8. REFERENCES

- Ashmawy, A., Darwish, E., Sotelo, N., and Muhammad, N. (2002). "Hydraulic performance of untreated and polymer-treated bentonite in inorganic landfill leachates." *Clays and Clay Minerals*, 50(5), 546-552.
- Avena, M., Cabrol, R., de Pauli, C. (1998). "Study of some physicochemical properties of pillared montmorillonites: acid-base potentiometric titrations and electrophoretic measurements." *Clays and Clay Minerals*, 38(4), 356-362.
- Buchholz, F., Graham, A. (1998). *Modern Superabsorbent Polymer Technology*. John Wiley and Sons, New York.
- Deng, Y., Dixon, J.B., White, G.N. (2006). "Bonding between polyacrylamide and smectite." *Colloids and Surfaces*, 281(1), 82-91.
- Di Emidio, G., Van Impe, W., Mazziere, F. (2010). "A polymer enhanced clay for impermeable geosynthetic clay liners." *Proceedings of Sixth International Conference on Environmental Geotechnics*, International Society for Soil Mechanics and Geotechnical Engineers, New Delhi, India, 963-967.
- Di Emedio, G., Van Impe, W., Flores, V. (2011). "Advances in geosynthetic clay liners: polymer enhanced clays." *GeoFrontiers 2011. Advances in Geotechnical Engineering*, American Society of Civil Engineers, Reston, USA, 1931-1940.
- Flynn, B., and Carter, G. (1998). "Waterproofing material and method of fabrication thereof." *US Patent Number: 6,537,676 B1*.
- Heller, H., and Keren, R. (2003). "Anionic polyacrylamide polymer adsorption by pyrophyllite and montmorillonite." *Clays and Clay Minerals*, 51, 334-339.

- Jo, H., Benson, C., Shackelford, C., Lee, J., and Edil, T. (2005). "Long-term hydraulic conductivity of a non-prehydrated geosynthetic clay liner permeated with inorganic salt solutions." *J. of Geotech. and Geoenviron. Eng.*, 131(4), 405-417.
- Jo, H., Katsumi, T., Benson, C., and Edil, T. (2001). "Hydraulic conductivity and swelling of non-prehydrated GCLs permeated with single species salt solutions." *J. of Geotech. and Geoenviron. Eng.*, 127(7), 557-567.
- Katsumi, T., Ishimori, Ho, Onikata, M., and Fukagawa, R. (2008). "Long-term barrier performance of modified bentonite materials against sodium and calcium permeant solutions." *Geotextiles and Geomembranes*, 26(1), 14-30.
- Kriaa, A., Hamdi, N., and Srasra, E. (2007). "Acid-base chemistry of montmorillonitic and beidellitic-montmorillonitic smectite." *Russian Journal of Electrochemistry*, 43(2), 175-187.
- Kolstad, D., Benson, C., Edil, T., and Jo, H. (2004a). "Hydraulic conductivity of dense prehydrated GCL permeated with aggressive inorganic solutions." *Geosynthetics International*, 11(3), 233-241.
- Kolstad, D., Benson, C., and Edil, T. (2004b). "Hydraulic conductivity and swell of nonprehydrated GCLs permeated with multi-species inorganic solutions." *J. of Geotech. and Geoenviron. Eng.*, 130(12), 1236-1249.
- Lee, J. and Shackelford, C. (2005). "Impact of bentonite quality on hydraulic conductivity of geosynthetic clay liners." *J. of Geotech. and Geoenviron. Engr.*, 131(1), 64-77.
- Lee, L., Rahbari, R. Lecourtier, J., and Chauveteau, G., (1991). "Adsorption of polyacrylamides on the different faces of kaolinites." *Journal of Colloid and Interface Science*, 147, 351-357.

- Mazzieri, F., Emidio, G., Van Impe, P. (2010a). "Diffusion of calcium chloride in a modified bentonite: Impact on osmotic efficiency and hydraulic conductivity." *Clays and Clay Minerals*, 58(3), 351-363.
- Mazzieri, F., Pasqualini, E., Emidio, G. (2010b). "Migration of heavy metals through conventional and factory-prehydrated GCL materials." *Proceedings of Sixth International Conference on Environmental Geotechnics*, International Society for Soil Mechanics and Geotechnical Engineers, New Delhi, India, 963-967.
- McBride M. (1994). *Environmental Chemistry of Soils*. Oxford University Press, New York.
- O'Brien N. (1970). "Fabric of kaolinite and illite floccules." *Clays and Clay Minerals*, 19, 353-359.
- Onikata, M., Kondo, M., and Kamon, M. (1996). "Development and characterization of a multiswellable bentonite." *Environmental Geotechnics*. Taylor and Francis, Rotterdam, 587-590.
- Onikata, M., Kondo, M., Hayashi, N., and Yamanaka, S. (1999). "Complex formation of cation-exchanged montmorillonites with propylene carbonate: Osmotic swelling in aqueous electrolyte solutions." *Clays and Clay Minerals*, 47(5), 672-677.
- Scalia, J., Benson, C. H., Edil, T. B., Bohnhoff, G. L., and Shackelford, C. D. (2011). "GCLs containing bentonite polymer nanocomposite." *GeoFrontiers 2011. Advances in Geotechnical Engineering*, American Society of Civil Engineers, Reston, USA, 2001-2009.
- Schroeder, C., Monjoie, A., Illing, P., Dosquet, D., and Thorez, J. (2001). "Testing a factory-prehydrated GCL under several conditions." *Proceedings, Sardinia*

- 2001, 8th International Waste Management and Landfill Symposium, CISA Environmental Sanitary Engineering Centre, Cagliari, Italy, 187-196.
- Shackelford, C., Benson, C., Katsumi, T., Edil, T., and Lin, L. (2000). "Evaluating the hydraulic conductivity of GCLs permeated with non-standard liquids." *Geotextiles and Geomembranes*, 18(2-3), 133-161.
- Siffert B., and Espinasse, P. (1980). "Adsorption of organic diacids and sodium polyacrylate onto montmorillonite." *Clays and Clay Minerals*, 28(5), 381-387.
- Stumm, W. (1992). *Chemistry of the Solid-Water Interface*. John Wiley and Sons, New York.
- Stumm, W., and Morgan, J. (1996). *Aquatic Chemistry*, 3rd ed. Wiley, New York.
- Theng, B. (1970). "Interactions of clay minerals with organic polymers. Some practical applications." *Clays and Clay Minerals*, 18, 357-362.
- Trauger R. and Darlington J. (2000). "Next-generation geosynthetic clay liners for improved durability and performance." *TR-220*. Colloid Environmental Technologies Company, Arlington Heights, 2-14.
- Tournassat, C., Greneche, J-M., Tisserant, D., and Charlet, L. (2003a). "The titration of clay minerals. I. Discontinuous backtitration technique combined with CEC measurements." *J. of Colloid and Interface Science*, 273, 224-233.
- Tournassat, C., Ferrage, E., Poinssingnon, C., and Charlet, L. (2003b). "The titration of clay minerals. II. Structure-based model and implications for clay reactivity." *J. of Colloid and Interface Science*, 273, 234-246.
- U.S. EPA. (2007). *Method 6010B: Inductively coupled plasma-atomic emission spectrometry, physical/chemical methods SW846*, 3rd Ed. US Environmental

Protection Agency, Office of Solid Waste and Emergency Response, Washington, DC.

Wieland, E., and Stumm, W. (1992). "Dissolution kinetics of kaolinite in acid aqueous solutions at 25 C." *Geochimica et Cosmochimica*, 56(9), 3339-3355.

Wieland, W., Wehrli, B., and Stumm W. (1988). "The coordination chemistry of weathering: III. A generalization on the dissolution rates of minerals." *Geochimica et Cosmochimica*, 52(8), 1969-1981.

Zhuang, J., and Gui-Rui, Y. (2002). "Effects of surface coatings on electrochemical properties and containment sorption of clay materials." *Chemosphere*, 49(6), 619-628.

5.9. ABBREVIATIONS

BB – Base sodium bentonite

BC – Bound cations

BPA – Bentonite-polymer alloy

BPB – Bentonite-polyacrylate blend

BPN – Bentonite-polymer nanocomposite

BSC – Base-bentonite-superabsorbent composite

BSM – Bentonite-superabsorbent mixture

CEC – Cation-exchange capacity

DW – Deionized water

ESI – Expedite swell-index

GCL – Geosynthetic-clay liner

GT – Geotextile

GSD – Grain-size distribution

HC – HYPER clay

ICP-OES – Inductively coupled plasma-optical emissions spectroscopy

k – Hydraulic conductivity

MSB – Multi-swellable bentonite

M_w – Weight average molecular weight

Na-B – GCL-grade sodium-bentonite

PDI – Polydispersivity index

PZNPC – Point-of-zero net-proton-charge

SAP – Superabsorbent sodium polyacrylate

SC – Soluble cations

SI – Swell index

WSP – Water-soluble polyacrylate

USCS – Unified Soil Classification System

XRD – X-ray diffraction

5.10. TABLES

Table 5.1 Properties of Na-bentonite (Na-B), base bentonite (BB), Na-polyacrylate (SAP), BB-SAP mixture (BSM) at a BB-SAP ratio of 100:1, and Na-B-SAP composites (BSC) at Na-B-to-SAP ratios of 100:1 and 1280:1.

Material	Soluble cations (cmol+/kg)				Bound cations (mole fractions)				CEC	d ₀₀₁ spacing
	Na ⁺	K ⁺	Ca ²⁺	Mg ²⁺	Na ⁺	K ⁺	Ca ²⁺	Mg ²⁺	(cmol+/kg)	nm
Na-B	18.1	0.4	0.2	0.1	0.44	0.02	0.36	0.17	78	1.4
BB	23.3	0.4	0.2	0.1	0.42	0.04	0.42	0.12	85.5	1.4
SAP	173	0.0	0.0	0.0	0.95	0.00	0.00	0.05	194	-
BSM 100:1	17.7	0.5	1.8	0.3	0.47	0.02	0.34	0.17	79	1.4
BSC 100:1	13.4	0.2	6.4	0.4	0.52	0.03	0.29	0.17	80	1.4
BSC 1280:1	18.3	0.3	5.1	0.1	0.42	0.02	0.39	0.16	79	1.4

Table 5.2 Cation exchange capacity (CEC) and hydraulic conductivity (k) of soils used in porosity clogging experiments with water-soluble polyacrylate (WSP).

Barrier material	CEC (cmol+/kg)	k (soil only) (m/s)	k (plus WSP) (m/s)
Clean sand	0.0	4.2×10^{-6}	4.1×10^{-6}
Non-plastic silt	0.1	1.3×10^{-8}	1.3×10^{-8}
Low-plasticity silt	0.9	3.9×10^{-8}	2.4×10^{-8}
Kaolinite	1.8	1.0×10^{-7}	1.3×10^{-11}
Na-bentonite	78	1.8×10^{-7}	1.6×10^{-10}

Table 5.3 Measured indicator parameters of permeant solutions.

Testing liquid	Electrical conductivity (mS/cm)	pH
5 mM CaCl_2	1.34	6.1
50 mM CaCl_2	11.0	6.5
500 mM CaCl_2	98.9	6.8

Table 5.4 Swell index (SI) or expedited swell index (ESI) and hydraulic conductivity (k) of sodium-bentonite (Na-B), superabsorbent-polymer (SAP), bentonite-SAP mixture (BPM) at a ratio of 100:1, and bentonite-SAP composites (BPC) at ratios of 100:1 and 1280:1.

Test liquid	Na-B		SAP		BPM 100:1		BPC 100:1		BPC 1280:1	
	SI (mL/2 g)	k (m/s)	SI (mL/2 g)	k (m/s)	ESI (mL/2 g)	k (m/s)	ESI (mL/2 g)	k (m/s)	ESI (mL/2 g)	k (m/s)
DW	30.7	2.1×10^{-11}	1790	2.7×10^{-12}	23.5	-	40.0	-	39.0	-
5 mM CaCl_2	28.7	2.3×10^{-11}	445	2.1×10^{-11}	22.0	1.9×10^{-11}	36.5	1.7×10^{-11}	36.0	1.9×10^{-11}
50 mM CaCl_2	10.2	1.7×10^{-7}	80	2.5×10^{-7}	9.5	6.1×10^{-8}	10.0	1.6×10^{-10}	9.0	1.3×10^{-9}
500 mM CaCl_2	8.0	4.5×10^{-7}	13	4.0×10^{-7}	8.0	6.2×10^{-8}	8.0	1.6×10^{-7}	7.3	3.1×10^{-7}

Table 5.5 Hydraulic conductivity (k) tests performed on polymer clay composites.

Polymer Mw	Polymer mass percentage (%)	Permeant	k (m/s)
-	-		1.8×10^{-7}
Low	2		5.0×10^{-11}
Low	5		3.7×10^{-11}
Low	10		2.8×10^{-11}
Mid	0.75	50 mM	8.0×10^{-11}
Mid	2	CaCl ₂	3.5×10^{-11}
Mid	5		2.6×10^{-11}
Mid	10		1.1×10^{-11}
High	5		6.9×10^{-10}
High	10		5.1×10^{-7}
-	-		4.5×10^{-7}
Low	5		1.2×10^{-6}
Low	10		2.0×10^{-6}
Mid	2	500 mM	1.1×10^{-7}
Mid	5	CaCl ₂	3.4×10^{-7}
Mid	10		5.4×10^{-8}
Mid	20		8.2×10^{-9}
High	5		6.6×10^{-8}

5.11. FIGURES

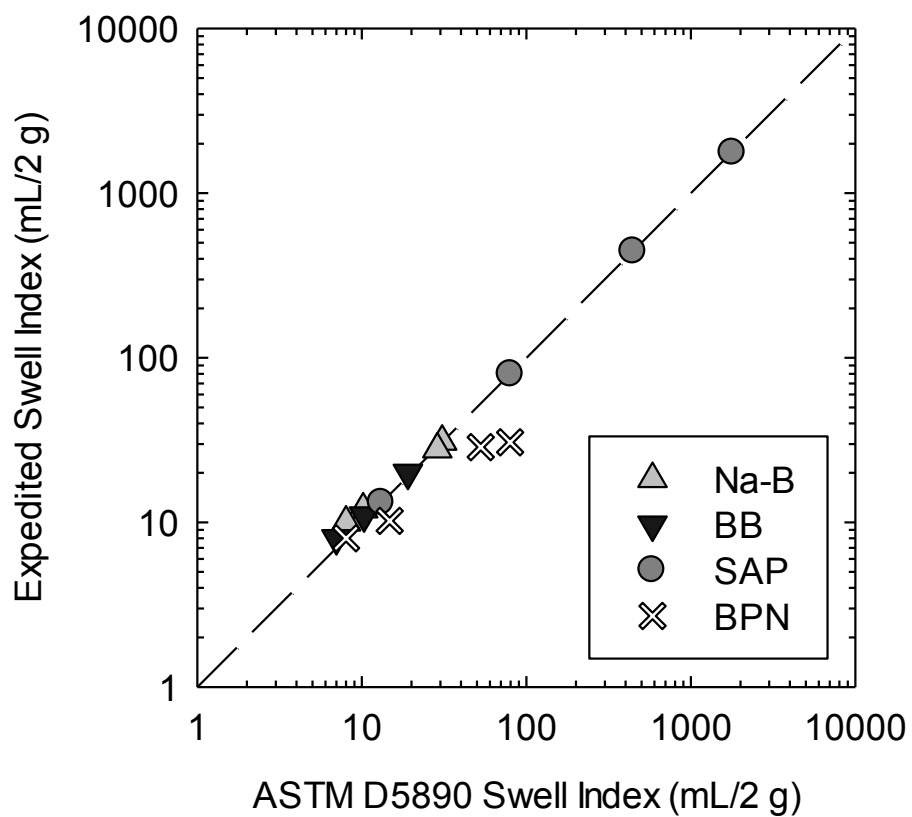


Fig. 5.1 Comparison of results by expedited swell index (ESI) method and the standard ASTM D5890 swell index (SI) method.

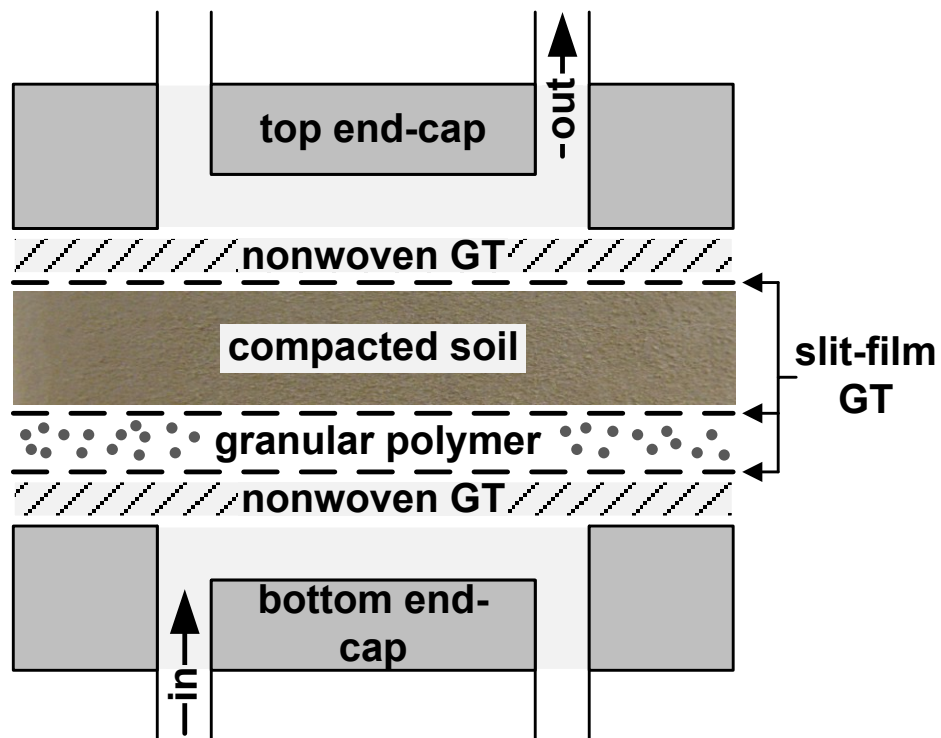


Fig. 5.2 Schematic of cell assembly used for testing polyacrylate clogging in compacted (down-gradient) soils.

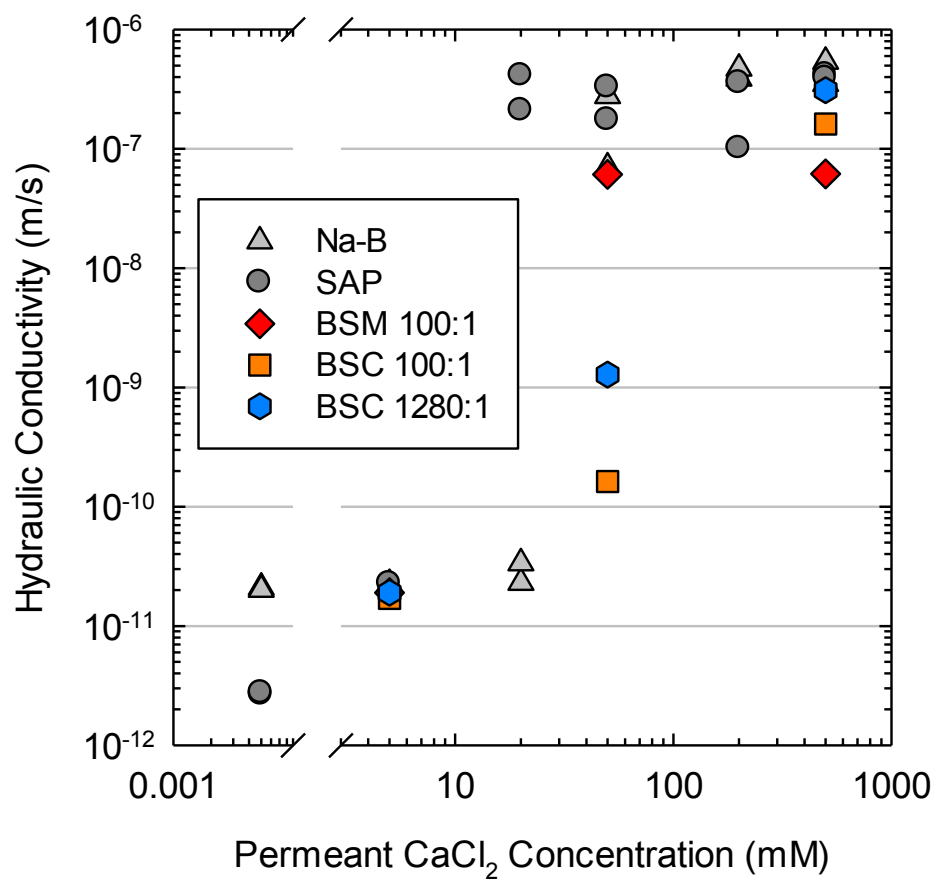


Fig. 5.3 Hydraulic conductivity versus the CaCl_2 concentration of the permeant solution.

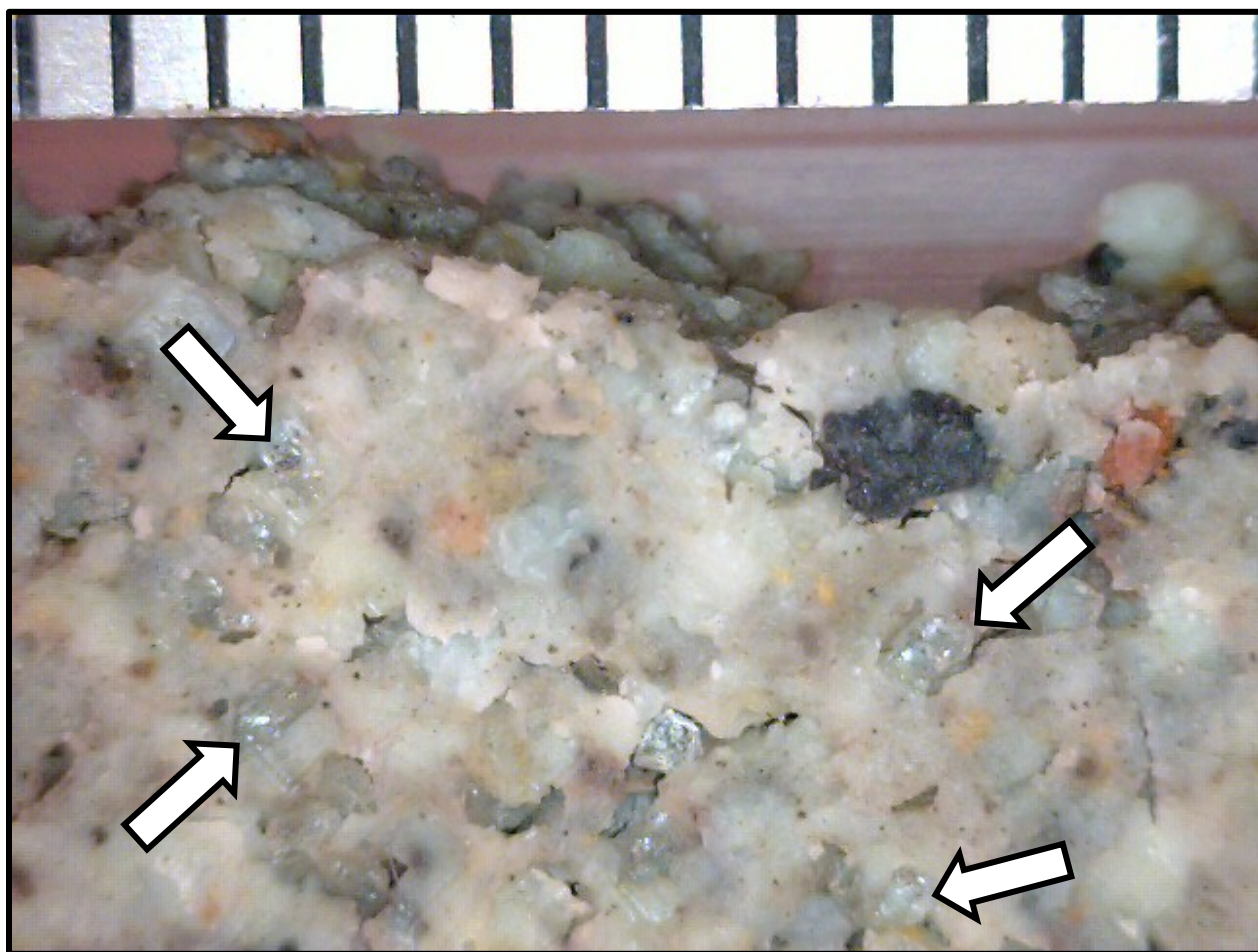


Fig. 5.4 Surface of BSM 100:1 specimen after permeation with 50 mM CaCl₂. Arrows denote some of the locations of visible SAP granules. Scale across top of picture is in mm.

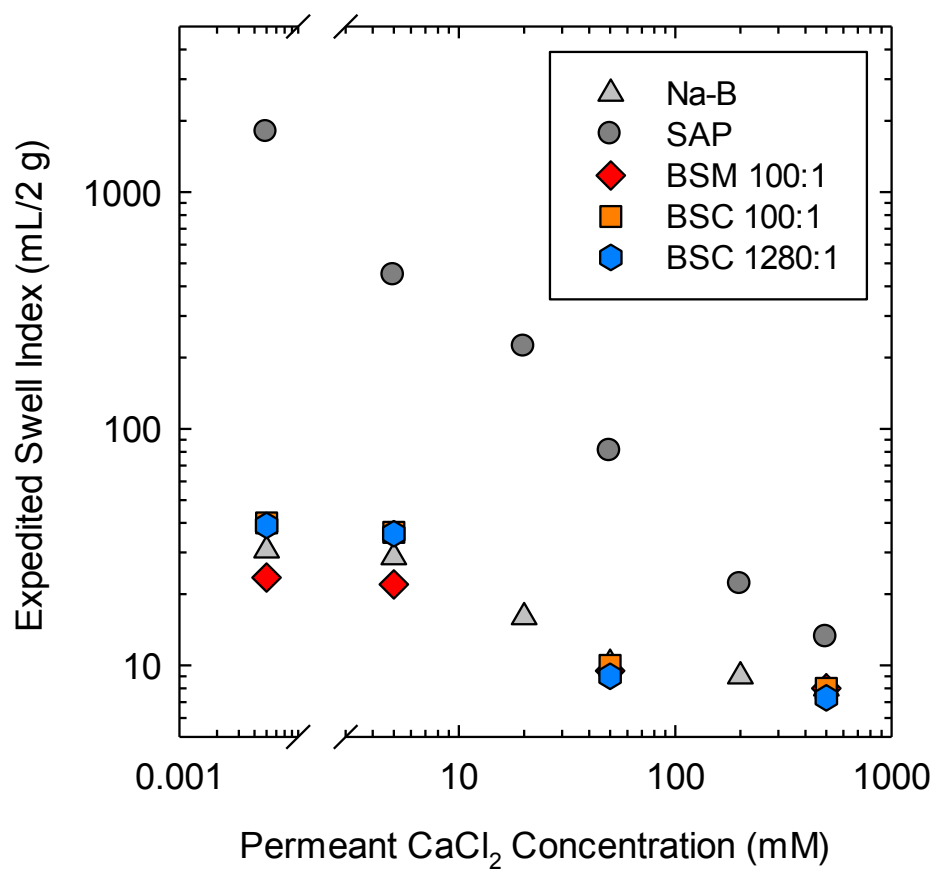


Fig. 5.5 Expedited swell index of Na-bentonite (Na-B), superabsorbent polymer (SAP), a granular Na-B-SAP mixture, and base-bentonite-SAP composites (BSCs) in the range of CaCl_2 concentrations used as permeants.

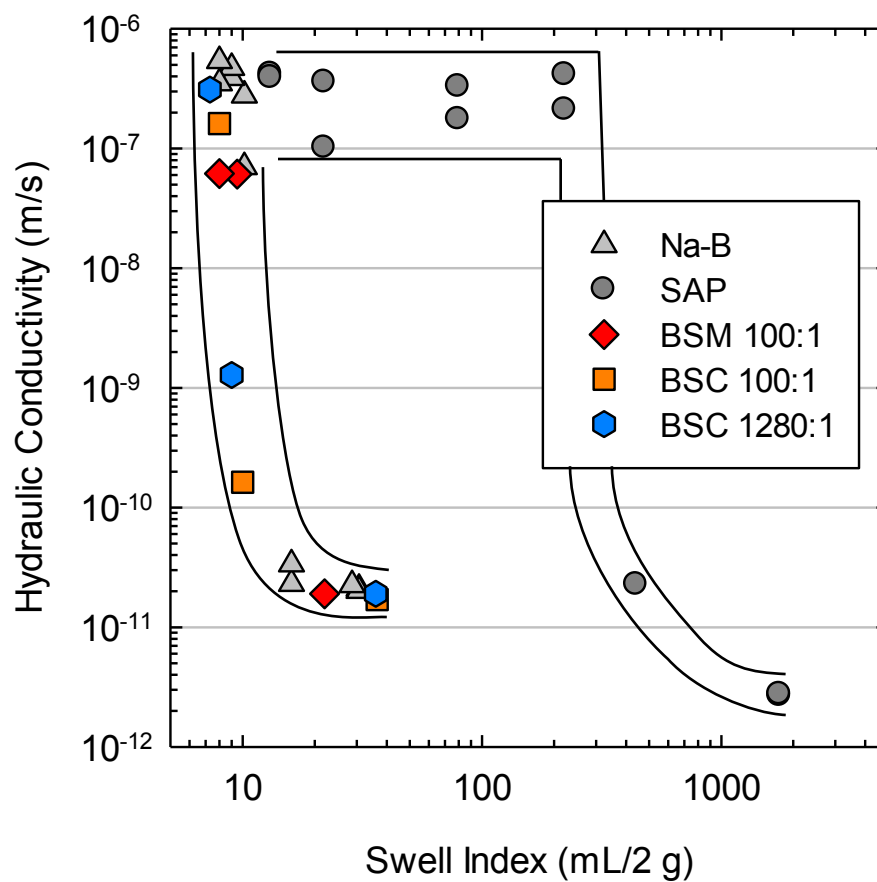


Fig. 5.6 Hydraulic conductivity of Na-bentonite (Na-B), superabsorbent polymer (SAP), a granular Na-B-SAP mixture, and base-bentonite-SAP composites (BSCs) versus swell index of the materials in corresponding solutions.

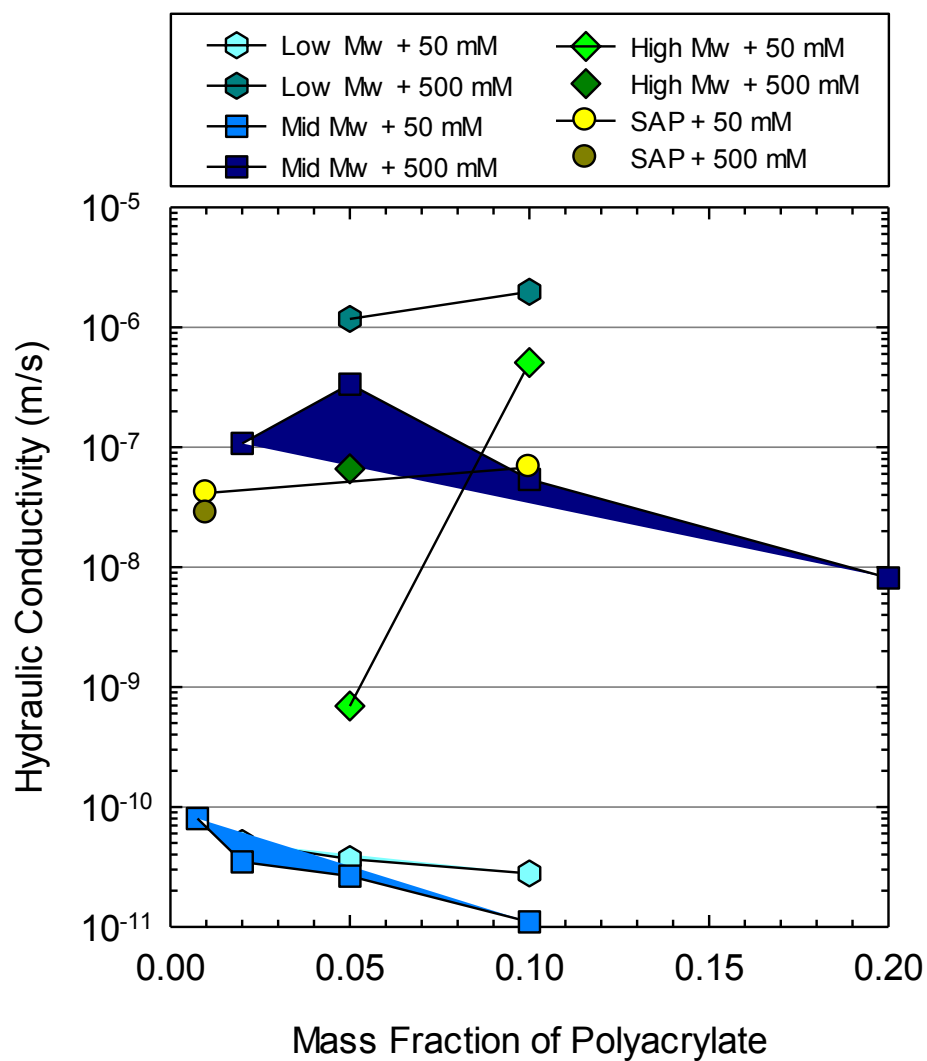


Fig. 5.7 Hydraulic conductivity at varying permeant CaCl_2 concentrations versus the mass fraction of polyacrylate granularly blended into granular Na-bentonite.

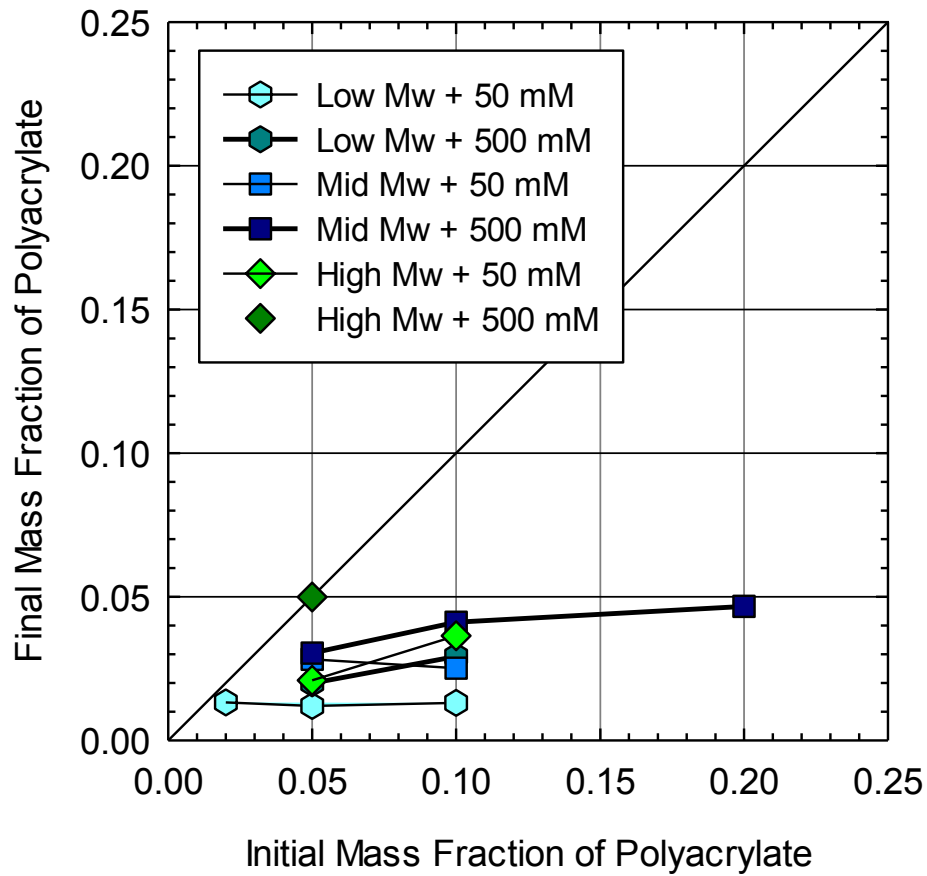


Fig. 5.8 Final fractional mass of water-soluble polyacrylate (WSP) in bentonite-WSP specimens relative to initial fractional mass of polymer mixed into specimen. Data are segregated by WSP weight average molecular weight (Mw) and the strength (in mM) of CaCl_2 used as a permeant solution.

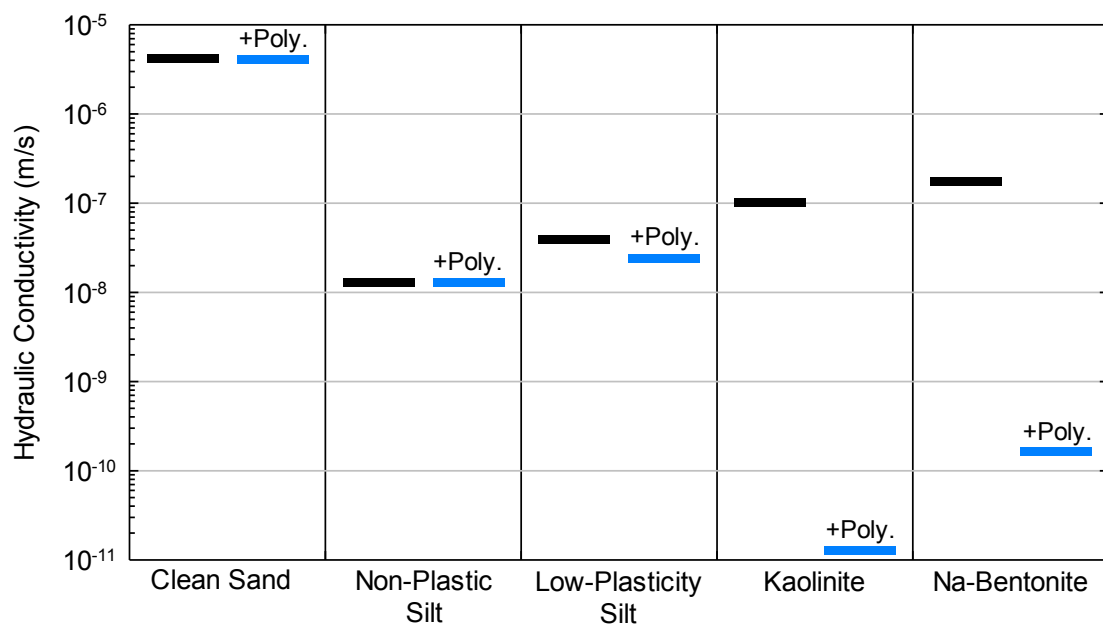


Fig. 5.9 Hydraulic conductivity of varying mineral-barrier layers for unmodified and water-soluble-polyacrylate up-gradient (+Poly.) specimens.

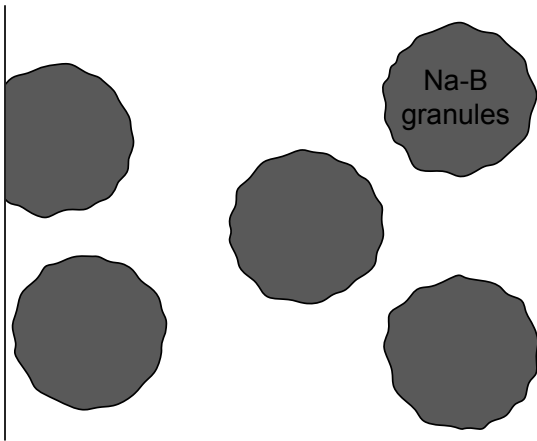
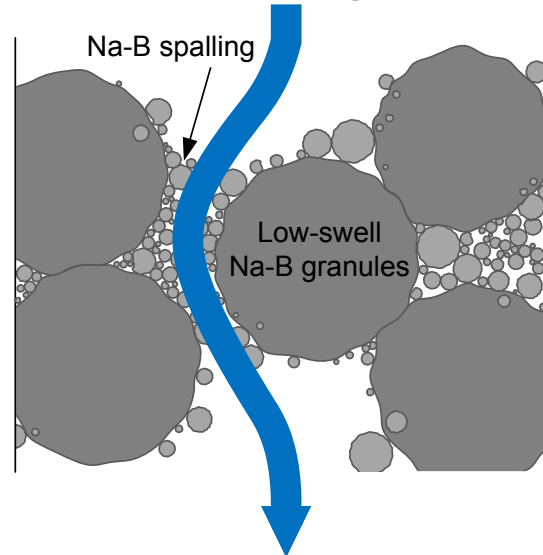
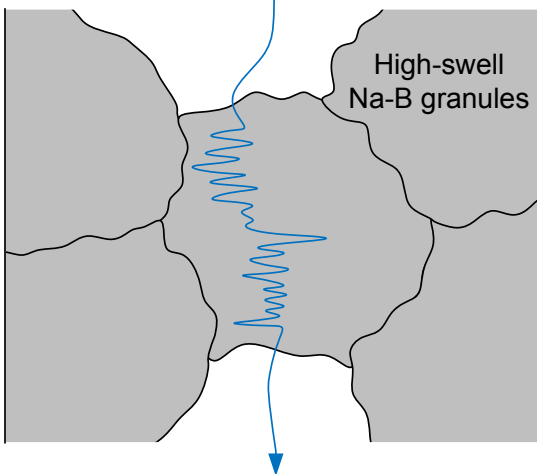
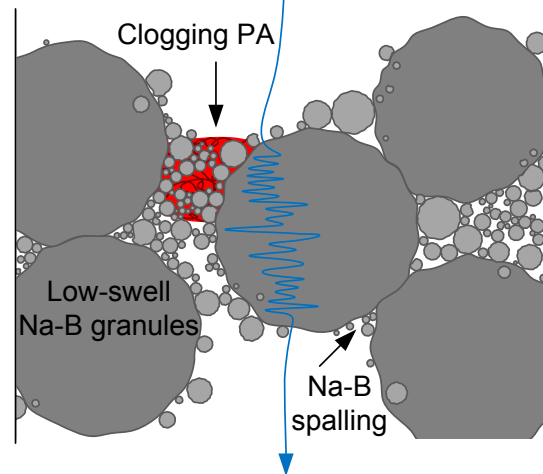
(a) Dry granules**(b) Low swell, high k** **(c) High swell, low k** **(d) PA clogged, low k** 

Fig. 5.10 Conceptual models for hydraulic behavior of granular Na-bentonite (Na-B) and water-soluble polyacrylate (WSP) clogged granular bentonite. The swell of dry granules of Na-B (a) depends on the ionic strength of the hydrating solution, with low swell occurring with 50 mM CaCl_2 and consequently a high hydraulic conductivity (k) (b). Na-bentonite granules hydrated with a dilute solution exhibit low k (c). Clogging of hydraulically active porosity by soluble WSP in within granular Na-B permeated with 50 mM CaCl_2 still yields a low k (d).

APPENDIX A

Lab-Fabricated Geosynthetic Clay Liner (GCL) Assembly Guide

1. Accumulate permeameter components necessary to construct Fig. A1 as well as a 250 or 500-mL bottle, and a 60-mL syringe that attaches to the top drain, base drain, and outflow tube.

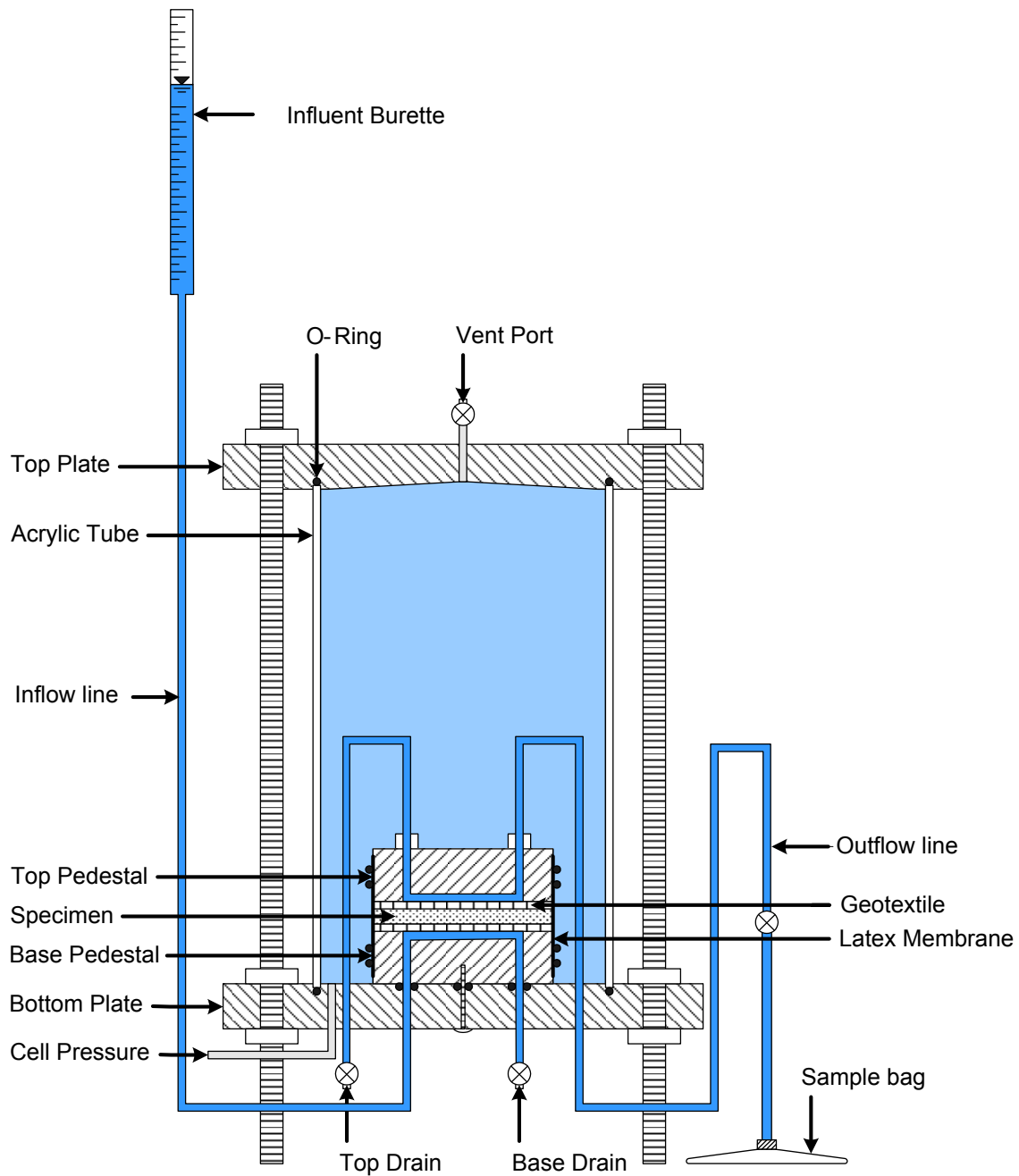
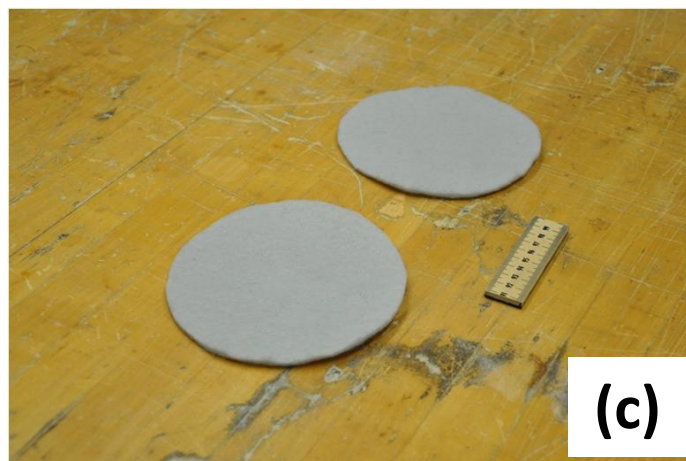
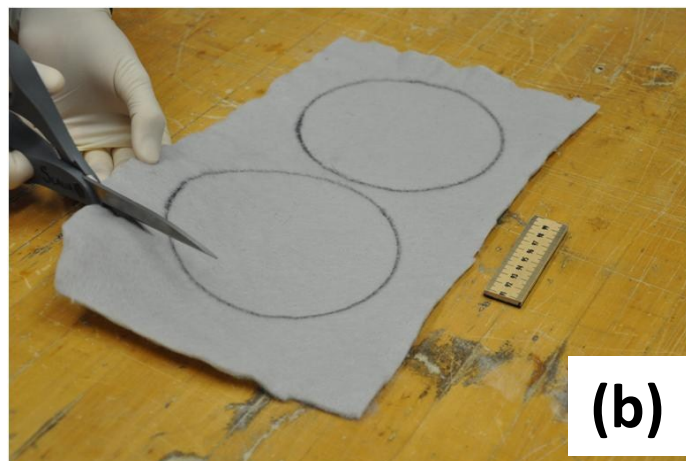
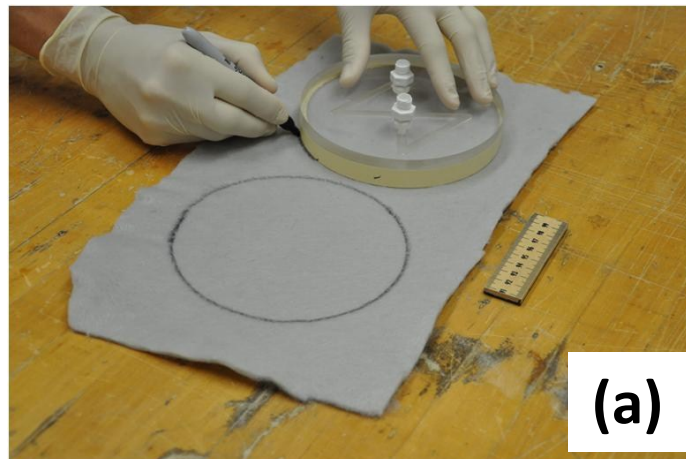
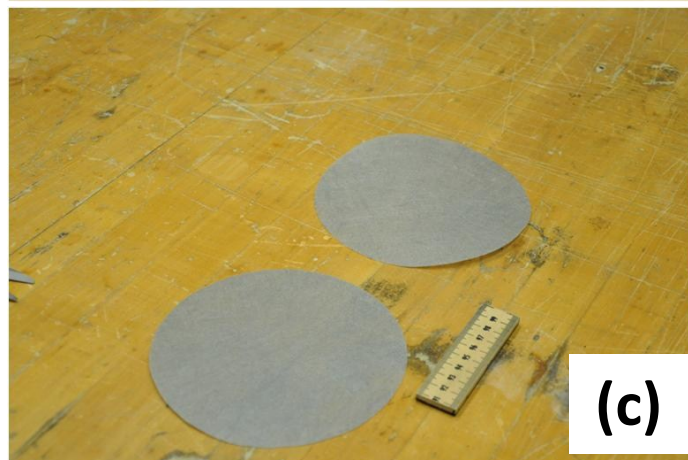
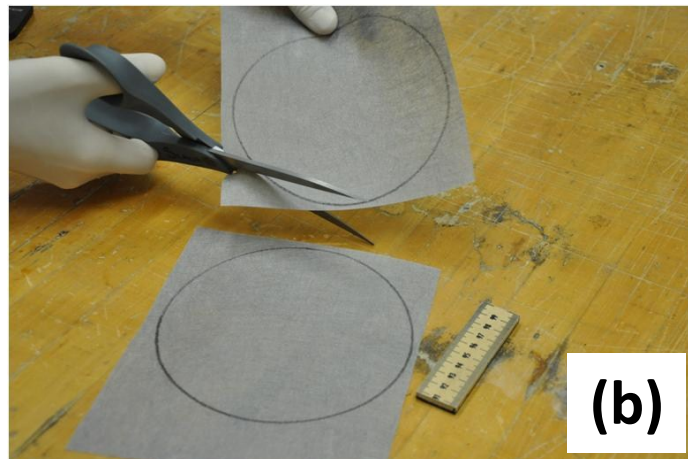
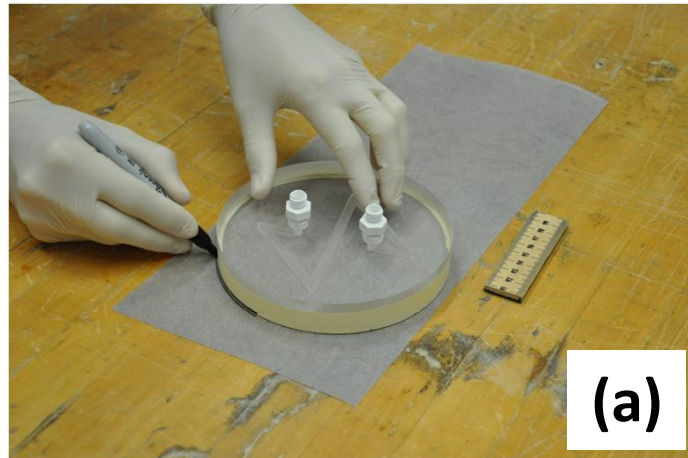


Fig. A1. Schematic of pseudo-GCL assembled in flexible wall permeameter.

2. Use the top pedestal (see Fig. A1) to trace two circles of pedestal diameter on heavy nonwoven geotextiles (gray). Carefully cut out both geotextiles circles.



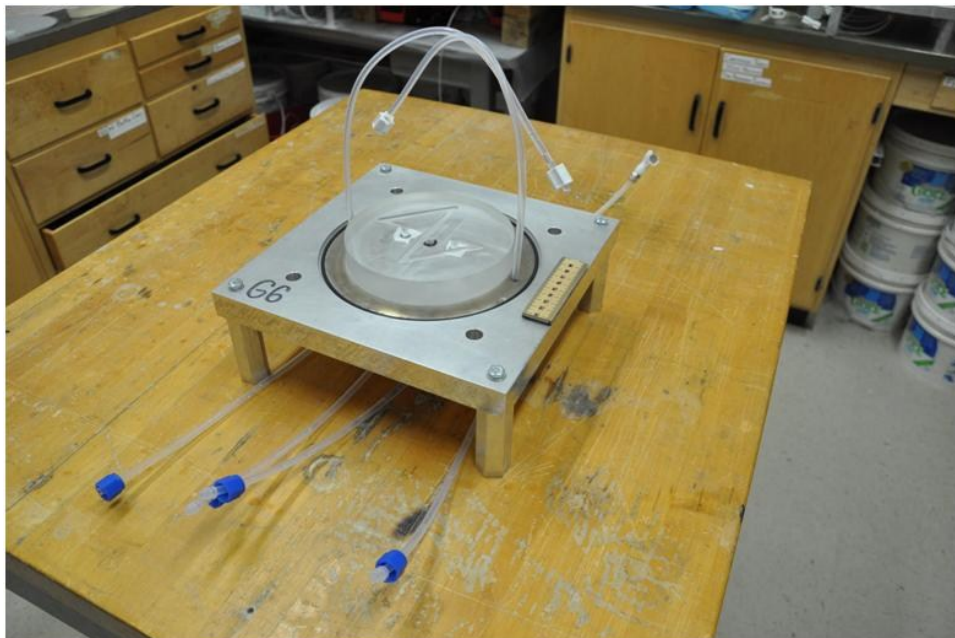
3. Use the top pedestal (see Fig. A1) to trace two circles matching the pedestal on heat bonded calendered nonwoven geotextiles (gray). Carefully cut out both geotextiles.



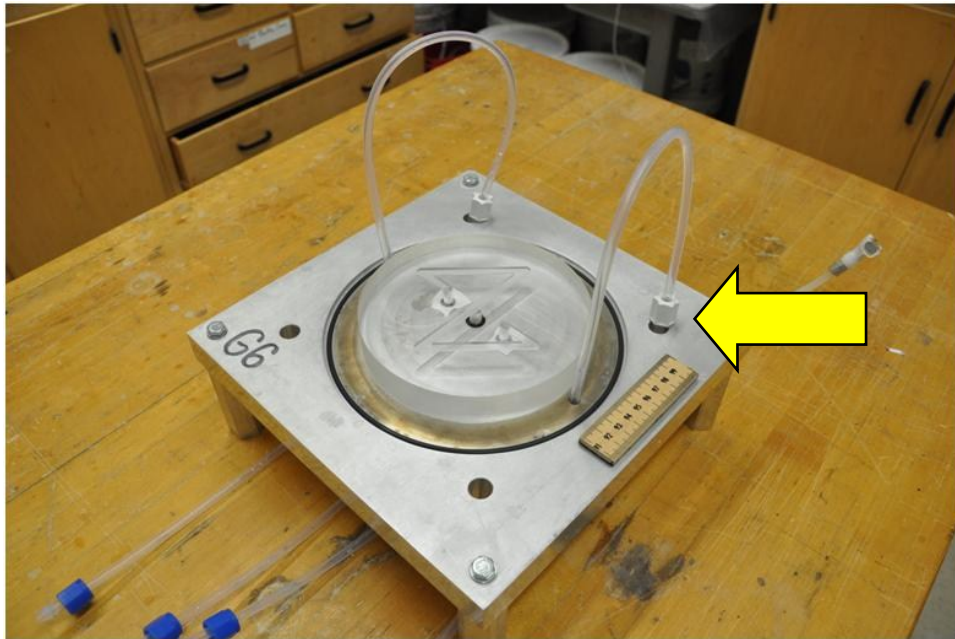
5. Put aside both sets of geotextiles disks.



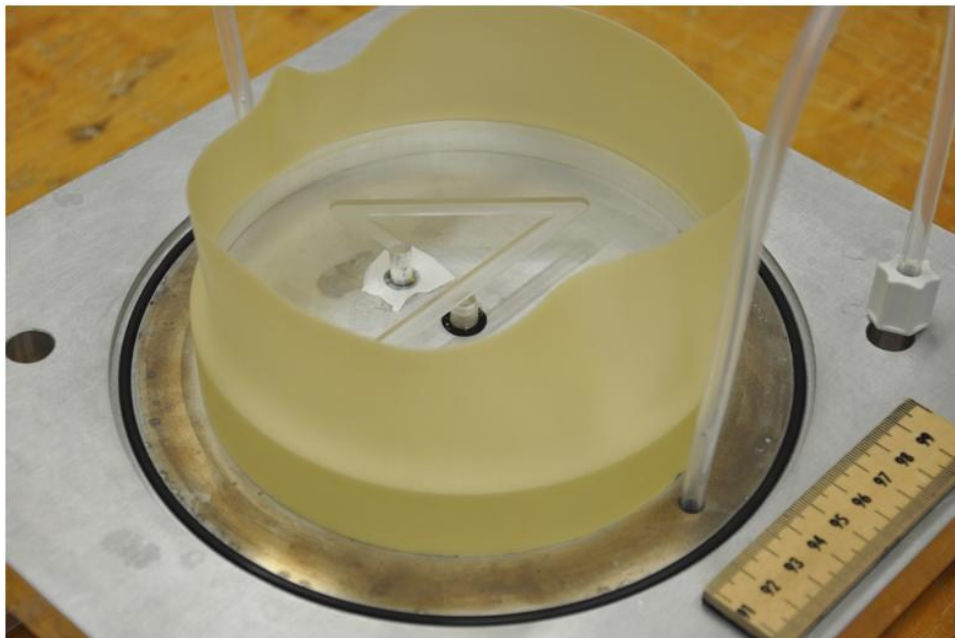
6. Place permeameter base on working surface, acid wash all tubing (flush with 10% Nitric Acid, followed by thorough flushing with deionized water (DW)). Finally flush DW water from tubing with air. A 60-mL syringe works well for this.



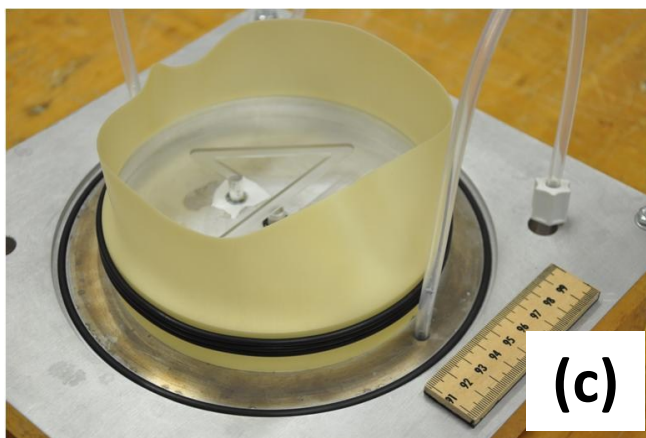
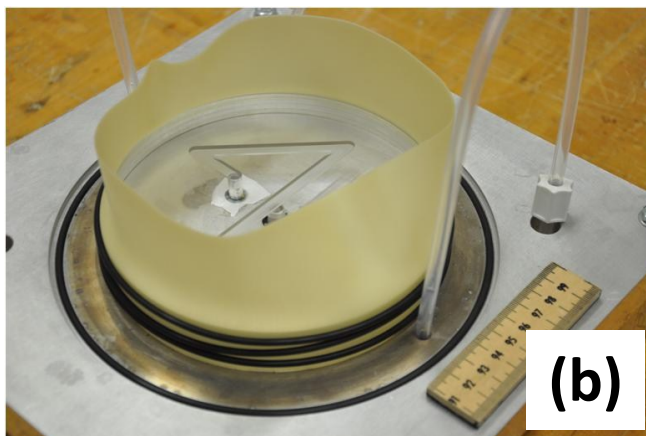
7. Tuck aside tubing that will be connected to top pedestal.



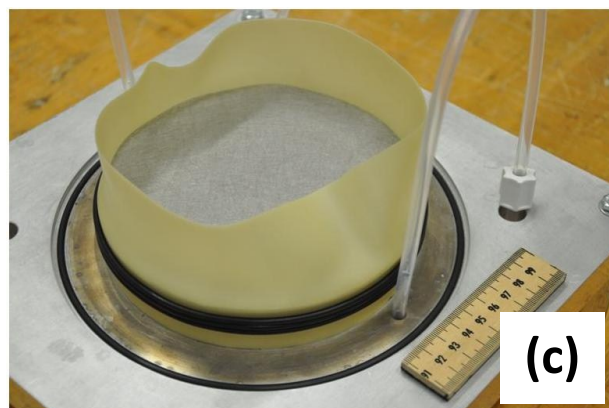
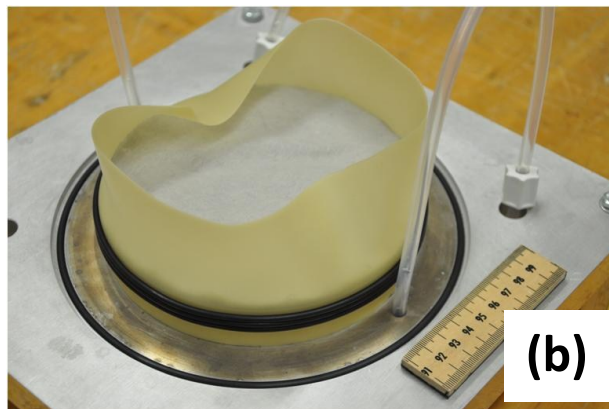
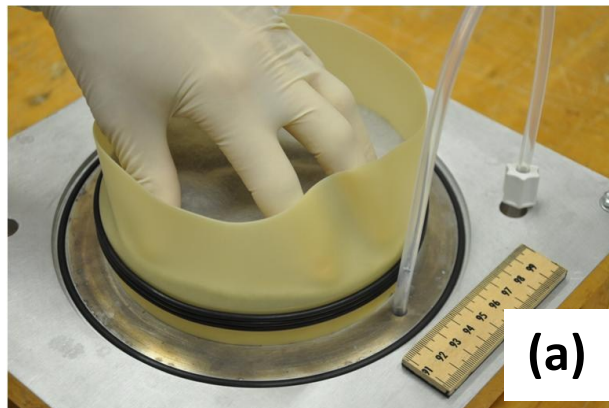
8. Slide latex membrane over base pedestal so that membrane reaches to the bottom plate, and is not twisted.



9. Stretch three O-rings over a rigid ring with an inside diameter slightly larger than the base pedestal + membrane (a). Delicately slide these O-rings off of rigid ring and around the base pedestal + O-rings (b). Using your fingertips, untwist O-rings. The top O-ring should be between 0.5-to-1.0 cm from the top of the base pedestal (c).



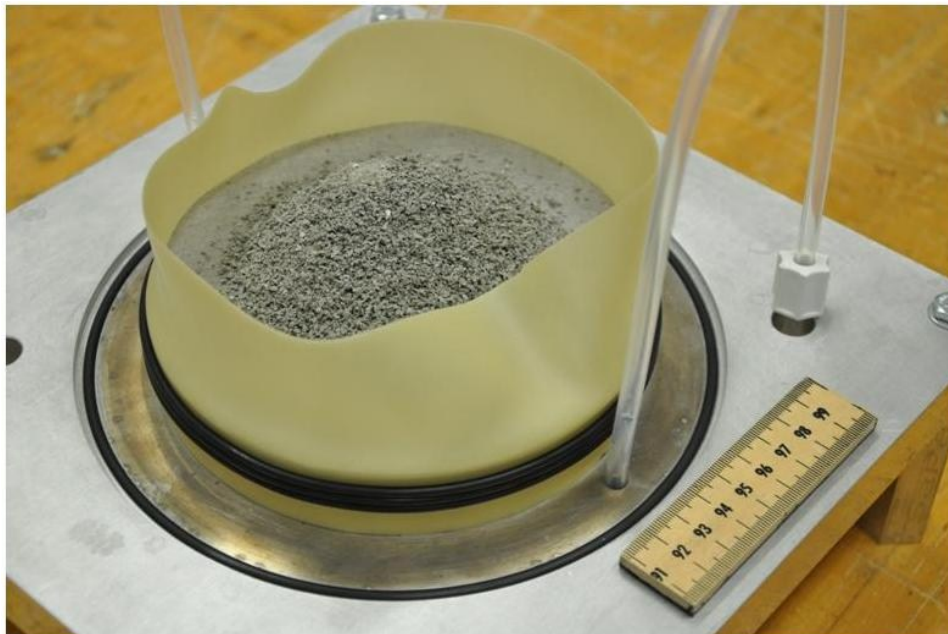
10. Place one heavy nonwoven geotextiles circle atop the base pedestal. Gently press the edges of the geotextiles circle down (a), so the circle is flat on the base pedestal (b). Next, place one heat bonded calendered nonwoven geotextiles atop the heavy nonwoven geotextiles circle. Again, gently press the edges of the geotextiles circle down so the circle is flat (c).



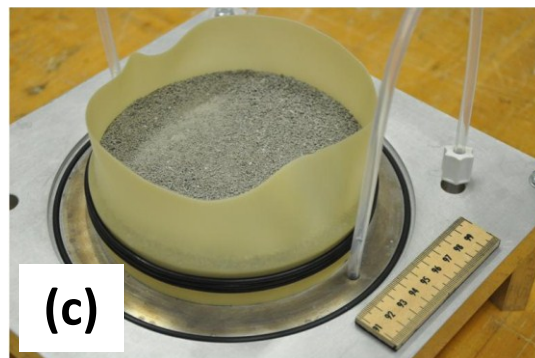
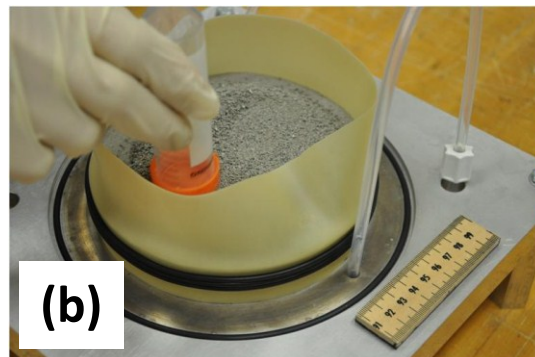
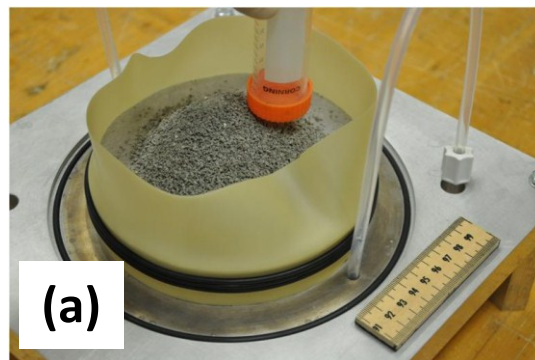
11. Weigh out the required mass of clay in a clean weighing dish.



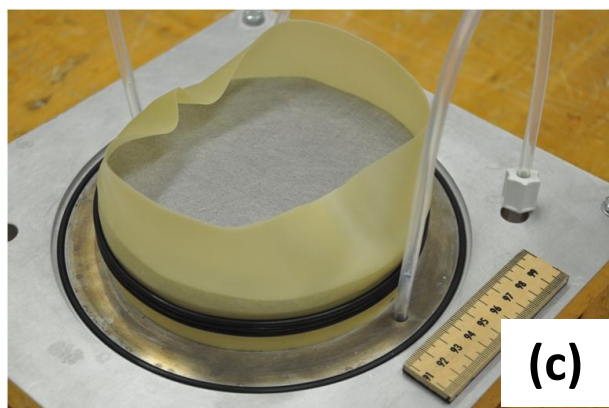
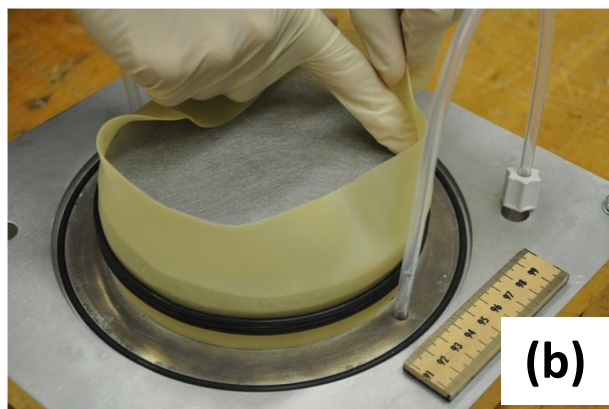
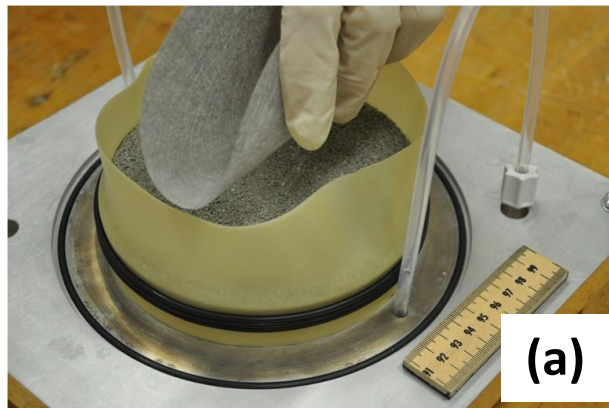
12. Gently pour the clay atop the center of the heat bonded calendered nonwoven geotextile.



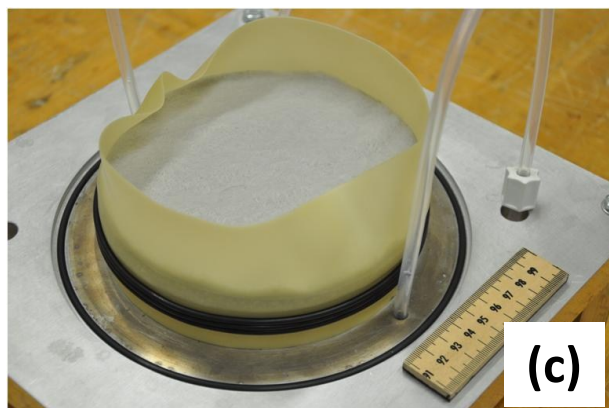
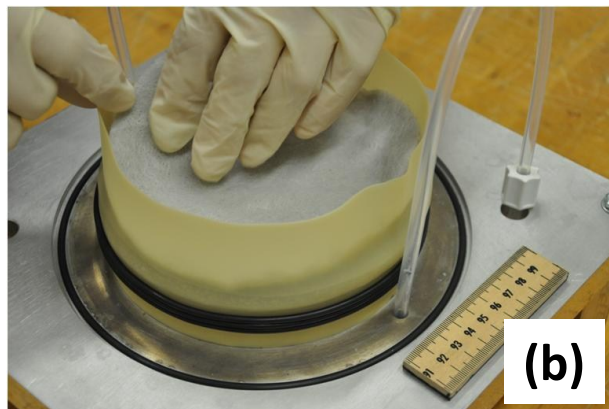
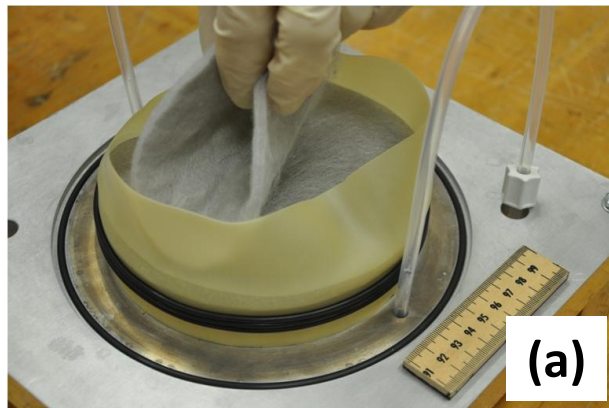
13. Use a small tamper with rounded edges (a 50 mL centrifuge tube works) to evenly distribute the clay across the surface of the heat bonded calendered nonwoven geotextiles. **Do not try to compact the clay**, merely distribute evenly. Be **very careful** to not overly deflect the latex membrane (**you do not want clay to fall between the latex membrane and the textiles or base pedestal**). Take your time; this is far and away the most critical step. The clay layer **must** be uniform in thickness.



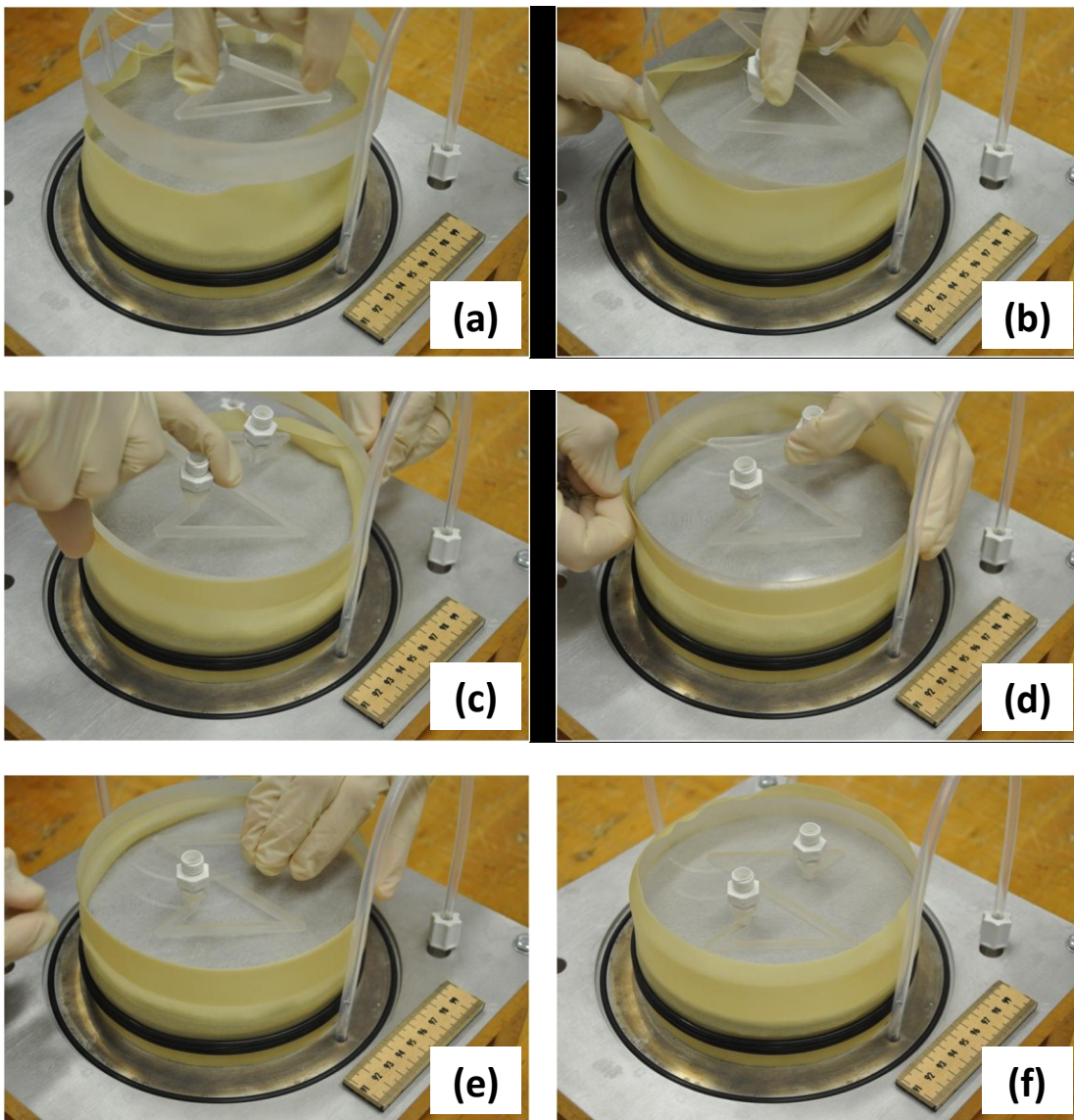
14. Carefully fold the other heat bonded calendered nonwoven geotextile and insert atop the center of the clay layer (a). Gently push down the edges of the textile circle while keeping the latex membrane tight against the base pedestal (b). **You do not want clay to fall between the latex membrane and the base pedestal.** Take your time (c).



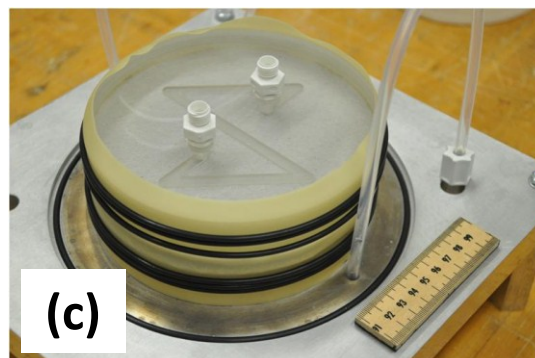
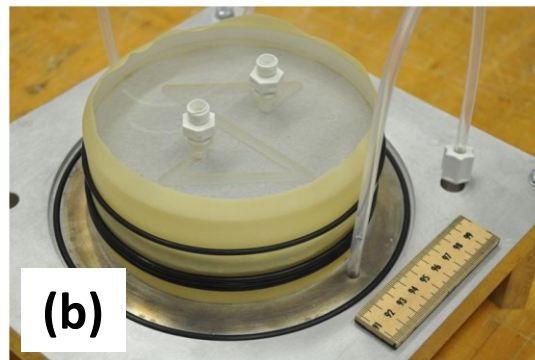
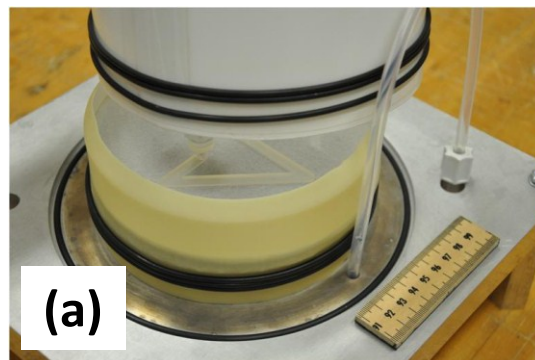
15. Carefully fold the other heavy nonwoven geotextile and insert atop the center of the top heat bonded calendered nonwoven geotextiles (a). Gently push down the edges of the textile circle while keeping the latex membrane tight against the base pedestal (b). **You do not want clay to fall between the latex membrane and the base pedestal.** Take your time (c).



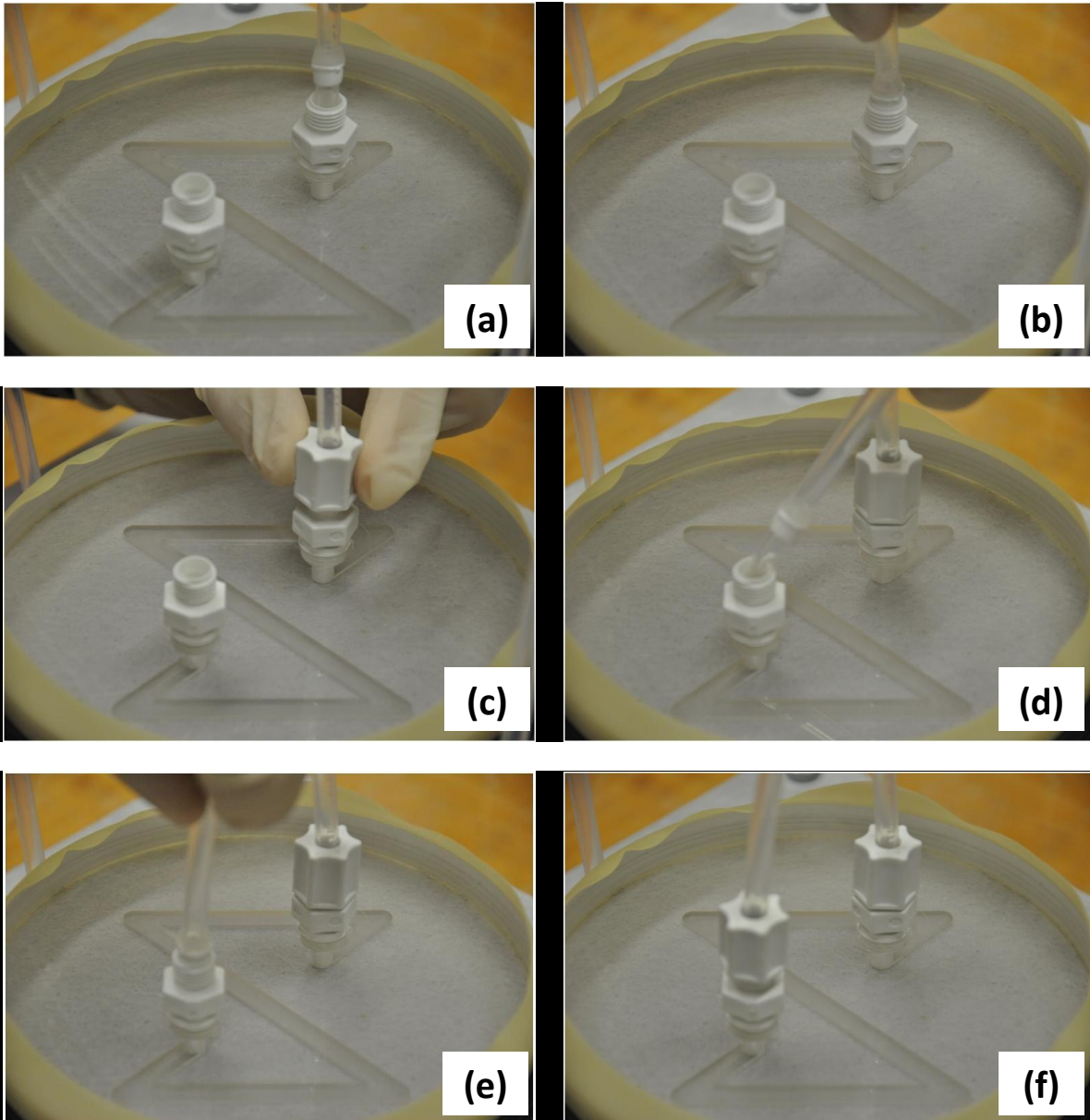
16. Hold the top cap (see Fig. A1) in one hand by the top fittings (a). Gently slip one side of the top edge of the top cap inside the latex membrane (b). Hold the cap with one hand, holding the membrane to the top cap with one thumb, and the cap level with your pointer finger (c). Slowly work up the membrane around the top cap, careful to not pull out the membrane from the base pedestal (d). Continue working the top cap down (e) by pulling the latex membrane up until the top cap is flush with the top geotextiles, and the latex membrane is taught (d).



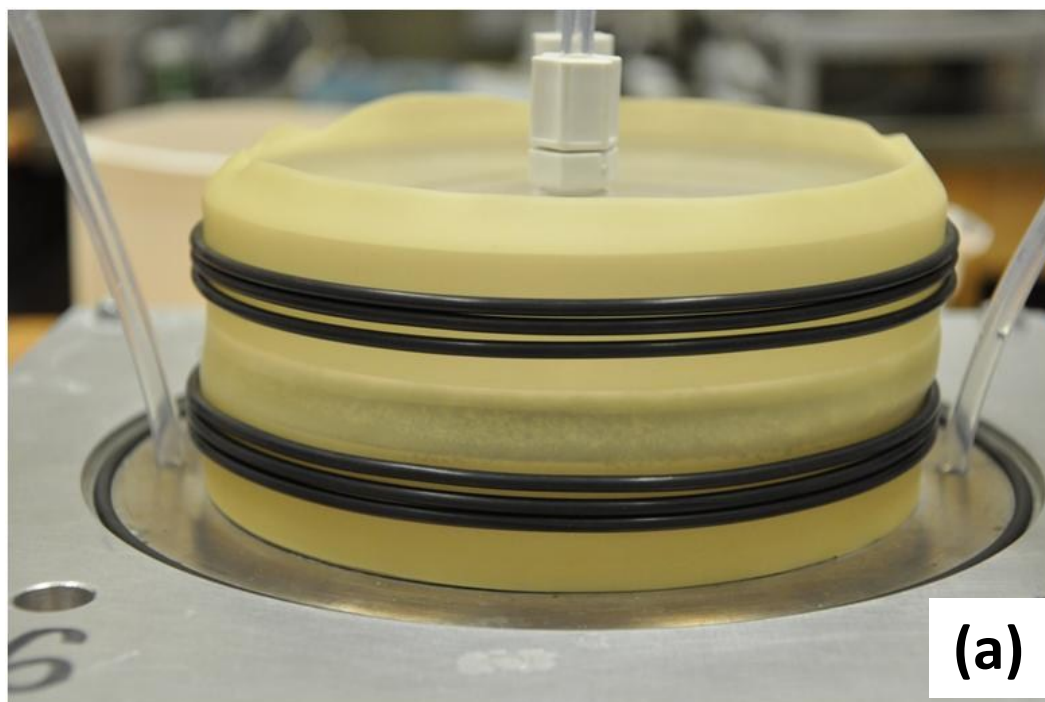
17. Stretch three O-rings over a rigid ring with an inside diameter slightly larger than the top cap + membrane (a). Delicately slide the first O-ring off of the rigid ring onto the upper portion of the top cap (b). Using finger tips untwist O-ring. The bottom O-ring should be 0.5 to 1.0 cm from the bottom of the top cap. Repeat this process with the other two O-rings, placing both above the first O-ring (c). **Be careful not to accidentally slide an O-ring onto the specimen, if this happens, you will have to start again at Step 7.**



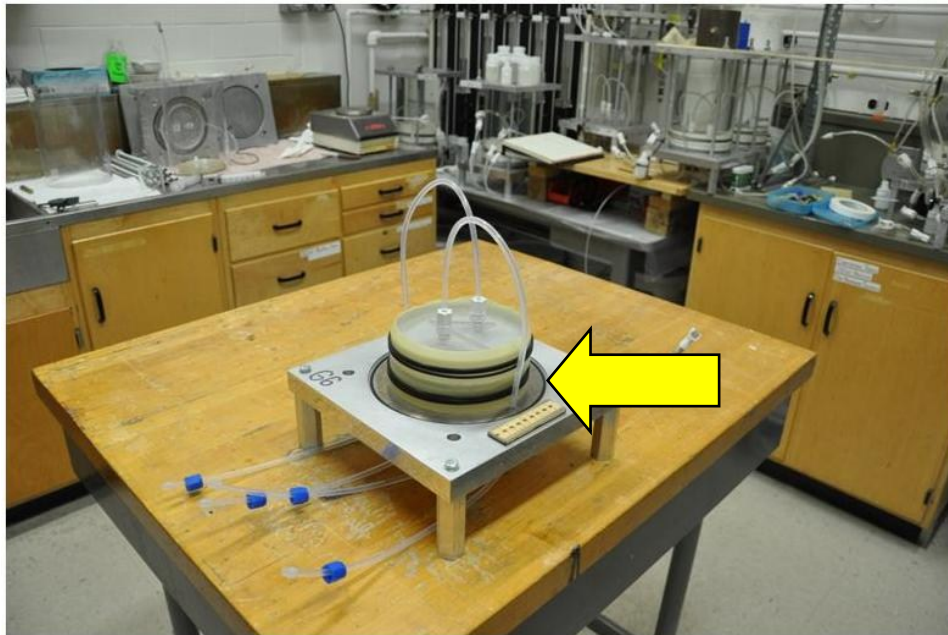
18. Un-tuck top tubing, and attach to top pedestal. Finger tightening is sufficient for tests at low effective stress. While tightening, hold top cap with other hand so that the membrane is not disturbed/shifted during tightening. You **do not** want clay to fall between the membrane and the base pedestal.



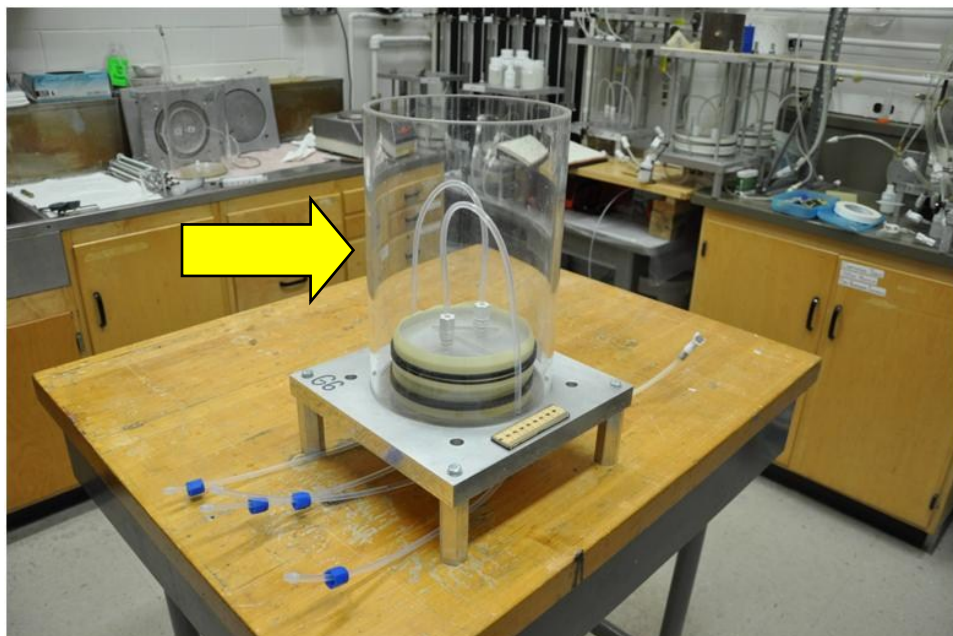
19. If more than a few granules of bentonite has fallen between the base pedestal and the latex membrane, or if the bentonite layer is not of even thickness, you will need to start again at Step. 7.



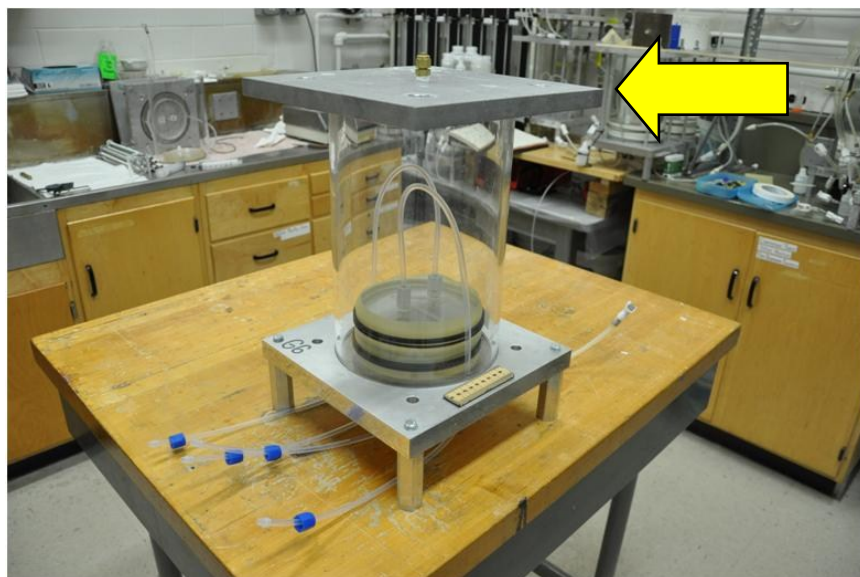
20. Ensure the cell O-ring is in place.



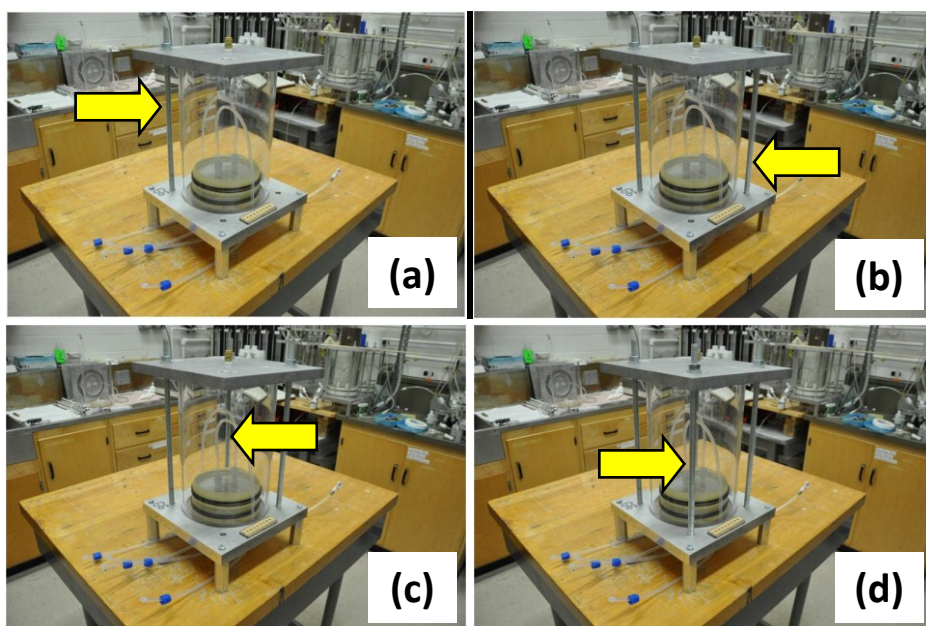
21. Place clear Acrylic cell on base plate. Ensure Acrylic cell is fitted against the cell O-ring.



22. Place the top plate atop the Acrylic cell. Ensure the Acrylic cell is in contact with the top plate O-rings. If you have trouble with the top plate O-ring falling out, flip over the top cap. Place the Acrylic cell on the O-rings of the top plate. Flip over top plate and Acrylic cell together, and place Acrylic cell on base plate (again ensuring Acrylic cell is uniformly touching the O-ring)



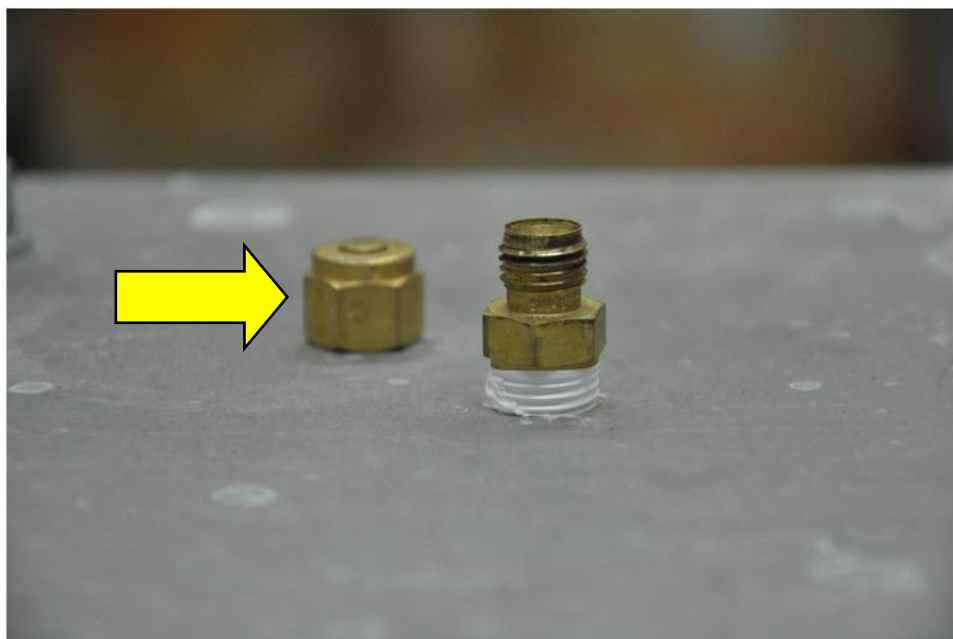
23. Install threaded rods between top and bottom plate.



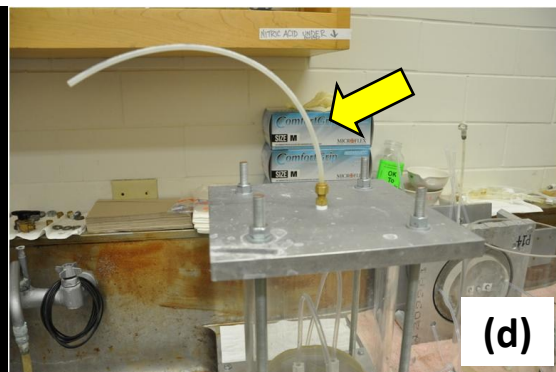
24. Tighten rods in a crosswise pattern. You will need to go around the four rods at least four times to get everything tightened down.



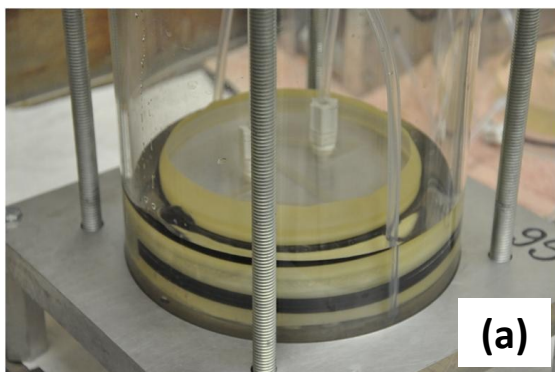
25. Remove cap for top vent.



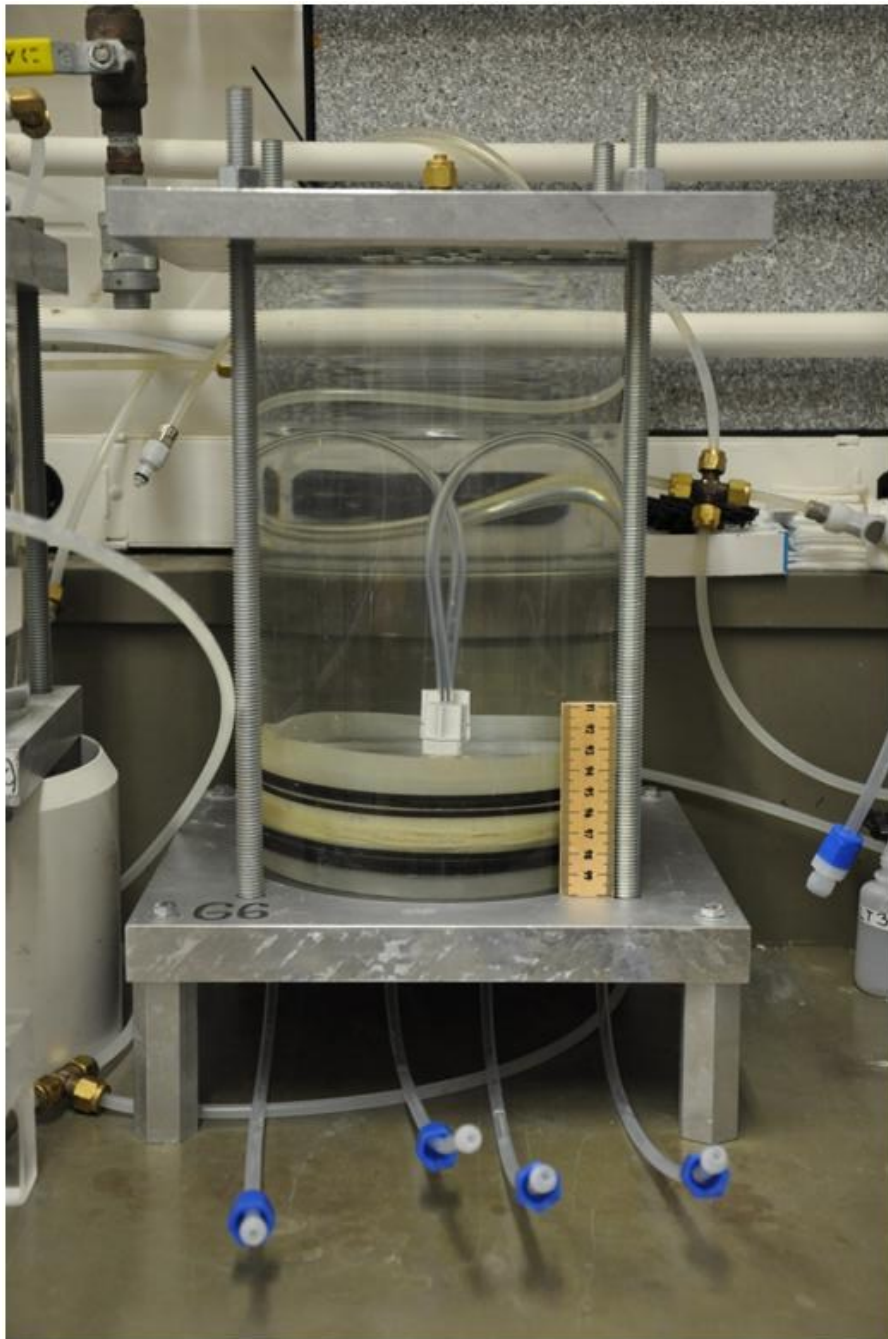
26. Attach overflow tube to top of permeameter. This will later be used to bleed air from the cell during filling.



27. Attach sink to cell pressure line. Slowly fill permeameter (a). Bleed air from under top cap (b). You will need to tilt the permeameter to do this, but do not disturb the clay specimen. Do not tilt the permeameter more than 1 cm out of plane and do not jar permeameter.

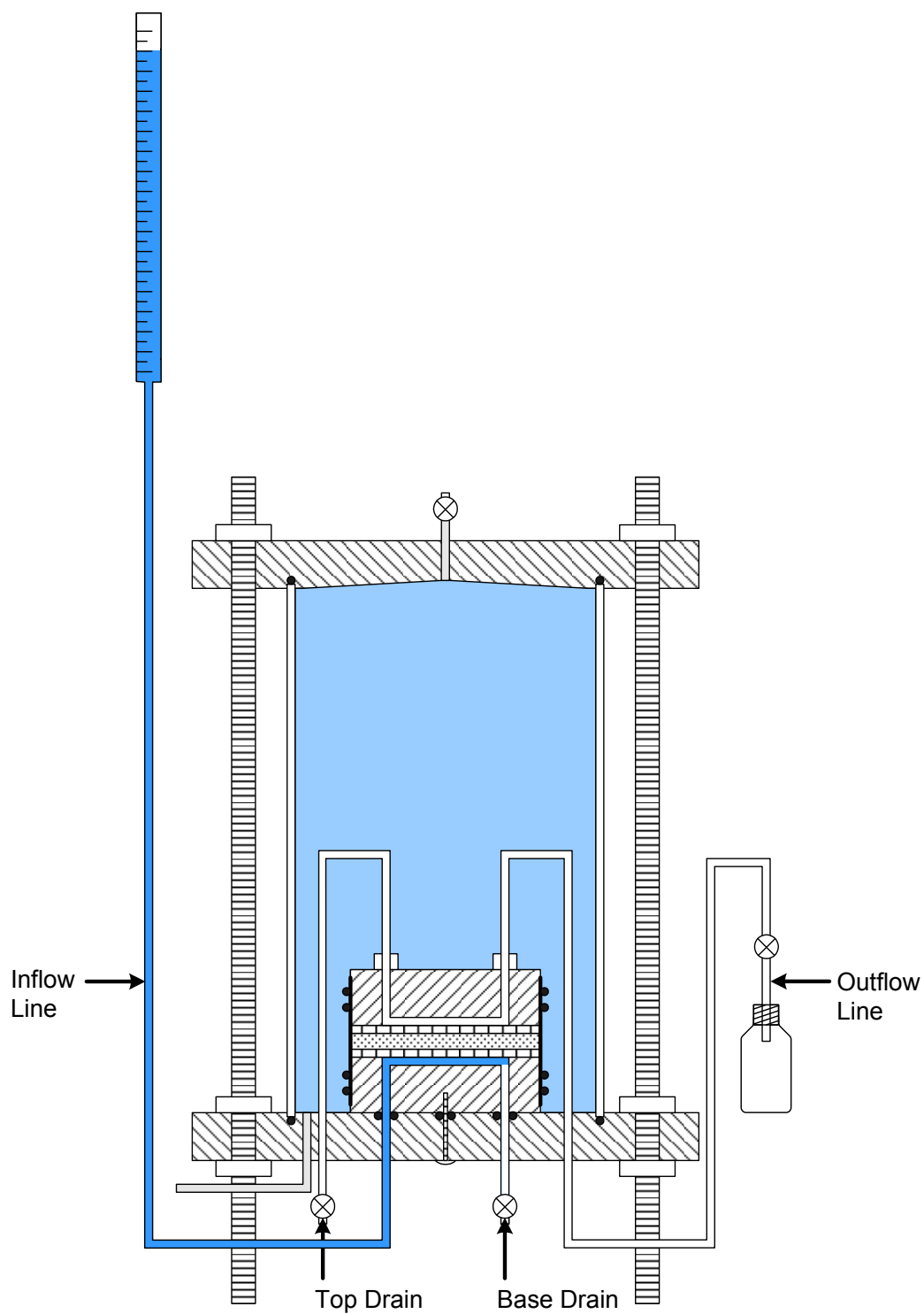


28. Delicately move permeameter to below inflow burette (where you will be performing the permeability experiment). **Apply cell pressure via cell-pressure line.**
- line.**

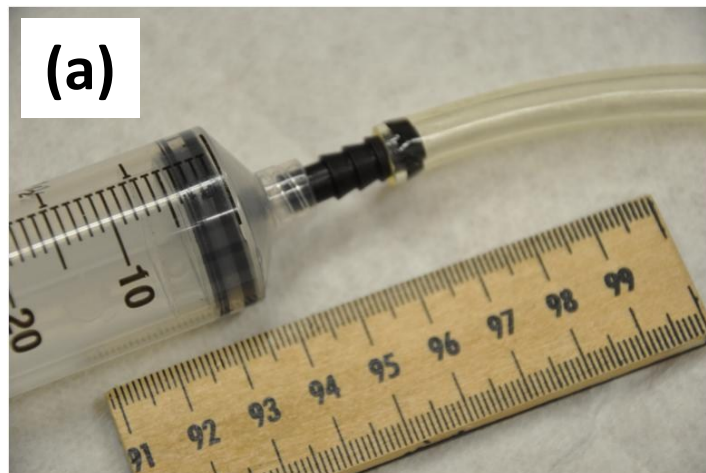




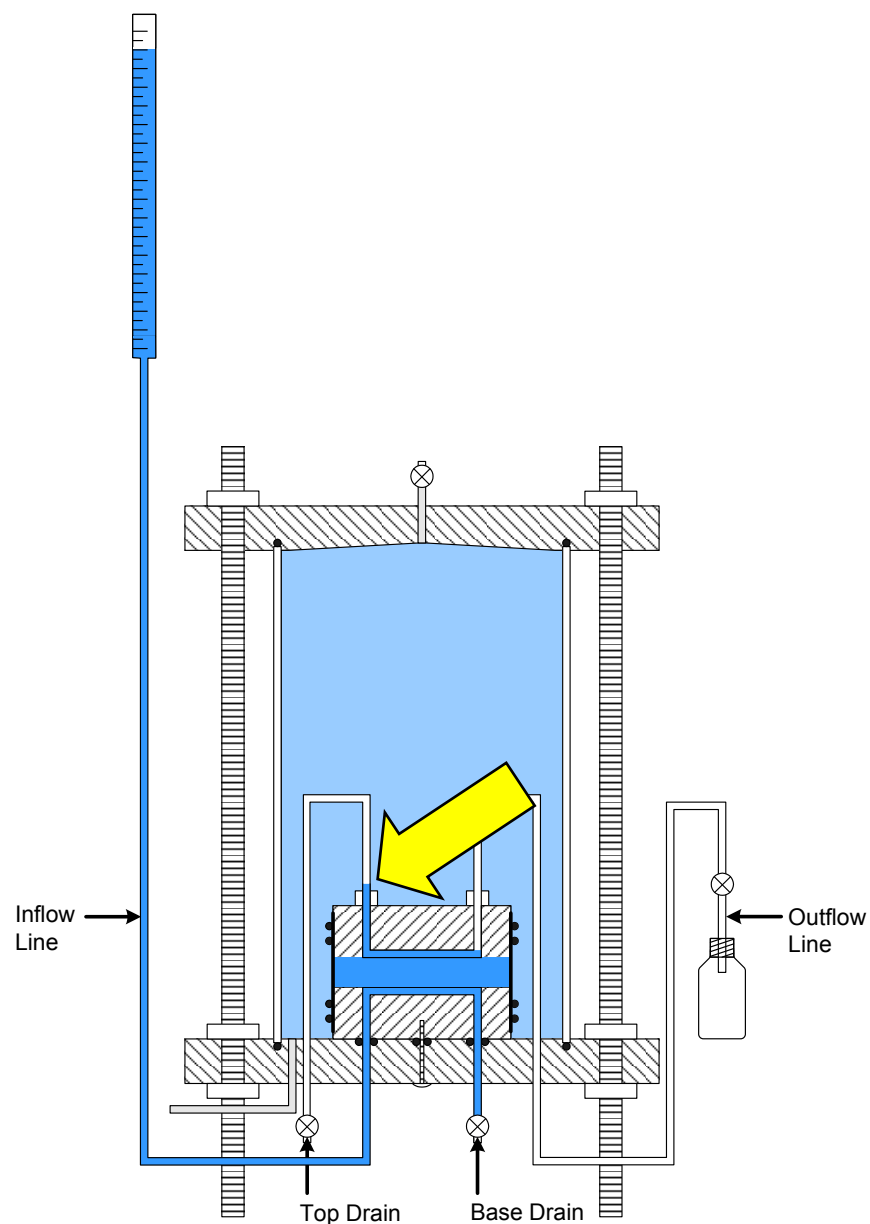
30. Fill inflow line with permeant. You will need to pinch the flexible tygon inflow line tubing to get all of the bubbles out of the line. Fill inflow burette to near the top.



31. Attach (a) a 60-mL syringe (b) to base drain line. Do not overly insert barbed tip or it will be impossible to remove. Open clamp on base drain line. Bleed air from the base of the pedestal. Once air (in form of bubbles) ceases to run from base drain tubing, clamp base drain line. You will need to refill the inflow burette when the water level nears the 50-mL mark. To do this, clamp the base drain line, remove the 50-mL syringe, discard liquid, refill inflow burette, reattach 60-mL syringe, open clamp on base drain, and continue to bleeding air. Close clamp on base drain line. Refill inflow burette to 30-mL mark. Remove 60-mL syringe and discard liquid (turn syringe 90° while tubing to easily detach).

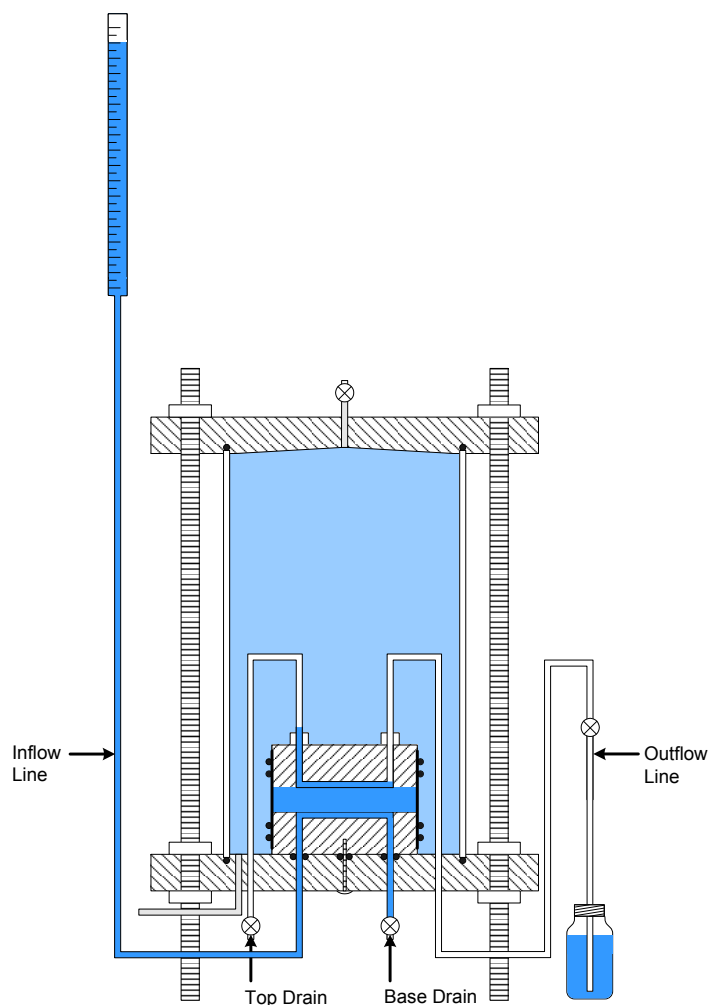


32. Attach a 60-mL syringe to the top drain line. Hold syringe so that flow does not occur through the specimen when the top drain clamp is opened. Open the top drain line clamp. Slowly allow flow through the specimen until water is visible above the top cap in the top drain line. Close top-drain line clamp. The intent here is to pass permeant into the specimen, through the hydrophobic flow-distribution geotextiles.



33. Fill inflow burette to mid-point (~25 mL mark). If inflow burette is above this mark, attach a 60-mL syringe to base drain, open clamp, slowly drain burette to required level, close clamp, detach 60-mL syringe, and discard extra permeant.
34. **Allow specimen in permeameter to hydrate for 48 hr. Refill inflow burette to 25 mL mark at least every 12 hours.**
35. After 48 hr, attach a 60-mL syringe to base drain line. Open clamp on base drain line. Bleed air from the base of the pedestal. Once air (in form of bubbles) ceases to run from base drain tubing, clamp base drain line. Remove 60-mL syringe and discard liquid. You may need refill inflow burette if the water level nears the 50-mL mark (bottom). To do this, clamp the base drain line, remove the 50-mL syringe, discard liquid, refill inflow burette, reattach 60-mL syringe, open clamp on base drain, and continue bleeding air. Refill inflow burette to top.
36. Attach a 60-mL syringe to top drain line. Hold syringe so that flow does not occur through the specimen when the top drain clamp is opened. Open the top drain line clamp. Slowly remove pressure holding syringe in place. If flow occurs rapidly from burette (burette level drops more than 20 mL within a minute) either the specimen is not fully hydrated, or the specimen is not compatible with the permeant. If inflow burette does not drop rapidly, continue to next step. If inflow burette drops rapidly, begin high hydraulic conductivity permeability testing.

37. Place outflow line into the bottom of a 250 or 500 mL bottle filled with permeant solution. Hold bottle with a clamp (the outflow line will tend to topple the bottle as the water is pulled out). The top drain line should be attached to a 60-mL syringe. The clamp should also be open on the base drain line. Pull permeant from the 250 or 500 mL bottle up outflow line, through top cap, and into 60-mL syringe. Continue to pull permeant until air (in form of bubbles) ceases to run from the top drain line. You may need to detach, drain and reattach 60-mL syringe multiple times and possibly refill 250 mL bottle while removing air. Once air is removed, close clamp on top drain.



38. All lines and geotextiles should now be de-aired, and the specimen should be at least partially hydrated. **Let the hydraulic conductivity testing commence!**

